

# **SARS Pathogenesis: Host Factors**

The studies presented in this thesis were carried out at the Department of Virology, Erasmus MC, Rotterdam, The Netherlands. Financial support was provided by the European Union, FP6 grant 5111060 (SP22-CT-2004), the National Institute of Health, Ro1 grant HL080621 and VIRGO.

The publication of this thesis was financially supported by:  
ViroClinics Biosciences B.V. and Greiner Bio-one

Cover design: Talita Groenendijk & Anna de Lang  
Layout by: Léonie Sijtsma, Serendipity ontwerp; [www.serendipity-ontwerp.nl](http://www.serendipity-ontwerp.nl)  
Printed by BOXPress B.V., Oisterwijk, The Netherlands

ISBN: 978-90-9026452-3

# SARS Pathogenesis: Host Factors

SARS PATHOGENESE: GASTHEERFACTOREN

## Proefschrift

ter verkrijging van de graad van doctor aan de Erasmus Universiteit  
Rotterdam op gezag van de rector magnificus  
Prof.dr. H.G. Schmidt  
en volgens besluit van het College voor Promoties.

De openbare verdediging zal plaatsvinden op  
donderdag 5 januari 2012 om 15:30 uur

door  
Anna de Lang  
geboren te Leusden



***Promotie commissie***

***Promotor:*** Prof.dr. A.D.M.E. Osterhaus

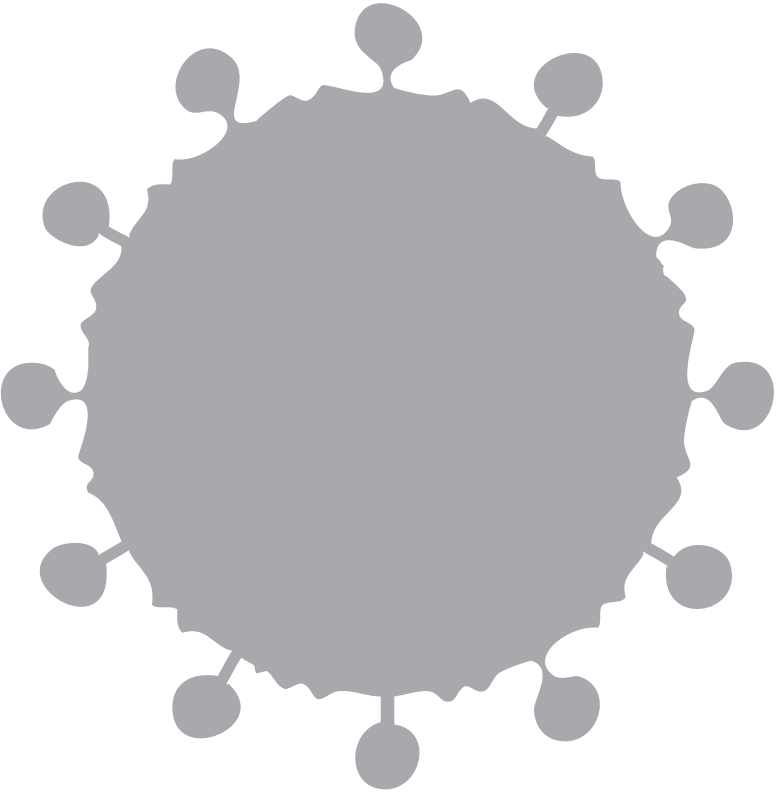
***Copromotor:*** Dr. B.L.Haagmans

***Overige leden:*** Prof.dr. T. Kuiken  
Prof.dr. J.J.M. van Dongen  
Prof.dr. P.J.M. Rottier



# Content

<b>Chapter 1</b>	
General introduction	7
<b>Chapter 2</b>	
Functional genomics highlights differential induction of antiviral pathways in the lungs of SARS-CoV infected macaques	33
<b>Chapter 3</b>	
Early host responses in peripheral blood mononuclear cells of SARS-CoV infected macaques	61
<b>Chapter 4</b>	
Plasmacytoid dendritic cells drive early antiviral and proinflammatory host responses in SARS-CoV infected mice	77
<b>Chapter 5</b>	
Interferon- $\gamma$ and interleukin-4 downregulate expression of the SARS-CoV receptor ACE2 in Vero E6 cells	103
<b>Chapter 6</b>	
Exacerbated innate host response to SARS-CoV in aged non-human primates	119
<b>Chapter 7</b>	
Repressed transcriptional host response in SARS-CoV infected ferrets	159
<b>Chapter 8</b>	
Summarizing discussion	183
Nederlandse samenvatting	205
Dankwoord	211
Curriculum Vitae	215
Publications	217
PhD portfolio	219



CHAPTER 1

# General introduction

Partially based on:

Anna de Lang, Tracey Baas, Saskia L. Smits, Michael G. Katze, Albert D.M.E. Osterhaus, Bart L. Haagmans

*Future Virology*. 2009; Jan 1;4(1):71-78



## Emergence of SARS

Severe acute respiratory syndrome (SARS) emerged late 2002/early 2003 in Guangdong Province, China, and spread rapidly to several countries in Asia, North America and Europe causing disease in 8096 people, of whom 774 died (World Health Organization statistics, [http://www.who.int/csr/sars/country/table2004\\_04\\_21/en/index.html](http://www.who.int/csr/sars/country/table2004_04_21/en/index.html), figure 1.1). While the number of deaths caused by SARS remained relatively low compared to for example the yearly influenza outbreaks, the impact of the SARS epidemic was very high, due to the rapid spread of the disease through air travel, immediate and intensive media coverage and the continuing globalization of the economy. The emergence of this new highly pathogenic disease brought on a quick response from the scientific world; only a few months after the first emergence of SARS, a newly discovered coronavirus (CoV) was identified as its etiological agent (26, 64, 66, 103).

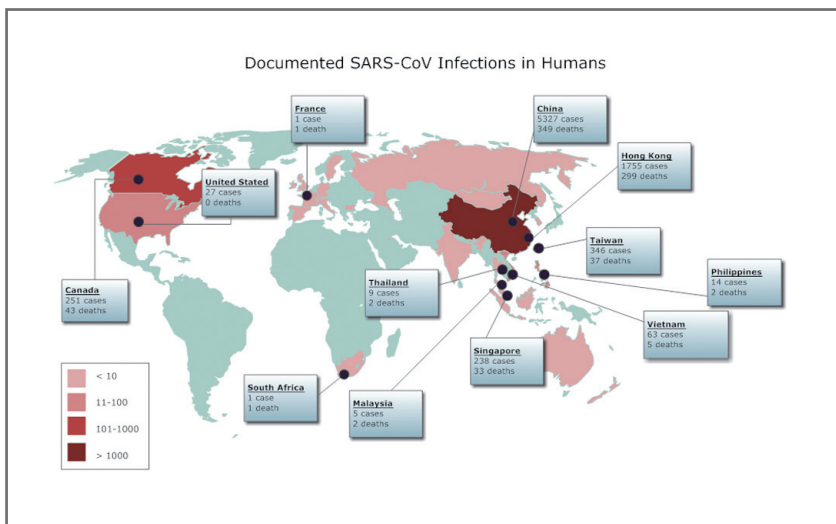


**Figure 1.1.** Countries affected by SARS-CoV. World map representing the number of documented SARS-CoV infections and SARS related deaths worldwide in the 2002/2003 epidemic. Countries with more than 10 cases or at least 1 death are mentioned specifically.

Until the SARS-CoV outbreak in 2003/2004 human infecting CoVs were associated with upper respiratory tract infections with mild disease symptoms. In fact, the only two human CoVs that were known before the emergence of SARS-CoV, HCoV-229E and HCoV-OC43, are believed to cause a significant percentage of all common colds in humans (70, 95). SARS-CoV was the first human CoV known to cause potentially severe disease of the lower respiratory tract, leading to death in almost 10% of people infected. The emergence of SARS-CoV had a catalyzing effect on CoV research, leading to the discovery of several previously unidentified CoVs. Two new human CoVs were identified, HCoV-NL63 and HCoV-HKU1, both viruses causing nonfatal upper and lower respiratory tract infections in infants, elderly and immunocompromised individuals (31, 131, 136). In addition, several novel animal CoVs have been identified such as avian CoVs

that infect mallards, geese and pigeons, enteric CoVs infecting ferrets and various bat infecting CoVs, one of them being a likely SARS-CoV precursor (57, 71, 78, 104, 106). The fact that during the SARS-CoV outbreak almost no SARS-CoV specific antibodies were found in non-SARS cases indicates that the virus had not been circulating at a large scale in the human population before the start of the epidemic in 2003, suggesting that the virus has been introduced into humans from animals (12, 64, 103). In line with this finding, many of the people that were infected with SARS-CoV early during the epidemic had been in close contact with live animals on Chinese wet markets (39). The current hypothesis is that bats are the main natural reservoirs of SARS-CoV-like viruses, and virus transmission to humans most likely occurred via civet cats, which are common trade animals on these wet markets (71, 78).

Like other CoVs, SARS-CoV can experimentally infect many different species, such as bats, civet cats, chickens, rats, mice, hamsters, guinea pigs, ferrets, pigs and non human primates (macaques and African green monkeys). Lungs of SARS-CoV infected macaques show type II pneumocyte hyperplasia and multiple foci of acute diffuse alveolar damage (DAD), characterized by flooding of the alveoli with oedema and infiltration of inflammatory cells (41, 66, 117). Although a wide range of animal species is susceptible to infection with SARS-CoV, most of these models do not exactly replicate SARS-CoV pathogenesis in humans. Not only does the pulmonary pathology differ from that seen in human cases, also the duration of viral replication is shorter in the animal models used for SARS research (20, 35, 66, 89). Interestingly, levels of viral replication are usually extremely high in the different animal models, whereas clinical disease is mostly limited.

### SARS-CoV: structure, replication and tropism

CoVs belong to the *Coronaviridae* family, based on their conserved genome organization and mechanism of replication, grouped within the order of the *Nidovirales* together with the *Roniviridae* and the *Arteriviridae* (36). These viruses are enveloped single stranded positive sense RNA viruses that infect a wide range of different animal species as well as humans. Transmission of CoVs occurs primarily via respiratory aerosols and via the faecal-oral route, mainly causing respiratory and enteric disease but sometimes also neurological disease or hepatitis, depending on the virus involved (91). The CoVs are ordered into three different groups based on entire genome sequence comparisons, roughly ascribing all the mammalian infecting CoVs to groups alpha and beta, including the human CoVs, and almost all the avian infecting CoVs to the gamma group (37). The initial classification of SARS-CoV in a new fourth group led to some controversy, however, subsequent analysis of SARS-CoV viral genes led to the conclusion that SARS-CoV has not diverged enough to form a completely new CoV group and, despite several unique features, it was concluded that SARS-CoV is best grouped with the beta group CoVs (91).

CoVs are enveloped viruses bearing distinctive spikes on their surface, appearing 'crown-like' (corona) when studied with electron microscopy, hence their name. SARS-CoV particle morphology is exemplary for CoV morphology in general; SARS-CoV particles are roughly spherical in shape and measure about 80-90 nm in diameter. The first SARS-CoV sequence, of the Tor2 strain, was already published in April 2003, only one month after the outbreak (87). With a genome that is approximately 29750 bases long, SARS-CoV is one of the largest RNA viruses known. The order and organization of genes within the SARS-CoV genome is similar to that of other CoVs with the replicase and protease genes at the 5' end

followed by 4 structural proteins present in all CoVs, namely the spike protein S, the membrane protein M, the envelope protein E and the nucleocapsid protein N. Interspersed between the structural protein genes are several other open reading frames (ORFs) (figure 1.2). The SARS-CoV genome contains 14 ORFs in total, for some of which the function is still unknown.

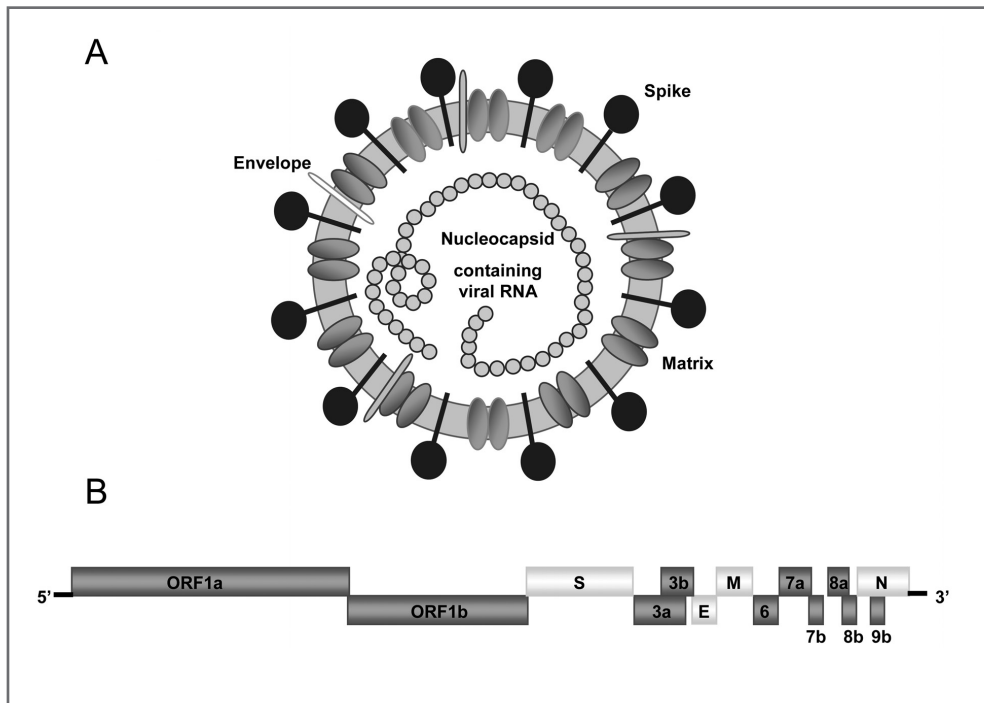


**Figure 1.2. Schematic diagram of CoV structure and genome organization.** The spike, membrane and envelope proteins are embedded in a lipid bilayer, which is derived from intracellular membranes. The viral RNA is associated with the nucleocapsid protein (A). The SARS-CoV genome consists of 14 ORFs. ORF1a and ORF1b both encode large polyproteins, containing the polymerase proteins among others. The structural gene region contains genes for the spike S, envelope E, membrane M and nucleocapsid N. Interspersed are the ORFs that encode the accessory proteins (B).

The SARS-CoV replication strategy is typical for CoVs; SARS-CoV RNA looks very much like the host RNA, having a 5' methylated cap and a 3' polyadenylated A tail, allowing the virus to use host ribosomes for translation after the viral RNA genome is released into the cytoplasm of the host cell. The first proteins produced are the replicase proteins (the non structural proteins), resulting from proteolytic processing of the pp1a and pp1ab polyproteins that are encoded by ORF1a and ORF1b. The SARS-CoV replicase allows for production of a nested set of mRNAs with a common 3' end, the subgenomic mRNAs, encoding the structural proteins that comprise the viral particles as well as some accessory proteins. Subsequently the N proteins assemble with the genomic RNA to form nucleocapsids in the cytoplasm, after which

these nucleocapsids bind the M proteins that are integrated into the ER membrane, just as the S and E proteins. After binding the M protein, the assembled nucleocapsids, including the viral RNA, bud into the ER lumen forming new viral particles that are exported out of the cells through the Golgi apparatus. S proteins that are not incorporated into the viral particle are transported to the cellular membrane, where they facilitate cell-to-cell fusion.

The heavily glycosylated S proteins on the surface of the viral particle are crucial for SARS-CoV to establish and maintain an infection cycle. SARS-CoV enters the host cell by binding of the S<sub>1</sub> domain of the S protein to the cellular receptor. Subsequently, the S<sub>2</sub> domain fuses with the cellular membrane (82). While SARS-CoV is able to bind the C-type lectins CD209L and DC-SIGN, the metalloproteinase angiotensin-converting enzyme 2 (ACE2) seems to be the key functional receptor for the virus (54, 77, 90, 139). SARS-CoV entry into the host cell is not dependent on the proteolytic activity of ACE2, since an enzymatically inactive ACE2 variant still binds SARS-CoV and facilitates entry (77). ACE2 is expressed in vascular endothelia, heart, kidney and testis, but also in epithelia of the small intestine and in alveolar epithelial cells (25, 42-43). Although ACE2 localization explains SARS-CoV tissue tropism in most areas such as the lungs, small intestine and the kidneys, there are also some discrepancies. For example, in colonic epithelium there are SARS-CoV infected cells although there is no ACE2 expression, on the other hand, in endothelial cells in the heart there is abundant expression of ACE2, but SARS-CoV infected cells have not been detected here (25, 42). These inconsistencies may be explained by the use of other receptors or co-receptors such as CD209L or DC-SIGN. Interestingly, the far less pathogenic HCoV-NL63 also uses ACE2 as a cellular receptor (47, 116). The HCoV-NL63 S protein and the SARS-CoV S protein both bind overlapping regions of ACE2, however, binding of the SARS-CoV S to ACE2 is more efficient than that of CoV-NL63 (79). Analysis of SARS-CoV RNA sequences from different isolates over time shows that the virus readily adapted once it was introduced in humans, especially in the beginning of the epidemic (1). Changes in the sequence of the S protein seem of particular importance for spread of SARS-CoV among humans, since the S protein from a SARS-CoV strain that spread globally more efficiently binds ACE2 than S proteins from civet cat SARS-CoV strains (80). Typical of CoVs is that the virally encoded RNA polymerases do not have proof-reading capability and typically have an error rate of about 1 in 10.000 nucleotides. Since CoV genomes are very large - 30 kb on average - each replication cycle will induce several mutations in the progeny virus. In addition, deletion and recombination may contribute to a rapid evolution of SARS-CoV strains (68-69, 93, 122, 145).

## SARS pathogenesis and treatment

SARS-CoV infection in humans initially causes lower respiratory tract disease, potentially causing a progressive atypical pneumonia with clinical symptoms that include fever, malaise, lymphopenia, and in some cases also diarrhoea (23, 75, 98, 102). Although SARS-CoV mainly causes respiratory disease, the virus can also be cultured from faeces and urine from SARS-CoV infected patients, indicating that SARS-CoV does not solely infect the lungs. About 20-30% of SARS patients suffered from severe disease and needed to be transferred to intensive care units. Ultimately the overall fatality rate approached 10% in adults, but the mortality rate was strongly correlated to the age of the patient. Strikingly, while the mortality rate in older patients (>60yrs) was very high, up to 50% in certain areas, children seemed to



be relatively resistant to SARS (24, 48, 81). Although SARS complications can be fatal, most SARS patients recovered, suggesting that protective immune responses are operational. The clinical course of SARS follows three phases. The first phase is characterized by active viral replication and patients experience the first symptoms of disease. Virus levels start to decrease while antibodies, which are effective in controlling infection, increase in the second phase. Nonetheless, pneumonia and immunopathological injury also develop in this phase. Eventually, in the third phase, fatal cases of SARS develop severe pneumonia and acute respiratory distress syndrome (ARDS), characterized by the presence of DAD (98).

ARDS is a severe form of acute lung failure and can not only be triggered by SARS-CoV, but also by other pathogens like H5N1 avian influenza and anthrax (38, 40). Furthermore, a variety of other conditions like sepsis, pancreatitis, and severe trauma, can lead to ARDS (133). Despite today's modern intensive care medicine, no pharmacological therapies have yet been developed that can alleviate ARDS symptoms and the mortality associated with ARDS remains very high. ARDS is characterized by massive infiltration of immune cells, such as neutrophils and macrophages, in the lungs, oedema formation and the induction of an array of inflammatory cytokines and chemokines, such as CXCL10, CCL2, IL-6, IL-8, IL-12, IL-1 $\beta$  and interferon (IFN)- $\gamma$  (133). Significant induction of these inflammatory agents has also been observed in SARS patients and has been described as a "cytokine storm" (49, 56, 108, 128, 135, 146). Additionally, it has been shown that these inflammatory cytokines are produced at higher levels in elderly people as compared to the young, making them more vulnerable for the development of ARDS after SARS-CoV infection, which corresponds with mortality rates observed in young and older patients (17) (110). Furthermore, high levels of CXCL10 in the first week after onset of fever have been associated with an adverse outcome of SARS-CoV infection (127). CXCL10, produced at high levels by activated bronchial epithelial cells in response to infection, acts on the CXCR3 receptor and is a chemoattractant for activated Th-1 cells and natural killer cells (10, 96, 113). Excessive CXCL10 production has also been reported for other respiratory viral infection, such as the human influenza A H5N1, where high levels of CXCL10 are associated with fatal outcome (22).

During the SARS epidemic several different therapies have been tested in SARS patients, however no trials with randomized placebo controls were performed. In humans, the first phase of viral replication peaks around day 10 after onset of symptoms, suggesting that there is a window of time to start an effective treatment and to reduce viral levels in order to prevent immunopathological damage, especially since high viral load in the second week of illness is associated with adverse outcome (50). Both ribavirin combined with lopinavir/ ritonavir and corticosteroids as well as treatment with IFN alfacon-1 were beneficial for SARS patients (15, 84). Several potential agents that could serve as SARS treatments, considering IFNs, glycyrrhizin, baicalin, reserpine, niclosamide, luteolin, tetra-O-galloyl- $\beta$ -D-glucose and the protease inhibitors all have been reported to be active against SARS-CoV *in vitro*, but the only approved medication that has been tested in an animal model so far is pegylated IFN- $\alpha$ , which protects type I pneumocytes from SARS-CoV infection in macaques (41).

### **SARS-CoV induced pathogenic pathways in target cells**

*In vitro* experiments have shown that diverse potentially pathogenic pathways are activated in cells infected with or exposed to SARS-CoV, such as pathways involved in induction of apoptosis, stress

responses and procoagulation (125). Most prominent however is the induction of pathways involved in the immune response after SARS-CoV infection, characterized by the induction of a range of proinflammatory cytokines and chemokines of the CXC and CCL family, as well as elevated transcription of genes involved in cell to cell signaling and cellular movement (14, 72, 97, 121, 125, 141, 144). Induction of cytokines like IL-6, IL-8 and chemokines like CXCL10, CCL2, CCL3 and CCL5 has been observed in several different cell lines derived from organs as kidney, colon, liver and lung, as well as in dendritic cells and macrophages exposed to SARS-CoV. Interestingly, productive SARS-CoV infection is not necessary for induction of these genes (14, 72). As mentioned previously, excessive induction of proinflammatory cytokines and chemokines may be associated with SARS pathology seen in human patients.

SARS-CoV not only induces the production of potentially pathogenic cytokines and chemokines in its target cells, but might also cause pathology through effects on its cellular receptor ACE2. Before ACE2 was known as a SARS-CoV receptor, this enzyme was first described in 2000 as one of the key players in the renin angiotensin system (RAS) (25, 129). The RAS is a peptide hormone system that has an essential role in regulation of heart function and maintaining blood pressure homeostasis and consists of a cascade of various multifunctional enzymes, receptors and mediators (5, 21). In summary, the protease renin hydrolyzes angiotensinogen, generating angiotensin I (ANG I). The C-terminal aminoacids from ANG I can be cleaved by angiotensin converting enzyme (ACE), resulting in the production of the biologically active angiotensin II (ANG II). Subsequently, ANG II binds its specific receptor  $AT_1$ , leading to several adverse biological effects such as vasoconstriction, proliferation, cardiac hypertrophy and pulmonary fibrosis. For years it was thought that the RAS was an endocrine system with ANG I as its main effector hormone, however in recent years, along with the discovery of ACE2, a whole new axis was established besides the pathogenic ACE/ANG II/ $AT_1$  axis, namely the ACE2/ANG-(1-7)/Mas receptor axis (28, 137). ACE and ACE2 share a high percentage of sequence similarity in their catalytic domains, but these two homologues act on different substrates, giving them distinct biological functions (25, 129). While ACE removes 2 residues from the decapeptide ANG I, generating ANG II, ACE2 cleaves only 1 residue, leading to the production of the biologically inactive ANG (1-9) which then can be converted to the vasodilatory peptide ANG-(1-7) by ACE or other peptidases. Alternatively, ANG II can be directly metabolized by ACE2 to generate ANG-(1-7). The biological properties of ANG (1-7) are completely opposite compared to those of ANG II. Mainly through the Mas receptor, but also through the  $AT_2$  receptor, ANG (1-7) stimulates vasodilation, antiproliferation and antihypertrophy. By cleaving ANG II into ANG (1-7), ACE2 plays an important role in counterbalancing adverse actions of the ACE/ANG II/ $AT_1$  receptor axis. Thus, the vasoconstrictor/proliferative actions of the RAS, mediated by ANG II, versus its vasodilator/antiproliferative actions, mediated by ANG (1-7), are mainly driven by the balance between ACE2 and ACE (figure 1.3).

In the last decade several studies have reported about a role for the RAS in the development of ARDS (51, 55, 88). For instance, there seems to be a correlation between ACE gene polymorphisms and the susceptibility and mortality of ARDS. Moreover, it has been shown that ACE2 protects murine lungs from severe acute lung injury in different ARDS models and that ARDS in mice can be attenuated by either inhibiting the ACE/ANG II/ $AT_1$  receptor axis or by treatment with an enzymatically active recombinant ACE2 (51). Interestingly, SARS-CoV infection or treatment with a recombinant SARS-CoV Spike protein in mice decreases ACE2 expression levels in the lungs, favoring the pathogenic ACE/ANG II/ $AT_1$  receptor axis.

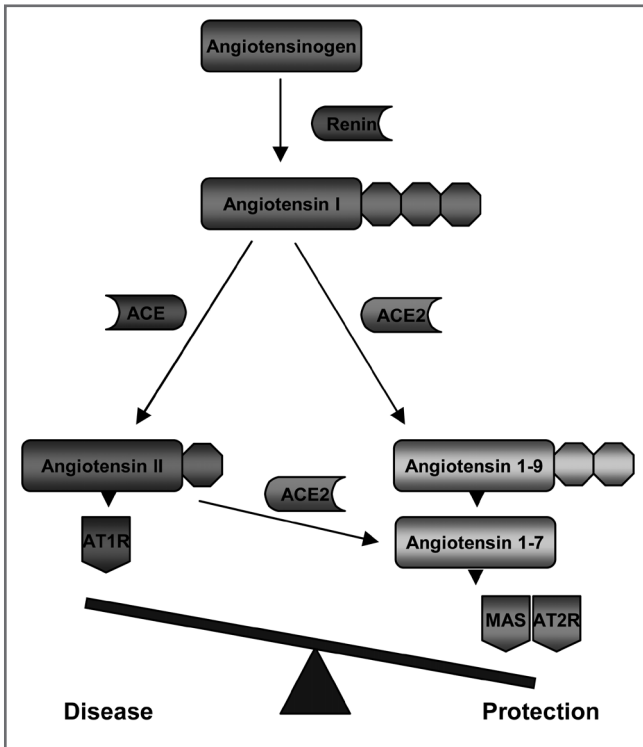


**Figure 1.3. RAS pathways.** Schematic diagram showing the counterregulatory axes of the RAS, the ACE/ANG II/AT<sub>1</sub>R axis and the ACE2/ANG (1-7)/Mas receptor axis. The ACE enzymes play an important role in balancing these axes. ACE cleaves ANG I, generating ANG II, but ACE2 counterbalances this pathogenic axis by degrading ANG II into ANG (1-7).

Additionally, treatment with a recombinant Spike protein coincided with increased ANG II peptide levels and worsened ARDS symptoms in a murine ARDS model (65). Thus, SARS-CoV mediated downregulation of ACE2 might play a role in SARS induced pathogenesis and development of ARDS after SARS-CoV infection. SARS-CoV might also employ the ACE2 receptor as a signal transducer leading directly to induction of the proinflammatory CCL2 (11). CCL2 is a chemokine that attracts monocytes, memory T lymphocytes, and basophils and involved in inflammatory reactions. Increased levels of CCL2 are associated with ARDS but also with other inflammatory lung disorders like asthma and pulmonary fibrosis (111). Elevated levels of CCL2 were also detected in sera of SARS patients and in supernatants of cells infected with SARS-CoV (13, 56). Moreover, it was shown that direct interaction of the viral particle viral infection and replication was not necessary for production of CCL2 since incubation of cells with SARS-CoV virus like particles or SARS-CoV Spike protein were sufficient to induce CCL2 gene transcription and protein production (11). In addition, interaction of SARS-CoV virus like particles with the ACE2 receptor directly leads to induced expression of the proinflammatory CCL2 through casein kinase II mediated phosphorylation of ACE2 and subsequent activation of the MAPK pathway (11). This suggests that ACE2, besides counterbalancing the adverse actions of the ACE/ANG II/AT<sub>1</sub> receptor axis by enzymatically cleaving ANG II, might also function as a signal transducer in the cellular membrane and possibly contributes to SARS induced pathology via this route.

## IFN induction by SARS-CoV

Innate immune responses provide immediate defense against pathogens by recruiting immune cells to the site of infection by identifying and eliminating pathogens and subsequent induction of cytokines, activation of the complement system and adaptive immune responses. To specifically provide powerful protection against invading viruses, IFNs are produced. Type I IFNs, IFN- $\alpha$  (13 human subtypes) and IFN- $\beta$  (1 human subtype), together with type III IFNs, IFN- $\lambda_1$ , IFN- $\lambda_2$  and IFN- $\lambda_3$  (IL-29, IL-28A and IL-18B respectively) are induced in direct response to virus infection (100). IFN- $\gamma$ , a single type II IFN, is not secreted in direct response to viral infection but produced by activated T cells and natural killer cells. In principal, most mammalian cells are capable of producing type I IFNs; however the mechanism and amount of IFNs that are induced can differ among cell types. While fibroblasts, epithelial cells and neurons mainly secrete IFN- $\beta$  initially before they switch to IFN- $\alpha$  production, plasmacytoid dendritic cells (pDCs) initially make large amounts of IFN- $\alpha$  followed by a switch to IFN- $\beta$ . IFNs do not only function as direct antiviral proteins, they also have several other biological properties such as inhibition of cellular proliferation and immunomodulation, making their role in viral infections broader than just their direct antiviral activity (45, 74).

There are several routes by which cells can recognize the presence of an invading virus and by which IFNs can be produced subsequently. The relevance of a specific route depends on the type of virus, type of cell that is infected and the stage of infection in that same cell. The two major pathways through which cells sense invading viruses are the intracellular pathway and the endosomal pathway. In the intracellular pathway, IFN- $\beta$  is induced when pathogen associated molecular patterns (PAMPs), such as double stranded (ds) RNA and 5'-triphosphorylated single stranded (ss) RNA, are sensed by the RNA helicases RIG-I and MDA-5, the main intracellular receptors of viral RNA (2, 60, 142-143). When viral RNA binds to these helicases, a signaling chain is induced, eventually leading to the phosphorylation of the transcription factor IRF-3, a molecule that plays an essential role in the activation of the IFN- $\beta$  promoter (30, 46, 114). As soon as IRF-3 is phosphorylated, the molecule homo-dimerizes and is translocated to the nucleus where it recruits the co-factors CPB and p300 and binds the IFN- $\beta$  promoter in order to start IFN- $\beta$  gene transcription. Ongoing viral replication subsequently induces the activation of transcription factors NF- $\kappa$ B and AP-1 that both bind the IFN- $\beta$  promoter and further enhance IFN- $\beta$  gene expression (16,101). The induction of IFN leads to the production of IRF-7, which is only present in low amounts in most cells (112). Phosphorylated IRF-7 subsequently binds the IFN- $\beta$  promoter, resulting in enhanced induction of IFN- $\beta$  and the induction of the IFN- $\alpha$  genes through a positive feedback loop (86, 112).

Induction of IFN through the endosomal pathway involves the Toll like receptors (TLRs), like TLR3, TLR7, TLR8 and TLR9, which can detect viruses in endosomal compartments as they enter cells. This pathway is used by pDCs, which are also known as "professional type I IFN producers" (29). pDCs predominantly sense viral RNA through the endosomal receptors TLR7 and TLR8 (29, 53). When these TLRs become activated, the adapter molecule MyD88 is recruited, which in turn recruits IRAK-4 and IRAK-1. Subsequently, through activation of several signaling molecules, eventually IRF-7, NF- $\kappa$ B and IRF-3 are activated and translocated to the nucleus, leading to the production of IFN- $\alpha$  and IFN- $\beta$ . Interestingly, the pDC is the only known cell type that constitutively expresses high levels of IRF-7 and thus high levels of IFN can be produced by these cells (61, 105).

SARS-CoV typically does not induce an IFN response in infected cell cultures although substantial

amounts of the IFN inducing dsRNA are generated during infection (118, 119, 125, 134). This suggests that SARS-CoV is able to inhibit the induction of IFNs, either actively or passively. Several potential mechanisms through which SARS-CoV can inhibit IFN induction have been described recently. Double membrane vesicles are formed after CoV infection, and it is hypothesized that these complexes shield viral RNA from sensing molecules (118, 123). Recently it was shown that 2'-O-methylation of CoV mRNA is involved in inhibiting IFN responses in infected cells as well (150). In contrast to wild type CoVs, CoV mutants lacking the 2'-O-methyltransferase activity induced high levels of IFNs. Interestingly, induction of IFNs was dependent of the cytoplasmatic RNA sensor MDA-5. Another possibility is that one of the SARS-CoV viral proteins sequesters the genomic RNA in such a way that host-sensing proteins do not detect it as has been demonstrated for several other viruses, such as VP35 from Ebola and NS1 of influenza (44, 59). It remains to be proven if SARS-CoV actively inhibits IFN production or just escapes from the induction of IFNs. Spiegel et al. showed that although SARS-CoV does not induce IFN, IRF-3 initially translocates to the nucleus of infected cells in SARS-CoV infected cells (119). However, at a later time point after infection, IRF-3 was again localized in the cytoplasm. Furthermore, SARS-CoV interfered with IRF-3 hyperphosphorylation, dimerization, and binding to cofactor chromatin binding protein. Also studies using expression plasmids that contain one of the SARS-CoV proteins have demonstrated that SARS-CoV proteins ORF3b, ORF6, the N protein and the papain-like protease (PLP) are able to inhibit IFN production by affecting the IRF3 activation pathway (33, 62). More recently, other groups demonstrated that SARS-CoV does not activate IRF-3 and NF- $\kappa$ B or induce IFN in infected cells, but that subsequent treatment with Poly:IC or infection with Sendai virus still results in IFN production (32, 132, 148). In addition, when recombinant SARS-CoV, deleted for one of their accessory ORFs, was used to infect cells, none of the deletion mutants were able to induce IFN but Sendai virus infection did induce IFN- $\beta$  production in these cells (32). Apparently, SARS-CoV does not induce the IFN sensing pathway, but SARS-CoV does not actively block sensing of other viral proteins or stimuli either.

In contrast to most studies performed in *in vitro* cell cultures, human pDCs are able to produce IFN upon incubation with SARS-CoV (9). pDCs are known to be the most potent producers of IFN- $\alpha$  in the human body, producing 10-100 times more type I IFNs than other cell types, and type I and type III IFNs account for 60% of the total genes expressed in activated pDCs (115, 52). While IFNs cannot be detected in SARS-CoV infected myeloid DCs (mDCs), pDCs rapidly produce and secrete considerable amounts of IFN- $\alpha$  and IFN- $\beta$  upon SARS-CoV infection. Furthermore, using MHV as a CoV model, it was observed that rapid IFN induction in pDCs is dependent on TLR7 and MyD88. These sensing molecules induce expression of IFN- $\alpha$  upon viral infection through IRF-7, constitutively expressed in pDCs, suggesting that the pDC restricted TLR7/IRF-7 IFN induction pathway is not affected by the virus. It is still unclear whether DCs are infected by SARS-CoV, and so far no conclusive evidence on infection of DCs by SARS-CoV has been reported (8, 72, 130, 149). On the other hand, active viral replication may not be necessary to mount an efficient IFN response (8, 120). Castiletti et al. observed that SARS-CoV induces IFN- $\alpha$  and IFN- $\gamma$  in peripheral blood mononuclear cells (PBMCs) from healthy donors and that this IFN response was even more robust when PBMCs were incubated with (paraformaldehyde) fixed SARS-CoV infected Vero cells (8). In addition, Spiegel et al. found that both live and UV inactivated SARS-CoV were able to induce type I IFNs in DC cultures (120). In line with these results, a study analyzing IFN levels in 40 well described SARS

patients found high levels of type I IFNs in plasma and robust IFN stimulated gene expression in pre-crisis SARS patients (7). Although there is no direct proof yet that pDCs are responsible for the induction of IFNs during SARS-CoV infection *in vivo*, the fact that pDCs are able to produce type I IFNs upon SARS-CoV infection *in vitro* is suggestive for their role *in vivo*. However, it is still possible that another cell type is accountable for the IFN production during SARS. For example, for several other RNA viruses it has been shown that alveolar macrophages, not pDCs, are the main type I IFN producers early in infection (67).

### SARS-CoV blocks IFN signaling

As soon as IFN- $\alpha$  and IFN- $\beta$  bind to the common type I IFN receptor (composed of the products of the IFNAR1 and the IFNAR2 genes), conformational changes in the intracellular domain of the receptor lead to the activation of the JAK/STAT signaling pathway (94, 107). The cytoplasmic tails of IFNAR1 and IFNAR2 associate with tyrosine kinase 2 (Tyk2) and tyrosine kinase janus 1 (JAK1) respectively, leading to binding and activation of signal transducers and activators of transcription (STAT) 1 and STAT2. After STAT1 and STAT2 have formed a stable hetero-dimer, the complex is translocated into the nucleus where it associates with IRF-9 to form the heterotrimer ISGF3(4, 109). This complex binds to the IFN stimulated response element (ISRE) resulting in transcription of IFN stimulated genes (ISGs), like PKR, 2'5'OAS, MX, ISG15, ISG20 and ISG54. More than 300 ISGs are induced by IFN- $\alpha/\beta$ , leading to a wide array of biological effects in the host cell (107). For example, the G1/S phase specific cyclin-dependent kinase inhibitor p21 triggers cell-cycle arrest, while proteins such as procaspases, PKR and OAS, have an antiviral effect by causing apoptosis (3, 19, 85). Additionally, ISGs can have immunomodulatory effects by promoting the presentation of viral antigens through upregulated expression of the MHC class I molecules, by promoting maturation of DCs or by upregulating the activities of NK cells (73-74). The combined expression of these ISGs by a cell is collectively known as an "antiviral state".

Recently it was demonstrated that SARS-CoV does not only prevent the induction of type I IFNs, but that several SARS-CoV proteins also block different steps in the IFN signaling pathway (figure 1.4). For example, the ORF7a protein and the nsp1 gene product were shown to inhibit cellular protein synthesis and to promote host cell mRNA degradation, respectively (58, 63). In addition, the SARS-CoV proteins ORF3b and ORF 6 inhibit IFN signaling through the JAK/STAT pathway both passively and actively (62). Inhibition of IFN signaling by ORF6 was described in detail by Frieman et al.(34). They demonstrated that ORF6 tethers karyopherin  $\alpha$ 2 and karyopherin  $\beta$ 1 to the ER/Golgi membrane, inhibiting the nuclear import of STAT1 and thus preventing transcription of the ISGs.

The presence of type I IFNs and ISGs in SARS-CoV infected humans raises the question to what extent these pathways play a role in SARS pathogenesis. Pre-treatment of cells with IFN before infection prevents SARS-CoV replication in these cells (14, 72, 119). In addition, Haagmans et al. showed that IFN- $\alpha$  protects type I pneumocytes from SARS-CoV infection in macaques (41). Considering these observations, IFN treatment starting early after onset of clinical symptoms may also be effective in human SARS patients. Insights in the complex regulation of the IFN response during SARS-CoV may provide clues for intervention strategies based on the use of IFNs.

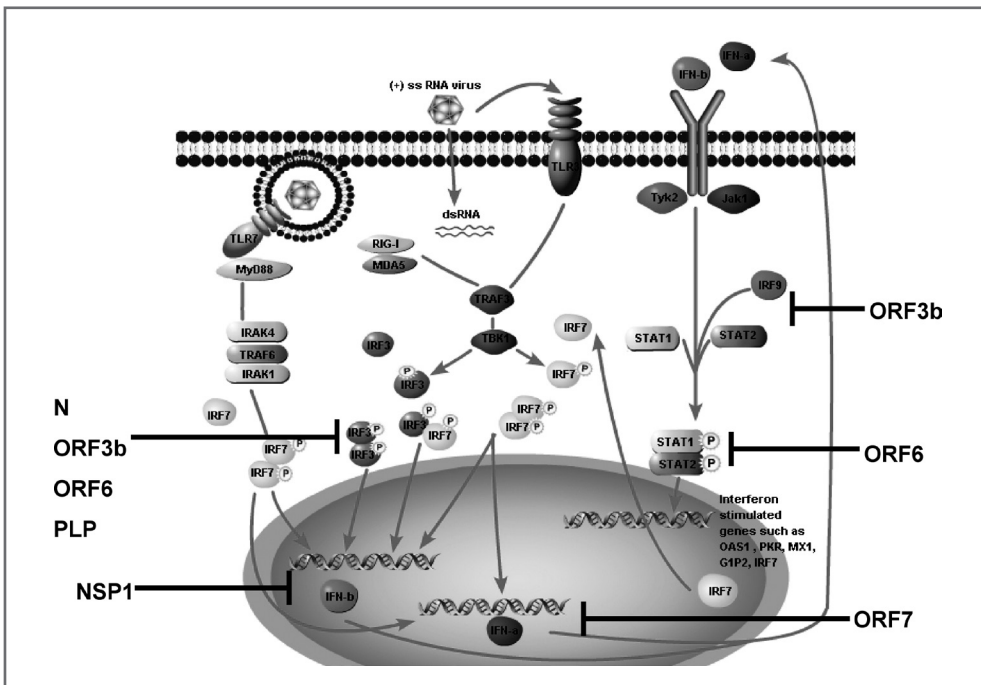


Figure 1.4. Impression of different routes of IFN induction and IFN signaling and how these can be affected by SARS-CoV proteins. For example, the SARS-CoV proteins ORF3B, ORF6, N and PLP block IFN induction by inhibiting IRF3 activation. In addition, the ORF7a protein and the nsp1 gene product inhibit cellular protein synthesis and promote host cell mRNA degradation, respectively. ORF3b and ORF 6 have been shown to interfere with IFN signaling.

## Adaptive immune response after SARS-CoV infection

Adaptive immune responses will develop shortly after innate immune responses have been triggered. In SARS-CoV infection, relatively little is known about the cells that participate in the early innate immune response. Studies in mice have demonstrated that NK cell-deficient mice clear SARS-CoV efficiently (35). On the other hand, SARS-CoV-specific antibodies, memory B cells as well as memory T cells have been detected in recovered SARS patients (27, 76, 83, 92, 138). Neutralizing antibodies to SARS-CoV are broadly elicited in SARS patients and immune sera of these patients cross-neutralize diverse human SARS-CoV strains (99). Immunization studies in African green monkeys with a chimeric virus containing a parainfluenza-spike protein and studies with spike protein-encoding DNA vaccines in SARS-CoV-challenged mice revealed that the SARS-CoV S protein is the dominant protective antigen (6, 140). In addition, it has been shown that the humoral response alone is sufficient to inhibit viral replication in SARS-CoV mouse model in which mice suffer from mild disease (124, 140). In another study, using a model in which mice were infected with the mouse-adapted SARS-CoV strain MA15, it was demonstrated that B cells alone do not suffice and that T cells are required for protection against SARS-CoV (147). T cell responses play an important role in viral infection, not only destroying virus-infected cells directly, but T cells are also key in activat-

ing other immune cells during infection and establishing memory to a renewed exposure to the same pathogen. It must be noted that the levels of antibodies, memory B cells and memory T cells decrease over time after SARS-CoV infection (126). It is not yet known what causes this decrease and how this might influence protection against a possible second SARS-CoV infection.



## OUTLINE OF THIS THESIS

Currently it is hypothesized that SARS pathology in humans is caused by a disproportional immune response by the host, characterized by excessive induction of a range of inflammatory cytokines. Despite the fact that many studies have been performed to unravel different aspects of SARS-CoV infection *in vitro*, relatively little is still known about the series of events leading up to the immunopathogenic host response *in vivo*, the cell types involved and how various host factors influence the outcome of disease. Pathological changes observed in SARS animal models differ from what is seen in natural human disease and infection with wild type SARS-CoV is rarely lethal in these animals. However, the fact that SARS-CoV causes limited clinical disease in most animal models - despite high viral loads in the lungs - may offer opportunities to unravel the pathogenic pathways that are activated in SARS-CoV infection and to identify the key players involved in the immune response against SARS-CoV. The aim of this thesis is to shed more light on the factors that determine the course of SARS pathogenesis and to identify some of the key host factors involved in this process.

A range of techniques was used to analyze and compare several “classic” parameters of SARS-CoV infection, such as viral replication, immunohistochemistry and histopathology in different models. Additionally, host responses to SARS-CoV infection in these models were analyzed using genomics, giving a broader view of the SARS-CoV mediated induction of antiviral and pathogenic pathways. Combining these techniques, we have studied different host parameters of SARS pathogenesis in several SARS-CoV infection models. We were able to compare the SARS induced host response at sequential time points after infection in different animal species, in young and aged hosts and in various organs.

In summary, viral replication and host gene expression profiles in the lungs of SARS-CoV infected macaques were analyzed during the acute phase of SARS to gain insight into the early events that take place after infection. This analysis revealed activation of a strong antiviral response, including the induction of IFNs, in the lungs of SARS-CoV infected macaques, as well as induction of several inflammatory cytokines (**chapter 2**). Further analysis of the SARS mediated host response was performed by comparing host gene expression in macaque lungs to gene expression in PBMCs from these same macaques. From this analysis we conclude that SARS-CoV does not replicate in PBMCs and that, although a significant host response was detected in these cells, this response is mainly driven by cytokines, like IFN, produced in the lung after infection (**chapter 3**). To study the source of antiviral IFNs produced in the lungs during SARS-CoV infection, experiments in SARS-CoV infected mice and dendritic cells *in vitro* were performed. In addition, pDCs were depleted in SARS-CoV infected BALB/c mice to unravel the host genomic response induced by these cells (**chapter 4**). Next, antiviral pathways induced by cytokines like IFN- $\gamma$  were further analyzed *in vitro* (**chapter 5**). On the other hand, pathogenic host pathways were further characterised in SARS-CoV infected (aged) macaques and ferrets, which show gross pathological changes in the lungs (**chapter 6 and 7**). Since SARS-CoV causes severe disease mainly in elderly people, SARS-CoV infection in young macaques was compared to the response in aged macaques, showing that aged macaques develop significantly more pathology coinciding with increased activation of pathogenic pathways, which both could be reduced by therapeutic treatment with recombinant IFN (**chapter 6**). Theoretically, several

pathogenic pathways may potentially contribute to SARS-CoV pathology, such as induction of proinflammatory cytokines, but also the RAS might be involved. Treatment with a recombinant ACE2 protein, the SARS-CoV cellular receptor, but also an important RAS enzyme, might have a beneficial effect on SARS mediated pathogenesis, which was tested in SARS-CoV infected ferrets. (*chapter 7*). Finally, the findings of this thesis are evaluated in the summarizing discussion (*chapter 8*).

## REFERENCES

1. 2004. Molecular evolution of the SARS coronavirus during the course of the SARS epidemic in China. *Science* **303**:1666-1669.
2. Andrejeva, J., K. S. Childs, D. F. Young, T. S. Carlos, N. Stock, S. Goodbourn, and R. E. Randall. 2004. The V proteins of paramyxoviruses bind the IFN-inducible RNA helicase, mda-5, and inhibit its activation of the IFN-beta promoter. *Proc Natl Acad Sci U S A* **101**:17264-17269.
3. Asefa, B., K. D. Klarmann, N. G. Copeland, D. J. Gilbert, N. A. Jenkins, and J. R. Keller. 2004. The interferon-inducible p200 family of proteins: a perspective on their roles in cell cycle regulation and differentiation. *Blood Cells Mol Dis* **32**:155-167.
4. Banninger, G., and N. C. Reich. 2004. STAT2 nuclear trafficking. *J Biol Chem* **279**:39199-39206.
5. Boehm, M., and E. G. Nabel. 2002. Angiotensin-converting enzyme 2--a new cardiac regulator. *N Engl J Med* **347**:1795-1797.
6. Bukreyev, A., E. W. Lamirande, U. J. Buchholz, L. N. Vogel, W. R. Elkins, M. St Claire, B. R. Murphy, K. Subbarao, and P. L. Collins. 2004. Mucosal immunisation of African green monkeys (*Cercopithecus aethiops*) with an attenuated parainfluenza virus expressing the SARS coronavirus spike protein for the prevention of SARS. *Lancet* **363**:2122-2127.
7. Cameron, M. J., L. Ran, L. Xu, A. Danesh, J. F. Bermejo-Martin, C. M. Cameron, M. P. Muller, W. L. Gold, S. E. Richardson, S. M. Poutanen, B. M. Willey, M. E. DeVries, Y. Fang, C. Seneviratne, S. E. Bosinger, D. Persad, P. Wilkinson, L. D. Greller, R. Somogyi, A. Humar, S. Keshavjee, M. Louie, M. B. Loeb, J. Brunton, A. J. McGeer, S. R. N. Canadian, and D. J. Kelvin. 2007. Interferon-mediated immunopathological events are associated with atypical innate and adaptive immune responses in patients with severe acute respiratory syndrome. *J Virol* **81**:8692-8706.
8. Castilletti, C., L. Bordin, E. Lalle, G. Rozera, F. Poccia, C. Agrati, I. Abbate, and M. R. Capobianchi. 2005. Coordinate induction of IFN-alpha and -gamma by SARS-CoV also in the absence of virus replication. *Virology* **341**:163-169.
9. Cervantes-Barragan, L., R. Züst, F. Weber, M. Spiegel, K. S. Lang, S. Akira, V. Thiel, and B. Ludewig. 2007. Control of coronavirus infection through plasmacytoid dendritic-cell-derived type I interferon. *Blood* **109**:1131-1137.
10. Charo, I. F., and R. M. Ransohoff. 2006. The many roles of chemokines and chemokine receptors in inflammation. *N Engl J Med* **354**:610-621.
11. Chen, I. Y., S. C. Chang, H. Y. Wu, T. C. Yu, W. C. Wei, S. Lin, C. L. Chien, and M. F. Chang. 2010. Upregulation of the chemokine (C-C motif) ligand 2 via a severe acute respiratory syndrome coronavirus spike-ACE2 signaling pathway. *J Virol* **84**:7703-7712.
12. Chen, X., B. Zhou, M. Li, X. Liang, H. Wang, G. Yang, and X. Le. 2004. Serology of severe acute respiratory syndrome: implications for surveillance and outcome. *J Infect Dis* **189**:1158-1163.
13. Cheng, Z. J., H. Vapaatalo, and E. Mervaala. 2005. Angiotensin II and vascular inflammation. *Med Sci Monit* **11**:RA194-205.
14. Cheung, C. Y., L. L. Poon, I. H. Ng, W. Luk, S. F. Sia, M. H. Wu, K. H. Chan, K. Y. Yuen, S. Gordon, Y. Guan, and J. S. Peiris. 2005. Cytokine responses in severe acute respiratory syndrome coronavirus-infected macrophages *in vitro*: possible relevance to pathogenesis. *J Virol* **79**:7819-7826.
15. Chu, C. M., V. C. Cheng, I. F. Hung, M. M. Wong, K. H. Chan, K. S. Chan, R. Y. Kao, L. L. Poon, C. L. Wong, Y. Guan, J. S. Peiris, and K. Y. Yuen. 2004. Role of lopinavir/ritonavir in the treatment of SARS: initial virological and clinical findings. *Thorax* **59**:252-256.16. Chu, W. M., D. Ostertag, Z. W. Li, L. Chang, Y. Chen, Y. Hu, B. Williams, J. Perrault, and M. Karin. 1999. JNK2 and IKKbeta are required for activating the innate response to viral infection. *Immunity* **11**:721-731.
17. Chung, H. Y., B. Sung, K. J. Jung, Y. Zou, and B. P. Yu. 2006. The molecular inflammatory process in aging. *Antioxid Redox Signal* **8**:572-581.
18. Cinatl, J., Jr., G. Hoever, B. Morgenstern, W. Preiser, J. U. Vogel, W. K. Hofmann, G. Bauer, M. Michaelis, H. F. Rabenau, and H. W. Doerr. 2004. Infection of cultured intestinal epithelial cells with severe acute respiratory syndrome coronavirus. *Cell Mol Life Sci* **61**:2100-2112.
19. Clemens, M. J. 2003. Interferons and apoptosis. *J Interferon Cytokine Res* **23**:277-292.
20. Cowling, B. J., M. P. Muller, I. O. Wong, L. M. Ho, M. Louie, A. McGeer, and G. M. Leung. 2007. Alternative methods of estimating an incubation distribution: examples from severe acute respiratory syndrome. *Epidemiology* **18**:253-259.
21. Crackower, M. A., R. Sarao, G. Y. Oudit, C. Yagil, I. Koziarzdzki, S. E. Scanga, A. J. Oliveira-dos-Santos, J. da Costa, L. Zhang, Y. Pei, J. Scholey, C. M. Ferrario, A. S. Manoukian, M. C. Chappell, P. H. Backx, Y. Yagil, and J. M. Penninger. 2002. Angiotensin-converting enzyme 2 is an essential regulator of heart function. *Nature* **417**:822-828.

22. de Jong, M. D., C. P. Simmons, T. T. Thanh, V. M. Hien, G. J. Smith, T. N. Chau, D. M. Hoang, N. V. Chau, T. H. Khanh, V. C. Dong, P. T. Qui, B. V. Cam, Q. Ha do, Y. Guan, J. S. Peiris, N. T. Chinh, T. T. Hien, and J. Farrar. 2006. Fatal outcome of human influenza A (H5N1) is associated with high viral load and hypercytokinemia. *Nat Med* 12:1203-1207.
23. Denison, M. R. 2004. Severe acute respiratory syndrome coronavirus pathogenesis, disease and vaccines: an update. *Pediatr Infect Dis J* 23:S207-214.
24. Donnelly, C. A., A. C. Ghani, G. M. Leung, A. J. Hedley, C. Fraser, S. Riley, L. J. Abu-Raddad, L. M. Ho, T. Q. Thach, P. Chau, K. P. Chan, T. H. Lam, L. Y. Tse, T. Tsang, S. H. Liu, J. H. Kong, E. M. Lau, N. M. Ferguson, and R. M. Anderson. 2003. Epidemiological determinants of spread of causal agent of severe acute respiratory syndrome in Hong Kong. *Lancet* 361:1761-1766.
25. Donoghue, M., F. Hsieh, E. Baronas, K. Godbout, M. Gosselin, N. Stagliano, M. Donovan, B. Woolf, K. Robison, R. Jeyaseelan, R. E. Breitbart, and S. Acton. 2000. A novel angiotensin-converting enzyme-related carboxypeptidase (ACE2) converts angiotensin I to angiotensin 1-9. *Circ Res* 87:E1-9.
26. Drosten, C., S. Gunther, W. Preiser, S. van der Werf, H. R. Brodt, S. Becker, H. Rabenau, M. Panning, L. Kolesnikova, R. A. Fouchier, A. Berger, A. M. Burguiere, J. Cinatl, M. Eickmann, N. Escriou, K. Grywna, S. Kramme, J. C. Manuguerra, S. Muller, V. Rickerts, M. Sturmer, S. Vieth, H. D. Klenk, A. D. Osterhaus, H. Schmitz, and H. W. Doerr. 2003. Identification of a novel coronavirus in patients with severe acute respiratory syndrome. *N Engl J Med* 348:1967-1976.
27. Fan, Y. Y., Z. T. Huang, L. Li, M. H. Wu, T. Yu, R. A. Koup, R. T. Bailer, and C. Y. Wu. 2009. Characterization of SARS-CoV-specific memory T cells from recovered individuals 4 years after infection. *Arch Virol* 154:1093-1099.
28. Ferreira, A. J., R. A. Santos, C. N. Bradford, A. P. Mecca, C. Sumners, M. J. Katovich, and M. K. Raizada. 2010. Therapeutic implications of the vasoprotective axis of the renin-angiotensin system in cardiovascular diseases. *Hypertension* 55:207-213.
29. Fitzgerald-Bocarsly, P., J. Dai, and S. Singh. 2008. Plasmacytoid dendritic cells and type I IFN: 50 years of convergent history. *Cytokine Growth Factor Rev* 19:3-19.
30. Fitzgerald, K. A., S. M. McWhirter, K. L. Faia, D. C. Rowe, E. Latz, D. T. Golenbock, A. J. Coyle, S. M. Liao, and T. Maniatis. 2003. IKKepsilon and TBK1 are essential components of the IRF3 signaling pathway. *Nat Immunol* 4:491-496.
31. Fouchier, R. A., N. G. Hartwig, T. M. Bestebroer, B. Niemeyer, J. C. de Jong, J. H. Simon, and A. D. Osterhaus. 2004. A previously undescribed coronavirus associated with respiratory disease in humans. *Proc Natl Acad Sci U S A* 101:6212-6216.
32. Frieman, M., M. Heise, and R. Baric. 2008. SARS coronavirus and innate immunity. *Virus Res* 133:101-112.
33. Frieman, M., K. Ratia, R. E. Johnston, A. D. Mesecar, and R. S. Baric. 2009. Severe acute respiratory syndrome coronavirus papain-like protease ubiquitin-like domain and catalytic domain regulate antagonism of IRF3 and NF-kappaB signaling. *J Virol* 83:6689-6705.
34. Frieman, M., B. Yount, M. Heise, S. A. Kopecky-Bromberg, P. Palese, and R. S. Baric. 2007. Severe acute respiratory syndrome coronavirus ORF6 antagonizes STAT1 function by sequestering nuclear import factors on the rough endoplasmic reticulum/Golgi membrane. *J Virol* 81:9812-9824.
35. Glass, W. G., K. Subbarao, B. Murphy, and P. M. Murphy. 2004. Mechanisms of Host Defense following Severe Acute Respiratory Syndrome-Coronavirus (SARS-CoV) Pulmonary Infection of Mice. *J Immunol* 173:4030-4039.
36. Gorbalenya, A. E., L. Enjuanes, J. Ziebuhr, and E. J. Snijder. 2006. Nidovirales: evolving the largest RNA virus genome. *Virus Res* 117:17-37.
37. Gorbalenya, A. E., E. J. Snijder, and W. J. Spaan. 2004. Severe acute respiratory syndrome coronavirus phylogeny: toward consensus. *J Virol* 78:7863-7866.
38. Grose, C., and K. Chokephaibulkit. 2004. Avian influenza virus infection of children in Vietnam and Thailand. *Pediatr Infect Dis J* 23:793-794.
39. Guan, Y., B. J. Zheng, Y. Q. He, X. L. Liu, Z. X. Zhuang, C. L. Cheung, S. W. Luo, P. H. Li, L. J. Zhang, Y. J. Guan, K. M. Butt, K. L. Wong, K. W. Chan, W. Lim, K. F. Shortridge, K. Y. Yuen, J. S. Peiris, and L. L. Poon. 2003. Isolation and characterization of viruses related to the SARS coronavirus from animals in southern China. *Science* 302:276-278.
40. Guarner, J., J. A. Jernigan, W. J. Shieh, K. Tatti, L. M. Flannagan, D. S. Stephens, T. Popovic, D. A. Ashford, B. A. Perkins, S. R. Zaki, and G. Inhalational Anthrax Pathology Working. 2003. Pathology and pathogenesis of bioterrorism-related inhalational anthrax. *Am J Pathol* 163:701-709.
41. Haagmans, B. L., T. Kuiken, B. E. Martina, R. A. Fouchier, G. F. Rimmelzwaan, G. van Amerongen, D. van Riel, T. de Jong, S. Itamura, K. H. Chan, M. Tashiro, and A. D. Osterhaus. 2004. Pegylated interferon-alpha protects type 1 pneumocytes

- against SARS coronavirus infection in macaques. *Nat Med* **10**:290-293.
42. Hamming, I., W. Timens, M. L. Bulthuis, A. T. Lely, G. J. Navis, and H. van Goor. 2004. Tissue distribution of ACE2 protein, the functional receptor for SARS coronavirus. A first step in understanding SARS pathogenesis. *J Pathol* **203**:631-637.
  43. Harmer, D., M. Gilbert, R. Borman, and K. L. Clark. 2002. Quantitative mRNA expression profiling of ACE 2, a novel homologue of angiotensin converting enzyme. *FEBS Lett* **532**:107-110.
  44. Hartman, A. L., J. S. Towner, and S. T. Nichol. 2004. A C-terminal basic amino acid motif of Zaire ebolavirus VP35 is essential for type I interferon antagonism and displays high identity with the RNA-binding domain of another interferon antagonist, the NS1 protein of influenza A virus. *Virology* **328**:177-184.
  45. Hertzog, P. J., L. A. O'Neill, and J. A. Hamilton. 2003. The interferon in TLR signaling: more than just antiviral. *Trends Immunol* **24**:534-539.
  46. Hiscott, J. 2007. Triggering the innate antiviral response through IRF-3 activation. *J Biol Chem* **282**:15325-15329.
  47. Hofmann, H., K. Pyrc, L. van der Hoek, M. Geier, B. Berkhout, and S. Pohlmann. 2005. Human coronavirus NL63 employs the severe acute respiratory syndrome coronavirus receptor for cellular entry. *Proc Natl Acad Sci U S A* **102**:7988-7993.
  48. Hon, K. L., C. W. Leung, W. T. Cheng, P. K. Chan, W. C. Chu, Y. W. Kwan, A. M. Li, N. C. Fong, P. C. Ng, M. C. Chiu, C. K. Li, J. S. Tam, and T. F. Fok. 2003. Clinical presentations and outcome of severe acute respiratory syndrome in children. *Lancet* **361**:1701-1703.
  49. Huang, K. J., I. J. Su, M. Theron, Y. C. Wu, S. K. Lai, C. C. Liu, and H. Y. Lei. 2005. An interferon-gamma-related cytokine storm in SARS patients. *J Med Virol* **75**:185-194.
  50. Hung, I. F., V. C. Cheng, A. K. Wu, B. S. Tang, K. H. Chan, C. M. Chu, M. M. Wong, W. T. Hui, L. L. Poon, D. M. Tse, K. S. Chan, P. C. Woo, S. K. Lau, J. S. Peiris, and K. Y. Yuen. 2004. Viral loads in clinical specimens and SARS manifestations. *Emerg Infect Dis* **10**:1550-1557.
  51. Imai, Y., K. Kuba, S. Rao, Y. Huan, F. Guo, B. Guan, P. Yang, R. Sarao, T. Wada, H. Leong-Poi, M. A. Crackower, A. Fukamizu, C. C. Hui, L. Hein, S. Uhlig, A. S. Slutsky, C. Jiang, and J. M. Penninger. 2005. Angiotensin-converting enzyme 2 protects from severe acute lung failure. *Nature* **436**:112-116.
  52. Ito, T., H. Kanzler, O. Duramad, W. Cao, and Y. J. Liu. 2006. Specialization, kinetics, and repertoire of type 1 interferon responses by human plasmacytoid dendritic cells. *Blood* **107**:2423-2431.
  53. Iwasaki, A., and R. Medzhitov. 2004. Toll-like receptor control of the adaptive immune responses. *Nat Immunol* **5**:987-995.
  54. Jeffers, S. A., S. M. Tusell, L. Gillim-Ross, E. M. Hemmila, J. E. Achenbach, G. J. Babcock, W. D. Thomas, Jr., L. B. Thackray, M. D. Young, R. J. Mason, D. M. Ambrosino, D. E. Wentworth, J. C. Demartini, and K. V. Holmes. 2004. CD209L (L-SIGN) is a receptor for severe acute respiratory syndrome coronavirus. *Proc Natl Acad Sci U S A* **101**:15748-15753.
  55. Jerng, J. S., C. J. Yu, H. C. Wang, K. Y. Chen, S. L. Cheng, and P. C. Yang. 2006. Polymorphism of the angiotensin-converting enzyme gene affects the outcome of acute respiratory distress syndrome. *Crit Care Med* **34**:1001-1006.
  56. Jiang, Y., J. Xu, C. Zhou, Z. Wu, S. Zhong, J. Liu, W. Luo, T. Chen, Q. Qin, and P. Deng. 2005. Characterization of cytokine/chemokine profiles of severe acute respiratory syndrome. *Am J Respir Crit Care Med* **171**:850-857.
  57. Jonassen, C. M., T. Kofstad, I. L. Larsen, A. Lovland, K. Handeland, A. Follestad, and A. Lillehaug. 2005. Molecular identification and characterization of novel coronaviruses infecting graylag geese (*Anser anser*), feral pigeons (*Columbia livia*) and mallards (*Anas platyrhynchos*). *J Gen Virol* **86**:1597-1607.
  58. Kamitani, W., K. Narayanan, C. Huang, K. Lokugamage, T. Ikegami, N. Ito, H. Kubo, and S. Makino. 2006. Severe acute respiratory syndrome coronavirus nsp1 protein suppresses host gene expression by promoting host mRNA degradation. *Proc Natl Acad Sci U S A* **103**:12885-12890.
  59. Kash, J. C., E. Muhlberger, V. Carter, M. Grosch, O. Perwitasari, S. C. Proll, M. J. Thomas, F. Weber, H. D. Klenk, and M. G. Katze. 2006. Global suppression of the host antiviral response by Ebola- and Marburgviruses: increased antagonism of the type I interferon response is associated with enhanced virulence. *J Virol* **80**:3009-3020.
  60. Kato, H., O. Takeuchi, S. Sato, M. Yoneyama, M. Yamamoto, K. Matsui, S. Uematsu, A. Jung, T. Kawai, K. J. Ishii, O. Yamaguchi, K. Otsu, T. Tsujimura, C. S. Koh, C. Reis e Sousa, Y. Matsuura, T. Fujita, and S. Akira. 2006. Differential roles of MDA5 and RIG-I helicases in the recognition of RNA viruses. *Nature* **441**:101-105.
  61. Kerkmann, M., S. Rothenfusser, V. Hornung, A. Towarowski, M. Wagner, A. Sarris, T. Giese, S. Endres, and G. Hartmann. 2003. Activation with CpG-A and CpG-B oligonucleotides reveals two distinct regulatory pathways of type I IFN synthesis in human plasmacytoid dendritic cells. *J Immunol* **170**:4465-4474.

62. Koepcke-Bromberg, S. A., L. Martinez-Sobrido, M. Frieman, R. A. Baric, and P. Palese. 2007. Severe acute respiratory syndrome coronavirus open reading frame (ORF) 3b, ORF 6, and nucleocapsid proteins function as interferon antagonists. *J Virol* **81**:548-557.
63. Koepcke-Bromberg, S. A., L. Martinez-Sobrido, and P. Palese. 2006. 7a protein of severe acute respiratory syndrome coronavirus inhibits cellular protein synthesis and activates p38 mitogen-activated protein kinase. *J Virol* **80**:785-793.
64. Ksiazek, T. G., D. Erdman, C. S. Goldsmith, S. R. Zaki, T. Peret, S. Emery, S. Tong, C. Urbani, J. A. Comer, W. Lim, P. E. Rollin, S. F. Dowell, A. E. Ling, C. D. Humphrey, W. J. Shieh, J. Guarner, C. D. Paddock, P. Rota, B. Fields, J. DeRisi, J. Y. Yang, N. Cox, J. M. Hughes, J. W. LeDuc, W. J. Bellini, and L. J. Anderson. 2003. A novel coronavirus associated with severe acute respiratory syndrome. *N Engl J Med* **348**:1953-1966.
65. Kuba, K., Y. Imai, S. Rao, H. Gao, F. Guo, B. Guan, Y. Huan, P. Yang, Y. Zhang, W. Deng, L. Bao, B. Zhang, G. Liu, Z. Wang, M. Chappell, Y. Liu, D. Zheng, A. Leibbrandt, T. Wada, A. S. Slutsky, D. Liu, C. Qin, C. Jiang, and J. M. Penninger. 2005. A crucial role of angiotensin converting enzyme 2 (ACE2) in SARS coronavirus-induced lung injury. *Nat Med* **11**:875-879.
66. Kuiken, T., R. A. Fouchier, M. Schutten, G. F. Rimmelzwaan, G. van Amerongen, D. van Riel, J. D. Laman, T. de Jong, G. van Doornum, W. Lim, A. E. Ling, P. K. Chan, J. S. Tam, M. C. Zambon, R. Gopal, C. Drosten, S. van der Werf, N. Escriu, J. C. Manuerra, K. Stohr, J. S. Peiris, and A. D. Osterhaus. 2003. Newly discovered coronavirus as the primary cause of severe acute respiratory syndrome. *Lancet* **362**:263-270.
67. Kumagai, Y., O. Takeuchi, H. Kato, H. Kumar, K. Matsui, E. Morii, K. Aozasa, T. Kawai, and S. Akira. 2007. Alveolar macrophages are the primary interferon-alpha producer in pulmonary infection with RNA viruses. *Immunity* **27**:240-252.
68. Lai, M. M. 1990. Coronavirus: organization, replication and expression of genome. *Annu Rev Microbiol* **44**:303-333.
69. Lai, M. M., and D. Cavanagh. 1997. The molecular biology of coronaviruses. *Adv Virus Res* **48**:1-100.
70. Larson, H. E., S. E. Reed, and D. A. Tyrrell. 1980. Isolation of rhinoviruses and coronaviruses from 38 colds in adults. *J Med Virol* **5**:221-229.
71. Lau, S. K., P. C. Woo, K. S. Li, Y. Huang, H. W. Tsoi, B. H. Wong, S. S. Wong, S. Y. Leung, K. H. Chan, and K. Y. Yuen. 2005. Severe acute respiratory syndrome coronavirus-like virus in Chinese horseshoe bats. *Proc Natl Acad Sci U S A* **102**:14040-14045.
72. Law, H. K., C. Y. Cheung, H. Y. Ng, S. F. Sia, Y. O. Chan, W. Luk, J. M. Nicholls, J. S. Peiris, and Y. L. Lau. 2005. Chemokine upregulation in SARS-coronavirus-infected, monocyte-derived human dendritic cells. *Blood* **106**:2366-2374.
73. Le Bon, A., N. Etchart, C. Rossmann, M. Ashton, S. Hou, D. Gewert, P. Borrow, and D. F. Tough. 2003. Cross-priming of CD8+ T cells stimulated by virus-induced type I interferon. *Nat Immunol* **4**:1009-1015.
74. Le Bon, A., and D. F. Tough. 2002. Links between innate and adaptive immunity via type I interferon. *Curr Opin Immunol* **14**:432-436.
75. Leung, C. W., and W. K. Chiu. 2004. Clinical picture, diagnosis, treatment and outcome of severe acute respiratory syndrome (SARS) in children. *Paediatr Respir Rev* **5**:275-288.
76. Li, C. K., H. Wu, H. Yan, S. Ma, L. Wang, M. Zhang, X. Tang, N. J. Temperton, R. A. Weiss, J. M. Brenchley, D. C. Douek, J. Mongkolsapaya, B. H. Tran, C. L. Lin, G. R. Screaton, J. L. Hou, A. J. McMichael, and X. N. Xu. 2008. T cell responses to whole SARS coronavirus in humans. *J Immunol* **181**:5490-5500.
77. Li, W., M. J. Moore, N. Vasilieva, J. Sui, S. K. Wong, M. A. Berne, M. Somasundaran, J. L. Sullivan, K. Luzuriaga, T. C. Greenough, H. Choe, and M. Farzan. 2003. Angiotensin-converting enzyme 2 is a functional receptor for the SARS coronavirus. *Nature* **426**:450-454.
78. Li, W., Z. Shi, M. Yu, W. Ren, C. Smith, J. H. Epstein, H. Wang, G. Crameri, Z. Hu, H. Zhang, J. Zhang, J. McEachern, H. Field, P. Daszak, B. T. Eaton, S. Zhang, and L. F. Wang. 2005. Bats are natural reservoirs of SARS-like coronaviruses. *Science* **310**:676-679.
79. Li, W., J. Sui, I. C. Huang, J. H. Kuhn, S. R. Radoshitzky, W. A. Marasco, H. Choe, and M. Farzan. 2007. The S proteins of human coronavirus NL63 and severe acute respiratory syndrome coronavirus bind overlapping regions of ACE2. *Virology* **367**:367-374.
80. Li, W., C. Zhang, J. Sui, J. H. Kuhn, M. J. Moore, S. Luo, S. K. Wong, I. C. Huang, K. Xu, N. Vasilieva, A. Murakami, Y. He, W. A. Marasco, Y. Guan, H. Choe, and M. Farzan. 2005. Receptor and viral determinants of SARS-coronavirus adaptation to human ACE2. *Embo J*.
81. Liang, W., Z. Zhu, J. Guo, Z. Liu, W. Zhou, D. P. Chin, and A. Schuchat. 2004. Severe acute respiratory syndrome, Beijing, 2003. *Emerg Infect Dis* **10**:25-31.

82. Liu, S., G. Xiao, Y. Chen, Y. He, J. Niu, C. R. Escalante, H. Xiong, J. Farmer, A. K. Debnath, P. Tien, and S. Jiang. 2004. Interaction between heptad repeat 1 and 2 regions in spike protein of SARS-associated coronavirus: implications for virus fusogenic mechanism and identification of fusion inhibitors. *Lancet* **363**:938-947.
83. Liu, W., A. Fontanet, P. H. Zhang, L. Zhan, Z. T. Xin, L. Baril, F. Tang, H. Lv, and W. C. Cao. 2006. Two-year prospective study of the humoral immune response of patients with severe acute respiratory syndrome. *J Infect Dis* **193**:792-795.
84. Loutfy, M. R., L. M. Blatt, K. A. Siminovitch, S. Ward, B. Wolff, H. Lho, D. H. Pham, H. Deif, E. A. LaMere, M. Chang, K. C. Kain, G. A. Farcas, P. Ferguson, M. Latchford, G. Levy, J. W. Dennis, E. K. Laj, and E. N. Fish. 2003. Interferon alfacon-1 plus corticosteroids in severe acute respiratory syndrome: a preliminary study. *JAMA* **290**:3222-3228.
85. Maher, S. G., A. L. Romero-Weaver, A. J. Scarzello, and A. M. Gamero. 2007. Interferon: cellular executioner or white knight? *Curr Med Chem* **14**:1279-1289.
86. Marie, I., J. E. Durbin, and D. E. Levy. 1998. Differential viral induction of distinct interferon-alpha genes by positive feedback through interferon regulatory factor-7. *Embo J* **17**:6660-6669.
87. Marra, M. A., S. J. Jones, C. R. Astell, R. A. Holt, A. Brooks-Wilson, Y. S. Butterfield, J. Khattri, J. K. Asano, S. A. Barber, S. Y. Chan, A. Cloutier, S. M. Coughlin, D. Freeman, N. Girn, O. L. Griffith, S. R. Leach, M. Mayo, H. McDonald, S. B. Montgomery, P. K. Pandoh, A. S. Petrescu, A. G. Robertson, J. E. Schein, A. Siddiqui, D. E. Smailus, J. M. Stott, G. S. Yang, F. Plummer, A. Andonov, H. Artsob, N. Bastien, K. Bernard, T. F. Booth, D. Bowness, M. Czub, M. Drebot, L. Fernando, R. Flick, M. Garbutt, M. Gray, A. Grolla, S. Jones, H. Feldmann, A. Meyers, A. Kabani, Y. Li, S. Normand, U. Stroher, G. A. Tipples, S. Tyler, R. Vogrig, D. Ward, B. Watson, R. C. Brunham, M. Kraiden, M. Petric, D. M. Skowronski, C. Upton, and R. L. Roper. 2003. The Genome sequence of the SARS-associated coronavirus. *Science* **300**:1399-1404.
88. Marshall, R. P., R. J. McAnulty, and G. J. Laurent. 2000. Angiotensin II is mitogenic for human lung fibroblasts via activation of the type 1 receptor. *Am J Respir Crit Care Med* **161**:1999-2004.
89. Martina, B. E., B. L. Haagmans, T. Kuiken, R. A. Fouchier, G. F. Rimmelzwaan, G. Van Amerongen, J. S. Peiris, W. Lim, and A. D. Osterhaus. 2003. Virology: SARS virus infection of cats and ferrets. *Nature* **425**:915.
90. Marzi, A., T. Gramberg, G. Simmons, P. Moller, A. J. Rennekamp, M. Krumbiegel, M. Geier, J. Eisemann, N. Turza, B. Saunier, A. Steinkasserer, S. Becker, P. Bates, H. Hofmann, and S. Pohlmann. 2004. DC-SIGN and DC-SIGNR interact with the glycoprotein of Marburg virus and the S protein of severe acute respiratory syndrome coronavirus. *J Virol* **78**:12090-12095.
91. Masters, P. S. 2006. The molecular biology of coronaviruses. *Adv Virus Res* **66**:193-292.
92. Mo, H., G. Zeng, X. Ren, H. Li, C. Ke, Y. Tan, C. Cai, K. Lai, R. Chen, M. Chan-Yeung, and N. Zhong. 2006. Longitudinal profile of antibodies against SARS-coronavirus in SARS patients and their clinical significance. *Respirology* **11**:49-53.
93. Monceyron Jonassen, C. 2006. SARS/avian coronaviruses. *Dev Biol (Basel)* **126**:161-169; discussion 326-167.
94. Murray, P. J. 2007. The JAK-STAT signaling pathway: input and output integration. *J Immunol* **178**:2623-2629.
95. Myint, S., S. Johnston, G. Sanderson, and H. Simpson. 1994. Evaluation of nested polymerase chain methods for the detection of human coronaviruses 229E and OC43. *Mol Cell Probes* **8**:357-364.
96. Neville, L. F., G. Mathiak, and O. Bagasra. 1997. The immunobiology of interferon-gamma inducible protein 10 kD (IP-10): a novel, pleiotropic member of the C-X-C chemokine superfamily. *Cytokine Growth Factor Rev* **8**:207-219.
97. Ng, L. F., M. L. Hibberd, E. E. Ooi, K. F. Tang, S. Y. Neo, J. Tan, K. R. Murthy, V. B. Vega, J. M. Chia, E. T. Liu, and E. C. Ren. 2004. A human *in vitro* model system for investigating genome-wide host responses to SARS coronavirus infection. *BMC Infect Dis* **4**:34.
98. Nicholls, J. M., L. L. Poon, K. C. Lee, W. F. Ng, S. T. Lai, C. Y. Leung, C. M. Chu, P. K. Hui, K. L. Mak, W. Lim, K. W. Yan, K. H. Chan, N. C. Tsang, Y. Guan, K. Y. Yuen, and J. S. Peiris. 2003. Lung pathology of fatal severe acute respiratory syndrome. *Lancet* **361**:1773-1778.
99. Nie, Y., G. Wang, X. Shi, H. Zhang, Y. Qiu, Z. He, W. Wang, G. Lian, X. Yin, L. Du, L. Ren, J. Wang, X. He, T. Li, H. Deng, and M. Ding. 2004. Neutralizing antibodies in patients with severe acute respiratory syndrome-associated coronavirus infection. *J Infect Dis* **190**:1119-1126.
100. Onoguchi, K., M. Yoneyama, A. Takemura, S. Akira, T. Taniguchi, H. Namiki, and T. Fujita. 2007. Viral infections activate types I and III interferon genes through a common mechanism. *J Biol Chem* **282**:7576-7581.
101. Paladino, P., D. T. Cummings, R. S. Noyce, and K. L. Mossman. 2006. The IFN-independent response to virus particle entry provides a first line of antiviral defense that is independent of TLRs and retinoic acid-inducible gene I. *J Immunol* **177**:8008-8016.

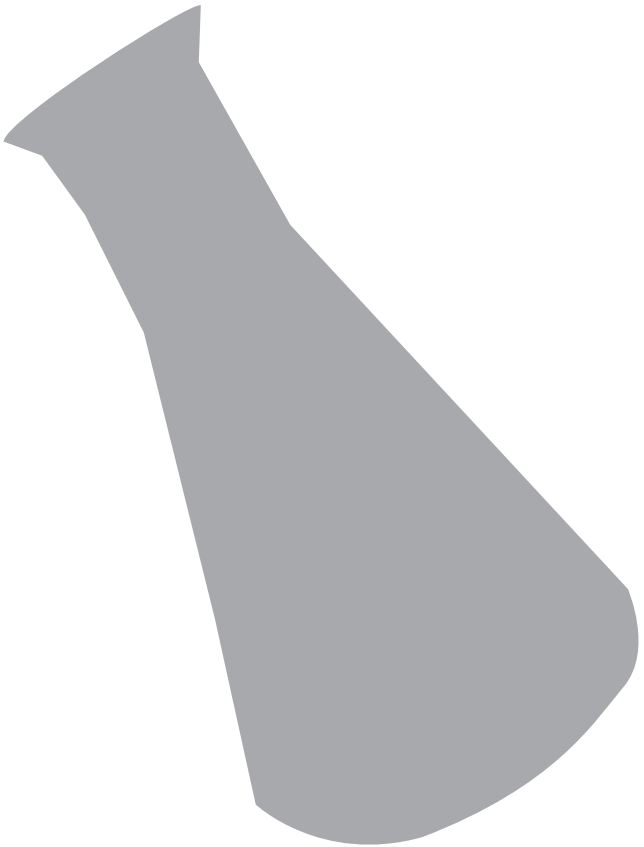
102. Peiris, J. S., C. M. Chu, V. C. Cheng, K. S. Chan, I. F. Hung, L. L. Poon, K. I. Law, B. S. Tang, T. Y. Hon, C. S. Chan, K. H. Chan, J. S. Ng, B. J. Zheng, W. L. Ng, R. W. Lai, Y. Guan, and K. Y. Yuen. 2003. Clinical progression and viral load in a community outbreak of coronavirus-associated SARS pneumonia: a prospective study. *Lancet* **361**:1767-1772.
103. Peiris, J. S., S. T. Lai, L. L. Poon, Y. Guan, L. Y. Yam, W. Lim, J. Nicholls, W. K. Yee, W. W. Yan, M. T. Cheung, V. C. Cheng, K. H. Chan, D. N. Tsang, R. W. Yung, T. K. Ng, and K. Y. Yuen. 2003. Coronavirus as a possible cause of severe acute respiratory syndrome. *Lancet* **361**:1319-1325.
104. Poon, L. L., D. K. Chu, K. H. Chan, O. K. Wong, T. M. Ellis, Y. H. Leung, S. K. Lau, P. C. Woo, K. Y. Suen, K. Y. Yuen, Y. Guan, and J. S. Peiris. 2005. Identification of a novel coronavirus in bats. *J Virol* **79**:2001-2009.
105. Prakash, A., E. Smith, C. K. Lee, and D. E. Levy. 2005. Tissue-specific positive feedback requirements for production of type I interferon following virus infection. *J Biol Chem* **280**:18651-18657.
106. Provacia, L. B., S. L. Smits, B. E. Martina, V. S. Raj, P. V. Doel, G. V. Amerongen, H. Moorman-Roest, A. D. Osterhaus, and B. L. Haagmans. 2011. Enteric coronavirus in ferrets, the Netherlands. *Emerg Infect Dis* **17**:1570-1571.
107. Randall, R. E., and S. Goodbourn. 2008. Interferons and viruses: an interplay between induction, signalling, antiviral responses and virus countermeasures. *J Gen Virol* **89**:1-47.
108. Reghunathan, R., M. Jayapal, L. Y. Hsu, H. H. Chng, D. Tai, B. P. Leung, and A. J. Melendez. 2005. Expression profile of immune response genes in patients with Severe Acute Respiratory Syndrome. *BMC Immunol* **6**:2.
109. Reich, N. C., and L. Liu. 2006. Tracking STAT nuclear traffic. *Nat Rev Immunol* **6**:602-612.
110. Rink, L., I. Cakman, and H. Kirchner. 1998. Altered cytokine production in the elderly. *Mech Ageing Dev* **102**:199-209.
111. Rose, C. E., Jr., S. S. Sung, and S. M. Fu. 2003. Significant involvement of CCL2 (MCP-1) in inflammatory disorders of the lung. *Microcirculation* **10**:273-288.
112. Sato, M., H. Suemori, N. Hata, M. Asagiri, K. Ogasawara, K. Nakao, T. Nakaya, M. Katsuki, S. Noguchi, N. Tanaka, and T. Taniguchi. 2000. Distinct and essential roles of transcription factors IRF-3 and IRF-7 in response to viruses for IFN-alpha/beta gene induction. *Immunity* **13**:539-548.
113. Sauty, A., M. Dziejman, R. A. Taha, A. S. Iarossi, K. Neote, E. A. Garcia-Zepeda, Q. Hamid, and A. D. Luster. 1999. The T cell-specific CXC chemokines IP-10, Mig, and I-TAC are expressed by activated human bronchial epithelial cells. *J Immunol* **162**:3549-3558.
114. Sharma, S., B. R. tenOever, N. Grandvaux, G. P. Zhou, R. Lin, and J. Hiscott. 2003. Triggering the interferon antiviral response through an IKK-related pathway. *Science* **300**:1148-1151.
115. Siegal, F. P., N. Kadowaki, M. Shodell, P. A. Fitzgerald-Bocarsly, K. Shah, S. Ho, S. Antonenko, and Y. J. Liu. 1999. The nature of the principal type 1 interferon-producing cells in human blood. *Science* **284**:1835-1837.
116. Smith, M. K., S. Tusell, E. A. Travanty, B. Berkhout, L. van der Hoek, and K. V. Holmes. 2006. Human angiotensin-converting enzyme 2 (ACE2) is a receptor for human respiratory coronavirus NL63. *Adv Exp Med Biol* **581**:285-288.
117. Smits, S. L., A. de Lang, J. M. van den Brand, L. M. Leijten, I. W. F. van, M. J. Eijkemans, G. van Amerongen, T. Kuiken, A. C. Andeweg, A. D. Osterhaus, and B. L. Haagmans. 2010. Exacerbated innate host response to SARS-CoV in aged non-human primates. *PLoS Pathog* **6**:e1000756.
118. Snijder, E. J., Y. van der Meer, J. Zevenhoven-Dobbe, J. J. Onderwater, J. van der Meulen, H. K. Koerten, and A. M. Mommaas. 2006. Ultrastructure and origin of membrane vesicles associated with the severe acute respiratory syndrome coronavirus replication complex. *J Virol* **80**:5927-5940.
119. Spiegel, M., A. Pichlmair, L. Martinez-Sobrido, J. Cros, A. Garcia-Sastre, O. Haller, and F. Weber. 2005. Inhibition of Beta interferon induction by severe acute respiratory syndrome coronavirus suggests a two-step model for activation of interferon regulatory factor 3. *J Virol* **79**:2079-2086.
120. Spiegel, M., K. Schneider, F. Weber, M. Weidmann, and F. T. Hufert. 2006. Interaction of severe acute respiratory syndrome-associated coronavirus with dendritic cells. *J Gen Virol* **87**:1953-1960.
121. Spiegel, M., and F. Weber. 2006. Inhibition of cytokine gene expression and induction of chemokine genes in non-lymphatic cells infected with SARS coronavirus. *Virol J* **3**:17.
122. Stavrinos, J., and D. S. Guttman. 2004. Mosaic evolution of the severe acute respiratory syndrome coronavirus. *J Virol* **78**:76-82.



123. Stertz, S., M. Reichelt, M. Spiegel, T. Kuri, L. Martinez-Sobrido, A. Garcia-Sastre, F. Weber, and G. Kochs. 2007. The intracellular sites of early replication and budding of SARS-coronavirus. *Virology* **361**:304-315.
124. Subbarao, K., J. McAuliffe, L. Vogel, G. Fahle, S. Fischer, K. Tatti, M. Packard, W. J. Shieh, S. Zaki, and B. Murphy. 2004. Prior infection and passive transfer of neutralizing antibody prevent replication of severe acute respiratory syndrome coronavirus in the respiratory tract of mice. *J Virol* **78**:3572-3577.
125. Tang, B. S., K. H. Chan, V. C. Cheng, P. C. Woo, S. K. Lau, C. C. Lam, T. L. Chan, A. K. Wu, I. F. Hung, S. Y. Leung, and K. Y. Yuen. 2005. Comparative host gene transcription by microarray analysis early after infection of the Huh7 cell line by severe acute respiratory syndrome coronavirus and human coronavirus 229E. *J Virol* **79**:6180-6193.
126. Tang, F., Y. Quan, Z. T. Xin, J. Wrarmert, M. J. Ma, H. Lv, T. B. Wang, H. Yang, J. H. Richardus, W. Liu, and W. C. Cao. 2011. Lack of peripheral memory B cell responses in recovered patients with severe acute respiratory syndrome: a six-year follow-up study. *J Immunol* **186**:7264-7268.
127. Tang, N. L., P. K. Chan, C. K. Wong, K. F. To, A. K. Wu, Y. M. Sung, D. S. Hui, J. J. Sung, and C. W. Lam. 2005. Early enhanced expression of interferon-inducible protein-10 (CXCL-10) and other chemokines predicts adverse outcome in severe acute respiratory syndrome. *Clin Chem* **51**:2333-2340.
128. Theron, M., K. J. Huang, Y. W. Chen, C. C. Liu, and H. Y. Lei. 2005. A probable role for IFN-gamma in the development of a lung immunopathology in SARS. *Cytokine* **32**:30-38.
129. Tipnis, S. R., N. M. Hooper, R. Hyde, E. Karran, G. Christie, and A. J. Turner. 2000. A human homolog of angiotensin-converting enzyme. Cloning and functional expression as a captopril-insensitive carboxypeptidase. *J Biol Chem* **275**:33238-33243.
130. Tseng, C. T., L. A. Perrone, H. Zhu, S. Makino, and C. J. Peters. 2005. Severe acute respiratory syndrome and the innate immune responses: modulation of effector cell function without productive infection. *J Immunol* **174**:7977-7985.
131. van der Hoek, L., K. Pyrc, M. F. Jebbink, W. Vermeulen-Oost, R. J. Berkhout, K. C. Wolthers, P. M. Wertheim-van Dillen, J. Kaandorp, J. Spaargaren, and B. Berkhout. 2004. Identification of a new human coronavirus. *Nat Med* **10**:368-373.
132. Versteeg, G. A., P. J. Bredenbeek, S. H. van den Worm, and W. J. Spaan. 2007. Group 2 coronaviruses prevent immediate early interferon induction by protection of viral RNA from host cell recognition. *Virology* **361**:18-26.
133. Ware, L. B., and M. A. Matthay. 2000. The acute respiratory distress syndrome. *N Engl J Med* **342**:1334-1349.
134. Weber, F., V. Wagner, S. B. Rasmussen, R. Hartmann, and S. R. Paludan. 2006. Double-stranded RNA is produced by positive-strand RNA viruses and DNA viruses but not in detectable amounts by negative-strand RNA viruses. *J Virol* **80**:5059-5064.
135. Wong, C. K., C. W. Lam, A. K. Wu, W. K. Ip, N. L. Lee, I. H. Chan, L. C. Lit, D. S. Hui, M. H. Chan, S. S. Chung, and J. J. Sung. 2004. Plasma inflammatory cytokines and chemokines in severe acute respiratory syndrome. *Clin Exp Immunol* **136**:95-103.
136. Woo, P. C., S. K. Lau, C. M. Chu, K. H. Chan, H. W. Tsoi, Y. Huang, B. H. Wong, R. W. Poon, J. J. Cai, W. K. Luk, L. L. Poon, S. S. Wong, Y. Guan, J. S. Peiris, and K. Y. Yuen. 2005. Characterization and complete genome sequence of a novel coronavirus, coronavirus HKU1, from patients with pneumonia. *J Virol* **79**:884-895.
137. Xu, P., S. Sriramula, and E. Lazartigues. 2011. ACE2/ANG-(1-7)/Mas pathway in the brain: the axis of good. *Am J Physiol Regul Integr Comp Physiol* **300**:R804-817.
138. Yang, L. T., H. Peng, Z. L. Zhu, G. Li, Z. T. Huang, Z. X. Zhao, R. A. Koup, R. T. Bailer, and C. Y. Wu. 2006. Long-lived effector/central memory T-cell responses to severe acute respiratory syndrome coronavirus (SARS-CoV) S antigen in recovered SARS patients. *Clin Immunol* **120**:171-178.
139. Yang, Z. Y., Y. Huang, L. Ganesh, K. Leung, W. P. Kong, O. Schwartz, K. Subbarao, and G. J. Nabel. 2004. pH-dependent entry of severe acute respiratory syndrome coronavirus is mediated by the spike glycoprotein and enhanced by dendritic cell transfer through DC-SIGN. *J Virol* **78**:5642-5650.
140. Yang, Z. Y., W. P. Kong, Y. Huang, A. Roberts, B. R. Murphy, K. Subbarao, and G. J. Nabel. 2004. A DNA vaccine induces SARS coronavirus neutralization and protective immunity in mice. *Nature* **428**:561-564.
141. Yen, Y. T., F. Liao, C. H. Hsiao, C. L. Kao, Y. C. Chen, and B. A. Wu-Hsieh. 2006. Modeling the early events of severe acute respiratory syndrome coronavirus infection *in vitro*. *J Virol* **80**:2684-2693.
142. Yoneyama, M., M. Kikuchi, K. Matsumoto, T. Imaizumi, M. Miyagishi, K. Taira, E. Foy, Y. M. Loo, M. Gale, Jr., S. Akira, S. Yonehara, A. Kato, and T. Fujita. 2005. Shared and unique functions of the DExD/H-box helicases RIG-I, MDA5, and LGP2 in antiviral innate immunity. *J Immunol* **175**:2851-2858.

143. Yoneyama, M., M. Kikuchi, T. Natsukawa, N. Shinobu, T. Imaizumi, M. Miyagishi, K. Taira, S. Akira, and T. Fujita. 2004. The RNA helicase RIG-I has an essential function in double-stranded RNA-induced innate antiviral responses. *Nat Immunol* 5:730-737.
144. Yoshikawa, T., T. E. Hill, N. Yoshikawa, V. L. Popov, C. L. Galindo, H. R. Garner, C. J. Peters, and C. T. Tseng. 2010. Dynamic innate immune responses of human bronchial epithelial cells to severe acute respiratory syndrome-associated coronavirus infection. *PLoS One* 5:e8729.
145. Zhang, X. W., Y. L. Yap, and A. Danchin. 2005. Testing the hypothesis of a recombinant origin of the SARS-associated coronavirus. *Arch Virol* 150:1-20.
146. Zhang, Y., J. Li, Y. Zhan, L. Wu, X. Yu, W. Zhang, L. Ye, S. Xu, R. Sun, Y. Wang, and J. Lou. 2004. Analysis of serum cytokines in patients with severe acute respiratory syndrome. *Infect Immun* 72:4410-4415.
147. Zhao, J., and S. Perlman. 2010. T cell responses are required for protection from clinical disease and for virus clearance in severe acute respiratory syndrome coronavirus-infected mice. *J Virol* 84:9318-9325.
148. Zhou, H., and S. Perlman. 2007. Mouse hepatitis virus does not induce Beta interferon synthesis and does not inhibit its induction by double-stranded RNA. *J Virol* 81:568-574.
149. Ziegler, T., S. Matikainen, E. Ronkko, P. Osterlund, M. Sillanpaa, J. Siren, R. Fagerlund, M. Immonen, K. Melen, and I. Julkunen. 2005. Severe acute respiratory syndrome coronavirus fails to activate cytokine-mediated innate immune responses in cultured human monocyte-derived dendritic cells. *J Virol* 79:13800-13805.
150. Züst, R., L. Cervantes-Barragan, M. Habjan, R. Maier, B. W. Neuman, J. Ziebuhr, K. J. Szretter, S. C. Baker, W. Barchet, M. S. Diamond, S. G. Siddell, B. Ludewig, and V. Thiel. 2011. Ribose 2'-O-methylation provides a molecular signature for the distinction of self and non-self mRNA dependent on the RNA sensor Mda5. *Nat Immunol* 12:137-143.





## Chapter 2

Functional genomics highlights differential induction of antiviral pathways in the lungs of SARS-CoV infected macaques

CHAPTER 2

# Functional genomics highlights differential induction of antiviral pathways in the lungs of SARS-CoV infected macaques

Based on:

Anna de Lang\*, Tracey Baas\*, Thomas Teal, Lonneke M. Leijten, Brandon Rain, Albert D.M.E. Osterhaus, Bart L. Haagmans and Michael G. Katze

\*These authors contributed equally

*PLoS Pathogens*, 2007; 10;3(8):e1112

## Chapter 2

Functional genomics highlights differential induction of antiviral pathways in the lungs of SARS-CoV infected macaques

## ABSTRACT

The pathogenesis of severe acute respiratory syndrome coronavirus (SARS-CoV) is likely mediated by disproportional immune responses and the ability of the virus to circumvent innate immunity. Using functional genomics, we analyzed early host responses to SARS-CoV infection in the lungs of adolescent cynomolgus macaques (*Macaca fascicularis*) that show lung pathology similar to that observed in human adults with SARS. Analysis of gene signatures revealed induction of a strong innate immune response characterized by the stimulation of various cytokine and chemokine genes, including interleukin (IL)-6, IL-8 and IP-10, which corresponds to the host response seen in acute respiratory distress syndrome (ARDS). As opposed to many *in vitro* experiments, SARS-CoV induced a wide range of type I interferons (IFN) and nuclear translocation of phosphorylated signal transducer and activator of transcription (STAT)<sub>1</sub> in the lungs of macaques. Using immunohistochemistry we revealed that these antiviral signaling pathways were differentially regulated in distinctive subsets of cells. Our studies emphasize that the induction of early IFN signaling may be critical to confer protection against SARS-CoV infection and highlight the strength of combining functional genomics with immunohistochemistry to further unravel the pathogenesis of SARS.

## INTRODUCTION

Infection with SARS-CoV causes lower respiratory tract disease with clinical symptoms that include fever, malaise, and lymphopenia (36). Approximately 20–30% of SARS patients required management in intensive care units, and the overall fatality rate approached 10%. Interestingly, children seemed to be relatively resistant to SARS, but the reason for this restriction is not known (10, 16, 27). The clinical course of SARS follows three phases (37–38). In the first phase, there is active viral replication and patients experience systemic symptoms. In the second phase, virus levels start to decrease while antibodies, which are effective in controlling infection, increase. However, pneumonia and immunopathological injury also develop in this phase. Ultimately, in the third phase, fatal cases of SARS progress to severe pneumonia and ARDS, characterized by the presence of diffuse alveolar damage (DAD) (25, 36). It has been hypothesized that the pathological changes are caused by a disproportional immune response, illustrated by elevated levels of inflammatory cytokines and chemokines, such as CXCL10 (IP-10), CCL2 (MCP-1), IL-6, IL-8, IL-12, IL-1 $\beta$  and IFN- $\gamma$  (17–18, 39, 50, 53, 55). These *in vivo* data have been confirmed with *in vitro* experiments, demonstrating that SARS-CoV infection induces a range of cytokines and chemokines in diverse cell types (5, 26, 35, 46, 48, 54).

In contrast, production of type I IFNs seems to be inhibited or delayed by SARS-CoV *in vitro* (5, 26, 35, 44–46, 48, 58). Moreover, no IFN- $\alpha$  or IFN- $\beta$  has been detected in the sera of SARS patients or in lungs of SARS-CoV infected mice (13, 32, 51). Recent *in vitro* studies demonstrated that type I IFN inhibition or delay may be orchestrated by SARS-CoV proteins ORF 3B, ORF 6 and N (23). The inhibition of IFN production would benefit SARS-CoV replication, since pre-treatment of cells with IFN before SARS-CoV infection efficiently prevents replication in these cells (7, 33, 40, 44, 57). Furthermore, prophylactic treatment of macaques with pegylated-IFN- $\alpha$  reduces SARS-CoV replication in the lungs (14).

Although IFN production was absent in clinical samples, gene and protein expression profiles in these patients were likely impacted by clinical treatments and concurrent pre-existing disease. In addition, most if not all virus-host response information is from clinical blood/sera samples that were taken relatively late during infection—little is known about what happens early during infection. Animal studies are of great value to decipher the host's initial innate immune response, without confounding clinical treatment (steroid and mechanical ventilation) or underlying co-morbidity. In order to elucidate early host responses during the acute phase of SARS-CoV infection, we infected cynomolgus macaques with SARS-CoV and used macaque-specific microarrays and RT-PCR techniques to study host gene expression profiles. Adolescent cynomolgus macaques infected with SARS-CoV develop DAD similar to SARS patients, but clear most of the virus in the lungs by day 6 (25). Because SARS-CoV replicates predominantly in the lower respiratory tract of macaques, the virus infects a range of cells, including type I and type II pneumocytes, that are different from those analyzed *in vitro*. The ability to simultaneously examine virus replication and host-response gene expression profiles in the lungs of these animals during the acute phase of SARS offers the opportunity to further unravel the pathogenesis of SARS.



## MATERIALS AND METHODS

### SARS-CoV infection

Six cynomolgus macaques (*Macaca fascicularis*) were infected intratracheally with  $1 \times 10^6$  TCID<sub>50</sub> SARS-CoV (HKU-39849) as described earlier (14). Virus stocks were generated in Vero E6 cells, defective in IFN production. Two animals were euthanized on day 1 after infection and four animals were euthanized on day 4. In addition, four animals were mock (PBS) infected and euthanized on day 4, serving as a negative control group. One lung from each monkey was fixed in 10% formalin for histopathology and immunohistochemistry while the other was used for real-time PCR and microarrays. Lung samples were randomly excised from three different lung areas (cranial, medial, caudal) and stored in RNeasy Lysis Buffer (Qiagen). Sixteen pieces of lung were taken from the SARS-CoV infected animals, 2-3 pieces of lung per animal. Twelve pieces of lung were taken from the mock-infected animals, 3 pieces of lung per animal. Individual lung samples in RNeasy Lysis Buffer were transferred to TRIzol Reagent (Invitrogen), homogenized using Polytron PT2100 tissue grinders (Kinematica), and then processed to extract RNA. All experiments were executed under a biosafety level 3, and approval for animal experiments was obtained from the Institutional Animal Welfare Committee.

### Oligonucleotide Microarray analysis

Infected macaque lung samples were co-hybridized with a reference mock-infected macaque lung sample on macaque oligonucleotide arrays containing 131 viral probes, corresponding to 26 viruses, and 22,559 rhesus probes, corresponding to ~18,000 rhesus genes. The reference mock-infected sample was created by pooling equal mass quantities of total RNA extracted from the 12 individual lung pieces from mock-infected animals. An Agilent 2100 bioanalyzer was used to check the purity of the total RNA prior to cRNA probe production with the Agilent Low RNA Input Fluorescent Linear Amplification kit (Agilent Technologies Inc., Palo Alto, CA). Arrays were scanned with an Agilent DNA microarray scanner, and image analysis was performed using Agilent Feature Extractor Software (Agilent Technologies). Each microarray experiment was done with two technical replicates using dye reversal (20). All data were entered into a custom-designed database (Expression Array Manager) and analyzed with Resolver® 4.0 (Rosetta Biosoftware) and Spotfire DecisionSite™ for Functional Genomics (Spotfire). In our data analysis, genes were selected to be included for transcriptional profile based on two criteria: a greater than 99.99% probability of being differentially expressed ( $p \leq 0.0001$ ) and an expression level change of 2 fold or greater. Ingenuity Pathway Analysis (Ingenuity Systems) was used to functionally annotate genes according to biological processes and canonical pathways. In accordance with proposed MIAME standards, primary data are available in the public domain through Expression Array Manager at <http://expression.microslu.washington.edu/expression/index.html> (2).

### Quantitative real time RT-PCR

RT-PCR was performed to detect SARS-CoV mRNA and to validate cellular gene expression changes as detected with microarrays. Each reaction was run in triplicate using Taqman 2x PCR Universal Master

Mix (Applied Biosystems, Foster City, CA) with primers and probe specific for the SARS-CoV nucleoprotein gene (25), or for macaque cellular genes (sequences shown in table 2.1). Differences in gene expression are represented as the fold change in gene expression relative to a calibrator and normalized to a reference, using the  $2^{-\Delta\Delta Ct}$  method (30). GAPDH (glyceraldehydes-3-phosphate dehydrogenase) or 18S rRNA were used as endogenous controls to normalize quantification of the target gene. The samples from the mock-infected macaques were used as a calibrator.

**Table 2.1. Primers and probes used for quantitative RT-PCR**

<i>Gene</i>	<i>Primer sequence</i>
<b><i>IFN-β</i></b>	fw: 5' GCC-TCA-AGG-ACA-GGA-TGA-ACT-T 3'
	rv: 5' CGT-CCT-CCT-TCT-GGA-ACT-GC 3'
	probe: 6-FAM-CAT-CCC-TGA-GGA-AAT-TAA-GCA-GCC-GC-TAMRA
<b><i>CXCL10</i></b>	fw: 5' CCA-AGT-CAA-TTT-TGT-CCA-CAT-GTT 3'
	rv: 5' CAG-ACA-CCT-CTT-CTC-ACC-CTT-CTT 3'
	probe: 6-FAM-AGA-TCA-TTG-CTA-CAA-TGA-A-TAMRA
<b><i>IL-6</i></b>	fw: 5' TGC-TTT-CAC-ACA-TGT-TAC-TCC-TGT-T 3'
	rv: 5' CAT-CCT-CGA-CGG-CAT-CTC-A 3'
	probe: 6-FAM-ATG-TCT-CCT-TTC-TCA-GGG-C-TAMRA
<b><i>IL-8</i></b>	fw: 5' CAG-CCT-TCC-TGC-TTT-CTG-CA 3'
	rv: 5' TGC-ACT-CAC-ATC-TAA-GTT-CTT-TAG-CAC 3'
	probe: 6-FAM-AAC-TGC-ACC-TTC-ACA-CAG-A-TAMRA

### Immunohistochemistry

Formalin-fixed, paraffin embedded lung samples from SARS-CoV infected and mock-infected macaques were stained for SARS-CoV, phosphorylated STAT1, and IFN-β using mouse-anti-SARS-nucleocapsid (Clone Ncap4, mouse IgG2b, Imgex), mouse-anti-phospho-STAT1 (Clone ST1P-11A5, mouse IgG2a-κ, Zymed Laboratories), and rabbit-anti-IFN-β (Chemicon) respectively. After deparaffinization, antigen retrieval was performed using a citrate buffer for the SARS-CoV and STAT1 staining. No antigen retrieval was performed when staining for IFN-β. Goat-anti-mouse IgG2a HRP, goat-anti-mouse IgG2b AP (Southern Biotech), and anti-rabbit IgG-HRP (DAKO) were used as secondary antibodies. Signals were developed with Fast Red and DAB (Sigma) and counterstained with Mayer's hematoxylin.

### *In vitro* SARS-CoV and STAT1 staining

MA104 cells (African Green Monkey foetal kidney cells, ECACC) were cultured in Eagle's Minimal Essential Medium (EMEM, Cambrex) supplemented with 2mM glutamine, 1% non-essential amino acids and 10% foetal bovine serum. Cells were seeded in 96-well plates (Greiner Bio-one) and infected with SARS-CoV

(MOI 0.5) and 24 hours after infection selected wells were treated with universal type I IFN (5000 U/ml, Sigma) for 30 minutes at 37°C. Subsequently, cells were fixed with 10% neutral-buffered formalin and treated with 70% ethanol. SARS-CoV infected cells were visualized using purified human IgG from a covalent SARS patient (CSL), followed by staining with an antibody to human IgG, linked to Alexa Fluor 594 (Invitrogen). Phosphorylated STAT1 was visualized using mouse-anti-phospho-STAT1 (Zymed), followed by staining with a FITC-linked antibody to mouse IgG.

## RESULTS

### **SARS-CoV replication and global gene expression in lungs of SARS-CoV infected macaques**

Six cynomolgus macaques were inoculated with SARS-CoV strain HKU-39849 and lung tissues were collected at day 1 ( $n = 2$ , 1A-1B) or day 4 ( $n = 4$ , 4A-4D). No lesions or clinical symptoms were detected on day 1 after SARS-CoV infection, whereas on day 4, three out of four monkeys were lethargic with one of these animals showing mildly labored breathing. Pathological changes at day 4 post infection included DAD, characterized by flooding of the alveoli with edema fluid, infiltration of neutrophils, damage to the alveolar and bronchial epithelia and occasional type 2 pneumocyte hyperplasia, as described earlier (14). Four mock-infected animals were included in the study to serve as a reference for host response without viral challenge and to examine outbred inter-animal variation. Our previous experience with A/Texas/36/91 influenza virus demonstrated that viral mRNA was detected in representative samples of the lung rather than throughout the whole lung (1). Based on this experience, the level of infection in separate lung samples was evaluated using RT-PCR.

SARS-CoV mRNA was detected in all animals, and 13 pieces out of the total of 16 lung pieces from infected animals contained high levels of virus, while the 3 remaining pieces of lung contained very low levels of virus (~3-4 logs lower, figure 2.1A). No viral RNA could be detected in the samples from the mock-infected animals. For gene expression experiments, lung samples from SARS-CoV infected animals were compared to a reference lung sample from mock-infected animals. The three samples with lower virus levels (1A-low, 4A-low, and 4D-low) were analyzed individually as not to dilute the gene expression of pooled pulmonary samples with higher SARS-CoV levels and also to potentially further define pulmonary infection. Samples from animals with high viral mRNA levels showed greater gene expression changes (~2000 genes day 1, ~800 genes day 4) compared to samples from animals with low-levels of viral mRNA (~400 genes), indicating a response of lung tissue to the virus (figure 2.1B). Additionally, the two day 1 animals showed higher numbers of differentially expressed genes than the day 4 animals. In contrast, gene expression analysis of the separate mock samples revealed limited differentially expressed genes.

In order to examine how gene expression would be influenced by presence of virus, timing after inoculation, and individual animal variation, global expression profiling was performed. Hierarchical clustering methods were used to order rows (genes) and columns (samples) to identify groups of genes

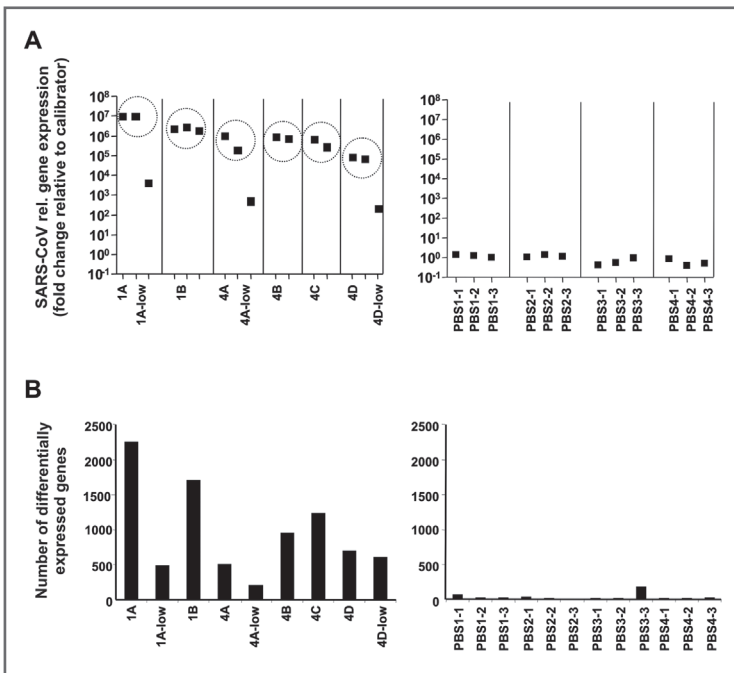


**Figure 2.1.** SARS-CoV mRNA levels and global gene expression in lungs of SARS-CoV infected macaques.

(A) RT-PCR was performed on all individual pulmonary samples from SARS-CoV infected animals and mock-infected animals to determine SARS-CoV levels. Samples from SARS-CoV infected animals that were pooled for microarray studies are indicated with circles. The 3 samples with lower levels of virus were hybridized separately. The 12 samples from mock-infected animals (i.e., PBS) were pooled and served as a reference sample. The number after PBS refers to the animal (i.e., PBS 1) while the number after the dash refers to the lung piece (i.e., PBS 1-1). (B) Using microarrays, gene expression in SARS-CoV infected animals was compared to gene expression in mock-infected animals. The bar graph shows the total number of genes considered to be differentially expressed, defined as an absolute fold change  $> 2$  with  $P < 0.0001$ . Samples 1A and 1B (day 1), and 4A-4D (day 4) are composed of the pooled individual pulmonary samples shown in figure 2.1A. Samples 1A low, 4A low, and 4B low are the outliers from figure 2.1A. Separate mock samples (i.e., PBS) were compared to the total mock pool.

or samples with similar expression patterns (6, 41). These data were plotted as a heat map where each matrix entry represents a gene expression value (figure 2.2A). Red corresponds to higher gene expression than that of the controls; green corresponds to lower gene expression. This analysis yielded 2050 genes with day 1 samples on one side of the heat map and day 4 samples on the other side of the heat map, indicating an influence of timing after inoculation. There are two major roots to the hierarchical dendrogram with the larger root composed of all the day 1 samples and the three day 4 samples with the highest virus levels. The smaller root is composed of the remaining day 4 samples with the lowest SARS-CoV

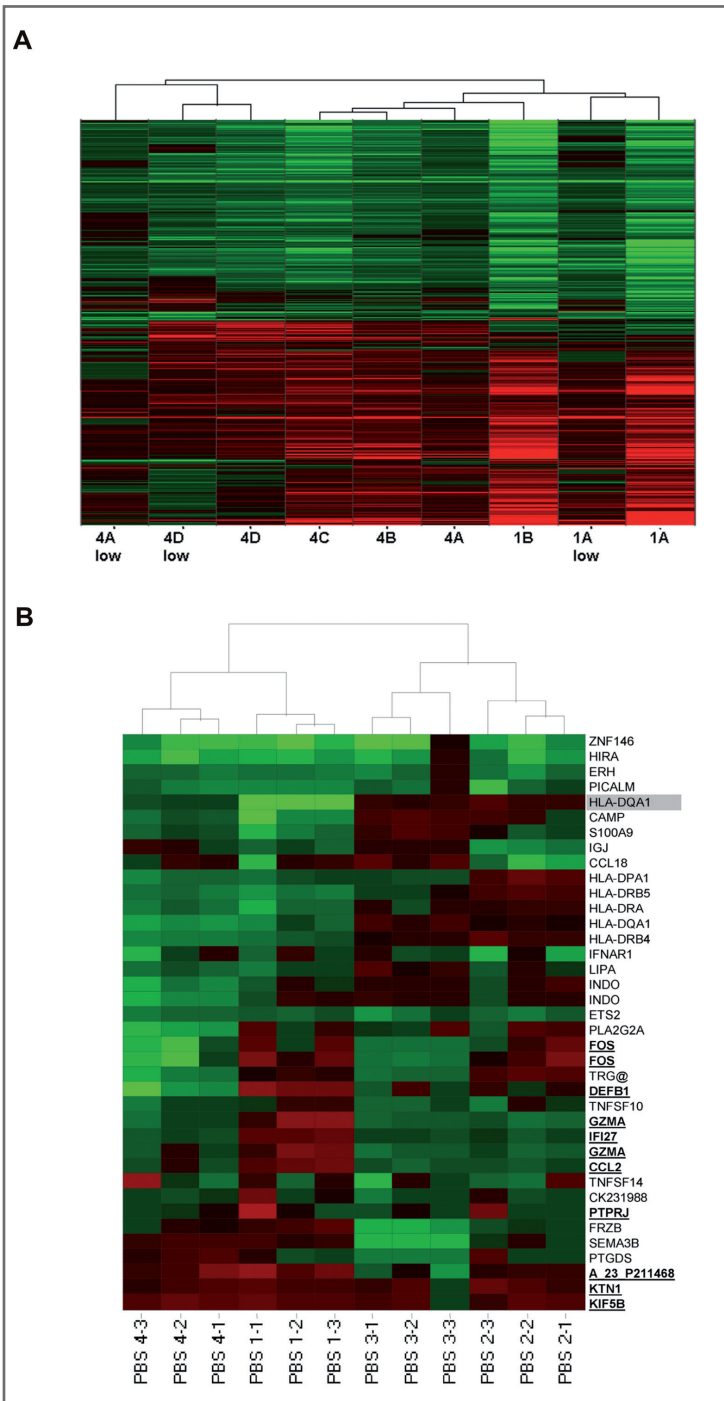


**Figure 2.2. Unsupervised Global Gene Expression Profile of SARS-CoV infected macaques and individual variation in mock-infected animals.**

(A) Gene expression profiles result from comparing gene expression in lungs of experimental animals versus gene expression in lungs of mock-infected animals (pooled). Genes were included if they met the criteria of a two-fold change or more ( $p < 0.0001$ ). A two-of-nine strategy allowed samples to cluster together if profile similarities existed based on timing of inoculation ( $n=2$  samples for day 1).

(B) The number after PBS refers to the animal (i.e., PBS 1) while the number after the dash refers to the lung piece (i.e., PBS 1-1). Thirty eight genes are displayed with an absolute fold change  $> 2$  and  $p < 0.0001$  in at least two animal samples. Upregulated genes are indicated in bold underline. Only one gene, HLA-DQA1, was downregulated  $> 5$ . No up-regulated genes met these criteria in mock-infected animals. Separate mock samples (i.e., PBS 1-1) were compared to the total mock pool.

levels. Although transcriptional profiling shows some variation when comparing samples from the same animal, the underlying gene expression is similar with a reduction in fold change in the “low” samples. These comparisons suggest that both individual animal variation and the “asynchronous” nature of the infection in the animals’ lungs are factors involved in determining transcription of cellular genes. To validate that the host-response from infected animals comprises a stronger transcriptional profile than individual variation from mock-infected animals, differential gene expression patterns in the separate mock samples were investigated, but only 38 genes were differentially expressed (figure 2.2B). These results suggest that underlying basal levels of gene transcription do not confound expression levels after infection. Even in a basal state, some low-level lung-to-lung variations were identified within the same animal but not enough to disrupt segregation of lung pieces based on animal.

### Common and unique temporal host responses to SARS-CoV infection

In order to elucidate common responses to SARS-CoV throughout the infection as well as unique responses at different time points after inoculation, a Venn diagram was generated with each set (circle) holding to the parameters of an absolute fold change  $> 2$  and  $p < 0.0001$  in at least two animals (figure 2.3A). The day 1 set contained 1278 genes and the day 4 set contained 950 genes. When examining host responses that were similar throughout the course of the infection, the intersection of the day 1 and day 4 sets indicates 597 genes show shared responses. The heat map of these 597 genes is shown in figure 2.3B. If more stringent criteria were used to find common responses in all six animals, using the 1278 genes from the day 1 set and the 129 genes that are differentially expressed in all day 4 animals, a subset of 97 genes was identified. This subset included IFN-stimulated genes (ISG), like IFITs, MX1, GBP1, and G1P2, and also various chemokines and cytokines, such as CXCL10 (IP-10), CCL2 (MCP-1), IL-6, and IL-8 (figure 2.51). These same cytokines and chemokines have been reported to be upregulated in human SARS cases (18, 39, 53, 55). This set also included cathepsin L (CTSL), which has been shown to be required for SARS-CoV entry into a cell (43). Even though only 97 genes were commonly regulated in all animals, indicated with blue bars in figure 2.3B, the heat map highlights that the other 500 genes show similar expression trends. Both sets of common-response genes showed similar functionality: cellular growth and proliferation, cell death, cellular movement, immune response, and cell-to-cell signaling.

Next, we analyzed genes that were differentially expressed exclusively on either day 1 or day 4, in order to find signature gene expression patterns for each day. Genes identified as unique responses at day 1 (681 genes) and at day 4 (353 genes) in the Venn diagram showed unique functionality (figure 2.3C). The gene expression profile at day 1 shows a prominent innate host response to viral infection; top functional categories on day 1 are the immune response, the hematological system, and the immune and lymphatic system. Genes like IFN- $\gamma$ , CCL4 (MIP-1- $\beta$ ), CSF3, IL1A and TNF are included in these categories. At day 4, a smaller panel of unique differentially expressed genes that play a role in cell cycle, cellular assembly, and DNA repair were identified like CCNB2, CCNE1, CDCA5, CENPA, CHAF1A and PRC1.

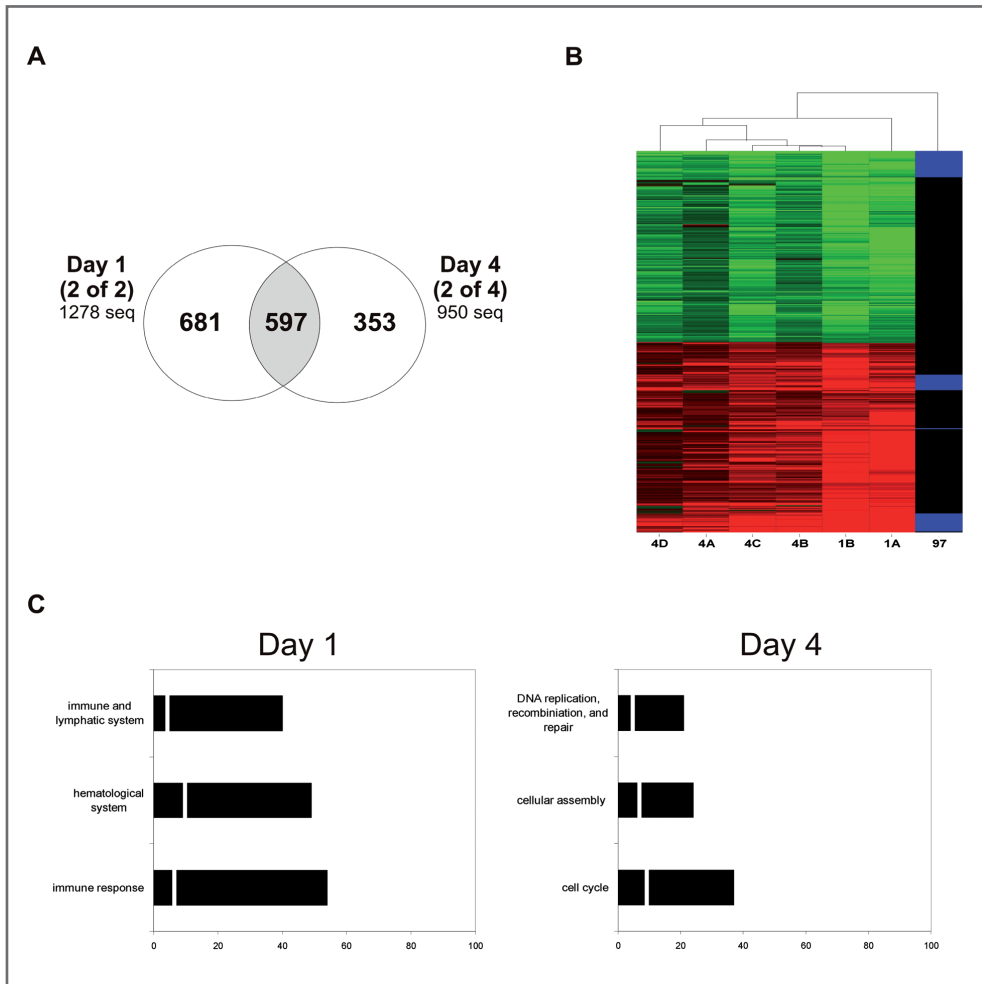


**Figure 2.3. Common and unique temporal gene responses to SARS-CoV infection.**

(A) The Venn diagram shows genes with an absolute fold change  $> 2$  and  $p < 0.0001$  in two of out of the two day 1 samples (left circle) or two out of the four day 4 samples (right circle). (B) The heat map includes the 597 genes from the grey Venn diagram intersections. The right column highlights the 97 genes that are commonly regulated in all 6 samples with blue. All 97 genes are listed in supplementary figure 2.S1. All gene expression profiles are the results of comparing gene expression in lungs of experimental animals versus gene expression in lungs of mock-infected animals (pooled). (C) Functional annotation was used to categorize the 681 unique genes at day 1, and the 353 unique genes at day 4. The percentage of genes within the top functional categories is indicated in the day 1 and the day 4 bargraph, with a white line indicating the percentage of genes found at the alternative day. Cell-to-cell signaling and cell death, other top categories on day 1, and cell death, cellular growth and proliferation, additional top categories on day 4, are not included in the bar graph as these categories were observed to have more genes differentially expressed in the common signature.

## Immune response, cell cycle and lung repair genes with strongly induced or reduced expression

In order to investigate genes that are most strongly regulated after SARS-CoV infection, genes included in the Venn diagram (figure 2.3A) that also held to an absolute fold change  $> 5$  were queried (figure 2.S2). From this set, genes that were involved in the immune response and lung repair processes were used to generate a heat map (figure 2.4). A number of genes that have been reported to be upregulated in SARS patient sera, such as CCL2 (MCP-1), CXCL10 (IP-10), IL-6, and IL-8, were strongly ( $\sim 20$  fold) induced in all animals. Many cell-cycle and matrix genes indicative of tissue repair processes were also highly differentially expressed at day 4 (e.g., ANLN, AREG, CDC2, CDKN3, CKS2, FOSL1, and KIF2C). Likewise, tissue factor pathway inhibitor 2 (TFPI2), an anticoagulant, was strongly upregulated during infection in all animals (averaging  $\sim 20$  fold), as well as PLSCR1, SERPINE1 (PAI1), and THBS1, all genes involved in pro-coagulation and platelet activation, were induced. Concomitant expression of TFPI2 with these pro-coagulation genes, might function as an inhibitory response to restrain the activation of the coagulation pathway during acute inflammation.

Surprisingly, expression of diverse IFN- $\alpha$  genes and expression of IFN- $\beta$  was upregulated  $\sim 10$ - $20$  fold in the day 1 samples. Furthermore, IFN- $\gamma$ , a type II IFN, was efficiently transcribed on day 1 after SARS-CoV infection ( $\sim 5$  fold). Other genes associated with the induction of IFNs like DDX58 (Rig-1), IRF-7, and STAT1, were also highly induced ( $\sim 8$  fold). Upregulation of type I IFNs in these SARS-CoV infected macaques is remarkable, since SARS-CoV inhibits IFN production in many *in vitro* studies. We did not detect induced IFN- $\beta$  mRNA expression using Ma104 cells or Caco2 cells and the SARS-CoV-HKU virus (data not shown). Not only IFNs, but also several IFN responsive genes (e.g., G1P2, GBP1/2, IFI/IFITs, MX1/2, ISG20 and OAS1/2/L) were highly transcribed, showing a persistent activation of the innate immune response. Furthermore, suppressor of cytokine signaling 1 (SOCS1) is induced at the onset of infection, presumably to establish negative feedback to attenuate cytokine signaling. Of note, IFIT1 (ISG56/IFI56), often used to gauge IFN induction, was upregulated an average of  $\sim 13$  fold.

## Pathogenic and antiviral pathways induced by SARS-CoV

To further explore some of the pathogenic and antiviral pathways that are induced after SARS-CoV infection, we investigated the transcription of various cytokines, chemokines, IFNs, ISGs and transcription factors involved in the JAK/STAT pathway. As can be seen in figure 2.5A, a wide range of chemokines and cytokines are differentially expressed after SARS-CoV infection in macaque lungs, especially on day 1 after infection. Besides previously mentioned chemokines, we detected monocyte chemotactic protein genes like CCL8 (MCP-2) and CCL7 (MCP-3), but also CCL11 (eotaxin), a chemotactic protein for eosinophils. In the samples with low SARS-CoV mRNA levels, the induction of chemokines is less evident, suggesting that the presence of these molecules is restricted to areas in the lung where virus is present. Furthermore, SARS-CoV infected macaques showed a stronger induction of IFNs (14 unique genes) and ISGs (20 unique genes) on day 1 than day 4 and when virus was present at high levels. Note that besides IFN- $\alpha$ , IFN- $\beta$  and IFN- $\gamma$  also the IFN- $\lambda$ 's (IL-29, IL-28A, IL-28B), which are type I IFNs, were induced in samples with high SARS-CoV levels. In the absence of viral RNA no IFNs, but interestingly, a number of ISGs (17 unique genes) were detected, suggesting paracrine stimulation (figure 2.5B).





Figure 2.4. Immune response, cell cycle and lung repair genes with strongly induced or reduced expression.

A selection of genes, involved in the immune response, cell cycle or lung repair processes, that showed an absolute fold change  $> 5$  and  $p < 0.0001$  in both day 1 animals and/or in at least two of the four day 4 animals was made. Genes with an absolute fold change  $> 5$  in both day 1 animals and in at least two of the four day 4 animals are indicated with bold, underlined text. A full summary of genes that show an absolute fold change  $> 5$  and  $p < 0.0001$  after SARS-CoV infection is given in supplementary figure 2.S2.

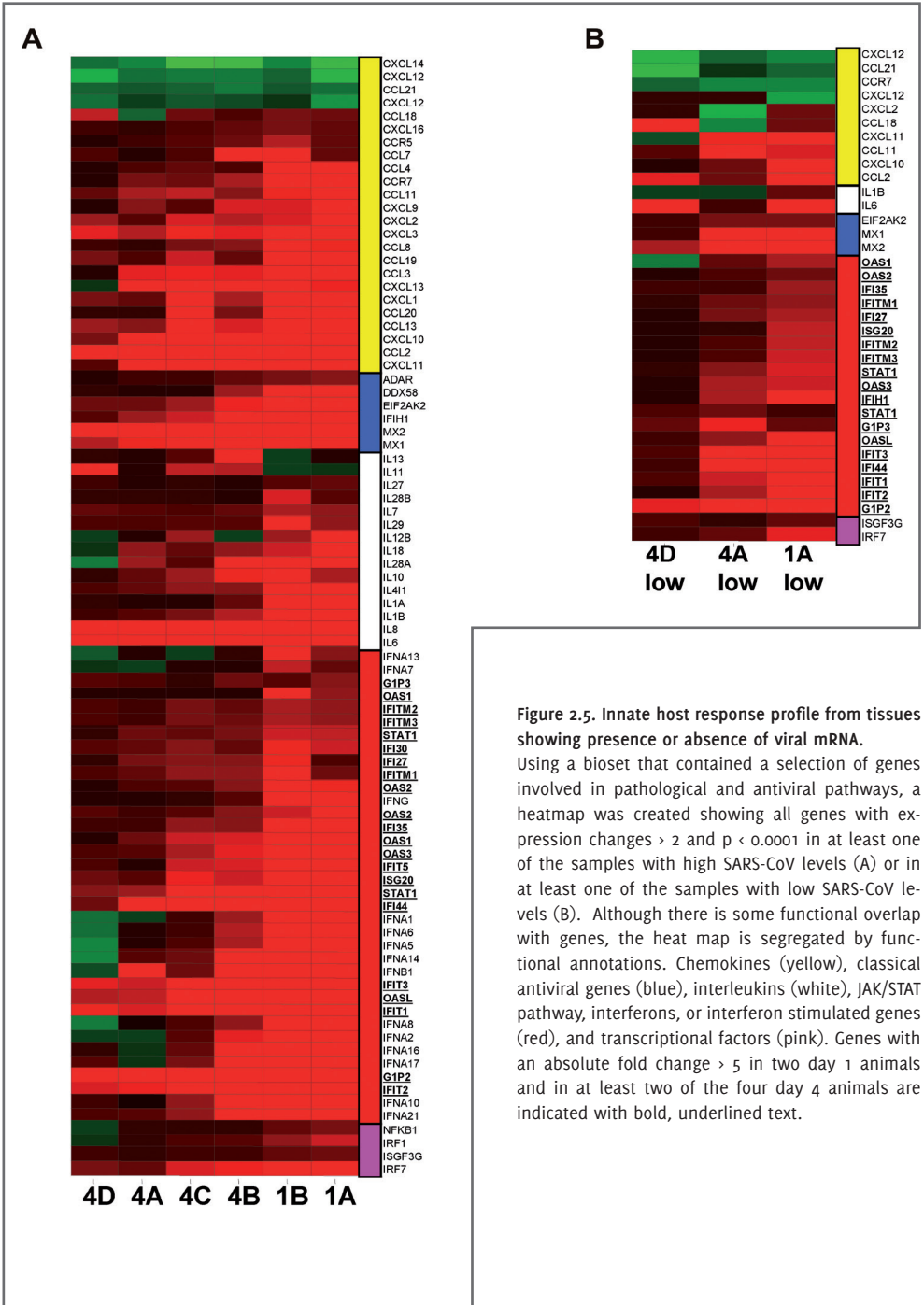


Figure 2.5. Innate host response profile from tissues showing presence or absence of viral mRNA.

Using a bioset that contained a selection of genes involved in pathological and antiviral pathways, a heatmap was created showing all genes with expression changes  $> 2$  and  $p < 0.0001$  in at least one of the samples with high SARS-CoV levels (A) or in at least one of the samples with low SARS-CoV levels (B). Although there is some functional overlap with genes, the heat map is segregated by functional annotations. Chemokines (yellow), classical antiviral genes (blue), interleukins (white), JAK/STAT pathway, interferons, or interferon stimulated genes (red), and transcriptional factors (pink). Genes with an absolute fold change  $> 5$  in two day 1 animals and in at least two of the four day 4 animals are indicated with bold, underlined text.

## Confirmation of IL-6, IL-8, IP-10/CXCL10 and IFN- $\beta$ expression with RT-PCR and correlation with SARS-CoV levels

Differential expression of a selection of strongly upregulated genes, CXCL10 (IP-10), IL-6, IL-8 and IFN- $\beta$ , was confirmed using RT-PCR (figure 2.6). In accordance to the microarray data, the RT-PCR data showed that CXCL10 (IP-10), IL-6, IL-8 and IFN- $\beta$  were all expressed at levels that were approximately 100 times higher in the SARS-CoV infected animals at day 1 than in the uninfected control animals and were still elevated on day 4 after infection. As can be seen in figure 2.6, the induction of IFN- $\beta$  was strongly correlated to the presence of virus ( $r_{\text{spearman}} = 0.88, p < 0.0001$ ). For CXCL10 (IP-10), IL-6 and IL-8 the correlation is less evident, which is not surprising since these cytokines can be induced by other factors than the virus itself.

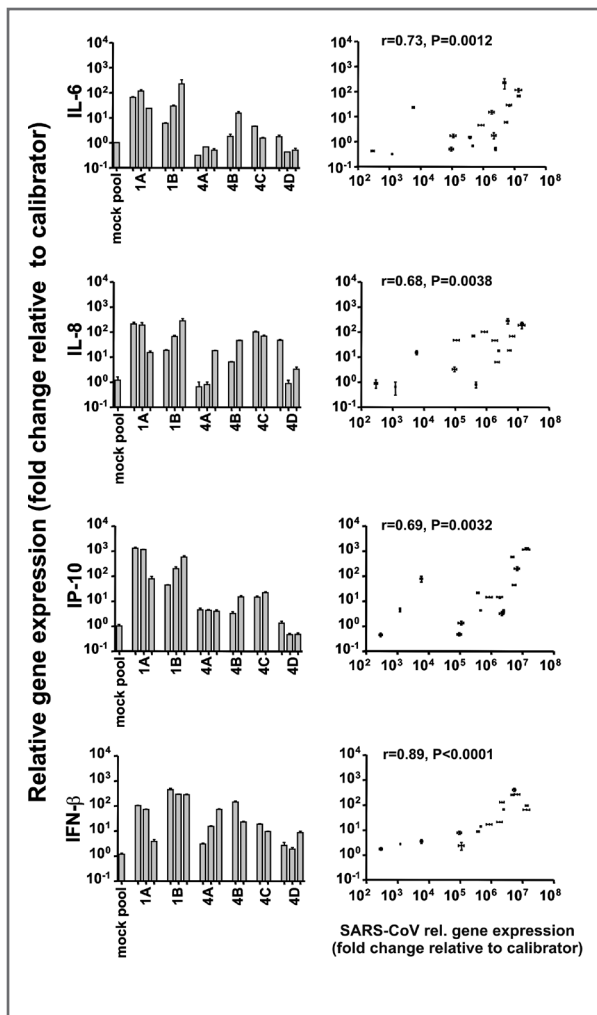
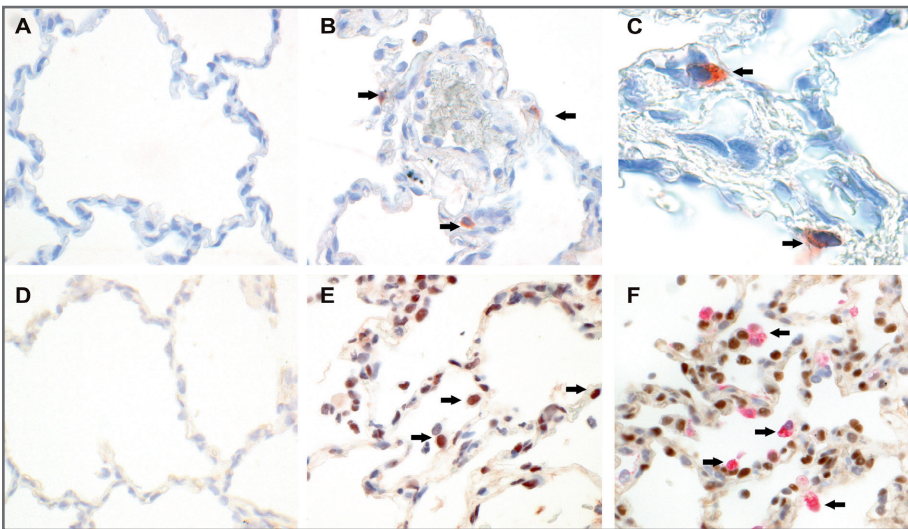


Figure 2.6. Confirmation of microarray results with RT-PCR and correlation of induced genes with presence of SARS-CoV. Quantitative RT-PCR for IL-6, IL-8, CXCL10 (IP-10) and IFN- $\beta$  was performed on all separate lung samples. Expression levels of these genes were plotted against the presence of SARS-CoV in these samples (as detected by RT-PCR). Correlation coefficients were determined using Spearman's correlation test.

## Detection of IFN- $\beta$ and phosphorylated STAT1 protein in lung of SARS-CoV infected macaques

In order to visualize the host response in the lungs of SARS-CoV infected macaques, IFN- $\beta$  production and translocation of phosphorylated STAT1 was studied using immunohistochemistry. In the lungs of the SARS-CoV infected macaques a modest number of cells stained positive for IFN- $\beta$  at day 1 post infection, whereas no IFN- $\beta$  positive cells could be detected in mock-infected macaques (figure 2.7A-C). Notably, most of the cells that stained positive for IFN- $\beta$  were located very close to blood vessels, but not in the alveoli where most SARS-CoV antigen positive cells (mainly type II pneumocytes at 1 day post infection) are located.

To examine if the IFNs that are produced in the lungs of these SARS-CoV infected macaques are biologically active and able to induce STAT1 phosphorylation and translocation, lung sections of the infected macaques were stained with antibodies against phosphorylated STAT1. As shown in figures 2.7D-E, no phosphorylated STAT1 could be detected in the lungs of PBS infected macaques, while in the lungs of SARS-CoV infected macaques cells with phosphorylated STAT1 in their nucleus were abundantly present. Subsequently, the same pieces of lung from SARS-CoV infected macaques at day 1 were double stained for phosphorylated STAT1 and SARS-CoV (figure 2.7F). Notably, phosphorylated STAT1 was not detected in the nucleus of SARS-CoV infected cells (type II pneumocytes), while cells directly adjacent to these SARS-CoV infected cells stained for phosphorylated STAT1, in many but not all foci containing SARS-CoV positive cells. Thus type I IFNs are produced in the lungs of SARS-CoV infected macaques, and are able to activate the JAK/STAT pathway. However, translocation of STAT1 does not occur in SARS-CoV infected pneumocytes.



**Figure 2.7.** Detection of IFN- $\beta$  and phosphorylated STAT1 in lung of SARS-CoV infected macaques using immunohistochemistry.

(A) Lack of IFN- $\beta$  expression in lungs of mock-infected macaques (40x) and (B-C) expression of IFN- $\beta$  (red) in lungs of SARS-CoV infected macaques at day 1 post infection (40x, 100x respectively, arrowheads). (D) Lack of phosphorylated STAT1 in lungs of mock-infected macaques (40x) and (E) abundant presence of phosphorylated STAT1 (brown) in lungs of SARS-CoV infected macaques at day 1 post infection (40x, arrowheads). No detection of phosphorylated STAT1 (brown) in SARS-CoV infected cells (red) (40x, arrowheads).

## Detection of STAT1 translocation after SARS-CoV infection *in vitro*

Although recent studies indicate that the SARS-CoV ORF6 protein is able to inhibit nuclear translocation of STAT1 *in vitro*, this was not demonstrated in experiments using infectious SARS-CoV (23). In order to assess if SARS-CoV inhibits phosphorylation and translocation of STAT1, MA104 cells were infected with SARS-CoV for 24 hours and then either fixed directly or treated with type I IFN. Cells infected with SARS-CoV, but not treated with IFN, stained positive for SARS-CoV (data not shown), but lacked staining for phosphorylated STAT1, indicating that SARS-CoV or other soluble mediators are not able to induce STAT1 phosphorylation (figure 2.8). After treatment of the MA104 cells with IFN, phosphorylated STAT1 could be detected in the nucleus of most cells, but not in the nucleus of SARS-CoV infected cells (figure 2.8). This demonstrates that SARS-CoV inhibits the translocation of phosphorylated STAT1 to the nucleus, confirming our *in vivo* data. Besides inhibiting translocation of phosphorylated STAT1, SARS-CoV also seems to reduce STAT1 phosphorylation, as the majority of SARS-CoV infected cells did not contain phosphorylated STAT1 in their cytoplasm, or at low levels.

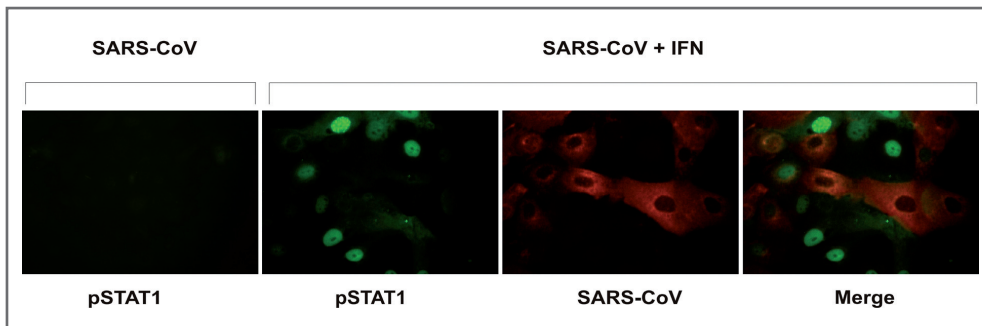


**Figure 2.8.** Inhibition of STAT1 phosphorylation and nuclear translocation in SARS-CoV infected MA104 cells. MA104 cells were infected with SARS-CoV for 24 hours and then either fixed directly (left panel) or treated with type I IFN and then fixed. Subsequently cells were stained for phosphorylated STAT1 and SARS-CoV. The most right panel shows a merge of the two middle panels, showing an inhibition on STAT1 phosphorylation and translocation in SARS-CoV infected cells.

## DISCUSSION

Pathogenic viruses escape the antiviral action of the IFN system by inhibiting both IFN production and signaling pathways. Here we report that, even though production and signaling of type I IFNs is inhibited by SARS-CoV *in vitro* as well as in SARS-CoV infected cells *in vivo*, high levels of type I IFNs are induced in the lungs of SARS-CoV infected macaques. These IFNs are able to activate STAT1, followed by the transcription of numerous ISGs. Using immunohistochemistry we revealed that these antiviral signaling pathways were differentially regulated in distinctive subsets of cells. Our results emphasize the strength of combining functional genomics with immunohistochemistry to further unravel the pathogenesis of SARS-CoV infection in cynomolgus macaques.

This study represents the first functional genomics investigation of SARS-CoV infection cynomolgus macaques. All experimental animals showed signs of infection because viral mRNA could be detected in random samples from the lung, indicating that the virus had spread throughout the whole lung at the time of necropsy. Furthermore, pathological examination of SARS-CoV infected macaques at day 4 post infection revealed multifocal DAD (14). Unlike 10% of humans with SARS, which are mainly restricted to the elderly, young-adult macaques used in this study do not succumb to SARS-CoV infection. However, the SARS-CoV induced pathology in these macaques likely resembles the pathological changes seen in the majority of human SARS patients that recover from the disease. Although none of the current animal models has fully reproduced all features of SARS, the most important aspects of this disease are observed in experimentally infected macaques, providing valuable insights into the initial innate immune response after infection, without confounding clinical treatment or underlying co-morbidity.

Using macaque-specific microarrays, we were able to observe that with early infection, high levels of viral mRNA corresponded to a strong cellular host response. This strong host response is dominated by genes involved in the immune response and includes a wide range of genes corresponding with what is seen in human ARDS. During the acute phase of human ARDS, activated neutrophils and macrophages enter the alveoli and produce a number of cytokines and chemokines such as IL-6, IL-8, and CXCL10 (IP-10) (52). These genes are also postulated to predict adverse SARS patient outcome (49) and were found in the lungs of our SARS-CoV infected macaques. During the chronic phase of human ARDS, type II pneumocytes start to proliferate and differentiate in order to repair the damaged lung. At day 4, the macaque lung shows similar evidence of lung repair and numerous genes are upregulated that are involved in cellular growth and proliferation, cell cycle, and DNA replication and repair. Genes involved in cell cycle regulation and proliferation have been previously reported in coronavirus infections other than SARS-CoV and characterized by an accumulation of infected cells in the G<sub>0</sub>/G<sub>1</sub> phase (47-48). We also detected a strong presence of genes involved in the coagulation pathway, including TFPI2, SERPINE1 (PAI1) and TIMP1. The idea of a pro-coagulation profile mimics the clinical-pathological observations of SARS patients that showed unusually disseminated small vessel thromboses in the lungs (12, 37). Additionally, cathepsin L was upregulated in all SARS-CoV infected macaques. Induction of this gene after SARS-CoV infection is quite interesting since cathepsin L is an endosomal protease that is necessary for SARS-CoV to infect a cell (43).

Remarkably, SARS-CoV infection in macaques leads to a strong transcription of IFNs. Not only IFN- $\alpha$ , IFN- $\beta$  and IFN- $\lambda$ , all type I IFNs, but also IFN- $\gamma$ , a type II IFN, were all highly upregulated, especially on day 1 after infection. The expression of IFN- $\beta$ , which strongly correlated to the amount of virus present, continued throughout day 4 and was confirmed using immunohistochemistry; IFN- $\beta$  positive cells could be detected in the lungs of the SARS-CoV infected macaques. The induction of IFN- $\beta$  in these SARS-CoV infected macaques is surprising since several reports have shown that SARS-CoV inhibits or delays type I IFN production in a number of cell types (5, 26, 35, 45-46, 48, 58). For example, SARS-CoV blocks a step in the activation of IRF-3, a transcription factor that is required for IFN- $\beta$  induction (44). In addition, the SARS-CoV proteins ORF3B, ORF6 and nucleocapsid have been shown to function as IFN antagonists as well as the SARS-CoV nsp1 gene that prevents the production of Sendai virus induced IFN- $\beta$  in 293 cells (19, 23). Interestingly, it was recently shown that plasmacytoid dendritic cells (pDCs) are able to produce IFN- $\alpha$

and IFN- $\beta$  after SARS-CoV infection, while conventional DCs did not produce these type I IFNs (4). pDCs are known for their ability to produce very high amounts of IFN- $\alpha$  and IFN- $\beta$  and are considered first-line sentinels in immune surveillance in the lung (3, 8-9, 31, 42). We speculate that the IFN- $\beta$  producing cells detected in the lungs of SARS-CoV infected macaques are pDCs. Future studies may address the nature of these IFN producing cells once technical difficulties in detecting pDCs in macaque tissues have been tackled. These studies may also shed light on whether decreasing numbers of pDCs observed in clinical blood samples from human SARS patients are caused by sequestering of pDCs by the lungs, destruction of pDCs by SARS-CoV, or destruction or suppression of pDCs by steroid treatment (56).

When IFNs are produced, they bind to their receptors on the cell membrane, after which STAT<sub>1</sub>, a key member of the JAK/STAT pathway, is phosphorylated and subsequently translocated to the nucleus, followed by the production of a wide range of IFN stimulated genes. *In vitro*, SARS-CoV inhibited translocation of STAT<sub>1</sub> to the nucleus and phosphorylation of STAT<sub>1</sub> was strongly reduced. However, the inhibition of STAT<sub>1</sub> phosphorylation was not absolute because cells with low levels of phosphorylated STAT<sub>1</sub> in their cytoplasm were also detected. In accordance with our data, Kopecky-Bromberg et al. recently showed that the SARS-CoV protein ORF6 is able to inhibit STAT<sub>1</sub> translocation (23). This strategy is not unique to SARS-CoV. Other viruses have been shown to be able to block signaling of IFNs by affecting phosphorylation and/or translocation of the STAT proteins. For example, Measles Virus V protein inhibits translocation of STAT<sub>1</sub>, but does not affect phosphorylation, whereas Measles Virus P protein blocks both these processes (11). Other paramyxoviruses, like Rinderpest Virus, Nipah Virus, Hendra Virus and Mumps Virus, but also flaviviruses like West Nile Virus and Japanese Encephalitis Virus are able to block activation of STAT<sub>1</sub> and STAT<sub>2</sub> (24, 28-29, 34). Inhibition of STAT<sub>1</sub> phosphorylation is not always complete. For example, Sendai virus suppresses tyrosine phosphorylation of STAT<sub>1</sub> during the early stages of infection, but this block becomes leaky after a couple of hours with phosphorylated STAT<sub>1</sub> accumulating in the cytoplasm (22). In contrast to these *in vitro* data, we observed phosphorylated STAT<sub>1</sub> in the nuclei of numerous cells in the lungs of SARS-CoV infected macaques, indicating that these cells had been activated by the IFNs produced in the lung. However, phosphorylated STAT<sub>1</sub> was not detected in SARS-CoV infected cells. The observations made in this study indicate that SARS-CoV infected macaques produce IFNs in response to virus infection and are further capable of activating the STAT<sub>1</sub> pathway in cells surrounding the SARS-CoV infected cells.

The importance of IFNs in controlling SARS-CoV infection has been suggested in several animal studies. Mice clear SARS-CoV in the absence of NK cells, T cells, or B cells, suggesting that innate immune responses are sufficient to limit SARS-CoV infection in these animals (13). Indeed, STAT<sub>1</sub> knock out mice, which are resistant to the effects of IFNs, to some extent show a worsening of pulmonary disease and an increase in viral replication in the lungs compared to normal mice after infection with SARS-CoV (15). Although IFN-treatment was not conducted in SARS-CoV infection mouse studies, prophylactic treatment of macaques with pegylated IFN- $\alpha$  protects type I pneumocytes from infection with SARS-CoV (14). In addition, potent antiviral activity is observed *in vitro* when cells are treated with IFNs before they are infected with SARS-CoV (7, 33, 40). Although we cannot determine the effect of neutralizing IFN- $\beta$  in SARS-CoV infected animals, based on the experiments utilizing recombinant IFNs in these animals, we postulate that type I IFNs are partly responsible for the relatively mild clinical symptoms that are seen in

SARS-CoV infected macaques. In addition, a recent study again demonstrated the importance of IFNs in viral infections, as macaques infected with the highly pathogenic and fatal 1918 influenza virus showed limited induction of type I IFNs (only IFNA4 reached fold changes > 5) and delayed induction of ISGs, while macaques infected with the low-pathogenic K173 influenza virus showed a strong induction of these antiviral molecules early during infection (21). Notably, IFN- $\beta$  was not upregulated (absolute fold change < 2) in any of the influenza virus infected animals, even in those animals that recovered, unlike SARS-CoV infected macaques that showed a very strong presence of IFN- $\beta$ .

In conclusion, our study demonstrates that cynomolgus macaques can be infected with SARS-CoV, as indicated by presence of viral mRNA at different locations throughout the lung at day 1 and day 4, with gross pathology becoming noticeable at day 4. Furthermore, we show that infection of cynomolgus macaques with SARS-CoV leads to a strong immune response, including the induction of various cytokines and chemokines, resembling the host response seen in human SARS patients. Strikingly, despite the fact that SARS-CoV infection blocks the production of IFNs *in vitro*, type I IFNs are strongly induced in the lungs of SARS-CoV infected macaques. The production of IFN early during infection, leads to wide spread activation of STAT1 and the production of IFN stimulated genes. This argues that, although SARS-CoV blocks IFN signaling in infected cells, locally produced IFNs are capable of activating non-infected cells and possibly can prevent infection of these cells. Thus, SARS-CoV infection in macaques leads to the differential activation of both pathogenic and antiviral signaling pathways *in vivo* and the outcome may be determined by the relative contribution of these signaling pathways.

## ACKNOWLEDGEMENTS

We thank S. Smits for her assistance with SARS-CoV infections and RNA isolations.



## SUPPORTING INFORMATION

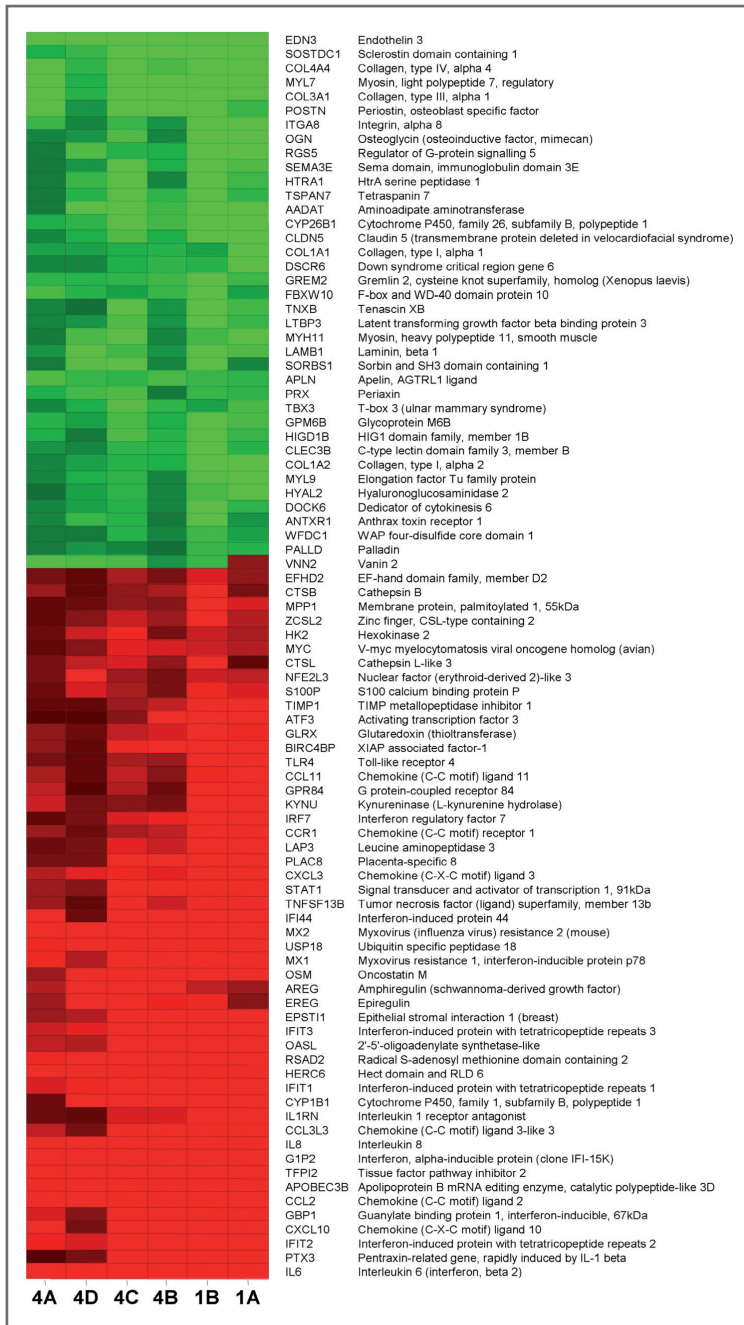


**Figure 2.S1. Heat map of common response genes that are observed in all animals.**

Depicted are all genes that adhere to an absolute fold change > 2 and  $p < 0.0001$  in all animals.

Day 1 ONLY	
AADAT	Aminoadipate aminotransferase
AGTR1L1	Angiotensin II receptor-like 1
APOL1	Apolipoprotein L1
APOL2	Apolipoprotein L2
APOL3	Apolipoprotein L3
APOL4	Apolipoprotein L4
AQP9	Aquaporin 9
ATF3	Activating transcription factor 3
BATF	Basic leucine zipper transcription factor, ATF-like
BCH1	Butyrylcholinesterase
CD44	Cluster of differentiation 44
BRG2	XAP corepressor factor-1
BRG3	Baculoviral IAP repeat-containing 7 (livin)
BRD51	BCR downstream signaling 1
C15orf48	Normal mucosa of esophagus specific 1
C1orf54	Chromosome 1 open reading frame 54
C3orf93	C-3 and tumor necrosis factor related protein 3
CD163	Chondroitin sulfate proteoglycan 1
CD169	Chromosome 8 open reading frame 19
CAV2	Caveolin 2
CBX7	Chromobox homolog 7
CCL13	Chemokine (C-C motif) ligand 13
CCL19	Chemokine (C-C motif) ligand 19
CCL20	Chemokine (C-C motif) ligand 20
CCR1	Chemokine (C-C motif) receptor 1
CCR7	Chemokine (C-C motif) receptor 7
CD163	CD163 antigen
CD169	CD169 antigen
CD274	CD274 antigen
CD80	CD80 antigen (CD28 antigen ligand 1, B7.1, antigen)
CD86	CD86 antigen (B7.2 antigen, B7.1 superfamily class II, CD137, B7.2)
CD147	CD147 antigen (FHL-2, CASP8 and FADD-like apoptosis regulator)
CHI3L2	Chitinase 3-like 2
CHST11	Carbohydrate (chondroitin 4) sulfotransferase 11
CIAS1	Cold autoimmune syndrome 1
CND5	Cold inducible transmembrane protein defined in velocardiofacial syndrome
CEACAM1	C-type lectin domain family 1, member A
CEACAM6	C-type lectin domain family 1, member B
COL1A2	Collagen type I alpha 2
COL4A3	Collagen type IV alpha 3 (Goodpasture antigen)
CTDSP1	CTD (carboxy-terminal domain, RNA polymerase II, polypeptide A), small phosphatase-like
CXCL1	Chemokine (C-X-C motif) ligand 1 (melanoma growth stimulating activity, alpha)
CXCL3	Chemokine (C-X-C motif) ligand 3
CXCL12	Chemokine (C-X-C motif) ligand 12
DEAF1	Deafness associated factor 1
DEAF2	Deafness associated factor 2
DEAF3	Deafness associated factor 3
DEAF4	Deafness associated factor 4
DEAF5	Deafness associated factor 5
DEAF6	Deafness associated factor 6
DEAF7	Deafness associated factor 7
DEAF8	Deafness associated factor 8
DEAF9	Deafness associated factor 9
DEAF10	Deafness associated factor 10
DEAF11	Deafness associated factor 11
DEAF12	Deafness associated factor 12
DEAF13	Deafness associated factor 13
DEAF14	Deafness associated factor 14
DEAF15	Deafness associated factor 15
DEAF16	Deafness associated factor 16
DEAF17	Deafness associated factor 17
DEAF18	Deafness associated factor 18
DEAF19	Deafness associated factor 19
DEAF20	Deafness associated factor 20
DEAF21	Deafness associated factor 21
DEAF22	Deafness associated factor 22
DEAF23	Deafness associated factor 23
DEAF24	Deafness associated factor 24
DEAF25	Deafness associated factor 25
DEAF26	Deafness associated factor 26
DEAF27	Deafness associated factor 27
DEAF28	Deafness associated factor 28
DEAF29	Deafness associated factor 29
DEAF30	Deafness associated factor 30
DEAF31	Deafness associated factor 31
DEAF32	Deafness associated factor 32
DEAF33	Deafness associated factor 33
DEAF34	Deafness associated factor 34
DEAF35	Deafness associated factor 35
DEAF36	Deafness associated factor 36
DEAF37	Deafness associated factor 37
DEAF38	Deafness associated factor 38
DEAF39	Deafness associated factor 39
DEAF40	Deafness associated factor 40
DEAF41	Deafness associated factor 41
DEAF42	Deafness associated factor 42
DEAF43	Deafness associated factor 43
DEAF44	Deafness associated factor 44
DEAF45	Deafness associated factor 45
DEAF46	Deafness associated factor 46
DEAF47	Deafness associated factor 47
DEAF48	Deafness associated factor 48
DEAF49	Deafness associated factor 49
DEAF50	Deafness associated factor 50
DEAF51	Deafness associated factor 51
DEAF52	Deafness associated factor 52
DEAF53	Deafness associated factor 53
DEAF54	Deafness associated factor 54
DEAF55	Deafness associated factor 55
DEAF56	Deafness associated factor 56
DEAF57	Deafness associated factor 57
DEAF58	Deafness associated factor 58
DEAF59	Deafness associated factor 59
DEAF60	Deafness associated factor 60
DEAF61	Deafness associated factor 61
DEAF62	Deafness associated factor 62
DEAF63	Deafness associated factor 63
DEAF64	Deafness associated factor 64
DEAF65	Deafness associated factor 65
DEAF66	Deafness associated factor 66
DEAF67	Deafness associated factor 67
DEAF68	Deafness associated factor 68
DEAF69	Deafness associated factor 69
DEAF70	Deafness associated factor 70
DEAF71	Deafness associated factor 71
DEAF72	Deafness associated factor 72
DEAF73	Deafness associated factor 73
DEAF74	Deafness associated factor 74
DEAF75	Deafness associated factor 75
DEAF76	Deafness associated factor 76
DEAF77	Deafness associated factor 77
DEAF78	Deafness associated factor 78
DEAF79	Deafness associated factor 79
DEAF80	Deafness associated factor 80
DEAF81	Deafness associated factor 81
DEAF82	Deafness associated factor 82
DEAF83	Deafness associated factor 83
DEAF84	Deafness associated factor 84
DEAF85	Deafness associated factor 85
DEAF86	Deafness associated factor 86
DEAF87	Deafness associated factor 87
DEAF88	Deafness associated factor 88
DEAF89	Deafness associated factor 89
DEAF90	Deafness associated factor 90
DEAF91	Deafness associated factor 91
DEAF92	Deafness associated factor 92
DEAF93	Deafness associated factor 93
DEAF94	Deafness associated factor 94
DEAF95	Deafness associated factor 95
DEAF96	Deafness associated factor 96
DEAF97	Deafness associated factor 97
DEAF98	Deafness associated factor 98
DEAF99	Deafness associated factor 99
DEAF100	Deafness associated factor 100

Figure 2.S2. Full summary of highly differentially expressed genes.

(A) Genes with an absolute fold change > 5 and p < 0.0001 in both day 1 animals. (B) Genes with an absolute fold change > 5 and p < 0.0001 in two of the four day 4 animals. (C) Genes with an absolute fold change > 5 and p < 0.0001 in both day 1 animals and in at least two of the four day 4 animals. Genes that were used for the heat map in figure 2.4 are highlighted in grey.



## REFERENCES

1. Baas, T., C. R. Baskin, D. L. Diamond, A. Garcia-Sastre, H. Bielefeldt-Ohmann, T. M. Tumpey, M. J. Thomas, V. S. Carter, T. H. Teal, N. Van Hoven, S. Proll, J. M. Jacobs, Z. R. Caldwell, M. A. Gritsenko, R. R. Hukkanen, D. G. Camp, 2nd, R. D. Smith, and M. G. Katze. 2006. Integrated molecular signature of disease: analysis of influenza virus-infected macaques through functional genomics and proteomics. *J Virol* 80:10813-10828.
2. Brazma, A., P. Hingamp, J. Quackenbush, G. Sherlock, P. Spellman, C. Stoeckert, J. Aach, W. Ansorge, C. A. Ball, H. C. Causton, T. Gaasterland, P. Glenisson, F. C. Holstege, I. F. Kim, V. Markowitz, J. C. Matese, H. Parkinson, A. Robinson, U. Sarkans, S. Schulze-Kremer, J. Stewart, R. Taylor, J. Vilo, and M. Vingron. 2001. Minimum information about a microarray experiment (MIAME)-toward standards for microarray data. *Nat Genet* 29:365-371.
3. Cella, M., D. Jarrossay, F. Facchetti, O. Alebardi, H. Nakajima, A. Lanzavecchia, and M. Colonna. 1999. Plasmacytoid monocytes migrate to inflamed lymph nodes and produce large amounts of type I interferon. *Nat Med* 5:919-923.
4. Cervantes-Barragan, L., R. Zust, F. Weber, M. Spiegel, K. S. Lang, S. Akira, V. Thiel, and B. Ludewig. 2007. Control of coronavirus infection through plasmacytoid dendritic-cell-derived type I interferon. *Blood* 109:1131-1137.
5. Cheung, C. Y., L. L. Poon, I. H. Ng, W. Luk, S. F. Sia, M. H. Wu, K. H. Chan, K. Y. Yuen, S. Gordon, Y. Guan, and J. S. Peiris. 2005. Cytokine responses in severe acute respiratory syndrome coronavirus-infected macrophages *in vitro*: possible relevance to pathogenesis. *J Virol* 79:7819-7826.
6. Chipman, H., and R. Tibshirani. 2006. Hybrid hierarchical clustering with applications to microarray data. *Biostatistics* 7:286-301.
7. Cinatl, J., B. Morgenstern, G. Bauer, P. Chandra, H. Rabenau, and H. W. Doerr. 2003. Treatment of SARS with human interferons. *Lancet* 362:293-294.
8. Colonna, M., G. Trinchieri, and Y. J. Liu. 2004. Plasmacytoid dendritic cells in immunity. *Nat Immunol* 5:1219-1226.
9. Demedts, I. K., K. R. Bracke, T. Maes, G. F. Joos, and G. G. Brusselle. 2006. Different roles for human lung dendritic cell subsets in pulmonary immune defense mechanisms. *Am J Respir Cell Mol Biol* 35:387-393.
10. Denison, M. R. 2004. Severe acute respiratory syndrome coronavirus pathogenesis, disease and vaccines: an update. *Pediatr Infect Dis J* 23:S207-214.
11. Devaux, P., V. von Messling, W. Songsungthong, C. Springfield, and R. Cattaneo. 2007. Tyrosine 110 in the measles virus phosphoprotein is required to block STAT1 phosphorylation. *Virology* 360:72-83.
12. Franks, T. J., P. Y. Chong, P. Chui, J. R. Galvin, R. M. Lourens, A. H. Reid, E. Selbs, C. P. McEvoy, C. D. Hayden, J. Fukuoka, J. K. Taubenberger, and W. D. Travis. 2003. Lung pathology of severe acute respiratory syndrome (SARS): a study of 8 autopsy cases from Singapore. *Hum Pathol* 34:743-748.
13. Glass, W. G., K. Subbarao, B. Murphy, and P. M. Murphy. 2004. Mechanisms of Host Defense following Severe Acute Respiratory Syndrome-Coronavirus (SARS-CoV) Pulmonary Infection of Mice. *J Immunol* 173:4030-4039.
14. Haagmans, B. L., T. Kuiken, B. E. Martina, R. A. Fouchier, G. F. Rimmelzwaan, G. van Amerongen, D. van Riel, T. de Jong, S. Itamura, K. H. Chan, M. Tashiro, and A. D. Osterhaus. 2004. Pegylated interferon-alpha protects type 1 pneumocytes against SARS coronavirus infection in macaques. *Nat Med* 10:290-293.
15. Hogan, R. J., G. Gao, T. Rowe, P. Bell, D. Flieder, J. Paragas, G. P. Kobinger, N. A. Wivel, R. G. Crystal, J. Boyer, H. Feldmann, T. G. Voss, and J. M. Wilson. 2004. Resolution of primary severe acute respiratory syndrome-associated coronavirus infection requires stat1. *J Virol* 78:11416-11421.
16. Hon, K. L., C. W. Leung, W. T. Cheng, P. K. Chan, W. C. Chu, Y. W. Kwan, A. M. Li, N. C. Fong, P. C. Ng, M. C. Chiu, C. K. Li, J. S. Tam, and T. F. Fok. 2003. Clinical presentations and outcome of severe acute respiratory syndrome in children. *Lancet* 361:1701-1703.
17. Huang, K. J., I. J. Su, M. Theron, Y. C. Wu, S. K. Lai, C. C. Liu, and H. Y. Lei. 2005. An interferon-gamma-related cytokine storm in SARS patients. *J Med Virol* 75:185-194.
18. Jiang, Y., J. Xu, C. Zhou, Z. Wu, S. Zhong, J. Liu, W. Luo, T. Chen, Q. Qin, and P. Deng. 2005. Characterization of cytokine/chemokine profiles of severe acute respiratory syndrome. *Am J Respir Crit Care Med* 171:850-857.

19. Kamitani, W., K. Narayanan, C. Huang, K. Lokugamage, T. Ikegami, N. Ito, H. Kubo, and S. Makino. 2006. Severe acute respiratory syndrome coronavirus nsp1 protein suppresses host gene expression by promoting host mRNA degradation. *Proc Natl Acad Sci U S A* **103**:12885-12890.
20. Kerr, M. K., and G. A. Churchill. 2001. Statistical design and the analysis of gene expression microarray data. *Genet Res* **77**:123-128.
21. Kobasa, D., S. M. Jones, K. Shinya, J. C. Kash, J. Copps, H. Ebihara, Y. Hatta, J. H. Kim, P. Halfmann, M. Hatta, F. Feldmann, J. B. Alimonti, L. Fernando, Y. Li, M. G. Katze, H. Feldmann, and Y. Kawaoka. 2007. Aberrant innate immune response in lethal infection of macaques with the 1918 influenza virus. *Nature* **445**:319-323.
22. Komatsu, T., K. Takeuchi, J. Yokoo, and B. Gotoh. 2002. Sendai virus C protein impairs both phosphorylation and dephosphorylation processes of Stat1. *FEBS Lett* **511**:139-144.
23. Kopecky-Bromberg, S. A., L. Martinez-Sobrido, M. Frieman, R. A. Baric, and P. Palese. 2007. Severe acute respiratory syndrome coronavirus open reading frame (ORF) 3b, ORF 6, and nucleocapsid proteins function as interferon antagonists. *J Virol* **81**:548-557.
24. Kubota, T., N. Yokosawa, S. Yokota, N. Fujii, M. Tashiro, and A. Kato. 2005. Mumps virus V protein antagonizes interferon without the complete degradation of STAT1. *J Virol* **79**:4451-4459.
25. Kuiken, T., R. A. Fouchier, M. Schutten, G. F. Rimmelzwaan, G. van Amerongen, D. van Riel, J. D. Laman, T. de Jong, G. van Doornum, W. Lim, A. E. Ling, P. K. Chan, J. S. Tam, M. C. Zambon, R. Gopal, C. Drosten, S. van der Werf, N. Escriou, J. C. Manuguerra, K. Stohr, J. S. Peiris, and A. D. Osterhaus. 2003. Newly discovered coronavirus as the primary cause of severe acute respiratory syndrome. *Lancet* **362**:263-270.
26. Law, H. K., C. Y. Cheung, H. Y. Ng, S. F. Sia, Y. O. Chan, W. Luk, J. M. Nicholls, J. S. Peiris, and Y. L. Lau. 2005. Chemokine upregulation in SARS-coronavirus-infected, monocyte-derived human dendritic cells. *Blood* **106**:2366-2374.
27. Leung, C. W., and W. K. Chiu. 2004. Clinical picture, diagnosis, treatment and outcome of severe acute respiratory syndrome (SARS) in children. *Paediatr Respir Rev* **5**:275-288.
28. Lin, R. J., B. L. Chang, H. P. Yu, C. L. Liao, and Y. L. Lin. 2006. Blocking of interferon-induced Jak-Stat signaling by Japanese encephalitis virus NS5 through a protein tyrosine phosphatase-mediated mechanism. *J Virol* **80**:5908-5918.
29. Liu, W. J., X. J. Wang, V. V. Mokhonov, P. Y. Shi, R. Randall, and A. A. Khromykh. 2005. Inhibition of interferon signaling by the New York 99 strain and Kunjin subtype of West Nile virus involves blockage of STAT1 and STAT2 activation by nonstructural proteins. *J Virol* **79**:1934-1942.
30. Livak, K. J., and T. D. Schmittgen. 2001. Analysis of relative gene expression data using real-time quantitative PCR and the 2(-Delta Delta C(T)) Method. *Methods* **25**:402-408.
31. Masten, B. J., G. K. Olson, C. A. Tarleton, C. Rund, M. Schuyler, R. Mehran, T. Archibeque, and M. F. Lipscomb. 2006. Characterization of myeloid and plasmacytoid dendritic cells in human lung. *J Immunol* **177**:7784-7793.
32. McCray, P. B., Jr., L. Pewe, C. Wohlford-Lenane, M. Hickey, L. Manzel, L. Shi, J. Netland, H. P. Jia, C. Halabi, C. D. Sigmund, D. K. Meyerholz, P. Kirby, D. C. Look, and S. Perlman. 2007. Lethal infection of K18-hACE2 mice infected with severe acute respiratory syndrome coronavirus. *J Virol* **81**:813-821.
33. Morgenstern, B., M. Michaelis, P. C. Baer, H. W. Doerr, and J. Cinatl, Jr. 2005. Ribavirin and interferon-beta synergistically inhibit SARS-associated coronavirus replication in animal and human cell lines. *Biochem Biophys Res Commun* **326**:905-908.
34. Nanda, S. K., and M. D. Baron. 2006. Rinderpest virus blocks type I and type II interferon action: role of structural and nonstructural proteins. *J Virol* **80**:7555-7568.
35. Ng, L. F., M. L. Hibberd, E. E. Ooi, K. F. Tang, S. Y. Neo, J. Tan, K. R. Murthy, V. B. Vega, J. M. Chia, E. T. Liu, and E. C. Ren. 2004. A human *in vitro* model system for investigating genome-wide host responses to SARS coronavirus infection. *BMC Infect Dis* **4**:34.
36. Nicholls, J. M., L. L. Poon, K. C. Lee, W. F. Ng, S. T. Lai, C. Y. Leung, C. M. Chu, P. K. Hui, K. L. Mak, W. Lim, K. W. Yan, K. H. Chan, N. C. Tsang, Y. Guan, K. Y. Yuen, and J. S. Peiris. 2003. Lung pathology of fatal severe acute respiratory syndrome. *Lancet* **361**:1773-1778.
37. Peiris, J. S., C. M. Chu, V. C. Cheng, K. S. Chan, I. F. Hung, L. L. Poon, K. I. Law, B. S. Tang, T. Y. Hon, C. S. Chan, K. H. Chan, J. S. Ng, B. J. Zheng, W. L. Ng, R. W. Lai, Y. Guan, and K. Y. Yuen. 2003. Clinical progression and viral load in a community outbreak of coronavirus-associated SARS pneumonia: a prospective study. *Lancet* **361**:1767-1772.

38. Peiris, J. S., K. Y. Yuen, A. D. Osterhaus, and K. Stohr. 2003. The severe acute respiratory syndrome. *N Engl J Med* **349**:2431-2441.
39. Reghunathan, R., M. Jayapal, L. Y. Hsu, H. H. Chng, D. Tai, B. P. Leung, and A. J. Melendez. 2005. Expression profile of immune response genes in patients with Severe Acute Respiratory Syndrome. *BMC Immunol* **6**:2.
40. Sainz, B., Jr., E. C. Mossel, C. J. Peters, and R. F. Garry. 2004. Interferon-beta and interferon-gamma synergistically inhibit the replication of severe acute respiratory syndrome-associated coronavirus (SARS-CoV). *Virology* **329**:11-17.
41. Shannon, W., R. Culverhouse, and J. Duncan. 2003. Analyzing microarray data using cluster analysis. *Pharmacogenomics* **4**:41-52.
42. Siegal, F. P., N. Kadowaki, M. Shodell, P. A. Fitzgerald-Bocarsly, K. Shah, S. Ho, S. Antonenko, and Y. J. Liu. 1999. The nature of the principal type 1 interferon-producing cells in human blood. *Science* **284**:1835-1837.
43. Simmons, G., D. N. Gosalia, A. J. Rennekamp, J. D. Reeves, S. L. Diamond, and P. Bates. 2005. Inhibitors of cathepsin L prevent severe acute respiratory syndrome coronavirus entry. *Proc Natl Acad Sci U S A* **102**:11876-11881.
44. Spiegel, M., A. Pichlmair, L. Martinez-Sobrido, J. Cros, A. Garcia-Sastre, O. Haller, and F. Weber. 2005. Inhibition of Beta interferon induction by severe acute respiratory syndrome coronavirus suggests a two-step model for activation of interferon regulatory factor 3. *J Virol* **79**:2079-2086.
45. Spiegel, M., K. Schneider, F. Weber, M. Weidmann, and F. T. Hufert. 2006. Interaction of severe acute respiratory syndrome-associated coronavirus with dendritic cells. *J Gen Virol* **87**:1953-1960.
46. Spiegel, M., and F. Weber. 2006. Inhibition of cytokine gene expression and induction of chemokine genes in non-lymphatic cells infected with SARS coronavirus. *Virol J* **3**:17.
47. Surjit, M., B. Liu, V. T. Chow, and S. K. Lal. 2006. The nucleocapsid protein of severe acute respiratory syndrome-coronavirus inhibits the activity of cyclin-cyclin-dependent kinase complex and blocks S phase progression in mammalian cells. *J Biol Chem* **281**:10669-10681.
48. Tang, B. S., K. H. Chan, V. C. Cheng, P. C. Woo, S. K. Lau, C. C. Lam, T. L. Chan, A. K. Wu, I. F. Hung, S. Y. Leung, and K. Y. Yuen. 2005. Comparative host gene transcription by microarray analysis early after infection of the Huh7 cell line by severe acute respiratory syndrome coronavirus and human coronavirus 229E. *J Virol* **79**:6180-6193.
49. Tang, N. L., P. K. Chan, C. K. Wong, K. F. To, A. K. Wu, Y. M. Sung, D. S. Hui, J. J. Sung, and C. W. Lam. 2005. Early enhanced expression of interferon-inducible protein-10 (CXCL-10) and other chemokines predicts adverse outcome in severe acute respiratory syndrome. *Clin Chem* **51**:2333-2340.
50. Theron, M., K. J. Huang, Y. W. Chen, C. C. Liu, and H. Y. Lei. 2005. A probable role for IFN-gamma in the development of a lung immunopathology in SARS. *Cytokine* **32**:30-38.
51. Tseng, C. T., C. Huang, P. Newman, N. Wang, K. Narayanan, D. M. Watts, S. Makino, M. M. Packard, S. R. Zaki, T. S. Chan, and C. J. Peters. 2007. Severe acute respiratory syndrome coronavirus infection of mice transgenic for the human Angiotensin-converting enzyme 2 virus receptor. *J Virol* **81**:1162-1173.
52. Ware, L. B., and M. A. Matthay. 2000. The acute respiratory distress syndrome. *N Engl J Med* **342**:1334-1349.
53. Wong, C. K., C. W. Lam, A. K. Wu, W. K. Ip, N. L. Lee, I. H. Chan, L. C. Lit, D. S. Hui, M. H. Chan, S. S. Chung, and J. J. Sung. 2004. Plasma inflammatory cytokines and chemokines in severe acute respiratory syndrome. *Clin Exp Immunol* **136**:95-103.
54. Yen, Y. T., F. Liao, C. H. Hsiao, C. L. Kao, Y. C. Chen, and B. A. Wu-Hsieh. 2006. Modeling the early events of severe acute respiratory syndrome coronavirus infection *in vitro*. *J Virol* **80**:2684-2693.
55. Zhang, Y., J. Li, Y. Zhan, L. Wu, X. Yu, W. Zhang, L. Ye, S. Xu, R. Sun, Y. Wang, and J. Lou. 2004. Analysis of serum cytokines in patients with severe acute respiratory syndrome. *Infect Immun* **72**:4410-4415.
56. Zhang, Z., D. Xu, Y. Li, L. Jin, M. Shi, M. Wang, X. Zhou, H. Wu, G. F. Gao, and F. S. Wang. 2005. Longitudinal alteration of circulating dendritic cell subsets and its correlation with steroid treatment in patients with severe acute respiratory syndrome. *Clin Immunol* **116**:225-235.
57. Zheng, B., M. L. He, K. L. Wong, C. T. Lum, L. L. Poon, Y. Peng, Y. Guan, M. C. Lin, and H. F. Kung. 2004. Potent inhibition of SARS-associated coronavirus (SCOV) infection and replication by type I interferons (IFN-alpha/beta) but not by type II interferon (IFN-gamma). *J Interferon Cytokine Res* **24**:388-390.
58. Ziegler, T., S. Matikainen, E. Ronkko, P. Osterlund, M. Sillanpaa, J. Siren, R. Fagerlund, M. Immonen, K. Melen, and I. Julkunen. 2005. Severe acute respiratory syndrome coronavirus fails to activate cytokine-mediated innate immune responses in cultured human monocyte-derived dendritic cells. *J Virol* **79**:13800-13805.





### **Chapter 3**

Early host responses in peripheral blood mononuclear cells of SARS-CoV infected macaques



CHAPTER 3

# Early host responses in peripheral blood mononuclear cells of SARS-CoV infected macaques

Based on:

Anna de Lang, Stewart Chang, Saskia L. Smits, Albert D.M.E. Osterhaus, Michael G. Katze and Bart L. Haagmans

In preparation

### **Chapter 3**

Early host responses in peripheral blood mononuclear cells of SARS-CoV infected macaques

## ABSTRACT

Severe acute respiratory syndrome coronavirus (SARS-CoV) infection causes acute lung injury and acute respiratory distress syndrome. While most pathogenesis studies have focused on the lower respiratory tract, few included other compartments. We analyzed the early transcriptional host response in PBMC from young-adult cynomolgus macaques infected with SARS-CoV. Although no viral RNA could be detected in PBMCs derived from SARS-CoV infected macaques, antiviral and proinflammatory pathways were induced in these cells. Pathway analysis revealed a dominance of genes involved in interferon signaling and pathogen recognition. On the other hand, genes induced in SARS-CoV infected cells like type I IFNs and CCL2, were not differentially expressed in PBMCs. Despite the fact that host gene expression in PBMCs and lungs of SARS-CoV infected macaques showed limited overlap, our analysis revealed that those transcriptional host responses in PBMCs may serve as bio-indicators that reflect early host responses in the lungs

## INTRODUCTION

SARS-CoV causes a severe infection of the lower respiratory tract that is hypothesized to be mediated by a disproportional host immune response, characterized by uncontrolled induction of proinflammatory cytokines. In severe cases SARS-CoV infection lead to acute respiratory distress syndrome (ARDS), characterized by inflammation, pulmonary oedema combined with infiltration of polymorphonuclear leukocytes and macrophages (34). Similar to SARS-CoV infection in humans, a wide range of cytokines and chemokines are detected in the lungs of SARS-CoV infected macaques (9). SARS-CoV replicates efficiently in the lungs of young adult macaques but only mild pathology is observed. In contrast, SARS-CoV mediated pathology in aged macaques is more severe and has characteristics similar to those seen in human SARS patients. The lack of a proper antiviral response in aged SARS-CoV infected macaques, characterized by lower levels of type I interferon (IFN) as compared to young adult macaques, might be one of the reasons for the observed differences (30).

Other SARS-CoV induced disease symptoms besides lower respiratory infection, include fever, myalgia and headaches, and in some patients diarrhea (19, 25). In line with these findings, SARS-CoV RNA has not only been detected in the lungs but also in respiratory secretions, faeces and urine (5). Although SARS-CoV does not seem to replicate in human PBMCs, analysis of the blood may be informative to further characterize the pathogenesis of SARS. A number of chemokines and cytokines have been detected in sera from SARS patients (4, 14, 32). Other studies have associated characteristics of the transcriptional host response in PBMCs to disease outcome in human SARS patients, suggesting host responses in the blood could function as a prognostic marker for disease severity (4). Since only few clinical samples are available, mainly taken relatively late during infection, more research is needed to determine whether SARS-CoV replicates in PBMCs and to characterize the SARS-CoV induced host responses in PBMCs. In this study, we employed an animal model to analyze the host response in PBMCs after SARS-CoV infection. We examined SARS-CoV replication and SARS-CoV induced host responses in PBMCs derived from SARS-CoV infected young adult macaques and compared host responses in the blood and lungs early during infection, which can be of value when using PBMCs for diagnostic and prognostic purposes.

## MATERIALS AND METHODS

### Lung and PBMC samples from SARS-CoV infected macaques

Lung tissues collected at time of necropsy at day 4 and peripheral blood samples collected just before infection (day 0) and at day 1, day 2 and day 4 after infection were used from four young adult cynomolgus macaques (*Macaca fascicularis*), 3-5 years old, that were inoculated with SARS-CoV strain HKU39849 in a previous study (30). Necropsies and sampling for histology/immunohistochemistry were performed as described previously (12). Upon collection, lung tissues were stored in RNA later (Invitrogen) and PBMCs were collected in Tempus Blood RNA tubes (Applied Biosystems) after which samples were frozen

at -80°C. Approval for animal experiments was obtained from the Institutional Animal Welfare Committee and performed according to Dutch guidelines for animal experimentation.

### **Isolation of RNA from lung tissue and PBMCs**

RNA was isolated from homogenized post mortem tissue samples using Trizol Reagent (Invitrogen) and the RNeasy mini kit (Qiagen). RNA was extracted from PBMCs using the Tempus Spin RNA isolation reagent kit (Applied Biosystems) according to the manufacturer's instructions. After RNA isolation from PBMC samples, RNA was purified by removing globin mRNA using the GLOBINclear kit (Ambion).

### **SARS-CoV specific RT-PCR**

cDNA synthesis was performed with 1 µg of total RNA and Superscript III RT (Invitrogen) with oligo(dT), according to the manufacturer's instructions. Semi-quantitative RT-PCR was performed to detect SARS-CoV mRNA (17). Differences in SARS-CoV gene expression are represented as the fold change in gene expression relative to a calibrator and normalized to a reference, using the  $2^{-\Delta\Delta Ct}$  method (20). GAPDH (glyceraldehydes-3-phosphate dehydrogenase) was used as endogenous control to normalize quantification of the target gene. RNA derived from lung tissue from four young macaques from a previous study was used as negative control and served as the calibrator. Average results ( $\pm$  S.E.M.) for SARS-CoV infected macaques were expressed as fold change compared to values in young adults PBS-infected animals, in the case of the lungs and to values in PBMCs at day 0 in the case of PBMC samples from day 1, day 2 and day 4 after SARS-CoV infection.

### **Microarray analysis**

Microarray analysis was performed using Agilent rhesus macaque 4x 44 K microarrays using the manufacturer's one-color analysis protocol (Agilent). Data from lung samples were normalized using a variance stabilization algorithm (VSN) and data from PBMC samples were normalized using quantile normalization (13). All gene expression data described here are publicly available at <http://viromics.washington.edu>. Differential gene expression between the different groups (lungs from SARS-CoV infected macaques versus lungs from PBS infected macaques, PBMCs from SARS-CoV macaques at day 1, day 2 or day 4 after infection versus PBMCs taken before SARS-CoV infection) was determined by LIMMA (version 2.12.0) (31). Correction for multiple testing was achieved by requiring a false discovery rate (FDR) of 0.05, calculated with the Benjamini-Hochberg procedure (3). To understand the gene functions and the biological processes represented in the data and obtain differentially expressed molecular and cellular functions, Ingenuity Pathways Knowledge Base (<http://www.ingenuity.com/>) was used. Heat maps were produced using complete linkage and Euclidian distance in Spotfire DecisionSite for Functional Genomics version 9.1 (<http://www.spotfire.com/>).

## RESULTS AND DISCUSSION

In order to analyze SARS-CoV mediated host responses in young adult macaques, four cynomolgus macaques were inoculated with SARS-CoV strain HKU-39849 after which blood samples were collected at days 1, 2 and 4 after infection and lung tissues at day 4 after infection. SARS-CoV infection of young adult macaques did not cause clinical symptoms and limited pulmonary consolidation was observed (30). The lesions in the lungs consisted of acute exudative diffuse alveolar damage and multifocal mild chronic lymphoplasmacytic tracheo-bronchoadenitis, characterized by moderate numbers of lymphocytes, plasma cells, macrophages, some neutrophils and occasional eosinophils in the lamina propria of the bronchi, focally surrounding and infiltrating the submucosal glands (30). RNA isolated from lungs and PBMCs from the SARS-CoV infected macaques was used to analyze SARS-CoV replication with a virus specific RT-PCR. Although SARS-CoV-induced pathological changes are limited in these young adult macaques, SARS-CoV efficiently replicates to high titers in the lungs of all SARS-CoV infected macaques (figure 3.1A). In PBMCs derived from these same animals, however, no virus could be detected at different days after infection (figure 3.1B).

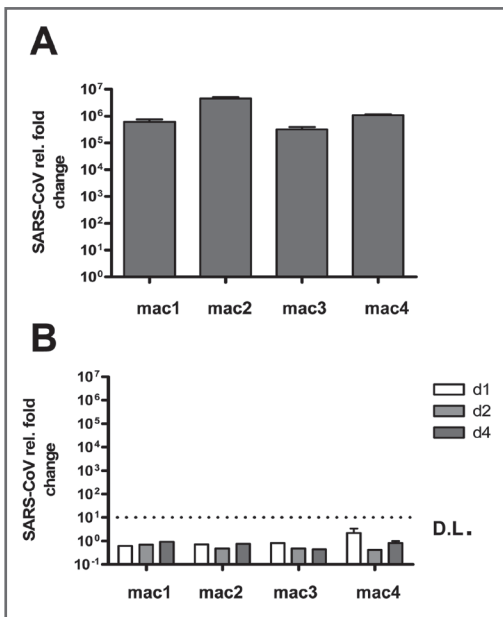


**Figure 3.1. SARS-CoV RNA levels in lung and PBMCs.** Fold increases in SARS-CoV gene transcripts in lungs from SARS-CoV infected macaques at day 4 after infection as compared to the lungs from PBS infected animals (A) and SARS-CoV gene transcripts in PBMCs from SARS-CoV infected macaques at day 1, day 2 and day 4 after SARS-CoV infection as compared to basal levels before infection (B) were determined using RT-PCR. The detection limit is represented as a dotted line.

To get a broad overview of host responses in PBMCs at the different time points after infection, microarray studies were performed and all genes differentially expressed at any of the time points were represented in a heatmap (figure 3.2A). Genes with an absolute fold change of at least 2 as compared to

expression in PBMCs taken before SARS-CoV infection, with a FDR lower than 0.05, were considered to be differentially expressed. Using these criteria, 611 genes were differentially expressed at day 1, 404 genes at day 2 and 186 genes at day 4 after SARS-CoV infection (figure 3.2B). A similar pattern, with numbers of differentially expressed genes peaking at day 1 and decreasing till day 4, was observed in the lungs of SARS-CoV infected macaques, but also in other SARS models (2, 9, 30) (de Lang et al., this thesis). Further analysis of host responses after SARS-CoV infection in macaque PBMCs showed that the majority of genes that were differentially expressed in PBMCs from SARS-CoV infected macaques were upregulated and a much smaller portion was downregulated.

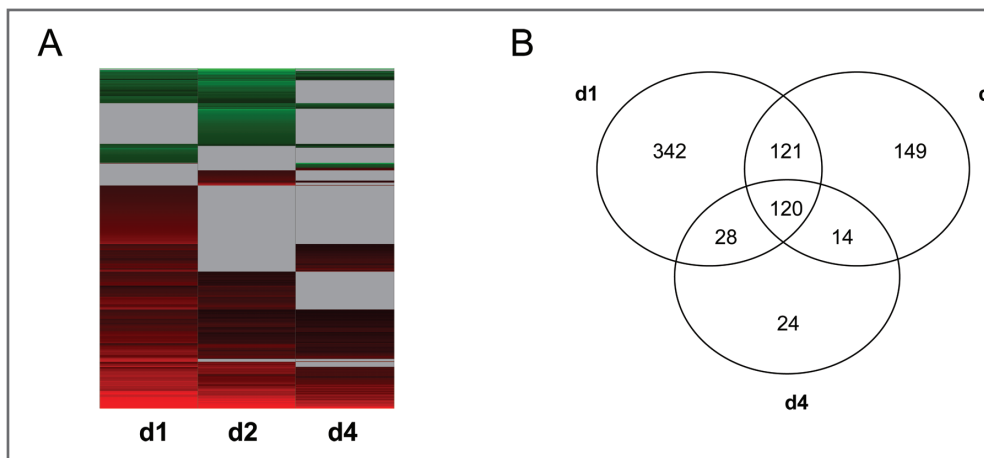


**Figure 3.2. Genes differentially expressed in PBMCs from SARS-CoV infected macaques.** All genes differentially expressed (absolute fold change  $>2$ ,  $p < 0.05$ ) either at day 1, 2 or 4 after infection in PBMCs from SARS-CoV infected macaques are represented in a heatmap (A). Genes depicted in red are upregulated compared to genes in the control group (PBMCs derived before SARS-CoV infection) and genes depicted in green are downregulated compared to the control group. Genes with a p-value higher than 0.05 were depicted in grey. The minimum and the maximum values of the color range in the heatmap were -4 and 4 respectively, using the log (base 2) fold change expression values. Common and unique genes within the sets of differentially expressed genes from PBMCs derived at the three different time points were determined by creating a Venn diagram (B).

Using Ingenuity Knowledge Base a more detailed analysis was performed to order the differentially expressed genes within a context of biological processes and pathways. These analyses revealed that pathways activated in macaque PBMCs were quite similar at the different days after infection, although the number of genes differentially expressed varied between the different time points. Overall, 120 genes were significantly regulated on all days, making up 20% of the total number of differentially expressed genes at day 1 and almost 65% of the genes significantly regulated at day 4. This indicates that the response on day 4 is mainly a remainder of genes activated at day 1 after infection (figure 3.2B). Early transcriptional host responses in PBMCs at day 1 after SARS-CoV infection are dominated by genes involved in recognition of invading pathogens and subsequent antiviral and inflammatory pathways.

Genes encoding for a range of pattern recognition receptors (PRRs), like the NOD-like receptors (NLRs) NLRP3 and NOD2, several Toll-like receptors (TLRs), the RNA helicases RIG-I (DDX58) and MDA-5 (IFIH1), but also molecules involved in transducing signals from the PRRs downstream like the adaptor molecule MyD88, are upregulated in PBMCs from SARS-CoV infected macaques (figure 3.3).

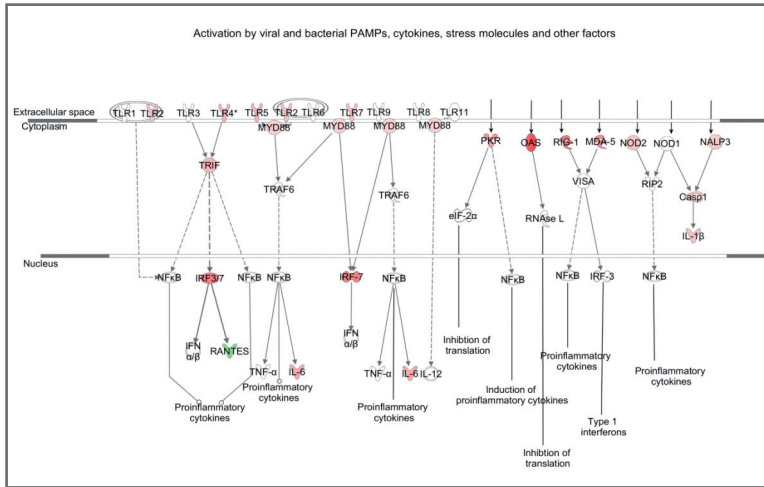


**Figure 3.3. Schematic representation of PRR signaling pathways activated in PBMCs.** Genes that were differentially expressed within these pathways (absolute fold change >2,  $p < 0.05$ ) in macaque PBMCs at day 1 after infection are depicted in red when upregulated or in green, when downregulated as compared to day 0. Intensity of coloring was relative to the log ratio fold changes in gene transcription which ranged from -1.02 to 5.60. The PRR signaling pathway was adapted from Ingenuity Knowledge Base.

NLRs are mainly involved in generating inflammatory and apoptotic responses. Together with PYCARD, caspase 1 and caspase 5, the latter two also induced in macaque PBMCs, the NLR protein NLRP3 can form an inflammasome (8, 22). The inflammasome is a multimeric structure that plays an important role in the activation of proinflammatory responses and is expressed in myeloid cells. Activation of the inflammasome leads to caspase 1 mediated processing and production of the proinflammatory cytokines IL-1 $\beta$  and IL-18. Different host factors, like moieties associated with danger and damage, as well as foreign molecules and pathogen-derived components can activate the inflammasome. In addition, several components of the inflammasome can be induced by IFN- $\gamma$ , which is induced in the lungs of SARS-CoV infected macaques. The fact that a number of genes involved in formation of the inflammasome are upregulated in PBMCs, further illustrated by induced expression of IL-1 $\beta$ , indicates that proinflammatory pathways are activated within these cells. Besides forming an inflammasome, activated NLRs are able to induce proinflammatory cytokines by engaging with the triggering receptor expressed on myeloid cells-1 (TREM1), also induced in macaque PBMCs upon SARS-CoV infection (24). This receptor is mainly expressed on subgroups of monocytes, macrophages and neutrophils and interaction between NLRs and



TREM1 leads to amplified induction of proinflammatory cytokines. CCL7, upregulated in PBMCs, is one of the cytokines typically upregulated after TREM1 activation (10, 29).

TREM1 does not only interact with the NLRs, but also with the TLRs, resulting in activation of proinflammatory genes as CCL2, CCL3, IL-8, IL-1 $\beta$  and TNF- $\alpha$ , through the transcription factor NF- $\kappa$ B (29). TLRs are another family of PRRs, involved in the induction of both inflammatory and antiviral responses. The TLRs are expressed both on the cell surface and within the cell in endosomes, depending on the subtype, and recognize the highly conserved pathogen-associated molecular patterns (PAMPs) after which they activate signaling pathways in the cell (1). Several TLR genes were upregulated in PBMCs from SARS-CoV infected macaques, namely TLR2, TLR3, TLR4, TLR5 and TLR7. Expression of TLRs can be regulated by various pathogens, but since no SARS-CoV RNA could be detected in these PBMCs, expression of these molecules is most likely induced by host factors, such as cytokines. For example, TLR2 and TLR4 expression can be induced by IL-1 $\beta$  and IFN- $\gamma$ , TLR3 expression can be induced by IFN- $\alpha$  and TLR5 and TLR7 can be induced by IL-6 (23, 27, 33, 37). All of these cytokines are upregulated in the macaque lung after SARS-CoV infection and could be responsible for the observed upregulation of TLRs in the blood.

Activation of TLRs does not only lead to activation of proinflammatory pathways, but induces antiviral pathways as well. Elevated expression levels of genes involved in IFN production, signaling as well as IFN stimulated genes (ISGs) indicate that antiviral pathways are readily activated in PBMCs from SARS-CoV infected macaques. For instance, the interferon regulatory factor (IRF)-7 and IRF9, which are activated by PRRs, are upregulated in PBMCs at day 1 after infection. Especially IRF7 plays an important role in the induction of type I IFNs, since it regulates many IFN- $\alpha$  genes (21). Although no IFNs were detected in PBMCs, several genes involved in IFN signaling, such as JAK2 and STAT1, as well as ISGs like IFIT1, IFIT3, IFI35, OAS genes and MX genes were induced in these cells.

At day 2 and 4 after SARS-CoV infection, similar canonical pathways were activated as on day 1 after infection, including pathways involved in recognition of viruses, IFN production and IFN signaling but also pathways involved in communication between innate and adaptive immunity. Although similar pathways were activated at different time points after infection in PBMCs, fewer genes within each pathway were differentially expressed. A set of 149 genes was uniquely expressed in PBMCs at day 2 after infection, as shown in the Venn diagram in figure 3.2B. Further analysis of this specific gene set showed that also these genes were mainly involved in the previously mentioned pathways. Apparently, at day 2 after infection other genes within these same pathways were additionally differentially expressed. IFNs were not differentially upregulated genes in macaque PBMCs at any time point. Thus, PBMCs in SARS-CoV infected macaques seem to respond to mediators released from the lungs at an early stage, illustrated by strong activation of IFN related pathways as well as proinflammatory pathways.

In comparison to 186 genes differentially expressed in macaque PBMCs at day 4 after infection, 358 genes were differentially expressed in the lungs of these macaques at the same day after infection. The higher number of differentially expressed genes in the lungs compared to PBMCs reflects the fact that the lungs are the main site of viral infection. As shown in the Venn diagram (figure 3.4), only 55 genes showed an overlap between both gene sets. A set of 48 genes was differentially expressed in lungs and PBMCs at all time points with the majority of these genes being involved in the recognition of invading pathogens and IFN signaling. This set included genes like DDX58, DHX58, IRF7, ISGs, IFIT genes, OAS genes

and STAT1, but also the proinflammatory chemokine CXCL10 and IFN- $\gamma$ . Interestingly, IFN- $\gamma$  was downregulated in PBMCs at all time points, but upregulated in the lung. One other gene in this set, the Charcot-Leyden crystal (CLC) gene, was downregulated both in PBMCs and in the lung. In SARS patients with severe disease the CLC protein is highly upregulated, possibly this induction takes place in a later phase of infection (16, 26). In the lungs, increased expression of IFNs and CCL2 could be detected. The fact that CCL2 is not induced in PBMCs at any of the time points, is indicative for the absence of viral particles in the blood, as CCL2 has been shown to be directly induced by SARS-CoV infection through signaling via the ACE2 receptor (6). Increased levels of CCL2, a monocyte attractant, have been associated with ARDS and have been observed in SARS patients as well (14, 28). In line with this, CCL2 is upregulated in the lungs of SARS-CoV infected macaques, mice and even ferrets, in which only a very limited number of genes is upregulated after SARS-CoV infection (9, 30)(de Lang et al., manuscript submitted and this thesis). IFN production has also been detected in lungs of mice and ferrets upon infection and we have shown that diverse types of IFNs are induced in murine pDCs by SARS-CoV particles (de Lang et al., manuscript submitted).

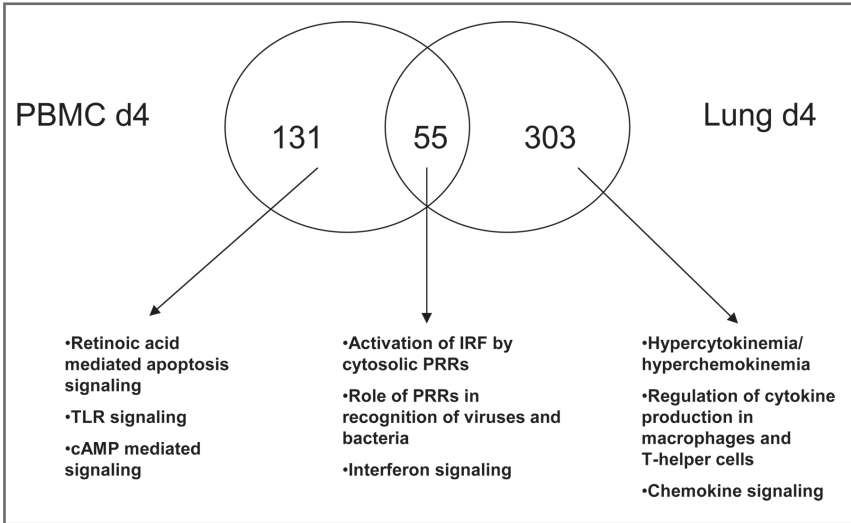


**Figure 3.4. Similarities and differences between host responses in PBMCs and the lung.** Common and unique genes within the sets of differentially expressed genes (absolute fold change  $>2$ ,  $p < 0.05$ ) at day 4 in PBMCs and at day 4 in the lungs of SARS-CoV infected macaques were represented in a Venn diagram. The most important canonical pathways, as determined with Ingenuity, are listed for each Venn area, representing pathways uniquely activated in either PBMCs or lungs at day 4 after SARS-CoV infection or pathways commonly activated in both compartments.

Besides IFNs and the proinflammatory chemokine CCL2 also other proinflammatory genes are induced in the macaque lung that are not detected in PBMCs, such as IL-6, CCL13, GZMB, CCL4, CCL8 and CXCL11, but also CCL11, and CXCL9. Many of these chemokines and cytokines are involved in respiratory diseases

such as damage of the lung, eosinophilia of the airway, asthma and airway hyperresponsiveness. On the other hand, in PBMCs from the SARS-CoV infected macaques 131 genes were uniquely expressed as compared to lung and this set included genes involved in retinoic acid mediated apoptosis, with upregulation of several PARP genes and TRAIL genes and genes involved in TLR signaling such as TLR2 and TLR3, which were upregulated at day 4 in PBMCs. In addition, a number of genes involved in cyclic adenosine monophosphate (cAMP) mediated signaling were uniquely expressed in PBMCs at day 4 after infection. cAMP is a second messenger that plays an important role in many biological processes by transferring and amplifying signals from the cell surface, from molecules such as hormones or cytokines, to target molecules inside the cell. In figure 3.5 the differences in cytokine and chemokine induction between PBMCs and lungs after SARS-CoV infection are illustrated by a heatmap that shows differential expression data of a wide range of cytokine and chemokine genes. While only few genes are differentially expressed both in PBMCs and the lung, such as CXCL10 and CXCL1, clearly more proinflammatory genes as well as IFNs are differentially expressed in the lung. Some cytokines such as IL-27 and CCL23 are exclusively upregulated in PBMCs. IL-27 is a cytokine related to IL-12A that is produced by antigen presenting cells and involved in the regulation of T-helper cell differentiation (35). CCL23 (MIP-3) and CXCL3 (MIP-2B) are chemoattractants for macrophages and T-cells. Expression of these cytokines can all be upregulated by IL-1 $\beta$ , expressed in PBMCs after SARS-CoV infection, but most likely also by other cytokines such as IFNs (7, 11).

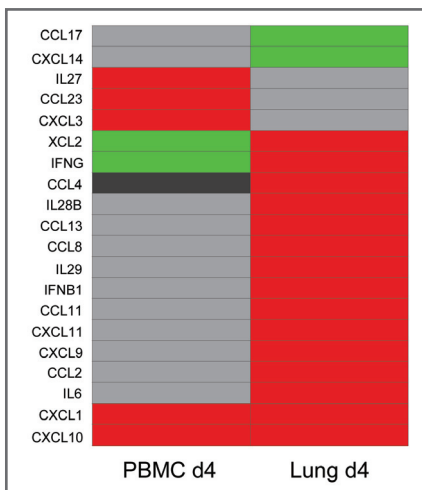


**Figure 3.5. Induction of cytokines and chemokines in PBMCs and lung after SARS-CoV infection.** Expression of a wide range of cytokines and chemokines was evaluated in PBMCs and lungs from SARS-CoV infected macaques. Genes depicted in red and green represent genes that are differentially expressed (absolute fold change >2,  $p < 0.05$ ) with upregulated genes represented in red and downregulated genes represented in green. Genes depicted in dark grey have a  $p$ -value  $< 0.05$  but do not make the fold change cutoff. Genes depicted in light grey have a  $p$ -value higher than 0.05.

In conclusion, this is the first study that examined SARS-CoV mediated host responses in PBMCs early during infection in an animal model. Using genomics, host responses in PBMCs from SARS-CoV infected macaques were analyzed and compared to host responses in the lung, the main site of infection. Although no viral RNA was detected in PBMCs, more than 600 genes were differentially expressed at day 1 after SARS-CoV infection, mainly involved in activation of antiviral and proinflammatory pathways.

However, IFNs and CCL2, indicative of the presence of SARS-CoV particles, were not upregulated in PBMCs, corresponding with the absence of viral RNA in RT-PCR analysis. Upregulation of PRRs like NLRs and TLRs and other genes involved in recognition of invading viruses, suggests that blood cells are being prepared for interaction with SARS-CoV, probably by IFNs and proinflammatory cytokines produced in the lung (15). The fact that a set of genes is induced in PBMCs but not in the lungs is most likely caused by the distinct cell types in the lungs and PBMC.

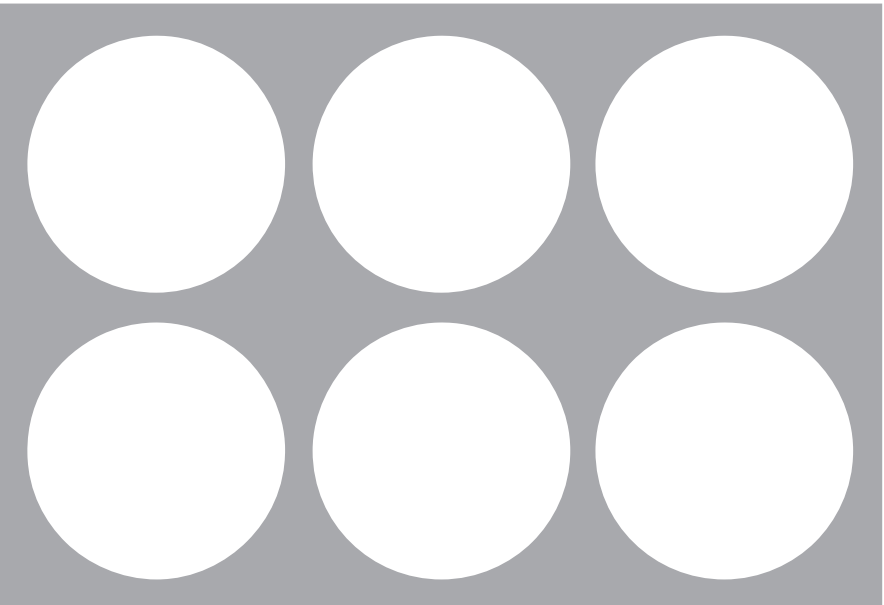
Transcriptional gene expression profiles in PBMCs from human SARS patients have been used to correlate to SARS disease outcome (4, 18, 26, 36). While Reghunathan et al. observed activation of proinflammatory pathways in PBMCs from SARS patients but no proinflammatory cytokines and chemokines, other groups did report increased transcription of proinflammatory cytokines and chemokines such as IL-1 $\beta$ , IL-8, TNF- $\alpha$ , CXCL10 and CCL2, some of which have been associated with poor disease outcome when detected early after the onset of disease symptoms (4, 32, 36). In addition, while IFN-induced genes are downregulated in PBMCs from acute phase SARS patients in one study, these same genes are upregulated in another study that also detected elevated levels of IFN- $\alpha$  protein in sera from human SARS patients during the acute phase of disease (4, 36). These mixed results found in PBMCs from human SARS patients may be explained by variation in type of patients included, treatments given, time of sampling and assays used to analyze results, but may also signify the great variety in host responses seen in different SARS patients due to factors as age and comorbidities. In this study we show that gene expression profiles in PBMCs do not accurately represent the genes activated in the lungs of SARS-CoV infected macaques early during infection but may reflect downstream activation of mediators, mainly IFNs, produced in the lungs.

## REFERENCES

1. Akira, S., K. Takeda, and T. Kaisho. 2001. Toll-like receptors: critical proteins linking innate and acquired immunity. *Nat Immunol* **2**:675-680.
2. Baas, T., A. Roberts, T. H. Teal, L. Vogel, J. Chen, T. M. Tumpey, M. G. Katze, and K. Subbarao. 2008. Genomic analysis reveals age-dependent innate immune responses to severe acute respiratory syndrome coronavirus. *J Virol* **82**:9465-9476.
3. Benjamini, Y., and Y. Hochberg. 1995. Controlling the False Discovery Rate - a Practical and Powerful Approach to Multiple Testing. *J Roy Stat Soc B Met* **57**:289-300.
4. Cameron, M. J., L. Ran, L. Xu, A. Danesh, J. F. Bermejo-Martin, C. M. Cameron, M. P. Muller, W. L. Gold, S. E. Richardson, S. M. Poutanen, B. M. Willey, M. E. DeVries, Y. Fang, C. Seneviratne, S. E. Bosinger, D. Persad, P. Wilkinson, L. D. Greller, R. Somogyi, A. Humar, S. Keshavjee, M. Louie, M. B. Loeb, J. Brunton, A. J. McGeer, S. R. N. Canadian, and D. J. Kelvin. 2007. Interferon-mediated immunopathological events are associated with atypical innate and adaptive immune responses in patients with severe acute respiratory syndrome. *J Virol* **81**:8692-8706.
5. Chan, K. H., L. L. Poon, V. C. Cheng, Y. Guan, I. F. Hung, J. Kong, L. Y. Yam, W. H. Seto, K. Y. Yuen, and J. S. Peiris. 2004. Detection of SARS coronavirus in patients with suspected SARS. *Emerg Infect Dis* **10**:294-299.
6. Chen, I. Y., S. C. Chang, H. Y. Wu, T. C. Yu, W. C. Wei, S. Lin, C. L. Chien, and M. F. Chang. 2010. Upregulation of the chemokine (C-C motif) ligand 2 via a severe acute respiratory syndrome coronavirus spike-ACE2 signaling pathway. *J Virol* **84**:7703-7712.
7. Chevillard, G., A. Derjuga, D. Devost, H. H. Zingg, and V. Blank. 2007. Identification of interleukin-1beta regulated genes in uterine smooth muscle cells. *Reproduction* **134**:811-822.
8. Davis, B. K., H. Wen, and J. P. Ting. 2011. The inflammasome NLRs in immunity, inflammation, and associated diseases. *Annu Rev Immunol* **29**:707-735.
9. de Lang, A., T. Baas, T. Teal, L. M. Leijten, B. Rain, A. D. Osterhaus, B. L. Haagmans, and M. G. Katze. 2007. Functional genomics highlights differential induction of antiviral pathways in the lungs of SARS-CoV-infected macaques. *PLoS Pathog* **3**:e112.
10. Dower, K., D. K. Ellis, K. Saraf, S. A. Jelinsky, and L. L. Lin. 2008. Innate immune responses to TREM-1 activation: overlap, divergence, and positive and negative cross-talk with bacterial lipopolysaccharide. *J Immunol* **180**:3520-3534.
11. Forssmann, U., M. B. Delgado, M. Uguccioni, P. Loetscher, G. Garotta, and M. Baggiolini. 1997. Ckbeta8, a novel CC chemokine that predominantly acts on monocytes. *FEBS Lett* **408**:211-216.
12. Haagmans, B. L., T. Kuiken, B. E. Martina, R. A. Fouchier, G. F. Rimmelzwaan, G. van Amerongen, D. van Riel, T. de Jong, S. Itamura, K. H. Chan, M. Tashiro, and A. D. Osterhaus. 2004. Pegylated interferon-alpha protects type 1 pneumocytes against SARS coronavirus infection in macaques. *Nat Med* **10**:290-293.
13. Huber, W., A. von Heydebreck, H. Sultmann, A. Poustka, and M. Vingron. 2002. Variance stabilization applied to microarray data calibration and to the quantification of differential expression. *Bioinformatics* **18 Suppl** 1:S96-104.
14. Jiang, Y., J. Xu, C. Zhou, Z. Wu, S. Zhong, J. Liu, W. Luo, T. Chen, Q. Qin, and P. Deng. 2005. Characterization of cytokine/chemokine profiles of severe acute respiratory syndrome. *Am J Respir Crit Care Med* **171**:850-857.
15. Khoo, J. J., S. Forster, and A. Mansell. 2011. Toll-like receptors as interferon-regulated genes and their role in disease. *J Interferon Cytokine Res* **31**:13-25.
16. Kong, S. L., P. Chui, B. Lim, and M. Salto-Tellez. 2009. Elucidating the molecular physiopathology of acute respiratory distress syndrome in severe acute respiratory syndrome patients. *Virus Res* **145**:260-269.
17. Kuiken, T., R. A. Fouchier, M. Schutten, G. F. Rimmelzwaan, G. van Amerongen, D. van Riel, J. D. Laman, T. de Jong, G. van Doornum, W. Lim, A. E. Ling, P. K. Chan, J. S. Tam, M. C. Zambon, R. Gopal, C. Drosten, S. van der Werf, N. Escriou, J. C. Manuguerra, K. Stohr, J. S. Peiris, and A. D. Osterhaus. 2003. Newly discovered coronavirus as the primary cause of severe acute respiratory syndrome. *Lancet* **362**:263-270.
18. Lee, Y. S., C. H. Chen, A. Chao, E. S. Chen, M. L. Wei, L. K. Chen, K. D. Yang, M. C. Lin, Y. H. Wang, J. W. Liu, H. L. Eng, P. C. Chiang, T. S. Wu, K. C. Tsao, C. G. Huang, Y. J. Tien, T. H. Wang, and H. S. Wang. 2005. Molecular signature of clinical severity in recovering patients with severe acute respiratory syndrome coronavirus (SARS-CoV). *BMC Genomics* **6**:132.
19. Leung, W. K., K. F. To, P. K. Chan, H. L. Chan, A. K. Wu, N. Lee, K. Y. Yuen, and J. J. Sung. 2003. Enteric involvement of severe acute respiratory syndrome-associated coronavirus infection. *Gastroenterology* **125**:1011-1017.

20. Livak, K. J., and T. D. Schmittgen. 2001. Analysis of relative gene expression data using real-time quantitative PCR and the 2(-Delta Delta C(T)) Method. *Methods* **25**:402-408.
21. Marie, I., J. E. Durbin, and D. E. Levy. 1998. Differential viral induction of distinct interferon-alpha genes by positive feedback through interferon regulatory factor-7. *EMBO J* **17**:6660-6669.
22. Martinon, F., K. Burns, and J. Tschopp. 2002. The inflammasome: a molecular platform triggering activation of inflammatory caspases and processing of proIL-beta. *Mol Cell* **10**:417-426.
23. Muzio, M., D. Bosisio, N. Polentarutti, G. D'Amico, A. Stoppacciaro, R. Mancinelli, C. van't Veer, G. Penton-Rol, L. P. Ruco, P. Allavena, and A. Mantovani. 2000. Differential expression and regulation of toll-like receptors (TLR) in human leukocytes: selective expression of TLR3 in dendritic cells. *J Immunol* **164**:5998-6004.
24. Netea, M. G., T. Azam, G. Ferwerda, S. E. Girardin, S. H. Kim, and C. A. Dinarello. 2006. Triggering receptor expressed on myeloid cells-1 (TREM-1) amplifies the signals induced by the NACHT-LRR (NLR) pattern recognition receptors. *J Leukoc Biol* **80**:1454-1461.
25. Peiris, J. S., C. M. Chu, V. C. Cheng, K. S. Chan, I. F. Hung, L. L. Poon, K. I. Law, B. S. Tang, T. Y. Hon, C. S. Chan, K. H. Chan, J. S. Ng, B. J. Zheng, W. L. Ng, R. W. Lai, Y. Guan, and K. Y. Yuen. 2003. Clinical progression and viral load in a community outbreak of coronavirus-associated SARS pneumonia: a prospective study. *Lancet* **361**:1767-1772.
26. Reghunathan, R., M. Jayapal, L. Y. Hsu, H. H. Chng, D. Tai, B. P. Leung, and A. J. Melendez. 2005. Expression profile of immune response genes in patients with Severe Acute Respiratory Syndrome. *BMC Immunol* **6**:2.
27. Ritter, M., D. Mennerich, A. Weith, and P. Seither. 2005. Characterization of Toll-like receptors in primary lung epithelial cells: strong impact of the TLR3 ligand poly(I:C) on the regulation of Toll-like receptors, adaptor proteins and inflammatory response. *J Inflamm (Lond)* **2**:16.
28. Rose, C. E., Jr., S. S. Sung, and S. M. Fu. 2003. Significant involvement of CCL2 (MCP-1) in inflammatory disorders of the lung. *Microcirculation* **10**:273-288.
29. Sharif, O., and S. Knapp. 2008. From expression to signaling: roles of TREM-1 and TREM-2 in innate immunity and bacterial infection. *Immunobiology* **213**:701-713.
30. Smits, S. L., A. de Lang, J. M. van den Brand, L. M. Leijten, I. W. F. van, M. J. Eijkemans, G. van Amerongen, T. Kuiken, A. C. Andeweg, A. D. Osterhaus, and B. L. Haagmans. 2010. Exacerbated innate host response to SARS-CoV in aged non-human primates. *PLoS Pathog* **6**:e1000756.
31. Smyth, G. K. 2004. Linear models and empirical bayes methods for assessing differential expression in microarray experiments. *Stat Appl Genet Mol Biol* **3**:Article3.
32. Tang, N. L., P. K. Chan, C. K. Wong, K. F. To, A. K. Wu, Y. M. Sung, D. S. Hui, J. J. Sung, and C. W. Lam. 2005. Early enhanced expression of interferon-inducible protein-10 (CXCL-10) and other chemokines predicts adverse outcome in severe acute respiratory syndrome. *Clin Chem* **51**:2333-2340.
33. Tissari, J., J. Siren, S. Meri, I. Julkunen, and S. Matikainen. 2005. IFN-alpha enhances TLR3-mediated antiviral cytokine expression in human endothelial and epithelial cells by upregulating TLR3 expression. *J Immunol* **174**:4289-4294.
34. Ware, L. B., and M. A. Matthay. 2000. The acute respiratory distress syndrome. *N Engl J Med* **342**:1334-1349.
35. Yoshida, H., M. Nakaya, and Y. Miyazaki. 2009. Interleukin 27: a double-edged sword for offense and defense. *J Leukoc Biol* **86**:1295-1303.
36. Yu, S. Y., Y. W. Hu, X. Y. Liu, W. Xiong, Z. T. Zhou, and Z. H. Yuan. 2005. Gene expression profiles in peripheral blood mononuclear cells of SARS patients. *World J Gastroenterol* **11**:5037-5043.
37. Zarembek, K. A., and P. J. Godowski. 2002. Tissue expression of human Toll-like receptors and differential regulation of Toll-like receptor mRNAs in leukocytes in response to microbes, their products, and cytokines. *J Immunol* **168**:554-561.





## Chapter 4

Plasmacytoid dendritic cells drive early antiviral and proinflammatory host responses in SARS-CoV infected mice



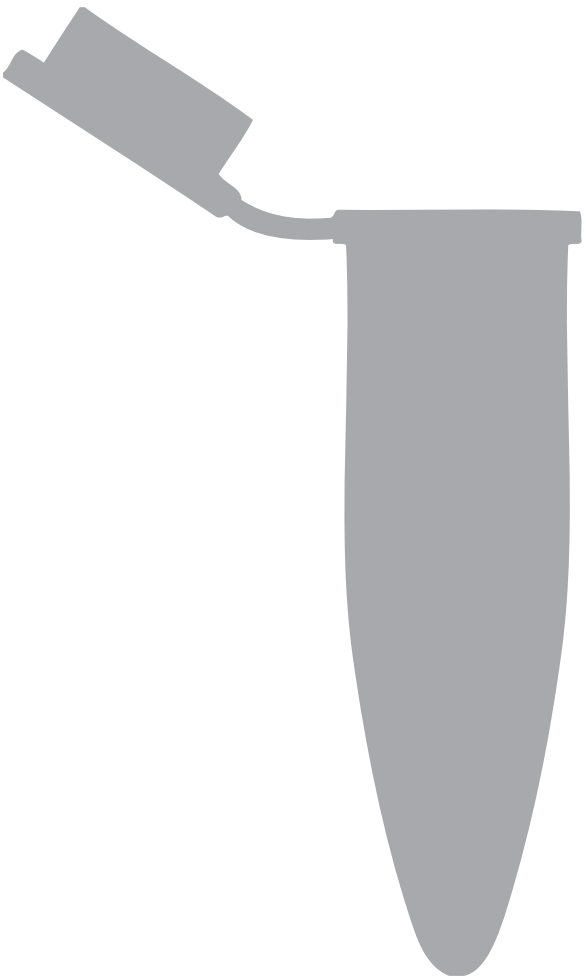
## CHAPTER 4

# Plasmacytoid dendritic cells drive early antiviral and proinflammatory host responses in SARS-CoV infected mice

Based on:

Anna de Lang, Corine H. Geurts van Kessel, Geert van Amerongen, Maarten A. Bijl, Fatiha Zaaoui-Boutahar, Louis Boon, Albert D.M.E. Osterhaus, Arno C. Andeweg and Bart L. Haagmans

submitted for publication



Interferon- $\gamma$  and interleukin-4 downregulate expression of the SARS-CoV receptor ACE2 in Vero E6 cells

CHAPTER 5

# Interferon- $\gamma$ and interleukin-4 downregulate expression of the SARS- CoV receptor ACE2 in Vero E6 cells

Based on:

Anna de Lang, Albert D.M.E Osterhaus and Bart L. Haagmans

*Virology*, 2006: 30;353(2):474-481

Interferon- $\gamma$  and interleukin-4 downregulate expression of the  
SARS-CoV receptor ACE2 in Vero E6 cells

## Chapter 5

## ABSTRACT

Interferons (IFNs) inhibit severe acute respiratory syndrome coronavirus (SARS-CoV) replication and might be valuable for SARS treatment. In this study we demonstrate that treatment of Vero E6 cells with interleukin-4 (IL-4) decreased the susceptibility of these cells to SARS-CoV infection. In contrast to IFNs, IL-4 did not show antiviral activity when administered immediately after SARS-CoV infection, suggesting that IL-4 acts early during the SARS-CoV replication cycle. Indeed, binding of recombinant SARS-CoV spike protein to Vero E6 cells was diminished on cells treated with IL-4, but also on cells exposed to IFN- $\gamma$ . Consistent with these observations, IL-4 and IFN- $\gamma$  downregulated cell-surface expression of angiotensin-converting enzyme 2 (ACE2), the SARS-CoV receptor. Besides diminished ACE2 cell-surface expression, ACE2 mRNA levels were also decreased after treatment with these cytokines. These findings suggest that IL-4 and IFN- $\gamma$  inhibit SARS-CoV replication partly through downregulation of ACE2.

## INTRODUCTION

Severe acute respiratory syndrome (SARS) emerged late 2002/early 2003 in Guangdong Province, China, and spread rapidly to several countries in Asia, North America and Europe, causing disease in almost 8000 people, of whom nearly 10% died. Only a few months after the first emergence of SARS, a newly discovered coronavirus (CoV) was identified as its etiological agent (6, 19, 31). SARS-CoV is a positive stranded RNA virus with a genome of about 30 kb in length that is structurally similar to that of other group 2 coronaviruses (27, 32, 35). It enters the host cell by binding of the spike (S) protein S<sub>1</sub> domain to angiotensin-converting enzyme 2 (ACE2), the SARS-CoV receptor (22). Subsequently, the S<sub>2</sub> domain fuses with the cellular membrane (24). ACE2 is a component of the renin-angiotensin system and mainly involved in the regulation of heart function and blood pressure (1, 4). It is expressed in vascular endothelia, heart, kidney and testis, but also in epithelia of the small intestine and in alveolar epithelial cells (5, 11-12). Recently it was shown that ACE2 also acts as a receptor for human coronavirus NL63 (HCoV-NL63) (13).

SARS-CoV replicates predominantly in the lower respiratory tract and causes diffuse alveolar damage, leading to severe respiratory distress (21, 30). Treatment of SARS patients was mainly based on the use of ribavirin and corticosteroids, but the efficacy of these drugs has not been proven. Several groups have examined the antiviral effect of interferons (IFNs) against SARS-CoV. *In vitro* studies have shown that human recombinant IFNs inhibit SARS-CoV replication and that IFN- $\beta$  and IFN- $\gamma$  combined have a synergistic antiviral effect against this virus (3, 29, 33). Furthermore, we have demonstrated that pegylated IFN- $\alpha$  protected type-I pneumocytes from infection with SARS-CoV in cynomolgous macaques (10). Usually IFNs achieve their antiviral effect through the induction of various proteins that block viral replication in the infected cell. To further explore the antiviral effect of IFNs and other cytokines specifically against SARS-CoV infection, we treated Vero E6 cells with various amounts of IFN- $\gamma$ , tumor necrosis factor (TNF)- $\alpha$  or interleukin (IL)-4 and infected these cells with SARS-CoV.

## MATERIALS AND METHODS

### Cells and cytokine treatment

Vero E6 cells (ATCC) were grown in Dulbecco's modified Eagle's medium (DMEM), supplemented with 10% fetal bovine serum (FBS), sodium bicarbonate and 20 mM Hepes buffer. Unless stated otherwise, recombinant human (r-hu) IL-4 (BD Pharmingen), r-hu IFN- $\gamma$ , r-hu TNF- $\alpha$ , r-hu IL-13, r-hu IL-10 (Peprotech Inc.) and r-hu IFN- $\alpha$  (Roche) were added to cell cultures at a concentration of 10 ng/ml, 48 h urs before infection. As a specificity control, r-hu IL-4 was pre-incubated with a neutralizing IL-4 antibody (Ebiosciences) for 30 minutes at 37° C before addition to the cells. All treatments were done in quadruplets (96-well experiments) or triplicate (6-well and 24-well experiments).

## Infection of Vero E6 cells and immunohistochemistry

Vero E6 cells grown in 96-well plates (Greiner Bio-one) were infected with  $10^5$  50% tissue culture infective doses (TCID<sub>50</sub>) SARS-CoV (HKU-39849) or HSV-1, by adding the virus directly to Vero E6 cell cultures. After 16 hours, cells were fixed with 10% neutral-buffered formalin and treated with 70% ethanol (10 min RT). SARS-CoV infected cells were visualized using purified human IgG from a convalescent SARS patient (CSL), followed by staining with an antibody to human IgG, linked to horseradish peroxidase (Amersham Biosciences). HSV infected cells were stained using a rabbit anti HSV-1 antiserum, followed by staining with an antibody to rabbit IgG, linked to horseradish peroxidase (DAKO). In the case of the HCoV-NL63 infection, Vero E6 cells cultured in the presence or absence of IL-4 were infected with  $10^4$  TCID<sub>50</sub> HCoV-NL63. The inoculum was removed after 1 hour and replaced with fresh medium. After 48 hours, the supernatant from these cells was titrated on fresh Vero E6 cells. Antiviral activity of IL-4 against SARS-CoV was determined by plaque titration. Vero E6 cells were grown in 24-well plates (Greiner Bio-one) in the presence or absence of IL-4 and infected with  $10^5$  TCID<sub>50</sub> SARS-CoV. After 1 h, the inoculum was removed and fresh medium was added. Supernatant from these cultures was taken at 16 h and plaque titrated by inoculating fresh Vero E6 cells, cultured in 6-well plates (Greiner Bio-one), for 1 h. Subsequently, cells were washed and culture medium containing 0.5% low melting point agarose was added. The plates were incubated at 37°C for 3 days, plaques were counted in wells containing approximately 10-100 plaques and the results were expressed as PFU/ml.

## SARS-CoV and ACE2 RT-PCR

RT-PCR with primers and probe specific for the nucleoprotein gene of SARS-CoV was used to quantify SARS-CoV in infected cells, as described earlier (21). Serial dilutions of the SARS-CoV stock were used as a standard. ACE2 mRNA levels were determined using the ACE2 Taqman Gene Expression Assay (Applied Biosystems). Differences in ACE2 expression were represented as the fold change in gene expression normalized to a reference, using the  $2^{-\Delta\Delta Ct}$  method (25). The housekeeping gene GAPDH was used as the reference and the IFN- $\gamma$ /TNF- $\alpha$  treated cells were used as the calibrator, since those cells had the lowest ACE2 expression.

## Spike protein binding studies

Binding of the SARS-CoV S protein was analyzed using flow cytometry. A His-tagged S protein (Protein Sciences) was incubated with cytokine-treated and mock-treated Vero E6 cells for 1 hour at 4°C, followed by  $\alpha$ His-FITC (Invitrogen) staining, to detect binding of the S protein.

## ACE2 expression studies

Vero E6 cells, with or without cytokine treatment, were stained with a polyclonal goat  $\alpha$ ACE2 antibody (R&D Systems) followed by staining with an anti-goat-FITC antibody (Sigma). As a control for background staining of the  $\alpha$ ACE2 antibody, cells were incubated with normal goat serum (MP Biomedicals). Staining of the ACE2 receptor on Vero E6 cells could be blocked with soluble ACE2 protein (R&D systems), but not with the soluble ACE protein (R&D systems), demonstrating the specificity of the ACE2 antibody (data not shown).

## RESULTS

### Susceptibility of Vero E6 cells to SARS-CoV or HSV infection after cytokine treatment

Vero E6 cells were treated with 1, 10 or 100 ng/ml of IL-4, IL-10, IFN- $\gamma$ , TNF- $\alpha$  or a combination of IFN- $\gamma$  and TNF- $\alpha$  and infected with SARS-CoV or herpes simplex virus (HSV)-1. While treatment with TNF- $\alpha$  (figure 5.1A) or IL-10 (data not shown) had no antiviral effect against SARS-CoV or HSV-1, pretreatment with IFN- $\gamma$  (figure 5.1B) or a combination of IFN- $\gamma$  and TNF- $\alpha$  (figure 5.1C) dose dependently reduced the number of infected cells per well after infection with either one of these viruses, as demonstrated previously (3, 7). Surprisingly, recombinant human IL-4 also exerted SARS-CoV antiviral activity, which was not observed against HSV infection (figure 5.1D), suggesting a virus specific antiviral activity. We also tested the antiviral activity of IL-4 against HCoV-NL63, another coronavirus that also uses the ACE2 receptor to enter the cell (13). Compared to untreated control cells, viral excretion from infected Vero E6 cells was reduced by more than 1 log after IL-4 treatment (figure 5.2).

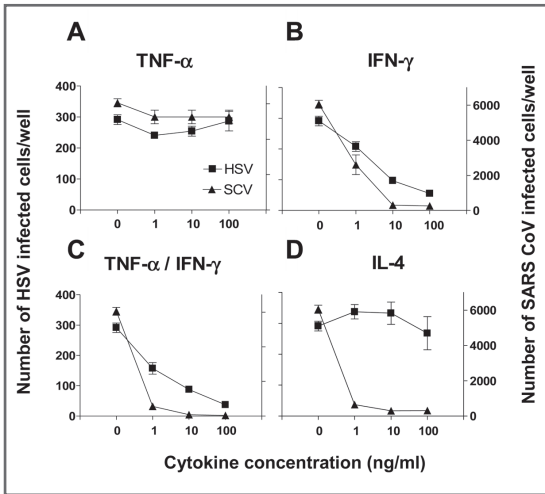


Figure 5.1. Susceptibility of Vero E6 cells to SARS-CoV or HSV-1 infection after treatment with TNF- $\alpha$  (A), IFN- $\gamma$  (B), IFN- $\gamma$  combined with TNF- $\alpha$  (C) or IL-4 (D). Triangle-shaped symbols represent SARS-CoV and rectangular symbols represent HSV-1. The left Y-axis indicates the number of infected cells per well after HSV infection, while the right Y-axis represents the number of infected cells per well after SARS-CoV (SCV) infection. Error bars indicate standard errors.

### Antiviral activity of IL-4 against SARS-CoV

We further evaluated the antiviral effect of IL-4 against SARS-CoV using a SARS-CoV-specific RT-PCR and plaque titration on Vero E6 cells. After pretreatment of the cells with 10 ng/ml IL-4 for 48 hours and subsequent infection, excretion of SARS-CoV from the treated cells was diminished by 1 log, just as SARS-CoV RNA levels in these cells (figure 5.3A-B). The antiviral effect of IL-4 was abrogated after pre-incubation with a neutralizing IL-4 antibody (figure 5.3A-B). These results further demonstrate that IL-4 has a modest antiviral activity against SARS-CoV infection in Vero E6 cells.

To determine which step of the SARS-CoV life cycle is affected by IL-4, conditioned medium from



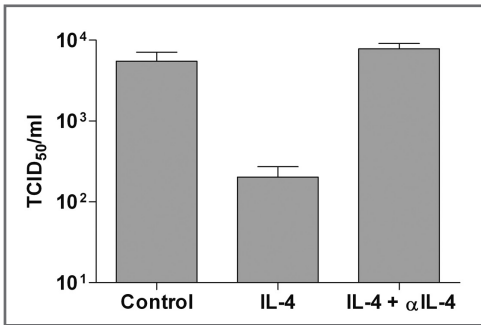


Figure 5.2. Antiviral activity of IL-4 against HCoV-NL63. Titration of supernatant after infection of Vero E6 cells with  $10^5$  TCID<sub>50</sub> HCoV-NL63. Error bars indicate standard errors.

Vero E6 cells that were treated with IL-4 (10 ng/ml) was removed and the cells were washed before they were infected with SARS-CoV. Removal of IL-4 conditioned medium from the Vero E6 cells after 48 hours of treatment still conferred protection against not inhibit replication of SARS-CoV once it has entered the cell and needs to be added to the cells at an earlier time point. Thus, IL-4 most likely has an antiviral effect on an early step of the SARS-CoV life cycle in Vero E6 cells.

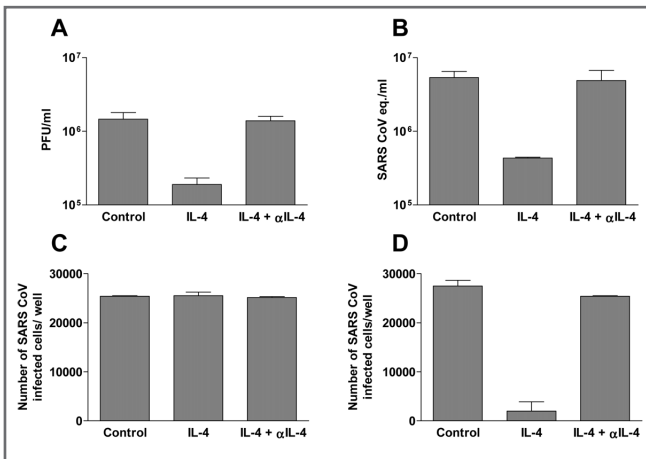
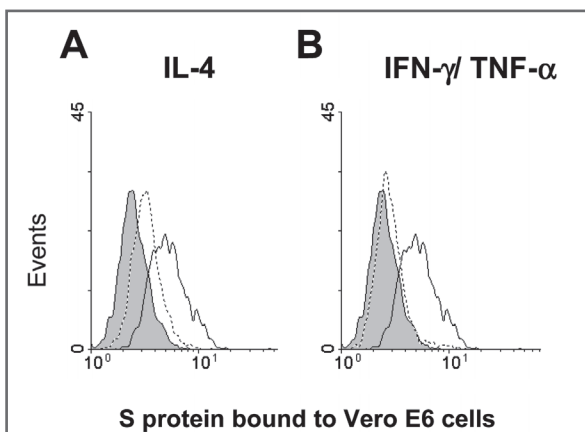


Figure 5.3. Antiviral activity of IL-4 against SARS-CoV. Plaque titration of supernatant (A) or amount of SARS-CoV RNA (B) present in mock (control), 10 ng/ml IL-4 or IL-4/ $\alpha$ -IL-4 treated cells that were infected with  $10^5$  TCID<sub>50</sub> SARS-CoV. Susceptibility of IL-4 treated Vero E6 cells to SARS-CoV infection after removal of IL-4 conditioned medium and subsequent washing (C) and susceptibility of fresh Vero E6 cells to SARS-CoV after receiving IL-4 conditioned medium just before infection with  $10^5$  TCID<sub>50</sub> SARS-CoV (D). Error bars indicate standard errors.

### Binding of recombinant SARS-CoV spike protein to cytokine treated Vero E6 cells

Since IL-4 treatment reduced excretion of virus, viral replication and infection, only when administered before SARS-CoV infection, binding of the SARS-CoV S protein to cytokine treated Vero E6 cells was analyzed using flow cytometry. As shown in figure 5.4A, treatment with IL-4 reduced the ability of Vero E6 cells to bind recombinant S protein. Because IFN- $\gamma$  combined with TNF- $\alpha$  also reduced susceptibility of Vero E6 cells to SARS-CoV, we analyzed binding of the S protein to these cells after IFN- $\gamma$ /TNF- $\alpha$  treatment and demonstrated that 10 ng/ml IFN- $\gamma$ /TNF- $\alpha$  reduced the binding capacity of the S protein to a

background level (figure 5.4B). These data suggest that these cytokines influence expression of the cellular receptor for SARS-CoV, ACE2.



**Figure 5.4.** Binding of recombinant SARS-CoV S protein to Vero E6 cells after treatment with 10 ng/ml IL-4 (A) or a combination of 10 ng/ml IFN- $\gamma$  and 10 ng/ml TNF- $\alpha$  (B). Dotted lines represent cytokine-treated cells, while thick lines represent mock treated control cells. The shaded areas represent background staining.

### Effect of cytokine treatment on ACE2 expression

To examine if IL-4 and IFN- $\gamma$ /TNF- $\alpha$  decrease susceptibility to SARS-CoV infection through an effect on cell surface ACE2 expression, we analysed ACE2 expression after cytokine treatment. As shown in figure 5.5A, 10 ng/ml IL-4 downregulated ACE2 expression and pre-incubation with a neutralizing IL-4 antibody abolished the IL-4 effect (figure 5.5B). Similarly, treatment of Vero E6 cells with 100 ng/ml IL-13 - also a Th2 cytokine - downregulated ACE2 expression and inhibited SARS-CoV replication (data not shown). Background staining was determined by incubating the cells with normal goat serum followed by the secondary antibody (figure 5.5).

A more pronounced decrease in ACE2 expression was observed after treatment with a combination of 10 ng/ml IFN- $\gamma$  and 10 ng/ml TNF- $\alpha$  compared to treatment with these cytokines separately (figure 5.5C-E). After removal of the cytokines, ACE2 expression was restored only gradually to pre-treatment levels (data not shown) whereas addition of fresh IFN- $\gamma$  and TNF- $\alpha$  at 48 h further decreased ACE2 expression to background level (figure 5.5F). Downregulation of ACE2 was not caused by an overall inhibitory effect on cell surface protein expression; IFN- $\gamma$  and IL-4 both upregulated MHC class I expression on Vero E6 cells (figure 5.5G and 5.5H).

When ACE2 expression on Vero E6 cells was followed in time after treatment with IL-4, a gradual decrease in ACE2 expression was observed, which was maximal at 48 hours after treatment (figure 5.6A). The decrease in ACE2 expression over time, correlated with decreased susceptibility to SARS-CoV infection (figure 5.6B). These experiments also demonstrate that IL-4 only displayed antiviral activity when administered at least 24 h before infection with SARS-CoV (figure 5.6B). In contrast, treatment with IFN- $\alpha$  1 hour after SARS-CoV infection reduced replication by at least 1 log (not shown). These results further substantiate our hypothesis that IL-4 inhibits SARS-CoV replication through downregulation of ACE2.

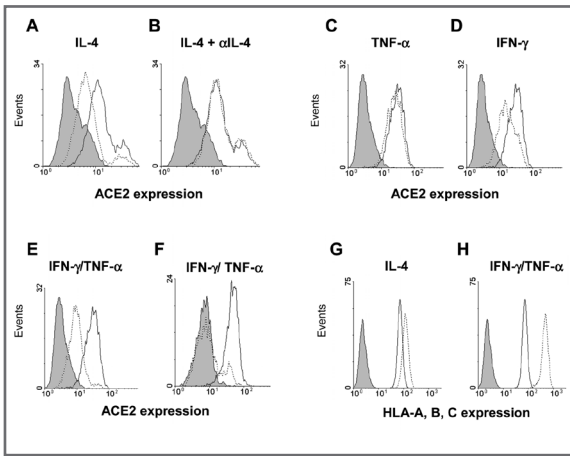


**Figure 5.5.** Influence of cytokine treatment on ACE2 expression. ACE2 expression was determined after treatment with 10 ng/ml IL-4 (A), IL-4 pre-incubated with a neutralizing antibody (B), 10 ng/ml TNF- $\alpha$  (C), 10 ng/ml IFN- $\gamma$  (D) or 10 ng/ml IFN- $\gamma$  combined with 10 ng/ml TNF- $\alpha$  (E), all at 48 h. Vero E6 cells were incubated for 96 h in the presence of 10 ng/ml IFN- $\gamma$  combined with 10 ng/ml TNF- $\alpha$  (F). HLA-A, B, C expression on Vero E6 cells after treatment with 10 ng/ml IL-4 (G) or IFN- $\gamma$  combined with TNF- $\alpha$  (H). Dotted lines represent cytokine-treated cells, while thick lines represent mock treated control cells. The shaded areas represent background staining.

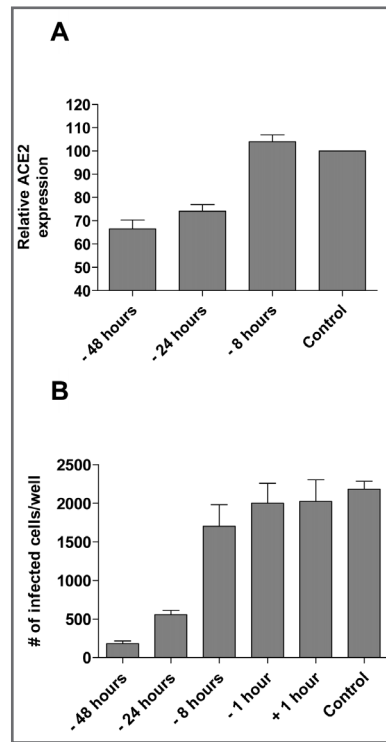


**Figure 5.6.** ACE2 expression and SARS-CoV susceptibility at different time points after IL-4 treatment. ACE2 expression on Vero E6 cells was monitored at different time points after IL-4 treatment relative to control cells (A). Susceptibility of Vero E6 cells to SARS-CoV was monitored at different time points before and after treatment with 10 ng/ml IL-4 (B). Shown is the number of SARS-CoV infected cells per well.

### ACE2 mRNA levels after cytokine treatment

The fact that ACE2 downregulation after IL-4 treatment is a gradual process and that ACE2 expression recovers slowly when cytokines are removed, suggests that ACE2 is downregulated at the mRNA level. Using an ACE2-specific Taqman, we observed reduced ACE2 mRNA levels in Vero E6 cells after 48 hours of IL-4 or IFN- $\gamma$ /TNF- $\alpha$  treatment (figure 5.7). This implicates that downregulation of ACE2 by these cytokines is regulated at transcription level.

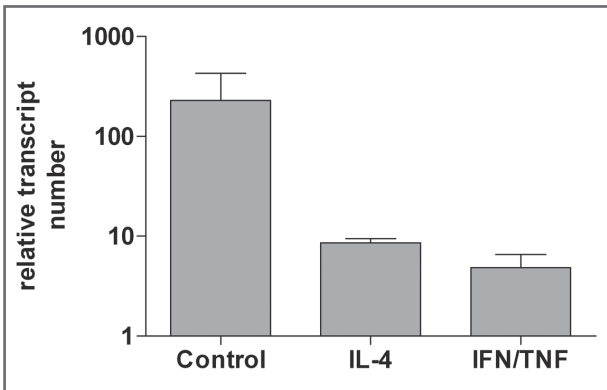


Figure 5.7. ACE2 mRNA levels in Vero E6 cells after treatment with 10 ng/ml IL-4 or a combination of 10 ng/ml IFN- $\gamma$  and 10 ng/ml TNF- $\alpha$  compared to ACE2 mRNA levels in untreated control cells. ACE2 mRNA levels in untreated control cell in IL-4 treated cells are represented as the fold change in gene expression relative to the IFN- $\gamma$ /TNF- $\alpha$  treated cells, which were used as the calibrator. GAPDH was used as an endogenous control.

## DISCUSSION

It is well established that IFNs inhibit replication of many different viruses, including SARS-CoV (3, 10, 29, 33). When IFNs bind to their receptors, downstream signaling from these receptors can block one or more steps in the virus life cycle. IL-4 on the other hand does not induce these proteins and may even antagonise the protective effects of IFN (26). In general, the Th2-derived cytokine IL-4 is not considered to display antiviral activity. In fact, only a few studies have demonstrated IL-4 mediated inhibition of viral replication (8, 23). Furthermore, expression of IL-4 by recombinant ectromelia virus or vaccinia virus exacerbated infection *in vivo* and the administration of recombinant IL-4 delayed virus clearance in influenza virus-infected mice (17, 28, 34). In this study we demonstrate that treatment of Vero E6 cells with IL-4 decreased susceptibility of these cells to SARS-CoV infection by 10-100 fold. Interestingly, ACE2 expression on the cell surface was downregulated after treatment with IL-4 or IFN- $\gamma$ . Therefore, we postulate that IL-4 and IFN- $\gamma$  may decrease susceptibility to SARS-CoV infection partially through modulation of ACE2 cell-surface expression. Cytokine-mediated downregulation of viral receptors has been reported earlier in the case of the coxsackievirus-adenovirus receptor, which can be downregulated synergistically by IFN- $\gamma$  and TNF- $\alpha$  *in vitro* (39).

In this study we show that the antiviral activity of IL-4 was not observed when IL-4 was added after SARS-CoV infection. This suggests that IL-4 inhibits entry of the virus, possibly through an effect on the viral receptor ACE2. In line with these observations, IL-4 does not have an antiviral effect against HSV, but does show antiviral activity against HCoV-NL63, which also utilizes ACE2 as a receptor. Subsequent experiments revealed that ACE2 expression indeed is downregulated by IL-4. Confirmation of ACE2's involvement as an intermediate of the IL-4 antiviral activity is hard to proof because of its essential role in SARS-CoV infection.

ACE2 is a component of the renin-angiotensin system and enzymatically cleaves angiotensin I into angiotensin 1-9 and angiotensin II into angiotensin 1-7 (5, 38). Several studies have reported regulation of ACE2 expression, most likely related to its enzymatic activity. ACE2 protein expression is downregu-

lated in the kidneys of hypertensive or diabetic rats (4, 37), whereas ACE2 upregulation has been demonstrated after blocking of the angiotensin II-receptors in the kidneys of rats during pregnancy, and in the human failing heart (2, 4, 9, 16, 37). Furthermore, it was recently shown that ACE2 is downregulated in the lungs of mice after acute lung injury, including SARS-CoV infection (20). Most probably, ACE2 can be regulated by several different factors and expression of this protein is dynamic on various cell types. Recently it was reported that ACE2 expression is dependent on the differentiation state of epithelia; ACE2 was poorly expressed on undifferentiated airway epithelial cells, while it was abundantly expressed on well-differentiated cells (18). It will be of interest to study the effect of IL-4 and IFN- $\gamma$  on ACE2 expression on these cells.

The ACE2 downregulation was cytokine-specific; while IFN- $\gamma$  and IL-4 both downregulated ACE2 expression, IFN- $\alpha$ , a cytokine that inhibits SARS-CoV replication *in vivo* and *in vitro*, did not affect ACE2 expression on Vero E6 cells (data not shown). Treatment of Vero E6 cells with IL-13 on the other hand also downregulated ACE2, suggesting the involvement of the IL-4 type II receptor in the IL-4 induced antiviral activity. However, this hypothesis could not be further substantiated because antibodies against the IL-4 type II receptor tested were not reactive on non-human primate Vero E6 cells. Forced downregulation of ACE2 expression by cytokines may reveal a novel antiviral strategy against SARS-CoV infection. Potentially, addition of cytokines able to downregulate ACE2 expression could further improve the efficacy of IFN- $\alpha$  based anti SARS-CoV therapy. However, downregulation of ACE2 may have a potential negative effects on SARS pathogenesis, since it was recently reported that ACE2 has a protective role in acute lung failure in mice (15). Therefore it will be necessary to explore the consequences of ACE2 downregulation on SARS pathogenesis.

The most important finding of this study is the observation that cytokines modulate ACE2 expression. The physiological relevance of the IL-4 induced antiviral activity may be limited because this cytokine is probably not produced in large quantities during natural SARS-CoV infection (14, 40). However, vaccination strategies utilizing inactivated SARS-CoV or subunits in the presence of specific alum based adjuvants, may skew immune response to TH2 or THo, allowing the production of IL-4 upon restimulation (36). The relevance of ACE2 expression modulation by IFN- $\gamma$  in the pathogenesis of SARS and NL-63 CoV needs further investigation.

## ACKNOWLEDGEMENTS

We thank R. Lonsdale, B. Martina and R.F. van Lavieren for their assistance with SARS-CoV infections.

## REFERENCES

1. Boehm, M., and E. G. Nabel. 2002. Angiotensin-converting enzyme 2—a new cardiac regulator. *N Engl J Med* **347**:1795-7.
2. Brosnihan, K. B., L. A. Neves, J. Joyner, D. B. Averill, M. C. Chappell, R. Sarao, J. Penninger, and C. M. Ferrario. 2003. Enhanced renal immunocytochemical expression of ANG-(1-7) and ACE2 during pregnancy. *Hypertension* **42**:749-53.
3. Cinatl, J., B. Morgenstern, G. Bauer, P. Chandra, H. Rabenau, and H. W. Doerr. 2003. Treatment of SARS with human interferons. *Lancet* **362**:293-4.
4. Crackower, M. A., R. Sarao, G. Y. Oudit, C. Yagil, I. Kozieradzki, S. E. Scanga, A. J. Oliveira-dos-Santos, J. da Costa, L. Zhang, Y. Pei, J. Scholey, C. M. Ferrario, A. S. Manoukian, M. C. Chappell, P. H. Backx, Y. Yagil, and J. M. Penninger. 2002. Angiotensin-converting enzyme 2 is an essential regulator of heart function. *Nature* **417**:822-8.
5. Donoghue, M., F. Hsieh, E. Baronas, K. Godbout, M. Gosselin, N. Stagliano, M. Donovan, B. Woolf, K. Robison, R. Jeyaseelan, R. E. Breitbart, and S. Acton. 2000. A novel angiotensin-converting enzyme-related carboxypeptidase (ACE2) converts angiotensin I to angiotensin 1-9. *Circ Res* **87**:E1-9.
6. Drosten, C., S. Gunther, W. Preiser, S. van der Werf, H. R. Brodt, S. Becker, H. Rabenau, M. Panning, L. Kolesnikova, R. A. Fouchier, A. Berger, A. M. Burguiere, J. Cinatl, M. Eickmann, N. Escriou, K. Grywna, S. Kramme, J. C. Manuguerra, S. Muller, V. Rickerts, M. Sturmer, S. Vieth, H. D. Klenk, A. D. Osterhaus, H. Schmitz, and H. W. Doerr. 2003. Identification of a novel coronavirus in patients with severe acute respiratory syndrome. *N Engl J Med* **348**:1967-76.
7. Feduchi, E., M. A. Alonso, and L. Carrasco. 1989. Human gamma interferon and tumor necrosis factor exert a synergistic blockade on the replication of herpes simplex virus. *J Virol* **63**:1354-9.
8. Goletti, D., A. L. Kinter, E. M. Coccia, A. Battistini, N. Petrosillo, G. Ippolito, and G. Poli. 2002. Interleukin (IL)-4 inhibits phorbol-ester induced HIV-1 expression in chronically infected U1 cells independently from the autocrine effect of endogenous tumour necrosis factor-alpha, IL-1beta, and IL-1 receptor antagonist. *Cytokine* **17**:28-35.
9. Goulter, A. B., M. J. Goddard, J. C. Allen, and K. L. Clark. 2004. ACE2 gene expression is upregulated in the human failing heart. *BMC Med* **2**:19.
10. Haagmans, B. L., T. Kuiken, B. E. Martina, R. A. Fouchier, G. F. Rimmelzwaan, G. van Amerongen, D. van Riel, T. de Jong, S. Itamura, K. H. Chan, M. Tashiro, and A. D. Osterhaus. 2004. Pegylated interferon-alpha protects type 1 pneumocytes against SARS coronavirus infection in macaques. *Nat Med* **10**:290-3.
11. Hamming, I., W. Timens, M. L. Bulthuis, A. T. Lely, G. J. Navis, and H. van Goor. 2004. Tissue distribution of ACE2 protein, the functional receptor for SARS coronavirus. A first step in understanding SARS pathogenesis. *J Pathol* **203**:631-7.
12. Harmer, D., M. Gilbert, R. Borman, and K. L. Clark. 2002. Quantitative mRNA expression profiling of ACE 2, a novel homologue of angiotensin converting enzyme. *FEBS Lett* **532**:107-10.
13. Hofmann, H., K. Pyrc, L. van der Hoek, M. Geier, B. Berkhout, and S. Pohlmann. 2005. Human coronavirus NL63 employs the severe acute respiratory syndrome coronavirus receptor for cellular entry. *Proc Natl Acad Sci U S A* **102**:7988-93.
14. Huang, K. J., I. J. Su, M. Theron, Y. C. Wu, S. K. Lai, C. C. Liu, and H. Y. Lei. 2005. An interferon-gamma-related cytokine storm in SARS patients. *J Med Virol* **75**:185-94.
15. Imai, Y., K. Kuba, S. Rao, Y. Huan, F. Guo, B. Guan, P. Yang, R. Sarao, T. Wada, H. Leong-Poi, M. A. Crackower, A. Fukamizu, C. C. Hui, L. Hein, S. Uhlig, A. S. Slutsky, C. Jiang, and J. M. Penninger. 2005. Angiotensin-converting enzyme 2 protects from severe acute lung failure. *Nature* **436**:112-6.
16. Ishiyama, Y., P. E. Gallagher, D. B. Averill, E. A. Tallant, K. B. Brosnihan, and C. M. Ferrario. 2004. Upregulation of angiotensin-converting enzyme 2 after myocardial infarction by blockade of angiotensin II receptors. *Hypertension* **43**:970-6.
17. Jackson, R. J., A. J. Ramsay, C. D. Christensen, S. Beaton, D. F. Hall, and I. A. Ramshaw. 2001. Expression of mouse interleukin-4 by a recombinant ectromelia virus suppresses cytolytic lymphocyte responses and overcomes genetic resistance to mousepox. *J Virol* **75**:1205-10.
18. Jia, H. P., D. C. Look, L. Shi, M. Hickey, L. Pewe, J. Netland, M. Farzan, C. Wohlford-Lenane, S. Perlman, and P. B. McCray, Jr. 2005. ACE2 receptor expression and severe acute respiratory syndrome coronavirus infection depend on differentiation of human airway epithelia. *J Virol* **79**:14614-21.
19. Ksiazek, T. G., D. Erdman, C. S. Goldsmith, S. R. Zaki, T. Peret, S. Emery, S. Tong, C. Urbani, J. A. Comer, W. Lim, P. E. Rollin, S. F. Dowell, A. E. Ling, C. D. Humphrey, W. J. Shieh, J. Guarner, C. D. Paddock, P. Rota, B. Fields, J. DeRisi, J. Y. Yang, N.

- Cox, J. M. Hughes, J. W. LeDuc, W. J. Bellini, and L. J. Anderson. 2003. A novel coronavirus associated with severe acute respiratory syndrome. *N Engl J Med* **348**:1953-66.
20. Kuba, K., Y. Imai, S. Rao, H. Gao, F. Guo, B. Guan, Y. Huan, P. Yang, Y. Zhang, W. Deng, L. Bao, B. Zhang, G. Liu, Z. Wang, M. Chappell, Y. Liu, D. Zheng, A. Leibbrandt, T. Wada, A. S. Slutsky, D. Liu, C. Qin, C. Jiang, and J. M. Penninger. 2005. A crucial role of angiotensin converting enzyme 2 (ACE2) in SARS coronavirus-induced lung injury. *Nat Med* **11**:875-9.
  21. Kuiken, T., R. A. Fouchier, M. Schutten, G. F. Rimmelzwaan, G. van Amerongen, D. van Riel, J. D. Laman, T. de Jong, G. van Doornum, W. Lim, A. E. Ling, P. K. Chan, J. S. Tam, M. C. Zambon, R. Gopal, C. Drosten, S. van der Werf, N. Escriou, J. C. Manuguerra, K. Stohr, J. S. Peiris, and A. D. Osterhaus. 2003. Newly discovered coronavirus as the primary cause of severe acute respiratory syndrome. *Lancet* **362**:263-70.
  22. Li, W., M. J. Moore, N. Vasilieva, J. Sui, S. K. Wong, M. A. Berne, M. Somasundaran, J. L. Sullivan, K. Luzuriaga, T. C. Greenough, H. Choe, and M. Farzan. 2003. Angiotensin-converting enzyme 2 is a functional receptor for the SARS coronavirus. *Nature* **426**:450-4.
  23. Lin, S. J., P. Y. Shu, C. Chang, A. K. Ng, and C. P. Hu. 2003. IL-4 suppresses the expression and the replication of hepatitis B virus in the hepatocellular carcinoma cell line Hep3B. *J Immunol* **171**:4708-16.
  24. Liu, S., G. Xiao, Y. Chen, Y. He, J. Niu, C. R. Escalante, H. Xiong, J. Farmer, A. K. Debnath, P. Tien, and S. Jiang. 2004. Interaction between heptad repeat 1 and 2 regions in spike protein of SARS-associated coronavirus: implications for virus fusogenic mechanism and identification of fusion inhibitors. *Lancet* **363**:938-47.
  25. Livak, K. J., and T. D. Schmittgen. 2001. Analysis of relative gene expression data using real-time quantitative PCR and the  $2^{-\Delta\Delta C_T}$  Method. *Methods* **25**:402-8.
  26. Lohoff, M., E. Marsig, and M. Rollinghoff. 1990. Murine IL-4 antagonizes the protective effects of IFN on virus-mediated lysis of murine L929 fibroblast cells. *J Immunol* **144**:960-3.
  27. Marra, M. A., S. J. Jones, C. R. Astell, R. A. Holt, A. Brooks-Wilson, Y. S. Butterfield, J. Khattri, J. K. Asano, S. A. Barber, S. Y. Chan, A. Cloutier, S. M. Coughlin, D. Freeman, N. Girn, O. L. Griffith, S. R. Leach, M. Mayo, H. McDonald, S. B. Montgomery, P. K. Pandoh, A. S. Petrescu, A. G. Robertson, J. E. Schein, A. Siddiqui, D. E. Smailus, J. M. Stott, G. S. Yang, F. Plummer, A. Andonov, H. Artsob, N. Bastien, K. Bernard, T. F. Booth, D. Bowness, M. Czub, M. Drebot, L. Fernando, R. Flick, M. Garbutt, M. Gray, A. Grolla, S. Jones, H. Feldmann, A. Meyers, A. Kabani, Y. Li, S. Normand, U. Stroher, G. A. Tipples, S. Tyler, R. Vogrig, D. Ward, B. Watson, R. C. Brunham, M. Krajden, M. Petric, D. M. Skowronski, C. Upton, and R. L. Roper. 2003. The Genome sequence of the SARS-associated coronavirus. *Science* **300**:1399-404.
  28. Moran, T. M., H. Isobe, A. Fernandez-Sesma, and J. L. Schulman. 1996. Interleukin-4 causes delayed virus clearance in influenza virus-infected mice. *J Virol* **70**:5230-5.
  29. Morgenstern, B., M. Michaelis, P. C. Baer, H. W. Doerr, and J. Cinatl, Jr. 2005. Ribavirin and interferon-beta synergistically inhibit SARS-associated coronavirus replication in animal and human cell lines. *Biochem Biophys Res Commun* **326**:905-8.
  30. Nicholls, J. M., L. L. Poon, K. C. Lee, W. F. Ng, S. T. Lai, C. Y. Leung, C. M. Chu, P. K. Hui, K. L. Mak, W. Lim, K. W. Yan, K. H. Chan, N. C. Tsang, Y. Guan, K. Y. Yuen, and J. S. Peiris. 2003. Lung pathology of fatal severe acute respiratory syndrome. *Lancet* **361**:1773-8.
  31. Peiris, J. S., S. T. Lai, L. L. Poon, Y. Guan, L. Y. Yam, W. Lim, J. Nicholls, W. K. Yee, W. W. Yan, M. T. Cheung, V. C. Cheng, K. H. Chan, D. N. Tsang, R. W. Yung, T. K. Ng, and K. Y. Yuen. 2003. Coronavirus as a possible cause of severe acute respiratory syndrome. *Lancet* **361**:1319-25.
  32. Rota, P. A., M. S. Oberste, S. S. Monroe, W. A. Nix, R. Campagnoli, J. P. Icenogle, S. Penaranda, B. Bankamp, K. Maher, M. H. Chen, S. Tong, A. Tamin, L. Lowe, M. Frace, J. L. DeRisi, Q. Chen, D. Wang, D. D. Erdman, T. C. Peret, C. Burns, T. G. Ksiazek, P. E. Rollin, A. Sanchez, S. Liffick, B. Holloway, J. Limor, K. McCaustland, M. Olsen-Rasmussen, R. Fouchier, S. Gunther, A. D. Osterhaus, C. Drosten, M. A. Pallansch, L. J. Anderson, and W. J. Bellini. 2003. Characterization of a novel coronavirus associated with severe acute respiratory syndrome. *Science* **300**:1394-9.
  33. Sainz, B., Jr., E. C. Mossel, C. J. Peters, and R. F. Garry. 2004. Interferon-beta and interferon-gamma synergistically inhibit the replication of severe acute respiratory syndrome-associated coronavirus (SARS-CoV). *Virology* **329**:11-7.
  34. Sharma, D. P., A. J. Ramsay, D. J. Maguire, M. S. Rolph, and I. A. Ramshaw. 1996. Interleukin-4 mediates down regulation of antiviral cytokine expression and cytotoxic T-lymphocyte responses and exacerbates vaccinia virus infection *in vivo*. *J Virol* **70**:7103-7.
  35. Snijder, E. J., P. J. Bredenbeek, J. C. Dobbe, V. Thiel, J. Ziebuhr, L. L. Poon, Y. Guan, M. Rozanov, W. J. Spaan, and A. E. Gorbalenya. 2003. Unique and conserved features of genome and proteome of SARS-coronavirus, an early split-off from the coronavirus group 2 lineage. *J Mol Biol* **331**:991-1004.

36. Spruth, M., O. Kistner, H. Savidis-Dacho, E. Hitter, B. Crowe, M. Gerencer, P. Bruhl, L. Grillberger, M. Reiter, C. Tauer, W. Mundt, and P. N. Barrett. 2006. A double-inactivated whole virus candidate SARS coronavirus vaccine stimulates neutralising and protective antibody responses. *Vaccine* **24**:652-61.
37. Tikellis, C., C. I. Johnston, J. M. Forbes, W. C. Burns, L. M. Burrell, J. Risvanis, and M. E. Cooper. 2003. Characterization of renal angiotensin-converting enzyme 2 in diabetic nephropathy. *Hypertension* **41**:392-7.
38. Vickers, C., P. Hales, V. Kaushik, L. Dick, J. Gavin, J. Tang, K. Godbout, T. Parsons, E. Baronas, F. Hsieh, S. Acton, M. Patane, A. Nichols, and P. Tummino. 2002. Hydrolysis of biological peptides by human angiotensin-converting enzyme-related carboxypeptidase. *J Biol Chem* **277**:14838-43.
39. Vincent, T., R. F. Pettersson, R. G. Crystal, and P. L. Leopold. 2004. Cytokine-mediated downregulation of coxsackievirus-adenovirus receptor in endothelial cells. *J Virol* **78**:8047-58.
40. Wong, C. K., C. W. Lam, A. K. Wu, W. K. Ip, N. L. Lee, I. H. Chan, L. C. Lit, D. S. Hui, M. H. Chan, S. S. Chung, and J. J. Sung. 2004. Plasma inflammatory cytokines and chemokines in severe acute respiratory syndrome. *Clin Exp Immunol* **136**:95-103.







CHAPTER 6

# Exacerbated innate host response to SARS-CoV in aged non-human primates

Based on:

Saskia L. Smits, Anna de Lang, Judith M. A. van den Brand, Lonneke M. Leijten, Wilfred F. van IJcken, Marinus J. C. Eijkemans, Geert van Amerongen, Thijs Kuiken, Arno C. Andeweg, Albert D.M.E. Osterhaus and Bart L. Haagmans

*PLoS Pathogens*, 2010; 5;6(2):e1000756



## ABSTRACT

The emergence of viral respiratory pathogens with pandemic potential, such as severe acute respiratory syndrome coronavirus (SARS-CoV) and influenza A H5N1, urges the need for deciphering their pathogenesis to develop new intervention strategies. SARS-CoV infection causes acute lung injury (ALI) that may develop into life-threatening acute respiratory distress syndrome (ARDS) with advanced age correlating positively with adverse disease outcome. The molecular pathways, however, that cause virus-induced ALI/ARDS in aged individuals are ill-defined. Here, we show that SARS-CoV-infected aged macaques develop more severe pathology than young adult animals, even though viral replication levels are similar. Comprehensive genomic analyses indicate that aged macaques have a stronger host response to virus infection than young adult macaques, with an increase in differential expression of genes associated with inflammation, with NF- $\kappa$ B as central player, whereas expression of type I interferon (IFN)- $\beta$  is reduced. Therapeutic treatment of SARS-CoV-infected aged macaques with type I IFN reduces pathology and diminishes proinflammatory gene expression, including interleukin-8 (IL-8) levels, without affecting virus replication in the lungs. Thus, ALI in SARS-CoV infected aged macaques developed as a result of an exacerbated innate host response. The anti-inflammatory action of type I IFN reveals a potential intervention strategy for virus-induced ALI.

## INTRODUCTION

The zoonotic transmission of severe acute respiratory syndrome coronavirus (SARS-CoV) caused pneumonic disease in humans with an overall mortality rate of ~10%. The exact reasons why some individuals succumbed to the infection while others remained relatively unaffected have not been clarified. Aging, an important risk factor in SARS-CoV-associated disease, is associated with changes in immunity (39, 42, 52). Consequently, elderly individuals are at greater risk of contracting more severe and longer lasting infections with increased morbidity and mortality, exemplified by respiratory tract infections caused by influenza A virus and severe acute respiratory syndrome (SARS) coronavirus (43, 50-51). The clinical course of SARS-CoV-induced disease follows a triphasic pattern (50). The first phase is characterized by fever, myalgia and other systemic symptoms that are likely caused by the increase in viral replication and cytolysis. The second phase of the disease is characterized by a decrease in viral replication that correlates with the onset of IgG conversion. Interestingly, it is also in this phase that severe clinical worsening is seen, which can not be explained by uncontrolled viral replication. It has been hypothesized that the diffuse alveolar lung damage in this phase is caused by an over exuberant host response (29, 32, 50). The majority of patients recovers after 1-2 weeks, but up to one-third of the patients progress to the third phase and develop severe inflammation of the lung, characterized by acute respiratory distress syndrome (ARDS) (63). The clinical course and outcome of SARS-CoV disease are more favorable in children younger than 12 years of age as compared to adolescents and adults (28, 38, 66); elderly patients have a poor prognosis, with mortality rates of up to ~50% (50).

For SARS-CoV-associated disease in humans, it has been hypothesized that seemingly excessive proinflammatory responses, illustrated by elevated levels of inflammatory cytokines and chemokines, mediate immune-pathology resulting in acute lung injury (ALI) and ARDS (11, 46, 50, 59, 65). Direct support for this concept, however, is scarce. ALI and ARDS are typified by inflammation, with increased permeability of the alveolar-capillary barrier, resulting in pulmonary edema, hypoxia, and accumulation of polymorphonuclear leukocytes and macrophages. Inflammatory cytokines, among which IL-1 $\beta$  and IL-8, play a major role in mediating and amplifying ALI/ARDS (63) and are elevated in SARS-CoV-infected patients as well (11, 46). *In vitro* experiments confirm that SARS-CoV infection induces expression of cytokines/chemokines in a range of cell types (13, 37, 59). Moreover, infection of cynomolgus macaques with SARS-CoV leads to a strong immune response, with expression of various cytokines/chemokines, resembling the host response seen in human SARS patients (15). Nevertheless, the determinants that lead to severe virus-associated ALI/ARDS and that cause people to succumb to infection remain largely obscure, restraining development of appropriate treatments.

As advanced age is a predictor of adverse clinical outcome in both ARDS and SARS-CoV infections (50, 62), we used age as predisposing factor to study the pathogenesis of SARS-CoV in a macaque model. By performing comparative analyses of young adult and aged SARS-CoV-infected macaques regarding pathology, virus replication and host response, insight into the pathogenesis of SARS-CoV is obtained and a potential therapeutic intervention strategy for virus-induced ALI is revealed.

## MATERIALS AND METHODS

### Macaque studies

Six young adult cynomolgus macaques (*Macaca fascicularis*), 3-5 years old, four of which carried active temperature transponders in the peritoneal cavity, and four aged cynomolgus macaques, 10-18 years old, which all carried active temperature transponders, were inoculated with SARS-CoV strain HKU39849, as described previously (15, 19, 26, 36). Two additional aged animals (17 and 19 years old), previously infected with SARS-CoV strain HKU39849 (26), were enrolled in this study as well. Four young adult mock (PBS) infected animals from a previous study (15) and four aged macaques were taken as controls. Lung tissues stored in RNA-later from three cynomolgus macaques, 13 years old, previously inoculated with SARS-CoV strain HKU39849 and treated with pegylated IFN- $\alpha$  at a dose of 3  $\mu\text{g}/\text{kg}$  intramuscularly on days 1 and 3 after infection, were taken along for molecular analyses (26). All animals were infected with the same dose of virus, using the same inoculation procedure, by the same person to minimize inter-experiment variation. All animals were checked daily for clinical signs and anaesthetised with ketamine on days 0, 2 and 4 after infection to collect oral, nasal, and rectal swabs (26). All animals were euthanized on day 4 post infection. Necropsies and sampling for histology/immunohistochemistry were performed as described (26). The percentage of affected lung tissue from each lung lobe was determined at necropsy, recorded on a schematic diagram of the lung and the area of affected lung tissue was subsequently calculated (gross pathology score).

### Ethics

Approval for animal experiments was obtained from the Institutional Animal Welfare Committee and performed according to Dutch guidelines for animal experimentation.

### Immunohistochemistry

Serial 3  $\mu\text{m}$  lung sections were stained using mouse-anti-SARS-nucleocapsid IgG2a (clone Ncap4; Imgenex) 1:1600, mouse-anti-human neutrophil elastase (clone NP-57; DAKO) 1:10, mouse-anti-human CD68 (clone KP1; DAKO) 1:200, mouse-anti-human pankeratin (clone AE1/AE3; Neomarkers) 1:100, rabbit anti p-NF- $\kappa\text{B}$  p65 (Santa Cruz) or rabbit control and isotype antibodies (clones 11711 and 20102; R&D), according to standard protocols (26, 36). Quantitative assessment of SARS-CoV infection in the lungs was performed as described previously (26).

### RNA-extraction and quantitative RT-PCR

RNA from 200  $\mu\text{l}$  of swabs was isolated with the Magnapure LC total nucleic acid isolation kit (Roche) external lysis protocol and eluted in 100  $\mu\text{l}$ . SARS-CoV RNA was quantified on the ABI prism 7700, with use of the Taqman Reverse Transcription Reagents and Taqman PCR Core Reagent kit (Applied Biosystems), using 20  $\mu\text{l}$  isolated RNA, 1x Taqman buffer, 5.5 mM  $\text{MgCl}_2$ , 1.2 mM dNTPs, 0.25 U Amplitaq gold DNA polymerase, 0.25 U Multiscribe reverse transcriptase, 0.4 U RNase-inhibitor, 200 nM primers, and 100 nM probe (36). Amplification parameters were 30 min at 48°C, 10 min at 95°C, and 40 cycles of 15 s at

95°C, and 1 min at 60°C. RNA dilutions isolated from a SARS-CoV stock were used as a standard. Average results ( $\pm$  s.e.m.) for young adult ( $n = 6$ ) and aged macaque ( $n = 4$ ) groups were expressed as SARS-CoV equivalents per ml swab medium.

Lung tissue samples (0.3-0.5 gram) were taken for RT-PCR and microarray analysis in RNA-later (Ambion, Inc.). RNA was isolated from homogenized post mortem tissue samples using Trizol Reagent (Invitrogen) and the RNeasy mini kit (Qiagen). cDNA synthesis was performed with 1  $\mu$ g total RNA and Superscript III RT (Invitrogen) with oligo(dT), according to the manufacturer's instructions. Semi-quantitative RT-PCR was performed to detect SARS-CoV mRNA and to validate cellular gene expression changes as detected with microarrays (15). Differences in gene expression are represented as the fold change in gene expression relative to a calibrator and normalized to a reference, using the  $2^{-\Delta\Delta Ct}$  method (40). GAPDH (glyceraldehydes-3-phosphate dehydrogenase) was used as endogenous control to normalize quantification of the target gene. The samples from the young adult PBS-infected macaques were used as a calibrator. Average results ( $\pm$  s.e.m.) for young adult ( $n = 6$ ), aged ( $n = 6$ ), and IFN- $\alpha$ -treated aged ( $n = 3$ ) macaque groups were expressed as fold change compared to young adult PBS-infected animals, respectively (40). In addition, groups were based on severity of pathology: young adult macaques ( $n = 6$ ), aged macaques with pathology ( $n = 4$ ), and aged macaques with severe pathology with >40% of lungs affected ( $n = 2$ ) (Supplementary figure 6.4). As titration of lung homogenates gave inconsistent results in our hands and because the effects of endogenous and exogenous IFN may influence titration outcomes, we chose taqman and immunohistochemistry to determine viral replication levels in the lung.

### Isolation and activation of PBMC

PBMC from healthy blood donors were isolated from heparinized venous blood using Lymphoprep (Axis-Shield). PBMC were resuspended at  $2 \times 10^6$ /ml in RPMI 1640 medium (Biowhittaker) supplemented with L-glutamine (2 mM), penicillin (100 U/ml), streptomycin (100  $\mu$ g/ml), and 10% fetal calf serum in 50-ml tubes (Greiner Bio-one). Freshly isolated PBMC were incubated with IL-1 $\beta$  (5 ng/ml; eBioscience), IFN- $\alpha$  2a (1000 U/ml, 100U/ml, or 10U/ml; Roferon-A; Roche) or both for 24 hours in duplo or triplo per donor. Total RNA from stimulated PBMC was isolated using Trizol Reagent (Invitrogen) and the RNeasy mini kit (Qiagen). cDNA synthesis was performed with 100 ng total RNA and Superscript III RT (Invitrogen) with oligo(dT), according to the manufacturer's instructions. Semi-quantitative RT-PCR was performed for IL-8 (15) and IL-1 $\beta$  (Taqman gene expression assays; Applied Biosystems) as described previously using the  $2^{-\Delta\Delta Ct}$  method (40). Average results ( $\pm$  s.e.m.) were expressed as fold change compared to untreated (mock) cells (40).

### Statistical analysis

Data (RT-PCR and gross pathology scores for SARS-CoV-infected young adult versus aged and aged versus aged animals treated with IFN) were compared using Student's t-test with Welch's correction. Differences were considered significant at  $p < 0.05$ . One-way ANOVA and Bonferroni's multiple comparison test were used for the comparison of data in groups based on severity of pathology (low, medium, high) and *in vitro* IFN inhibition experiments. Correlation coefficients were determined using Spearman's correlation test.



## **RNA labeling, microarray hybridization, scanning and data preprocessing**

Pooled total RNA (2.4 µg) from one-three separate lung pieces of all animals (including previously infected animals), with substantial SARS-CoV replication ( $> 10^5$  fold change), was labeled using the One-Cycle Target Labeling Assay (Affymetrix) and hybridized onto Affymetrix GeneChip Rhesus Macaque Genome Arrays (Affymetrix), according to the manufacturer's recommendations. Image analysis was performed using Gene Chip Operating Software (Affymetrix). Microarray Suite version 5.0 software (Affymetrix) was used to generate .dat and .cel files for each experiment. All data were normalized using a variance stabilization algorithm (VSN) (30). Transformed probe values were summarized into one value per probe set by the median polish method (60).

## **Microarray data analysis**

Probe set (gene) wise comparisons between the experimental conditions (aged, young adult and IFN-treated animals versus young adult or aged PBS-infected animals and directly compared to each other) were performed by LIMMA (version 2.12.0) (58). Correction for multiple testing was achieved by requiring a false discovery rate (FDR) of 0.05, calculated with the Benjamini-Hochberg procedure (8). To understand the gene functions and the biological processes represented in the data and obtain differentially expressed molecular and cellular functions, Ingenuity Pathways Knowledge Base (<http://www.ingenuity.com/>) was used. Heat maps of proinflammatory pathways were produced using complete linkage and Euclidian distance in Spotfire DecisionSite for Functional Genomics version 9.1 (<http://www.spotfire.com/>) and Ingenuity Pathways Knowledge Base (<http://www.ingenuity.com/>), using log (base 2) transformed expression values with minimum and maximum values of the color range being -4 and 4, respectively. Differences between conditions in expression of specific proinflammatory pathways, e.g. direct comparison of defined gene sets (aged versus young adult and aged versus aged IFN-treated animals), were tested by Goeman's global test procedure (24). Hierarchical clustering analysis of normalized log-2 based hybridization signals of individual young adult and aged macaques of a set of gene transcripts that were identified as being differentially regulated (fold change  $\geq 2$ ; FDR  $< 0.05$ ) in at least one of the comparisons of young adult versus young adult PBS or aged versus aged PBS animals were created using Spotfire DecisionSite for Functional Genomics version 9.1 (<http://www.spotfire.com/>) with complete linkage and Euclidian distance parameters.

# **RESULTS**

## **SARS-CoV causes more severe pathology in aged than in young adult macaques**

To obtain further insights in the pathogenesis of SARS-CoV, six aged (10-19 years old) and six young adult (3-5 years old) cynomolgus macaques were infected with SARS-CoV HKU39849 and euthanized four days after infection. Four young adult and four aged PBS-infected cynomolgus macaques were used as negative controls. During the 4-day experiment, some of the SARS-CoV-infected aged animals displayed decreased activity and mildly labored breathing. All aged infected macaques showed an increase in body

temperature either during the night or during the day one to two days after infection (figure 6.1A). The lungs of aged macaques showed large (multi)focal pulmonary consolidation that was severe (~40-60% of affected lung tissue) in two macaques (figure 6.1B and figure 6.S1).

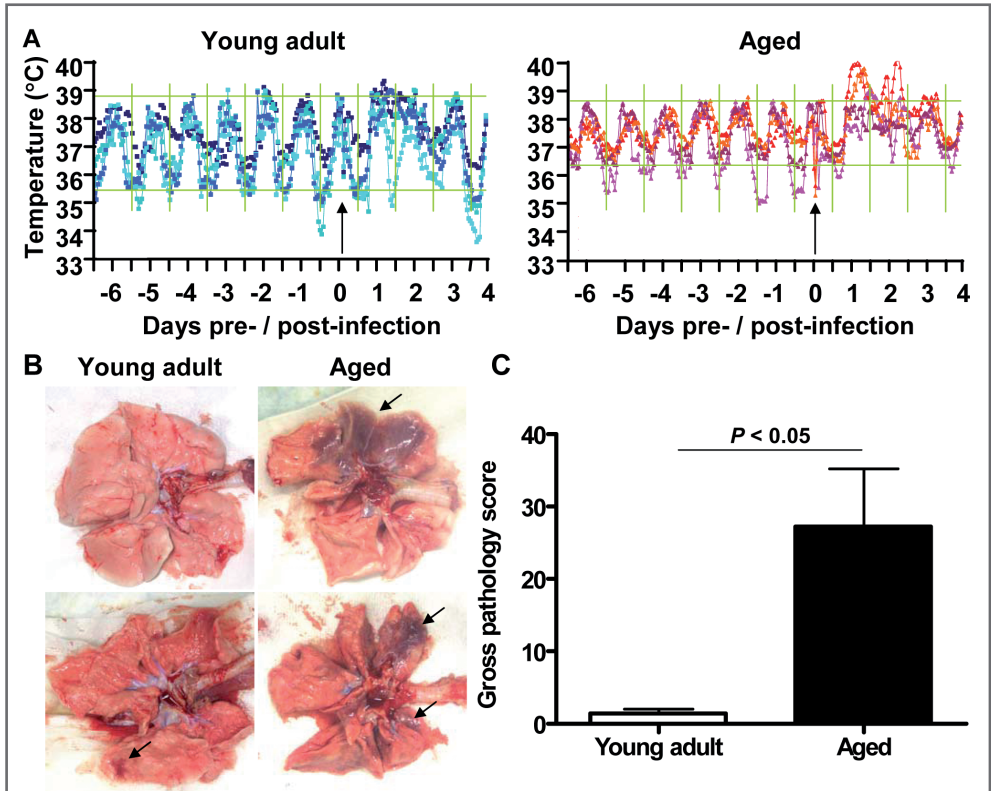


**Figure 6.1.** Aged macaques are more prone to develop SARS-CoV-associated disease than young adults. (A) Fluctuations in body temperatures in four young adult and four aged SARS-CoV-infected macaques measured by transponders in the peritoneal cavity. Temperatures are shown from day six prior to infection until four days post infection. The arrow indicates day zero when animals were infected. Grey horizontal lines mark the average range of temperature fluctuations prior to infection. (B) Macroscopic appearance of (consolidated) lung tissue of young adult and aged SARS-CoV infected macaques at day 4 post infection. Lesions are arrowed. (C) Gross pathology scores of aged and young adult macaque groups were determined after necropsy and averaged ( $\pm$  standard error of the mean (s.e.m.)).

Microscopic examination revealed typical ALI-associated lesions, similar to what has been seen in SARS-CoV-infected humans that progress to ARDS (51). Lesions involved the alveoli and terminal bronchioli, showing areas with acute or more advanced phases of diffuse alveolar damage (figure 6.2). Lumina of alveoli were variably filled with protein rich edema fluid, cellular debris, alveolar macrophages and neutrophils, eosinophils, and lymphocytes (figure 6.2 and figure 6.S2A-B). Moderately thickened alveolar walls

were lined by cuboidal epithelial cells (type II pneumocyte hyperplasia; figure 6.2 and figure 6.S2C). The epithelial origin of these enlarged type II pneumocytes with large vacuolated nuclei, prominent nucleoli and abundant vesicular cytoplasm was confirmed by keratin staining (figure 6.S2D). Hyaline membranes and multinucleated giant cells were occasionally observed in the alveoli (figure 6.S2E-F). In contrast, all young adult animals remained free of clinical symptoms and had no or less extensive pulmonary consolidation (figure 6.1A-C). Hyaline membranes were not observed in SARS-CoV-infected young adult macaques. A multifocal mild chronic lymphoplasmacytic tracheo-bronchoadenitis, characterized by moderate numbers of lymphocytes, plasma cells, macrophages, less neutrophils and occasional eosinophils in the lamina propria of the bronchi, focally surrounding and infiltrating the submucosal glands, was observed in all young adult macaques, but not in aged macaques (figure 6.2). Our data were confirmed by retrospective analysis of earlier experiments in which aged animals were used (15, 19, 26, 36). Overall, aged macaques develop more severe SARS-CoV-associated ALI than young adults.

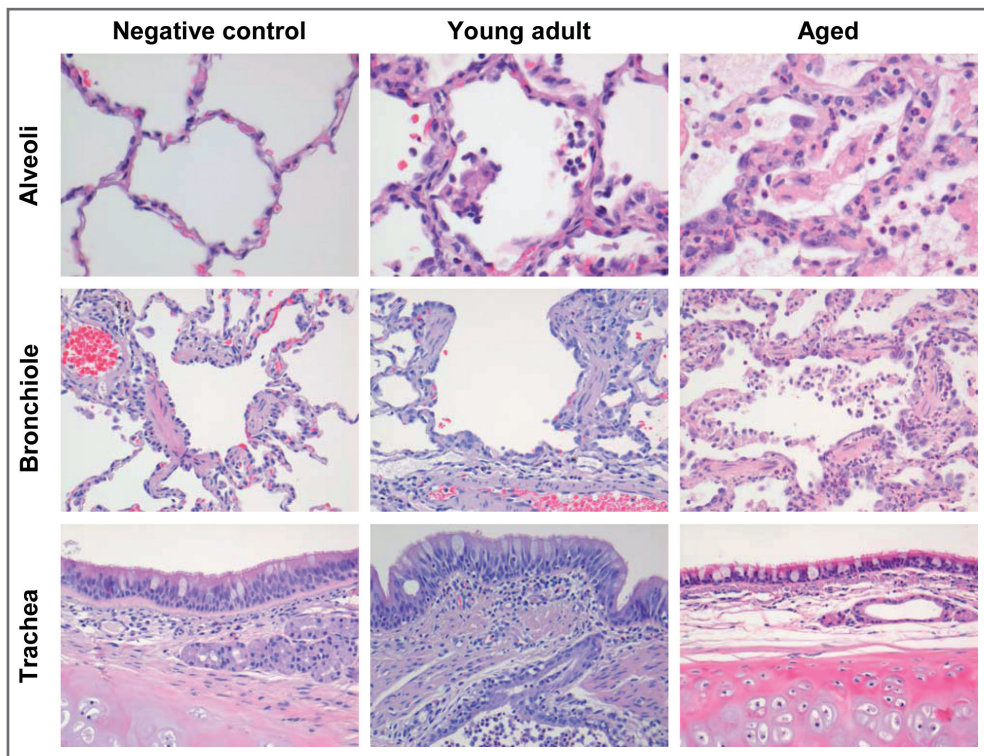


**Figure 6.2. Histology of lungs from SARS-CoV-infected aged macaques.** Lesions in lungs of PBS-infected (left panel) and SARS-CoV infected young adult (middle panel) and aged (right panel) macaques showing diffuse alveolar damage, characterized by disruption of alveolar walls causing edema and type II pneumocyte hyperplasia with influx of inflammatory cells in the alveoli and bronchioles. In the trachea, a multifocal mild chronic lymphoplasmacytic tracheobronchoadenitis was observed in young adult macaques.

### The level of viral replication in aged and young adult macaques is similar

Because viral replication is important for disease pathogenesis, we determined virus titers in aged and young adult animals. Virus excretion in the throat (figure 6.3A) and nose (figure 6.3B) of aged and young adult macaques at days 2 and 4 post infection was not significantly different. Moreover, no significant difference in quantity of SARS-CoV mRNA in the lungs of young adult and aged animals was observed (figure 6.3C). Differences in the nature and percentage of SARS-CoV-infected cells in the lungs of aged and young adult macaques were not seen either (figure 6.3D). Apparently, augmented pathology in aged macaques cannot be rationalized by increased viral replication.

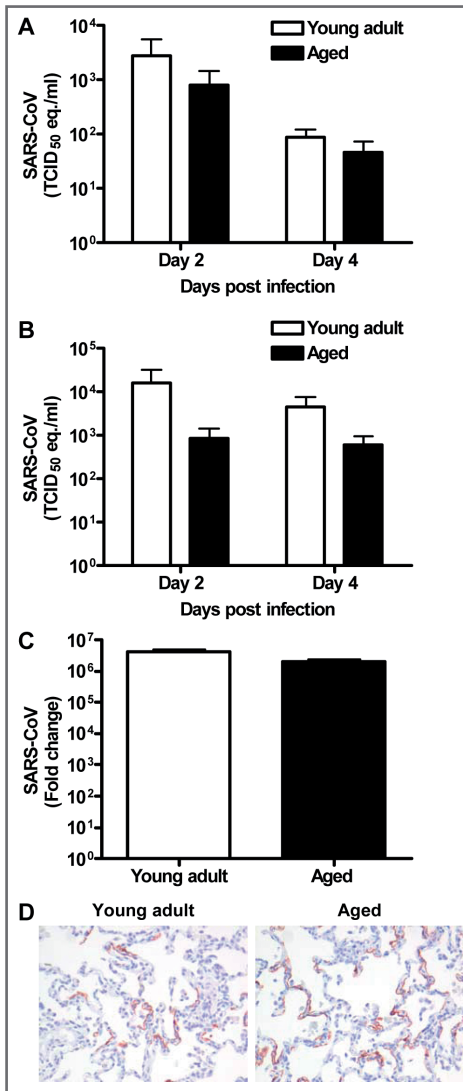


**Figure 6.3.** Viral replication levels in SARS-CoV-infected aged and young adult macaques are similar. (A-B) SARS-CoV replication in the throat (A) and nose (B) of SARS-CoV infected aged (black bars) and young adult (white bars) macaques at day 2 and 4 post infection as determined by real-time RT-PCR. Viral RNA levels are displayed as TCID<sub>50</sub> equivalents (eq.)/ml swab medium ( $\pm$  s.e.m.). (C) Average fold change in SARS-CoV mRNA levels ( $\pm$  s.e.m.) in the lungs of aged and young adult macaques compared to PBS-infected animals as determined by real-time RT-PCR and depicted on a log-scale. (D) Lung sections of SARS-CoV-infected aged and young adult macaques were stained with a mouse-anti-SARS-nucleocapsid IgG2a. Sections were counterstained with hematoxylin. Original magnifications are X20.

## The host response to SARS-CoV infection is stronger in aged than in young adult macaques

To understand why SARS-CoV-infection in aged macaques results in more severe pathology than in young adult macaques, we determined global gene expression profiles by analyzing total RNA isolated from the lungs using microarray analysis. Hierarchical clustering methods were used to order gene transcripts and individual aged and young adult animals to identify groups of animals with similar expression patterns. These data were plotted as a heat map in which each entry represents a gene expression value (figure 6.4). As expected in an animal experiment with outbred animals, the inter-animal variation was relatively high (figure 6.S3). There were two major roots to the hierarchical dendrogram, with one root containing the PBS-infected control animals, and the second root containing the SARS-CoV-infected animals. The root of the PBS-infected control animals was divided in two minor roots, clustering young adults together and aged animals as a group. These data suggest that the baseline expression patterns are different in young adult and aged macaques. The root of the SARS-CoV-infected animals was also divided in two minor roots, largely clustering young adult animals together and grouping aged infected macaques. The hierarchical clustering heat map suggests that both age and SARS-CoV infection are key factors involved in determining transcription of cellular genes.

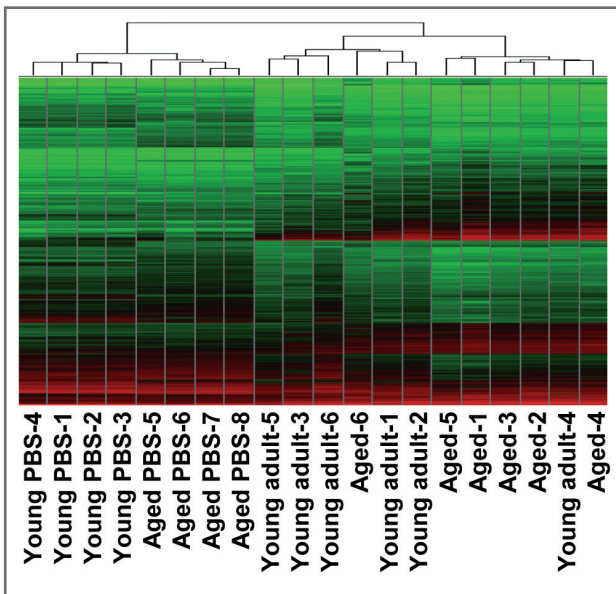


**Figure 6.4. Global gene expression profiles of individual young adult and aged animals.** Global gene expression profiles of normalized log<sub>2</sub> based hybridization signals of individual young adult and aged macaques of a set of gene transcripts that were identified as being differentially regulated (fold change  $\geq 2$ ; FDR  $< 0.05$ ) in at least one of the comparisons of gene expression in the lungs of experimentally SARS-CoV-infected aged and young adult macaques versus gene expression in the lungs of PBS-infected macaques, and genes were included if they met the criteria of an absolute fold change of  $\geq 2$ -fold (FDR  $< 0.05$ ) in at least one experiment. The data were plotted as a heat map, where each matrix entry represents a gene expression value. Normalized log<sub>2</sub> based hybridization signals ranged from 3 (green) to 14 (red). Dendrograms (trees) of the heat map represent the degree of relatedness between the samples, with short branches denoting a high degree of similarity and long branches denoting a low degree of similarity.

To determine whether aged and young adult animals respond differently to SARS-CoV-infection, their gene expression profiles were compared. In a direct comparison of aged ( $n = 6$ ) versus young adult ( $n = 6$ ) SARS-CoV-infected animals using an ANOVA-based analysis called LIMMA, 202 gene transcripts were differentially expressed (fold change  $\geq 2$ ;  $p < 0.05$ ; Table S1). Upon analysis of these gene transcripts within the context of biological processes and pathways using Ingenuity Pathways Knowledge Base, this subset of genes showed indications for an innate host response to viral infection. Among the top significantly differentially regulated ( $p < 0.005$ ) functional categories were immune response, inflammatory response and hematological system development and function, which included genes like  $F_3$ ,  $IL1RL1$ ,  $IL1RN$ ,  $IL-6$ ,  $IL-8$ ,  $S100A8$ ,  $SERPINA1$ ,  $SERPINA3$ ,  $NP$ ,  $ACPP$ ,  $TFPI2$ ,  $SPP1$ ,  $IGF1$ ,  $EDN3$ ,  $DEFB1$  and  $SOCS3$  (figure 6.5A) most of which were upregulated in SARS-CoV-infected aged animals compared to young adult infected animals. In addition, three of the most significantly regulated molecular/cellular functions ( $p < 0.005$ ) were associated with a proinflammatory response and included cell death, cell movement, and cell-to-cell signaling (figure 6.5A). The top gene interaction network, showing the interplay between genes during the host response to viral infection, contained NF- $\kappa$ B as central node (figure 6.5B). NF- $\kappa$ B is a redox-sensitive transcription factor implicated to play a major role in proinflammatory host responses and the development of ALI/ARDS (16, 31). Several of the 202 differentially expressed gene transcripts, among which  $IL1RN$ ,  $SERPINA1$ ,  $IL-8$ ,  $F_3$  and  $TFPI2$ , are target genes for NF- $\kappa$ B. Thus, significant differences exist in the host response to SARS-CoV infection, corresponding with age.

To obtain a more in-depth view of the host response to infection, global gene expression profiles were determined in lungs of SARS-CoV-infected aged ( $n = 6$ ) or young adult ( $n = 6$ ) macaques in comparison to aged or young adult PBS-infected macaques ( $n = 4$ ), respectively. Aged macaques differentially expressed 1577 gene transcripts (figure 6.6A). Gene ontology analysis revealed that the majority of genes in the aged macaque group compared to aged PBS-infected animals were associated with a proinflammatory response and included cellular growth and proliferation, cell death, cell movement, and cell-to-cell signaling (figure 6.6B). Although SARS-CoV-infected young adult macaques differentially expressed much less gene transcripts compared to young adult PBS-infected animals (figure 6.6A), the most significantly regulated molecular/cellular functions also included cellular growth and proliferation, cell death, cell movement, and cell-to-cell signaling (figure 6.6B). This suggested that the nature of the host response to infection in aged and young adult animals was strikingly similar, even though the severity was different.

Because the above described gene ontology molecular/cellular functions are very broad, genes were further subdivided based on available annotations to gain insight in differences in the host response to infection in aged and young adult macaques compared to aged and young adult PBS-infected animals, respectively. Heat maps were generated for differentially regulated genes with proinflammatory functions such as cell adhesion (figure 6.6C), apoptosis (figure 6.6D), and cytokine/chemokine signaling (figure 6.6E). The greater number of differentially expressed genes, as well as the brighter intensities (fold changes in transcripts) included in the heat map for aged macaques, suggested that aged macaques show a more zealous response to virus infection than young adult macaques. This assumption was corroborated using Goeman's global test (24) on the defined gene subsets cell adhesion, cytokine/chemokine signaling, and apoptosis. When macaques were grouped according to severity of pathology instead of age and compared to their respective PBS-infected controls, increased numbers of differentially



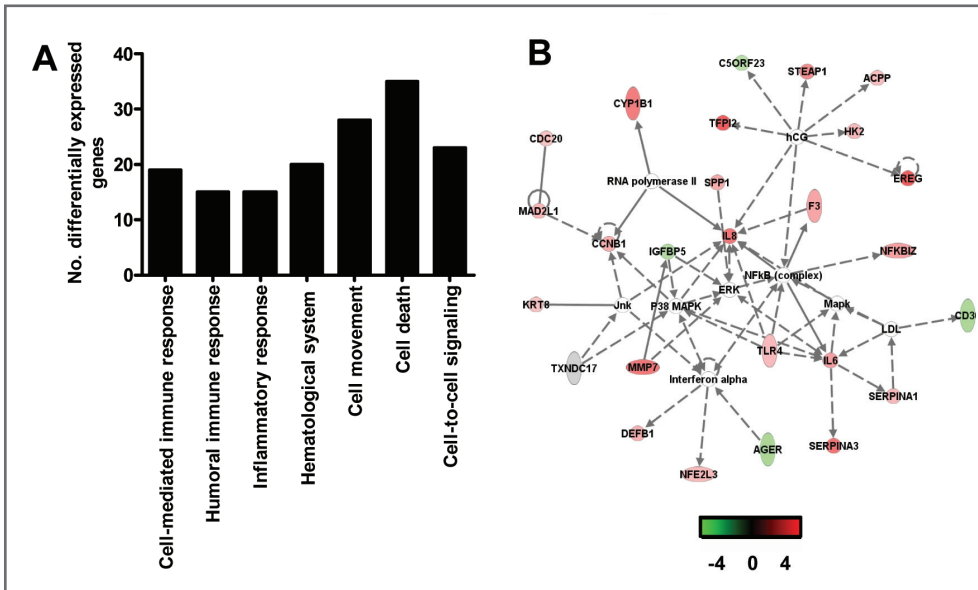
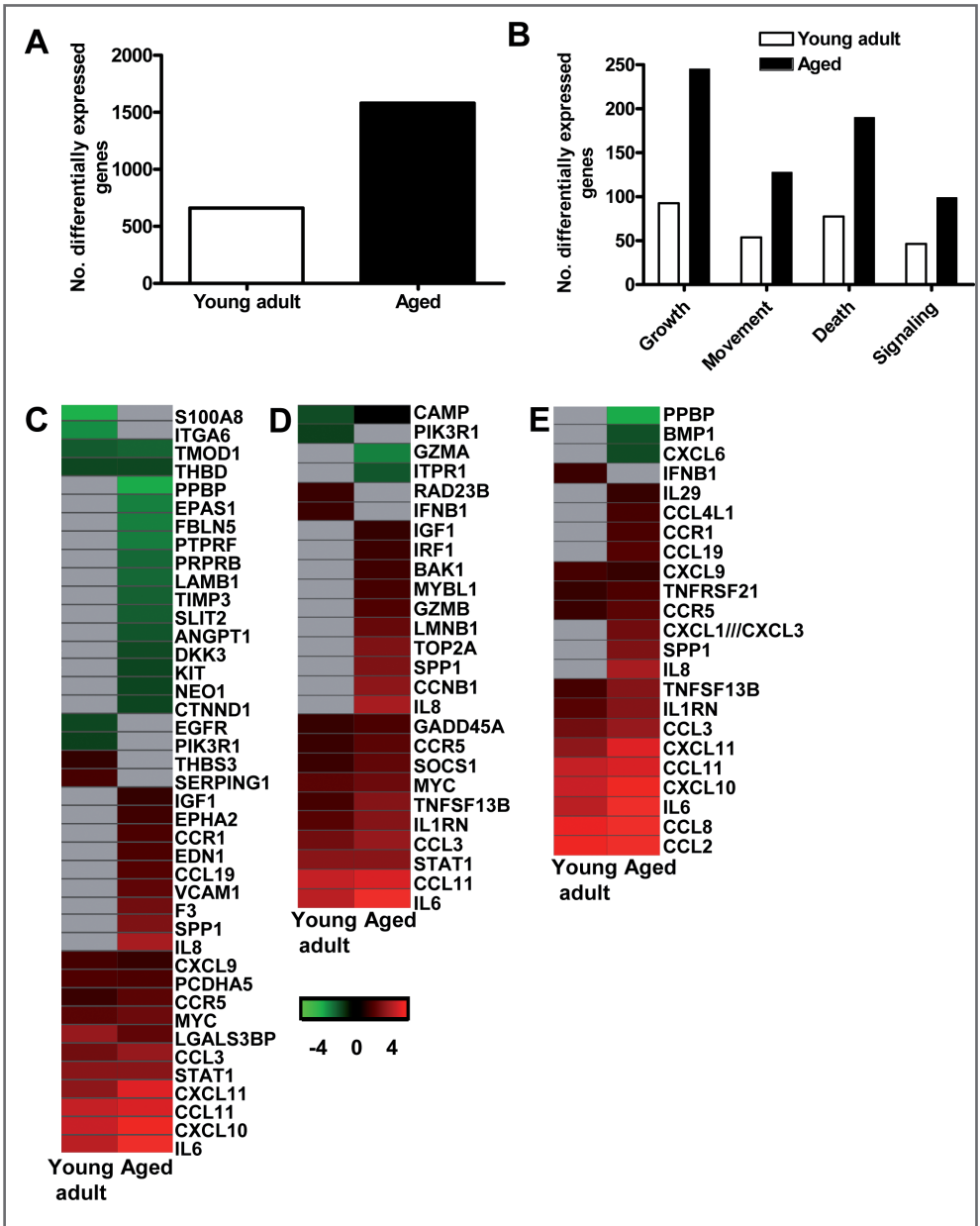


Figure 6.5. Direct comparison of gene expression profiles in the lungs of aged and young adult SARS-CoV-infected macaques. (A) Number of differentially expressed genes in the direct contrast of aged and young adult SARS-CoV-infected macaques with functions in immune response, inflammatory response, hematological system development and function, cell movement, cell death, or cell-to-cell signaling and interaction obtained from Ingenuity Pathways Knowledge Base. (B) This diagram shows a gene interaction network from Ingenuity Pathways Knowledge Base with genes that are differentially expressed in the contrast of aged and young adult SARS-CoV-infected animals. The central node is NF-κB, a key transcription factor in inflammation and ARDS. Genes depicted in green are downregulated and in red upregulated.

expressed gene transcripts and increased fold changes for differentially expressed genes in inflammatory pathways correlated positively with gross pathology scores as well (figure 6.S4). Our data show that the innate host response to SARS-CoV infection changes during aging in macaques; age, pathology, and proinflammatory host response go hand-in-hand.

In order to understand the host responses in the context of senescence, we directly compared lung samples from PBS-infected aged ( $n = 4$ ) and young adult ( $n = 4$ ) macaques. LIMMA analysis revealed that 518 gene transcripts were differentially expressed (fold change  $\geq 2$ ;  $p < 0.05$ ), with categories such as immunological disease, haematological system and development, cell death, cell movement, and cellular growth and proliferation among the top significantly differentially regulated functions ( $p < 0.005$ ). Only 14 out of the 518 differentially expressed gene transcripts were also differentially expressed in the direct contrast of SARS-CoV-infected aged and young adult macaques. Our data indicate that significant differences exist in the basal gene expression levels of aged and young adult macaques, which may partly explain why differences in pathology were observed after SARS-CoV infection.





**Figure 6.6. Aged macaques display a stronger host response to SARS-CoV infection than young adults.** (A) Number of differentially expressed gene transcripts in aged and young adult SARS-CoV-infected macaques compared to aged and young adult PBS-infected animals, respectively ( $\geq 2$ -fold change,  $FDR < 0.05$ , LIMMA analysis). (B) Number of differentially expressed genes in aged and young adult macaque groups compared to aged and young adult PBS-infected animals, respectively, with functions in cellular growth and proliferation, cell movement, cell death, or cell-to-cell signaling and interaction obtained from Ingenuity Pathways Knowledge Base. White bars for young adult and black bars for aged macaques. When SARS-CoV-infected aged and young adult macaques were compared directly, these cellular functions were significantly differentially expressed as well. (C-E) Gene expression profiles showing differentially expressed genes coding for proteins involved in cell adhesion (C), apoptosis (D), and cytokine/chemokine signaling (E) of aged and young adult macaques. Gene sets were obtained from Ingenuity Pathways Knowledge Base and changed  $\geq 2$ -fold in at least one of the macaque groups as compared to PBS-infected controls. The data presented are error-weighted fold change averages for six young adult and aged animals. Genes shown in red were upregulated, in green downregulated, and in grey not significantly differentially expressed in infected animals relative to PBS-infected animals (log (base 2) transformed expression values with minimum and maximum values of the color range being -4 and 4). Global test analysis of the direct contrast of SARS-CoV-infected aged versus young adult animals showed that these pathways were significantly differentially expressed ( $P < 0.05$ ). See Table S2 and S3 for full gene names and expression values.

### **NF- $\kappa$ B signaling in SARS-CoV-infected macaques**

As NF- $\kappa$ B target genes were differentially regulated in the direct comparison of SARS-CoV-infected aged and young adult macaques (figure 6.5), we focussed on NF- $\kappa$ B in the indirect comparison of aged and young adult SARS-CoV-infected macaques compared to aged and young adult PBS-infected animals, respectively. A gene interaction network, showing the interplay between “immune response”-type genes with NF- $\kappa$ B as central node, revealed that aged SARS-CoV-infected macaques showed a much more robust regulation of these genes than young adult infected animals (figure 6.7A) compared to their respective PBS-infected animals, which was corroborated by an analysis of differentially expressed target genes of NF- $\kappa$ B (figure 6.7B). Several of these genes, among which VCAM1, F3, PTX3, and IL-8, have also been implicated in development of ARDS (figure 6.7C) (18, 44, 63).

In order to visualize NF- $\kappa$ B-signaling in the lungs of SARS-CoV-infected aged and young adult macaques, translocation of NF- $\kappa$ B was studied using immunohistochemistry with antibodies against phosphorylated NF- $\kappa$ B on day 4 after infection. As shown in figure 6.7D, hardly any phosphorylated NF- $\kappa$ B could be detected in the nuclei of cells of PBS-infected macaques, while in the lungs of SARS-CoV-infected animals, cells with phosphorylated NF- $\kappa$ B in their nuclei were abundantly present. Phosphorylated NF- $\kappa$ B was detected primarily in the nuclei of non-infected cells (figure 6.7D). No obvious differences in the translocation of NF- $\kappa$ B in the lungs of aged and young adult macaques were observed.

### **Type I interferon- $\beta$ mRNA level is negatively correlated with gross pathology**

Overall, our data indicate that SARS-CoV-infected aged macaques display a stronger proinflammatory host response to infection than young adult macaques. For example, mRNA levels for IL-8, a key player in ALI/ARDS and a potent chemotactic factor essential in acute inflammation that is induced by a wide range of stimuli among which IL-1 $\beta$ , viral products, and oxidative stress, were strongly upregulated in SARS-CoV-infected aged macaques as compared to young adult animals (figure 6.5B, 6.7B, 6.8A). Despite the overall stronger activation of innate host gene responses in SARS-CoV-infected aged animals, microarray analyses revealed that IFN- $\beta$ , well-known for its antiviral activities, was not differentially expressed in aged

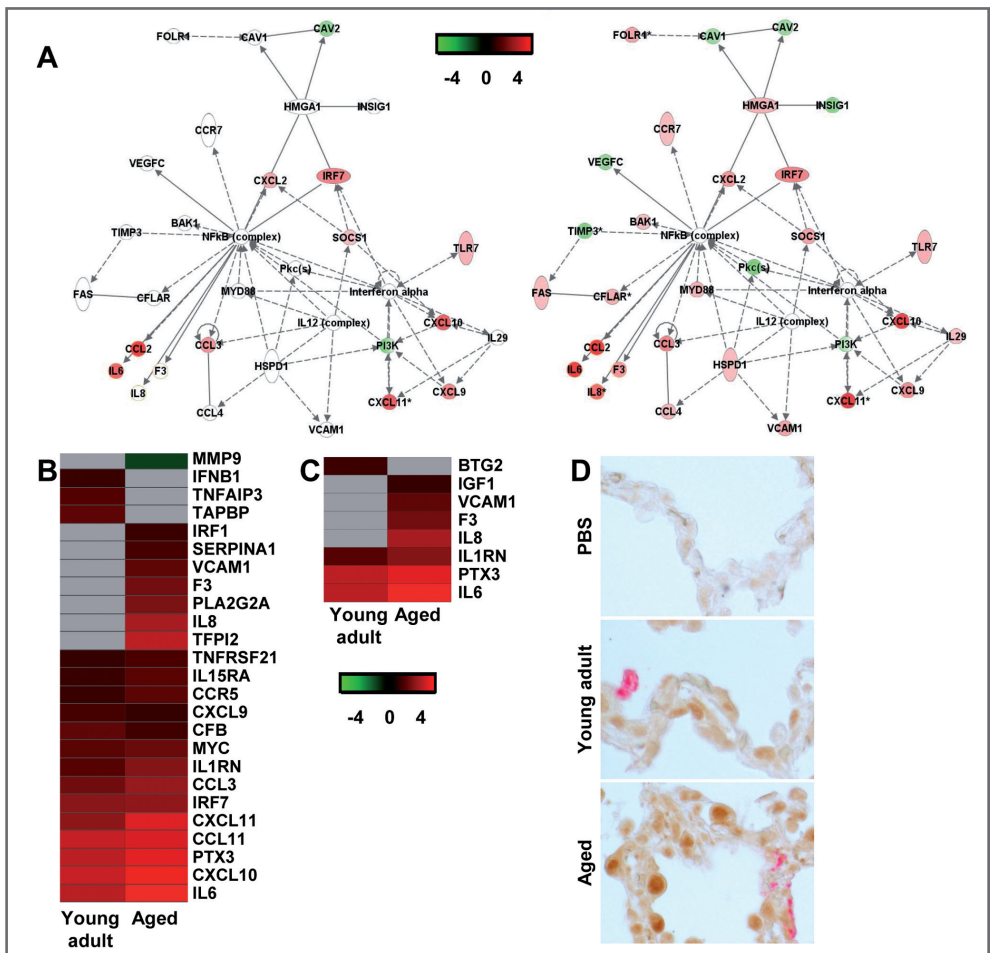


**Figure 6.7.** NF- $\kappa$ B signaling in aged and young adult macaques. (A) These diagrams show a gene interaction network from Ingenuity Pathways Knowledge Base with genes that are differentially expressed in the contrast of aged SARS-CoV-infected animals versus aged PBS-infected macaques. The central node is NF- $\kappa$ B, a key factor in inflammation and development of ARDS. Genes depicted in green are downregulated and in red upregulated. As a reference, the same network is shown for young adult animals (left panel) and aged animals (right panel). (B-C) Gene expression profiles showing differentially expressed NF- $\kappa$ B target genes (B) and genes coding for proteins involved ARDS (C) of aged and young adult macaques. Gene sets were obtained from Ingenuity Pathways Knowledge Base or literature and changed  $\geq 2$ -fold in at least one of the macaque groups as compared to PBS-infected controls. The data presented are error-weighted fold change averages for six young adult and aged animals. Genes shown in red were upregulated, in green downregulated, and in grey not significantly differentially expressed in infected animals relative to PBS-infected animals (log (base 2) transformed expression values with minimum and maximum values of the color range being -4 and 4). See Table S2 and S3 for full gene names and expression values. (D) Lung sections of PBS and SARS-CoV-infected aged and young adult macaques were stained with an antibody against phosphorylated NF- $\kappa$ B (brown) and with a mouse-anti-SARS-nucleocapsid IgG2a (red). Sections were counterstained with hematoxylin. Original magnifications are X40.

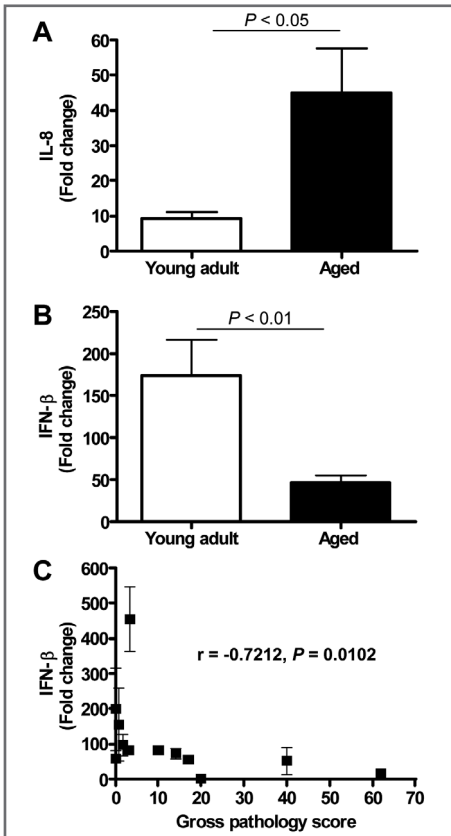


**Figure 6.8. Quantitative RT-PCR confirmation of IFN- $\beta$  mRNA levels.** (A) Quantitative RT-PCR for IL-8 was performed on two-three separate lung samples per animal with substantial virus replication. The data presented are error-weighted ( $\pm$  s.e.m.) averages of the fold-change as compared to PBS-infected controls for young adult ( $n = 6$ ) and aged ( $n = 6$ ) animals. (B) Quantitative RT-PCR for IFN- $\beta$  was performed on two-three separate lung samples per animal with substantial virus replication. The data presented are error-weighted ( $\pm$  s.e.m.) averages of the fold-change as compared to PBS-infected controls for young adult ( $n = 6$ ) and aged ( $n = 6$ ) animals. (C) The expression level of IFN- $\beta$  (fold change) per animal was plotted against gross pathology score and the correlation coefficient was determined using Spearman's correlation test.

macaques compared to PBS-infected animals, in contrast to young adults (figure 6.6E). RT-PCR analysis confirmed differential expression of IFN- $\beta$  mRNA between young adult and aged macaques (figure 6.8B). As shown in figure 6.3, this difference in IFN- $\beta$  levels in aged and young adult macaques did not affect viral replication efficiency. IFN- $\beta$  mRNA levels, however, negatively correlated with gross pathology (figure 6.8C).

### Anti-inflammatory action of type I interferon mitigates pathology in SARS-CoV-infected aged macaques

The observation of a reverse correlation of IFN- $\beta$  and IL-8 mRNA levels with age after SARS-CoV infection may reflect a physiological cross-regulation in which type I interferon and/or its respective signaling pathways modulate proinflammatory host responses (4, 35). To corroborate this hypothesis, we treated uninfected human PBMC with IL-1 $\beta$ , which is known to rapidly activate NF- $\kappa$ B-signaling (2, 5), and observed the induction of proinflammatory cytokines in uninfected human PBMC, such as IL-1 $\beta$  and IL-8 (figure 6.8A-B). An anti-inflammatory effect of pegylated IFN- $\alpha$  on IL-1 $\beta$ -induced responses was confirmed *in vitro*, as a dose-dependent inhibition of IFN- $\alpha$  on recombinant IL-1 $\beta$ -induced IL-1 $\beta$  and IL-8 mRNA levels in human PBMC was observed (figure 6.9A-B).

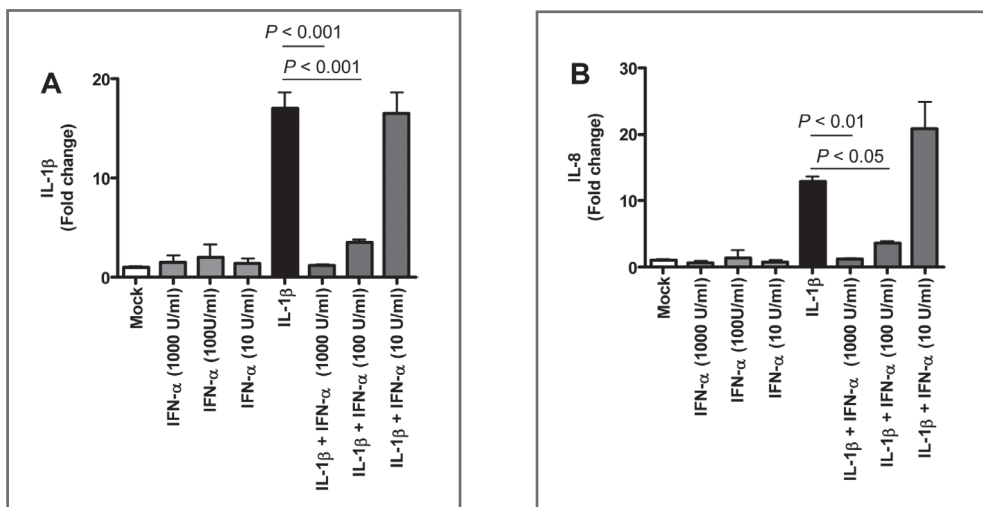


**Figure 6.9. Anti-inflammatory type I IFN inhibits IL-1 $\beta$ -induced proinflammatory cytokine production in PBMCs.** (A-B) Induction of IL-1 $\beta$  (A) and IL-8 (B) mRNAs after treatment of human PBMC with IL-1 $\beta$  (5 ng/ml), IFN- $\alpha$  (1000 U/ml, 100U/ml, or 10 U/ml) or both as determined by quantitative RT-PCR. The data presented are error-weighted ( $\pm$  s.e.m.) averages of the fold-change as compared to untreated (Mock) PBMC. Shown are representative data from one out of four donors.

Because type I IFNs can inhibit proinflammatory signaling pathways, among which NF- $\kappa$ B signaling pathways (4, 35), we examined whether exogenous administration of type I IFN in SARS-CoV-infected aged macaques could influence SARS-CoV pathogenesis. Retrospective analyses of the lungs of SARS-CoV-infected aged animals treated therapeutically with type I IFN (26) showed that SARS-CoV-infected IFN-treated aged animals remained free of clinical symptoms and had no or less extensive pulmonary consolidation than untreated aged macaques (figure 6.10A). Virus titers in the lungs, however, were similar between IFN-treated and untreated aged macaques (figure 6.10B) and viral antigen expression in the lungs was not significantly different (26).

In a direct comparison of the host response to infection in aged ( $n = 6$ ) versus IFN-treated aged ( $n = 3$ ) macaques using LIMMA, 961 gene transcripts were differentially expressed (fold change  $\geq 2$ ;  $p < 0.05$ ). Upon analysis of these gene transcripts within the context of genetic pathways, four of the most significantly regulated molecular/cellular functions ( $p < 0.005$ ) were associated with a proinflammatory response and included cellular growth and proliferation, cell death, cell movement, and cell-to-cell signaling, indicating that significant differences exist in the host response to SARS-CoV infection in animals treated with type I IFN compared to untreated aged macaques.

To obtain a broader view of the host response to infection, global gene expression profiles were determined in lungs of SARS-CoV-infected aged ( $n = 6$ ) or IFN-treated aged macaques ( $n = 3$ ) in comparison to aged PBS-infected macaques ( $n = 4$ ). IFN-treated macaques differentially expressed (fold change  $\geq 2$ ;  $p < 0.05$ ) approximately four-fold less gene transcripts than untreated aged macaques (figure 6.10C) as

compared to PBS-infected animals. The most significantly regulated molecular/cellular functions in the IFN-treated macaque group compared to PBS-infected animals were associated with a proinflammatory response and included cellular growth and proliferation, cell death, cell movement, and cell-to-cell signaling, similar to what was observed for the aged macaque group, although less genes per function were

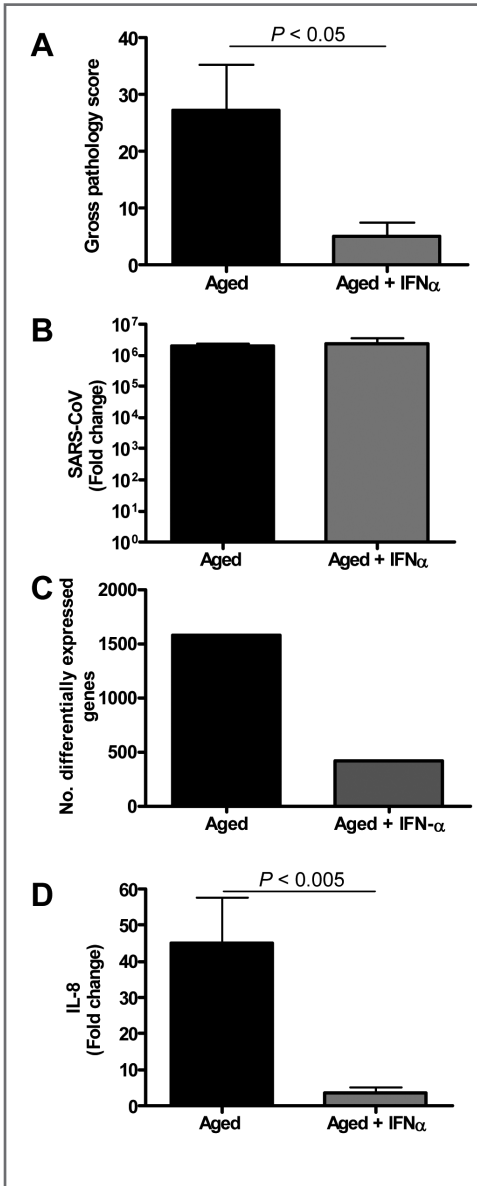


**Figure 6.10. Anti-inflammatory type I IFN inhibits virus-induced ALI in aged SARS-CoV-infected macaques.** (A) Gross pathology scores of lungs from macaques were determined during necropsy and averaged ( $\pm$  s.e.m.). (B) Average fold change ( $\pm$  s.e.m.) in SARS-CoV mRNA levels in the lungs of pegylated IFN- $\alpha$ -treated ( $n = 3$ ) and untreated aged ( $n = 6$ ) macaques compared to aged PBS-infected ( $n = 4$ ) animals as determined by real-time RT-PCR. (C) Number of differentially expressed gene transcripts compared to aged PBS-infected animals ( $\geq 2$ -fold change). (D) Quantitative RT-PCR for IL-8 was performed on two-three separate lung samples per animal with substantial virus replication. The data presented are error-weighted ( $\pm$  s.e.m.) averages of the fold-change as compared to PBS-infected controls for aged animals ( $n = 6$ ) and aged animals treated with IFN- $\alpha$  ( $n = 3$ ).

differentially expressed (figure 6.S5A). These data suggested a common nature of the host response to infection in aged and IFN-treated aged animals, although the severity seemed different.

To gain more insight in differences in the host response to infection in aged and IFN-treated macaques compared to PBS-infected animals, heat maps were generated for differentially regulated genes involved in proinflammatory pathways apoptosis (figure 6.S5B) and cell adhesion (figure 6.S5C). Using Goeman's global test (24) on the defined gene subsets cell adhesion and apoptosis, significant differences between aged and IFN-treated animals in these proinflammatory pathways were obtained, providing statistical evidence for a difference in host response of aged and IFN-treated animals to SARS-CoV infection. Moreover, a decrease in differentially expressed target genes of NF- $\kappa$ B was observed (figure 6.S5D). Most notably, a dramatic decrease in the expression of cytokine/chemokine mRNA levels was observed, among which IL-8 (figure 6.10D, figure 6.S5B-C). These data show that therapeutic treatment of SARS-CoV-infected aged macaques with type I IFN primarily results in downregulation of proinflammatory host responses.

## DISCUSSION

### Age, pathology and proinflammatory host response go hand-in-hand

The present study aimed at gaining insight into the pathogenesis of SARS-CoV by studying the relationship between age, pathology, virus replication, and host response in a macaque model. In humans, SARS-CoV infection progresses from an atypical pneumonia to acute diffuse alveolar damage and ARDS (50). The overall human fatality rate reached ~10% and up to 50% in elderly (50-51). The acute lung injury observed after SARS-CoV infection in aged macaques is similar to what has been seen in humans that progress to ARDS (51). This disease process includes an acute exudative phase, consisting of severe leukocyte infiltration, edema, the formation of hyaline membranes, and proliferation characterized by type II pneumocyte hyperplasia (27). SARS-CoV-infected aged macaques develop more severe pathology than young adult animals, even though viral replication levels are similar. The chronic phase, which is characterized by persistent intra-alveolar and interstitial fibrosis and mortality was not observed because animals were sacrificed early after infection.

Comparative analyses of gene expression in aged and young adult SARS-CoV-infected macaques revealed that the host response to SARS-CoV infection is similar in nature, but differs significantly in severity in proinflammatory responses. Aged macaques had a stronger host response to virus infection than young adult macaques, with an increase in differential expression of genes associated with inflammation that center around the transcription factor NF- $\kappa$ B. Comparative analysis of PBS-infected aged and young adult macaques revealed significant differences in gene expression as a result of aging only. These observations are in line with earlier hypotheses that age-related accumulated oxidative damage and a weakened antioxidative defense system cause a disturbance in the redox balance, resulting in increased reactive oxygen species. Subsequently, the oxidative stress-induced redox imbalance activates redox-sensitive transcription factors, such as NF- $\kappa$ B, followed by the induction of proinflammatory genes

including IL-1 $\beta$ , IL-6, TNF $\alpha$  and adhesion molecules, key players in the inflammatory process (14). Oxidative stress may also potentiate the cellular responses to IL-1 $\beta$  (57), an early mediator of inflammation (23). Thus, aging is associated not only with alterations in the adaptive immune responses, but also with a proinflammatory state in the host (6, 10, 14, 20). Oxidative stress and toll-like receptor-4 signaling via NF- $\kappa$ B triggered by viral lung pathogens, such as SARS-CoV, may further amplify the host response ultimately resulting in ALI (31). Taking the host gene expression profiles of PBS-infected aged and young adult macaques into account, we also observed a stronger activation of the proinflammatory pathways in SARS-CoV-infected aged macaques than in young adults. The finding that genes activated by NF- $\kappa$ B are significantly differentially upregulated in aged macaques infected with SARS-CoV is in line with the role of NF- $\kappa$ B as a redox-sensitive transcription factor in proinflammatory host responses and the development of ALI/ARDS (16, 31). Given the fact that several SARS-CoV proteins block NF- $\kappa$ B signaling (17, 21, 34), we hypothesize that NF- $\kappa$ B-signaling in non-infected cells is largely responsible for the upregulated expression of NF- $\kappa$ B target genes, such as IL-8, in aged compared to young adult macaques.

These observations are largely in line with transcriptome analyses in mice and SARS patients. In severe SARS patients, cytokines/chemokine involvement as the illness progresses may lead to widespread immune dysregulation and serious pathogenic events (11). Aged mice show more pathology than young adult mice and the transcriptional profile in aged mice generally indicates a more robust proinflammatory response to virus infection than in young mice (7, 55).

### **Type I IFN signaling**

Previously, we demonstrated IFN induction and signaling in SARS-CoV-infected macaques early after infection(15). Based on the observation that plasmacytoid dendritic cells are able to produce type I IFNs after SARS-CoV infection *in vitro* (12), it was speculated that these cells are the IFN-producing cells in lungs of SARS-CoV-infected macaques. In addition, phosphorylated STAT-1 was observed in the nuclei of numerous cells in the lungs of SARS-CoV-infected macaques, indicating that these cells had been activated by IFNs or other agonists produced in the lung (15). In SARS-CoV-infected cells, however, STAT-1 signaling was blocked (15), consistent with the fact that a range of SARS-CoV proteins can function as interferon antagonists that inhibit IFN production and signaling (21, 34). Therefore, a large part of the genes activated downstream of STAT-1, observed in genomics analyses, is likely due to signaling in non-infected cells (15). In the current study, we observed that aged macaques expressed significantly lower levels of IFN- $\beta$  mRNA than young adult macaques and that IFN- $\beta$  mRNA levels correlated negatively with severity of pathology. Interestingly, aged and young adult SARS-CoV-infected macaques showed opposite expression patterns for type I IFN- $\beta$  and certain proinflammatory cytokines, such as IL-8. These data are corroborated by previous observations showing that higher amounts of proinflammatory cytokines, such as IL-1 $\beta$  and IL-8, are produced upon stimulation of leukocytes of the elderly, whereas induction of type I IFNs is decreased compared to young adults (33, 54, 67).

### **Cross-regulation between type I IFN and NF- $\kappa$ B signaling cascades**

The observation of a reverse correlation of IFN- $\beta$  and IL-8 mRNA levels with age after SARS-CoV infection may reflect a physiological cross-regulation between antiviral STAT-1 and proinflammatory NF- $\kappa$ B

pathways. Evidence for such a cross-regulation between type I IFN/STAT-1 and proinflammatory/NF- $\kappa$ B signaling pathways exists. Type I interferons exert significant anti-inflammatory effects and provide at least partial protection from disease in collagen-induced arthritis, auto-immune encephalitis, and multiple sclerosis (1, 9, 25, 53, 61). Not only inhibits IFN-beta expression of the IL-8 gene at the transcriptional level (47), type I IFNs can also activate TAM receptor tyrosine kinases that inhibit toll-like receptor-induced cytokine-receptor cascades (48, 56) and induce the immunosuppressive cytokine IL-10 (3). Direct NF- $\kappa$ B/STAT-1 protein-protein interactions (22) and modification of STAT-1 by acetylation, may be involved in this process (35). A loss of type I IFN/STAT-1 signaling in aged macaques may negatively regulate interferon-induced gene expression and type I IFN signaling, which may lead to enhanced inflammatory responses. On the other hand, increased activation of NF- $\kappa$ B signaling pathways in aged macaques may negatively regulate interferon-induced gene expression and type I IFN signaling (4, 49, 64), which may enhance proinflammatory responses even further.

We have integrated our data and other findings on cross-regulation in a model (figure 6.11). The model depicts the innate immune response to SARS-CoV infection as a coordinated series of signaling pathways aimed at clearing the virus while not harming host cells. Upon SARS-CoV infection, infected cells, depicted in the model as pneumocytes, produce inflammatory mediators that activate NF- $\kappa$ B, resulting in the production of proinflammatory cytokines and chemokines, such as IL-8. IL-1 is one of the cytokines highly upregulated on day 1 after infection upon SARS-CoV infection of macaques (15) and capable of activating NF- $\kappa$ B. At the same time, the virus is recognized by sentinel cells, such as pDCs, that produce type I IFNs to signal that a foreign invader has entered the host. The production of IFN induces neighboring non-infected cells to remodel the intracellular environment by producing a range of antiviral proteins,

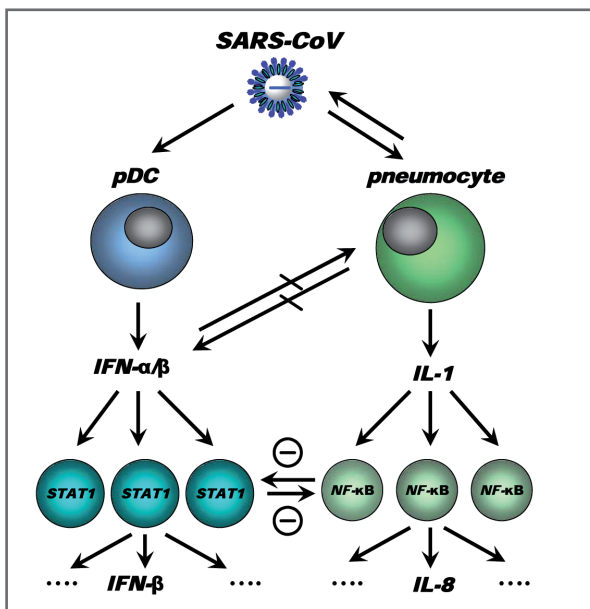


Figure 6.11. Model for cross-talk between “proinflammatory” and “antiviral” pathways during SARS-CoV infection. SARS-CoV infection results in activation of both “antiviral” and “proinflammatory” pathways. Subsets of uninfected cells, depicted by pDCs, start producing type I IFN (IFN- $\alpha$ ), which results in STAT-1 activation in neighbouring cells, which in turn may produce other mediators (e.g. IFN- $\beta$ ). The SARS-CoV-infected cells produce inflammatory mediators, supposedly IL-1, which results in NF- $\kappa$ B activation in neighbouring uninfected cells and subsequent production of inflammatory mediators, such as IL-8. Cross-regulation between “antiviral” and “proinflammatory” pathways allows polarisation of antiviral or proinflammatory responses thereby modulating pathology. Modulation of transcription factors in the uninfected cells, e.g. by aging, may affect the overall outcome of the infection.



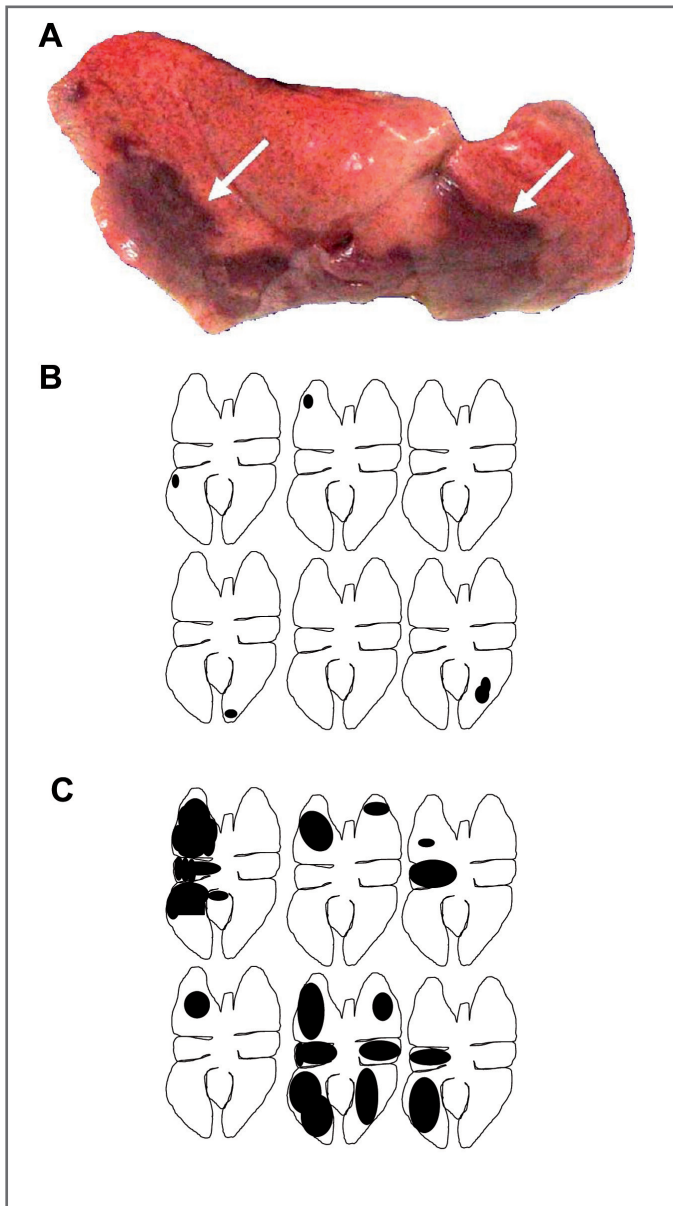
aiding in a block of viral replication. A cross-regulation between the “antiviral” and “proinflammatory” pathways occurs, which is a critical requirement to allow fine-tuning of the host response to infection and return to homeostasis. Disease outcome may be determined by the relative contribution of “antiviral” and “proinflammatory” pathways and apparently aging influences this intricate balance significantly.

Causal relationships between “antiviral” and “proinflammatory” pathways in macaques are difficult to prove and future studies in specific gene knock-out mice should therefore further clarify the complex interactions in the response to SARS-CoV. Our own *in vitro* experiments and the type I IFN intervention in SARS-CoV-infected aged macaques indicate that type I IFNs can play a role in mitigating proinflammatory host responses and severity of pathology. Therapeutic treatment of SARS-CoV-infected aged macaques with type I IFN reduces pathology and diminishes proinflammatory gene expression, including IL-8 levels, without affecting virus replication in the lungs. Antiviral effects of type I IFNs were not obvious, probably due to the fact that SARS-CoV infected cells inhibit STAT-1 signaling and viral replication peaks early after infection when treatment with pegylated IFN- $\alpha$  started. Given the fact that phosphorylated NF- $\kappa$ B was present mainly in the nuclei of non-infected cells in the lungs of SARS-CoV-infected macaques, these cells are potential targets for the action of IFN and subsequent STAT-1 signaling. It remains uncertain whether endogenously produced IFNs in young adult macaques are essential in the control of inflammatory responses or that enhanced activation of inflammatory pathways simply does not occur. Our data are in line with the observation that treatment of SARS-CoV-infected aged mice with type II IFN- $\gamma$ , which like type I IFN also signals via STAT-1, protected against lethal respiratory illness, seemingly without an effect on viral replication (45). Moreover, in humans with SARS, use of type I IFNs was associated with reduced disease-associated hypoxia and a more rapid resolution of radiographic lung abnormalities (41). Whether the anti-inflammatory action of type I/II IFNs in macaques, mice and humans occurs via common pathways and is interchangeable between host species remains to be determined. Assuming that there is a conserved pathway in ALI/ARDS induced by multiple pathogens, including pandemic viruses that may emerge from avian influenza, modulation of the host response by type I IFNs provides a promising outlook for novel intervention strategies.

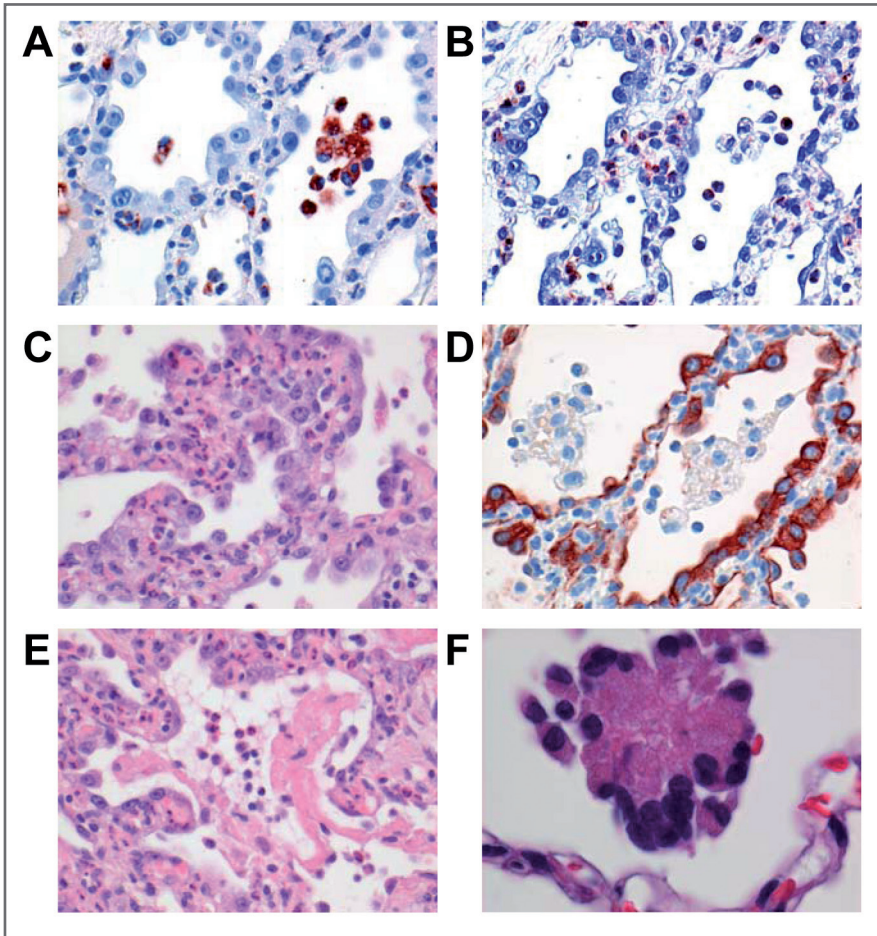
## ACKNOWLEDGEMENTS

We thank R. Dias d’Ullois, M.A. Bijl, F. Zaaraoui-Boutahar and R. Lonsdale for technical assistance.

## SUPPORTING INFORMATION



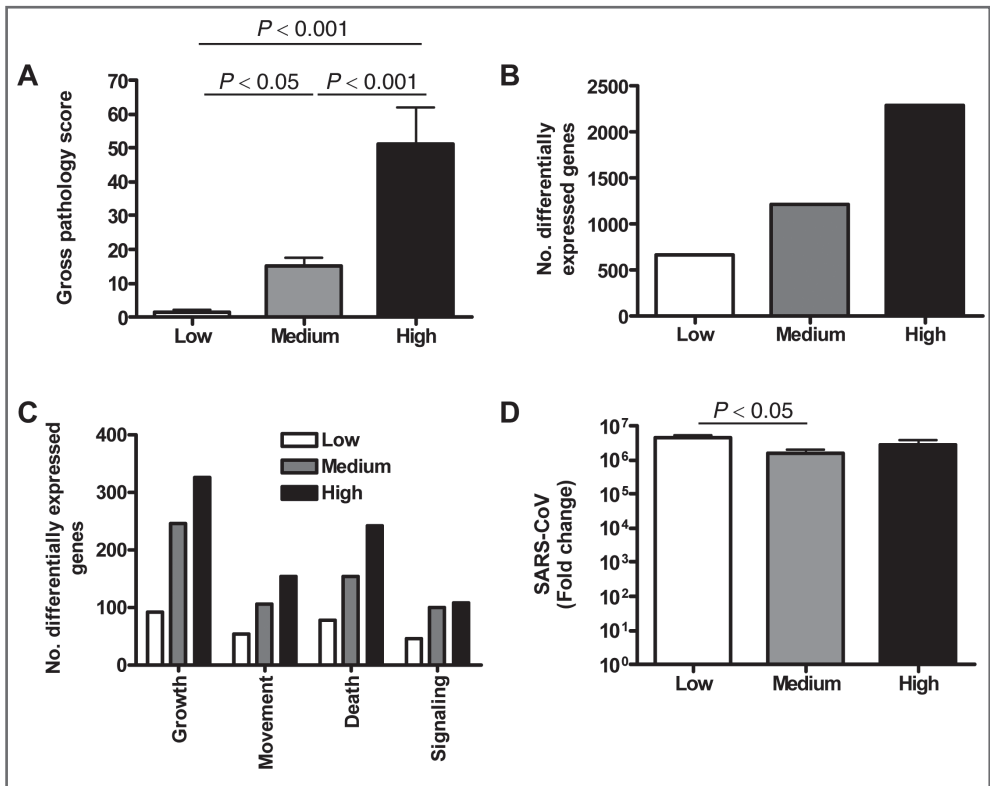
**Figure 6.S1: Gross lesions in aged macaque.** (A) SARS-CoV-induced lesions (white arrows) in the lung are still visible after inflation with 10% neutral-buffered formalin. (B-C) Schematic diagrams of the lungs showing gross pathology lesions of SARS-CoV-infected young adult (B) and aged (C) macaques.



**Figure 6.S2: Histology and immunohistochemical detection of cells in lungs from SARS-CoV-infected macaques.** (A-B) Lesion in the lung of a SARS-CoV-infected aged macaque, characterized by thickened alveolar walls lined by type II pneumocytes (type II pneumocyte hyperplasia) with influx of inflammatory cells. Consecutive sections were stained with a mouse monoclonal anti-human CD68 antibody for macrophages (A) and a mouse monoclonal anti-human neutrophil elastase antibody for neutrophils (B). Sections were counterstained with hematoxylin. Original magnifications are X40. (C) Lesions in the lung of a SARS-CoV infected aged macaque showing diffuse alveolar damage, characterized by type II pneumocyte hyperplasia with influx of inflammatory cells. (D) Lesion in the lung of a SARS-CoV-infected aged macaque, characterized by thickened alveolar walls lined by type II pneumocytes stained with a mouse monoclonal anti-human pankeratin antibody for epithelial cells. (E-F) Hyaline membranes (E) and syncytia (F) were occasionally observed in the lungs of aged macaques.

Gene symbol	Young adult						Aged					
	1	2	3	4	5	6	1	2	3	4	5	6
<b>BMP1</b>	6,62	6,93	6,88	6,68	7,22	7,06	6,15	6,23	6,24	6,63	6,62	7,14
<b>CCL11</b>	9,31	11,02	9,14	10,84	7,86	7,30	9,91	8,81	10,33	10,84	8,82	7,54
<b>CCL19</b>	7,41	6,97	7,97	8,50	7,14	6,15	7,36	8,06	7,58	7,99	8,28	8,29
<b>CCL3</b>	8,44	9,41	7,03	9,31	9,24	8,99	10,25	9,70	9,11	10,64	9,76	8,38
<b>CCL4L1</b>	8,05	8,85	6,87	8,75	8,82	8,80	9,52	8,53	8,61	9,49	8,90	8,13
<b>CCL8</b>	9,82	10,13	7,18	10,72	8,61	7,83	11,27	10,78	10,20	10,66	8,86	8,91
<b>CXCL1 /// CXCL3</b>	8,97	9,27	8,99	9,92	7,83	8,01	11,08	8,76	9,57	11,60	9,47	8,73
<b>CXCL10</b>	10,51	11,47	9,11	11,30	9,21	9,13	11,99	11,60	10,99	11,97	10,34	8,13
<b>CXCL11</b>	8,94	10,13	8,00	9,83	8,00	8,23	10,82	10,37	10,04	10,50	9,62	7,37
<b>CXCL9</b>	6,98	7,20	6,80	6,64	6,61	6,93	6,33	7,15	6,64	7,30	6,27	5,23
<b>IFNB1</b>	6,41	7,65	5,84	6,51	5,88	5,77	6,55	6,49	6,13	6,55	5,89	5,36
<b>IL1RN</b>	9,24	9,43	8,19	9,50	8,66	8,57	10,78	10,12	10,07	11,07	9,60	8,97
<b>IL6</b>	9,16	8,82	8,14	9,52	6,73	7,45	10,20	9,76	9,85	11,47	9,17	8,72
<b>IL8</b>	7,59	8,57	7,64	8,84	7,36	7,02	11,46	8,06	9,40	11,77	10,41	9,38
<b>MCP-1</b>	10,89	11,36	9,55	11,83	9,25	9,00	12,32	11,62	11,54	12,27	11,09	10,97
<b>PPBP</b>	5,53	5,34	5,43	5,35	5,88	6,58	5,31	7,02	5,13	5,44	5,25	5,58
<b>SPP1</b>	6,50	7,35	6,01	7,58	6,19	5,92	9,34	7,35	7,47	8,75	7,89	7,11
<b>TNFSF13B</b>	10,49	10,65	9,63	11,01	9,45	9,38	11,28	11,24	10,79	11,16	10,61	9,78

Figure 6.53: Global gene expression profiles of individual young adult and aged animals. For a subset of gene transcripts, cytokines and chemokines, normalized log-2 based hybridization values for individual aged and young adult macaques are shown.



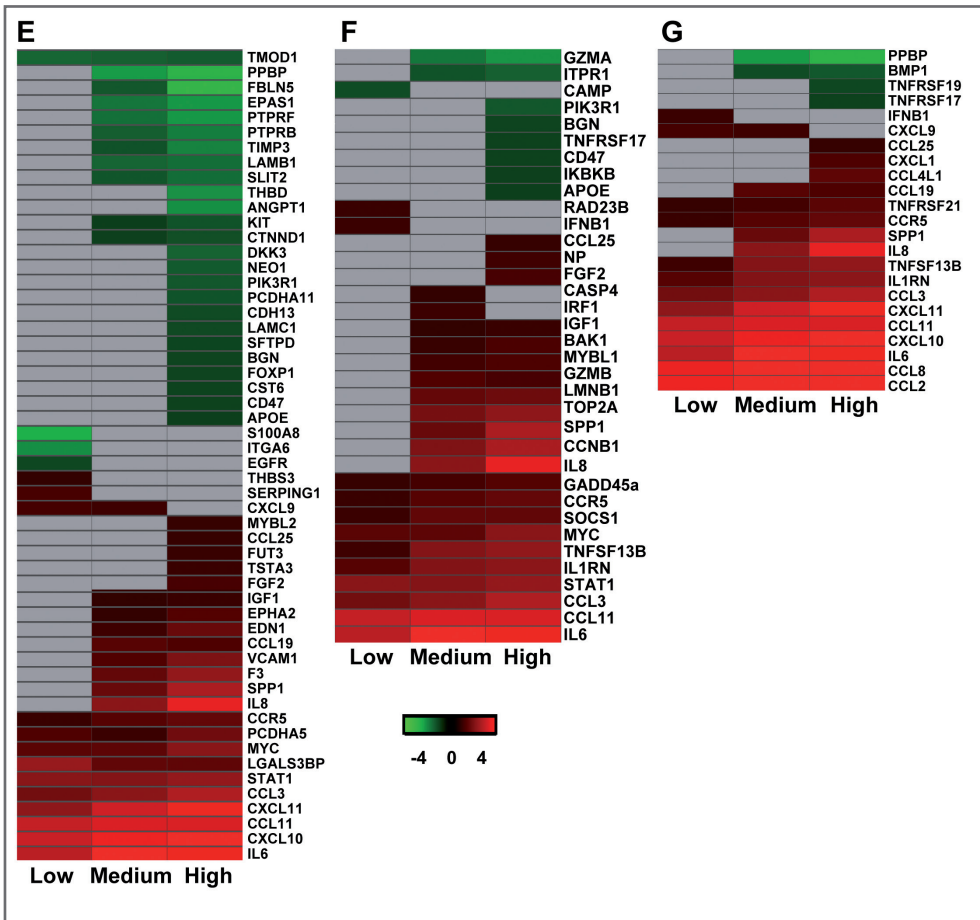
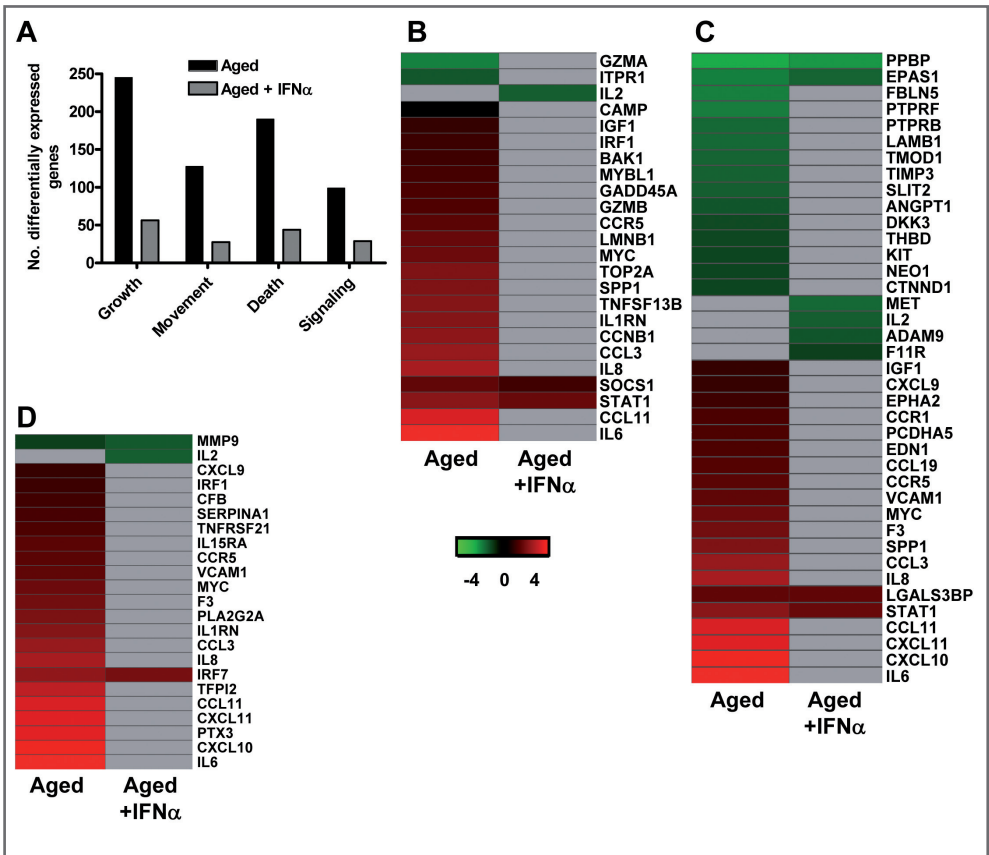


Figure 6.S4: Microarray analyses of the lower respiratory tract of SARS-CoV-infected macaques displaying different levels of severity of pathology. (A) Gross pathology scores of the lungs from aged and young adult macaques were determined. Based on the severity of pathology, macaques were divided in three groups (low (young adult animals; n = 6), medium (aged; n = 4), and high (aged; n = 2) pathology score), and average pathology scores ( $\pm$  s.e.m.) are shown. (B) Number of differentially expressed gene transcripts compared to uninfected animals ( $\geq 2$ -fold change) in macaque groups. (C) Number of differentially expressed genes in macaque groups compared to PBS-infected animals with functions in cellular growth and proliferation, cell movement, cell death, or cell-to-cell signaling and interaction obtained from Ingenuity Pathways Knowledge Base. (D) Average fold change ( $\pm$  s.e.m.) in SARS-CoV mRNA levels in the lungs of macaques with low, medium and high pathology scores as compared to PBS-infected animals as determined by real-time RT-PCR. (E-G) Gene expression profiles showing differentially expressed genes coding for proteins involved in cell adhesion (E), proteins involved in apoptosis (F), and cytokines and chemokines (G) of macaque groups with low, medium and high pathology scores as compared to PBS-infected animals. Genes displayed were obtained from Ingenuity Pathways Knowledge Base and changed  $\geq 2$ -fold in at least one of the macaque groups as compared to PBS-infected controls. The data presented are error-weighted averages. Genes shown in red were upregulated and in green downregulated in infected animals relative to PBS-infected animals ( $\log_2$  transformed expression values with minimum and maximum values of the color range being  $-4$  and  $4$ ). Genes shown in grey were not significantly differentially regulated. See Table S2 and S4 for full gene names and expression values.



**Figure 6.5:** Microarray analyses of the lower respiratory tract of SARS-CoV-infected aged and aged macaques treated with pegylated IFN- $\alpha$ . (A) Number of differentially expressed genes in macaque groups compared to PBS-infected animals with functions in cell growth and proliferation, cell movement, cell death, or cell-to-cell signaling and interaction obtained from Ingenuity Pathways Knowledge Base. When SARS-CoV-infected aged macaques were compared directly to IFN-treated aged macaques, these gene sets were significantly differentially expressed. (B-D) Gene expression profiles showing differentially expressed genes coding for proteins involved in apoptosis (B), cell adhesion (C), or NF- $\kappa$ B-signaling (D) of IFN $\alpha$ -treated and untreated aged macaques. Genes displayed were obtained from Ingenuity Pathways Knowledge Base or literature and changed  $\geq 2$ -fold in at least one of the groups as compared to PBS-infected controls. The data presented are error-weighted averages. Genes shown in red were upregulated, in green downregulated, and in grey not significantly differentially expressed in infected animals relative to PBS-infected animals ( $\log_2$  transformed expression values with minimum and maximum values of the color range being  $-4$  and  $4$ ). Global test analysis of the direct contrast of SARS-CoV-infected aged versus IFN-treated aged animals showed that the cell adhesion and apoptosis pathways were significantly differentially expressed ( $p < 0.05$ ). See Table S2 and S3 for full gene names and expression values.



**Supplementary Table S1****Annotated differentially expressed genes in aged versus young adult SARS-CoV infected macaques.**

<b>Symbol</b>	<b>Fold change</b>	<b>Annotation</b>
ACPP	1.09	acid phosphatase, prostate
ADRBK2	-1.02	adrenergic, beta, receptor kinase 2
AGER	-1.25	advanced glycosylation end product-specific receptor
AGTR1	-1.30	angiotensin II receptor, type 1
ANLN	1.64	anillin, actin binding protein
ANXA10	1.13	annexin A10
AQP3	1.42	aquaporin 3 (Gill blood group)
AREG	2.67	amphiregulin
ARL5B	1.18	ADP-ribosylation factor-like 5B
ASIP	-1.47	agouti signaling protein, nonagouti homolog (mouse)
ATP1B1	1.05	ATPase, Na <sup>+</sup> /K <sup>+</sup> transporting, beta 1 polypeptide
C12ORF5	1.51	chromosome 12 open reading frame 5
C15ORF48	1.34	chromosome 15 open reading frame 48
C4ORF43	1.27	chromosome 4 open reading frame 43
C5ORF23	-1.01	chromosome 5 open reading frame 23
CCNB1	1.34	cyclin B1
CD300LG	-1.44	CD300 molecule-like family member g
CD36	-1.21	CD36 molecule (thrombospondin receptor)
CDC20	1.01	cell division cycle 20 homolog ( <i>S. cerevisiae</i> )
CDO1	1.31	cysteine dioxygenase, type I
CEACAM5	1.83	carcinoembryonic antigen-related cell adhesion molecule 5
CLDN1	1.40	claudin 1
COL3A1	-1.62	collagen, type III, alpha 1
COL4A3	-1.32	collagen, type IV, alpha 3 (Goodpasture antigen)
CSNK1A1	1.32	casein kinase 1, alpha 1
CTSL1	1.11	cathepsin L1
CYP1B1	2.10	cytochrome P450, family 1, subfamily B, polypeptide 1
CYP4B1	-1.08	cytochrome P450, family 4, subfamily B, polypeptide 1
DDX3Y	-2.85	DEAD (Asp-Glu-Ala-Asp) box polypeptide 3, Y-linked
DEFB1	1.28	defensin, beta 1
DPP4	1.04	dipeptidyl-peptidase 4
ECT2	1.08	epithelial cell transforming sequence 2 oncogene
EDN3	-1.16	endothelin 3
EGFL6	-1.33	EGF-like-domain, multiple 6
EIF1AX	1.17	eukaryotic translation initiation factor 1A, X-linked
EIF1AY	-2.02	eukaryotic translation initiation factor 1A, Y-linked
EIF5A	1.55	eukaryotic translation initiation factor 5A
EMP2	-1.08	epithelial membrane protein 2
ENPP6	-1.04	ectonucleotide pyrophosphatase/phosphodiesterase 6
EREG	2.69	epiregulin
F3	1.48	coagulation factor III (thromboplastin, tissue factor)
FAM162B	-1.18	family with sequence similarity 162, member B
FBLN5	-1.03	fibulin 5
FFAR2	1.35	free fatty acid receptor 2
FMO2	-1.62	flavin containing monooxygenase 2 (non-functional)
FNDC1	-1.54	fibronectin type III domain containing 1
GALNT3	1.28	UDP-N-acetyl-alpha-D-galactosamine:polypeptide N-acetylgalactosaminyltransferase 3
GAPDH	1.01	glyceraldehyde-3-phosphate dehydrogenase
GJA5	-1.05	gap junction protein, alpha 5, 40kDa
GLS	1.01	glutaminase
GPM6B	-1.03	glycoprotein M6B
GPR84	1.05	G protein-coupled receptor 84
GSTM5	-1.06	glutathione S-transferase mu 5
HHIP	-1.13	hedgehog interacting protein
HK2	1.15	hexokinase 2
HPSE	1.04	heparanase
HTRA1	-1.02	HtrA serine peptidase 1
IGFBP5	-1.09	insulin-like growth factor binding protein 5

IGL@	1.40	immunoglobulin lambda locus
IGSF10	-1.68	immunoglobulin superfamily, member 10
IL1RL1	1.48	interleukin 1 receptor-like 1
IL1RN	1.17	interleukin 1 receptor antagonist
IL6	1.56	interleukin 6 (interferon, beta 2)
IL8	2.24	interleukin 8
IMAA	1.45	SLC7A5 pseudogene
INMT	-1.25	indolethylamine N-methyltransferase
ITGA8	-1.51	integrin, alpha 8
JUP	1.01	junction plakoglobin
KIAA0101	1.10	KIAA0101
KRT6A	1.59	keratin 6A
KRT6B	1.19	keratin 6B
KRT8	1.03	keratin 8
KRT8L2	1.48	keratin 8 pseudogene 12
LAMB1	-1.01	laminin, beta 1
LIF	1.03	leukemia inhibitory factor (cholinergic differentiation factor)
LRP4	-1.28	low density lipoprotein receptor-related protein 4
LY86	1.09	lymphocyte antigen 86
MAD2L1	1.20	MAD2 mitotic arrest deficient-like 1 (yeast)
MAFB	1.03	v-maf musculoaponeurotic fibrosarcoma oncogene homolog B (avian)
MIR21	1.08	microRNA 21
MMP7	2.20	matrix metalloproteinase 7 (matrilysin, uterine)
MPZL2	1.58	myelin protein zero-like 2
N4BP2L1	-1.45	NEDD4 binding protein 2-like 1
NFE2L3	1.14	nuclear factor (erythroid-derived 2)-like 3
NFKBIZ	1.56	nuclear factor of kappa light polypeptide gene enhancer in B-cells inhibitor, zeta
NP	1.22	nucleoside phosphorylase
NPM1	1.02	nucleophosmin (nucleolar phosphoprotein B23, numatrin)
OGN	-1.32	osteoglycin
PADI2	1.43	peptidyl arginine deiminase, type II
PAPSS2	-1.24	3'-phosphoadenosine 5'-phosphosulfate synthase 2
PHLDA2	1.31	pleckstrin homology-like domain, family A, member 2
PKIB	1.33	protein kinase (cAMP-dependent, catalytic) inhibitor beta
PLA1A	1.59	phospholipase A1 member A
PPA1	1.22	pyrophosphatase (inorganic) 1
PTCH1	-1.05	patched homolog 1 (Drosophila)
REV3L	1.26	REV3-like, catalytic subunit of DNA polymerase zeta (yeast)
RICTOR	1.51	RPTOR independent companion of MTOR, complex 2
RIMKLB	-1.01	ribosomal modification protein rimK-like family member B
RRM2	1.13	ribonucleotide reductase M2 polypeptide
S100A8	2.18	S100 calcium binding protein A8
SCD5	-1.30	stearoyl-CoA desaturase 5
SCN7A	-1.13	sodium channel, voltage-gated, type VII, alpha
SEC24D	1.13	SEC24 family, member D (S. cerevisiae)
SEMA6D	-1.14	sema domain, transmembrane domain (TM), and cytoplasmic domain, (semaphorin) 6D
SERPINA1	1.15	serpin peptidase inhibitor, clade A (alpha-1 antiproteinase, antitrypsin), member 1
SERPINA3	2.26	serpin peptidase inhibitor, clade A (alpha-1 antiproteinase, antitrypsin), member 3
SERPINB1	1.53	serpin peptidase inhibitor, clade B (ovalbumin), member 1
SERPINB5	1.24	serpin peptidase inhibitor, clade B (ovalbumin), member 5
SLC2A3	1.15	solute carrier family 2 (facilitated glucose transporter), member 3
SLC6A14	1.20	solute carrier family 6 (amino acid transporter), member 14
SLIT3	-1.28	slit homolog 3 (Drosophila)
SOCS3	1.04	suppressor of cytokine signaling 3
SOSTDC1	-2.03	sclerostin domain containing 1
SPP1	1.39	secreted phosphoprotein 1
SPRR1B	1.68	small proline-rich protein 1B (cornifin)
STEAP1	1.86	six transmembrane epithelial antigen of the prostate 1
TFPI2	2.65	tissue factor pathway inhibitor 2
TLR4	1.14	toll-like receptor 4
TNFRSF21	1.00	tumor necrosis factor receptor superfamily, member 21
TRIP13	1.10	thyroid hormone receptor interactor 13
TUBA1C	1.23	tubulin, alpha 1c
TUBB2A	1.20	tubulin, beta 2A



TXNDC17	1.00	thioredoxin domain containing 17
UBE2C	1.33	ubiquitin-conjugating enzyme E2C
UGCG	1.73	UDP-glucose ceramide glucosyltransferase
UGT8	1.05	UDP glycosyltransferase 8
UHRF1	1.30	ubiquitin-like with PHD and ring finger domains 1
WDFY1	1.17	WD repeat and FYVE domain containing 1
WNK1	-1.41	WNK lysine deficient protein kinase 1
XIST	3.29	X (inactive)-specific transcript (non-protein coding)
XPO1	1.12	exportin 1 (CRM1 homolog, yeast)
ZDHC9	1.06	zinc finger, DHHC-type containing 9

## Supplementary Table S2 Description of genes

Gene name	Gene description
ADAM9	ADAM metallopeptidase domain 9
ANGPT1	Angiopietin 1
APOE	Apolipoprotein E
BAK1	Bcl2-homologous antagonist/killer
BGN	Biglycan
BMP1	Bone morphogenetic protein 1
BTG2	B-cell translocation gene 2
CAMP	Cathelicidin antimicrobial peptide
CASP4	Caspase 4
CCL11	Chemokine (C-C motif) ligand 11
CCL19	Chemokine (C-C motif) ligand 19
CCL25	Chemokine (C-C motif) ligand25
CCL3	Chemokine (C-C motif) ligand 3
CCL4L1	Chemokine (C-C motif) ligand 4 like 1
CCL8	Chemokine (C-C motif) ligand 8
CCNB1	Cyclin B1
CCR1	Chemokine (C-C motif) receptor 1
CCR5	Chemokine (C-C motif) receptor 5
CD47	CD47 antigen
CDH13	Cadherin 13
CFB	Complement factor B
CST6	Cytostatin 6
CTNND1	Catenin, delta 1
CXCL1	Chemokine (C-X-C motif) ligand 1
CXCL1 /// CXCL3	Chemokine CXCL1///CXCL3
CXCL10	Chemokine (C-X-C motif) ligand 10
CXCL11	Chemokine (C-X-C motif) ligand 11
CXCL6	Chemokine (C-X-C motif) ligand 6
CXCL9	Chemokine (C-X-C motif) ligand 9
DKK3	Dickkopf homolog 3
EDN1	Endothelin 1
EGFR	Epidermal growth factor receptor
EPAS1	Endothelial PAS domain protein 1
EPHA2	Ephrin receptor A2
F11R	F11 receptor

F3	Coagulation factor III
FBLN5	Fibulin 5
FGF2	Heparin-binding growth factor 2
FOXP1	Forkhead box F1
FUT3	Fucosyltransferase 3
GADD45A	Growth arrest & DNA-damage-inducible protein 45 $\alpha$
GZMA	Granzyme A
GZMB	Granzyme B
IFNB1	Interferon, beta
IGF1	Insulin-like growth factor 1
IKBKB	Inhibitor $\kappa$ light polypeptide gene enhancer B-cells kinase beta
IL15RA	Interleukin 15 receptor, alpha
IL1RN	Interleukin 1 receptor antagonist
IL2	Interleukin 2
IL29	Interleukin 29
IL6	Interleukin 6
IL8	Interleukin 8
IRF1	Interferon regulatory factor 1
IRF7	Interferon regulatory factor 7
ITGA6	Integrin A6
ITPR1	Inositol 1,4,5-triphosphate receptor, type 1
KIT	V-kit Hardy-Zucker man4 feline sarcoma viral oncogene homolog
LAMB1	Laminin, beta 1
LAMC1	Laminin, gamma 1
LGALS3BP	Galectin 3 binding protein
LMNB1	Lamin B1
MCP-1	Chemokine (C-C motif) ligand 2
MET	Met proto-oncogene tyrosine kinase
MMP9	Matrix metalloproteinase 9
MYBL1	V-myb myeloblastosis viral oncogene homolog-like 1
MYBL2	V-myb myeloblastosis viral oncogene homolog-like 2
MYC	Myc proto-oncogene protein
NEO1	Neogenin homolog 1
NP	Nucleoside phosphorylase
PCDHA11	Protocadherin 11
PCDHA5	Protocadherin 5
PIK3R1	Phosphoinositide-3-kinase, regulatory subunit 1
PLA2G2A	Phospholipase A2, group IIA
PPBP	Chemokine (C-X-C motif) ligand 7
PTPRB	Protein tyrosine phosphatase, receptor type, B
PTPRF	Protein tyrosine phosphatase, receptor type, F
PTX3	Pentraxin 3
RAD23B	UV excision repair protein RAD23B homolog B
S100A8	S100 calcium-binding protein A8
SERPINA1	Alpha-1-antitrypsin
SERPING1	Serpin peptidase inhibitor 1 G1
SFTPD	Surfactant protein D
SLIT2	Slit homolog 2
SOCS1	Suppressor of cytokine signaling 1
SPP1	Osteopontin
STAT1	Signal transducer and activator of transcription 1

STAT1	Signal transducer and activator of transcription 1
TAPBP	TAP-binding protein
TFPI2	Tissue factor pathway inhibitor 2
THBD	Thrombomodulin
THBS3	Thrombospondin 3
TIMP3	Tissue inhibitor of matrix metalloproteinase-3
TMOD1	Tropomodulin 1
TNFAIP3	Tumor necrosis factor, alpha-induced protein 3
TNFRSF17	Tumor necrosis factor receptor superfamily, member 17
TNFRSF19	Tumor necrosis factor receptor superfamily, member 19
TNFRSF21	Tumor necrosis factor receptor superfamily, member 21
TNFSF13B	Tumor necrosis factor superfamily, member 13B
TOP2A	DNA topoisomerase II, alpha isozyme
TSTA3	Tissue specific transplantation antigen P35B
VCAM1	Vascular cell adhesion molecule 1

**Supplementary Table S3** Log (base 2)-transformed expression values of genes in heat maps in Fig 6, Fig. 7, and Fig. S5.

Symbol	Young	Aged	Aged + IFN $\alpha$
ADAM9	0	0	-1.316
ANGPT1	0	-1.321	0
BAK1	0	1.153	0
BMP1	0	-1.244	0
BTG2	1.099	0	0
CAMP	-1.181	0	0
CCL11	3.067	3.337	0
CCL19	0	1.463	0
CCL2	3.717	4.639	0
CCL3	1.886	2.425	0
CCL4L1	0	1.268	0
CCL8	3.556	4.467	2.57
CCNB1	0	2.285	0
CCR1	0	1.32	0
CCR5	1.069	1.56	0
CFB	1.631	1.183	0
CTNND1	0	-1.086	0
CXCL1 /// CXCL3	0	1.877	0
CXCL10	3.124	3.769	0
CXCL11	2.294	3.409	0
CXCL6	0	-1.161	-1.078
CXCL9	1.251	1.037	0
DKK3	0	-1.155	0
EDN1	0	1.344	0
EGFR	-1.128	0	0
EPAS1	0	-1.901	-1.517
EPHA2	0	1.154	0
F11R	0	0	-1.029
F3	0	1.897	0
FBLN5	0	-1.89	0
GADD45A	1.037	1.318	0
GZMA	0	-1.914	0
GZMB	0	1.365	0
IFNB1	1.084	0	0
IGF1	0	1.029	0
IL15RA	1.087	1.538	0
IL1RN	1.495	2.164	0

IL2	0	0	-1.436
IL29	0	1.047	0
IL6	2.924	4.009	0
IL8	0	2.665	0
IRF1	0	1.103	0
IRF7	2.228	2.33	1.962
ITGA6	-2.092	0	0
ITPR1	0	-1.334	0
KIT	0	-1.093	0
LAMB1	0	-1.572	0
LGALS3BP	2.431	1.638	1.632
LMNB1	0	1.739	0
MET	0	0	-1.575
MMP9	0	-1.007	-1.378
MYBL1	0	1.245	0
MYC	1.552	1.808	0
NEO1	0	-1.093	0
PCDHA5	1.369	1.342	0
PIK3R1	-1.03	0	0
PLA2G2A	0	2.039	0
PPBP	0	-2.438	-2.204
PTPRB	0	-1.575	0
PTPRF	0	-1.856	0
PTX3	2.954	3.46	0
RAD23B	1.082	0	0
S100A8	-2.516	0	0
SERPINA1	0	1.271	0
SERPING1	1.27	0	0
SLIT2	0	-1.435	0
SOCS1	1.087	1.649	1.161
SPP1	0	2.085	0
STAT1	2.226	2.222	1.758
TAPBP	1.594	0	0
TFPI2	0	2.966	0
THBD	-1.121	-1.114	0
THBS3	1.015	0	0
TIMP3	0	-1.488	0
TMOD1	-1.382	-1.518	0
TNFAIP3	1.444	0	0
TNFRSF21	1.036	1.335	0
TNFSF13B	1.244	2.158	0
TOP2A	0	2.081	0
VCAM1	0	1.618	0

**Supplementary Table S4** Log (base 2)-transformed expression values of genes in heat maps in Fig. S4.

Symbol	Low	Medium	High
ADAM9	1.18	0	0
ANGPT1	0	0	-2.105
APOE	0	0	-1.012
BAK1	0	1.066	1.327
BGN	0	0	-1.072
BMP1	0	-1.186	-1.36
BTG2	0	1.099	0
CAMP	-1.181	0	0
CASP4	0	1.014	0
CCL11	3.067	3.343	3.326
CCL19	0	1.518	1.354
CCL25	0	0	1.048
CCL3	1.886	2.242	2.791
CCL4L1	0	0	1.268
CCL8	0	3.556	4.467
CCNB1	0	2.08	2.696
CCR1	0	0	1.32
CCR5	1.069	1.503	1.674
CD47	0	0	-1.036
CDH13	0	0	-1.175

CFB	0	1.631	1.183
CST6	0	0	-1.054
CTNND1	0	0	-1.086
CXCL1	0	0	1.359
CXCL1 /// CXCL3	0	0	1.877
CXCL10	0	3.124	3.769
CXCL11	2.294	3.192	3.842
CXCL6	1.172	0	-1.161
CXCL9	0	1.251	1.037
DKK3	0	0	-1.492
EDN1	0	0	1.344
EGFR	-1.128	0	0
EPAS1	1.386	0	-1.901
EPHA2	0	1.014	1.434
F11R	0	0	0
F3	0	0	1.897
FBLN5	0	0	-1.89
FGF2	0	0	1.281
FOXP1	0	0	-1.067
FUT3	0	0	1.057
GADD45A	1.037	1.248	1.458
GZMA	0	-1.785	-2.171
GZMB	0	1.406	1.283
IFNB1	1.084	0	0
IGF1	0	1.003	1.081
IKBKB	0	0	-1.035
IL15RA	0	1.087	1.538
IL1RN	1.495	2.119	2.252
IL2	0	0	0
IL29	0	0	1.047
IL6	2.924	4.099	3.83
IL8	0	2.238	3.517
IRF1	0	1.112	0
IRF7	0	2.228	2.33
ITGA6	0	-2.092	0
ITPR1	0	-1.271	-1.459
KIT	0	0	-1.093
LAMB1	0	-1.532	-1.653
LAMC1	0	0	-1.133
LGALS3BP	0	2.431	1.638
LMNB1	0	1.694	1.829
MCP-1	3.717	4.603	4.712
MET	1.634	0	0
MMP9	1.11	0	-1.007
MYBL1	0	1.193	1.347
MYBL2	0	0	1.04
MYC	1.552	1.599	2.224
NEO1	0	0	-1.396
NP	0	0	1.167
PCDHA11	0	0	-1.296
PCDHA5	0	1.369	1.342
PIK3R1	0	0	-1.339
PLA2G2A	0	0	2.039
PPBP	0	-2.267	-2.781
PTPRB	0	0	-1.575
PTPRF	1.088	0	-1.856
PTX3	0	2.954	3.46
RAD23B	1.082	0	0
S100A8	0	-2.516	0
SERPINA1	0	0	1.271
SERPING1	0	1.27	0
SFTPD	0	0	-1.083
SLIT2	0	-1.333	-1.641
SOCS1	1.087	1.648	1.651
SPP1	0	1.771	2.712
STAT1	2.226	2.145	2.377
TAPBP	1.611	1.594	0
TFPI2	0	0	2.966
THBD	0	-1.121	-1.114
THBS3	0	1.015	0
TIMP3	0	0	-1.488
TMOD1	0	-1.382	-1.518
TNFAIP3	0	1.444	0
TNFRSF17	0	0	-1.047
TNFRSF19	0	0	-1.122
TNFRSF21	1.036	1.222	1.562
TNFSF13B	1.146	2.148	2.348
TOP2A	0	1.967	2.309
TSTA3	0	0	1.067
VCAM1	0	1.406	2.042

## REFERENCES

1. **Abreu, S. L.** 1982. Suppression of experimental allergic encephalomyelitis by interferon. *Immunol Commun* **11**:1-7.
2. **Akira, S., S. Uematsu, and O. Takeuchi.** 2006. Pathogen recognition and innate immunity. *Cell* **124**:783-801.
3. **Aman, M. J., T. Tretter, I. Eisenbeis, G. Bug, T. Decker, W. E. Aulitzky, H. Tilg, C. Huber, and C. Peschel.** 1996. Interferon-alpha stimulates production of interleukin-10 in activated CD4+ T cells and monocytes. *Blood* **87**:4731-6.
4. **Amit, I., M. Garber, N. Chevrier, A. P. Leite, Y. Donner, T. Eisenhaure, M. Guttman, J. K. Grenier, W. Li, O. Zuk, L. A. Schubert, B. Birditt, T. Shay, A. Goren, X. Zhang, Z. Smith, R. Deering, R. C. McDonald, M. Cabili, B. E. Bernstein, J. L. Rinn, A. Meissner, D. E. Root, N. Hacohen, and A. Regev.** 2009. Unbiased reconstruction of a mammalian transcriptional network mediating pathogen responses. *Science* **326**:257-63.
5. **Auron, P. E.** 1998. The interleukin 1 receptor: ligand interactions and signal transduction. *Cytokine Growth Factor Rev* **9**:221-37.
6. **Aw, D., A. B. Silva, and D. B. Palmer.** 2007. Immunosenescence: emerging challenges for an ageing population. *Immunology* **120**:435-46.
7. **Baas, T., A. Roberts, T. H. Teal, L. Vogel, J. Chen, T. M. Tumpey, M. G. Katze, and K. Subbarao.** 2008. Genomic Analysis Reveals Age Dependent Innate Immune Responses to SARS Coronavirus. *J Virol*.
8. **Benjamini, Y., and Y. Hochberg.** 1995. Controlling the false discovery rate: a practical and powerful approach to multiple testing. *J R Soc B* **57**:289-300.
9. **Billiau, A.** 2006. Anti-inflammatory properties of Type I interferons. *Antiviral Res* **71**:108-16.
10. **Bruunsgaard, H., M. Pedersen, and B. K. Pedersen.** 2001. Aging and proinflammatory cytokines. *Curr Opin Hematol* **8**:131-6.
11. **Cameron, M. J., L. Ran, L. Xu, A. Danesh, J. F. Bermejo-Martin, C. M. Cameron, M. P. Muller, W. L. Gold, S. E. Richardson, S. M. Poutanen, B. M. Willey, M. E. DeVries, Y. Fang, C. Seneviratne, S. E. Bosinger, D. Persad, P. Wilkinson, L. D. Greller, R. Somogyi, A. Humar, S. Keshavjee, M. Louie, M. B. Loeb, J. Brunton, A. J. McGeer, and D. J. Kelvin.** 2007. Interferon-mediated immunopathological events are associated with atypical innate and adaptive immune responses in patients with severe acute respiratory syndrome. *J Virol* **81**:8692-706.
12. **Cervantes-Barragan, L., R. Zust, F. Weber, M. Spiegel, K. S. Lang, S. Akira, V. Thiel, and B. Ludewig.** 2007. Control of coronavirus infection through plasmacytoid dendritic-cell-derived type I interferon. *Blood* **109**:1131-7.
13. **Cheung, C. Y., L. L. Poon, I. H. Ng, W. Luk, S. F. Sia, M. H. Wu, K. H. Chan, K. Y. Yuen, S. Gordon, Y. Guan, and J. S. Peiris.** 2005. Cytokine responses in severe acute respiratory syndrome coronavirus-infected macrophages *in vitro*: possible relevance to pathogenesis. *J Virol* **79**:7819-26.
14. **Chung, H. Y., B. Sung, K. J. Jung, Y. Zou, and B. P. Yu.** 2006. The molecular inflammatory process in aging. *Antioxid Redox Signal* **8**:572-81.
15. **de Lang, A., T. Baas, T. Teal, L. M. Leijten, B. Rain, A. D. Osterhaus, B. L. Haagmans, and M. G. Katze.** 2007. Functional genomics highlights differential induction of antiviral pathways in the lungs of SARS-CoV-infected macaques. *PLoS Pathog* **3**:e112.
16. **Fan, J., R. D. Ye, and A. B. Malik.** 2001. Transcriptional mechanisms of acute lung injury. *Am J Physiol Lung Cell Mol Physiol* **281**:L1037-50.
17. **Fang, X., J. Gao, H. Zheng, B. Li, L. Kong, Y. Zhang, W. Wang, Y. Zeng, and L. Ye.** 2007. The membrane protein of SARS-CoV suppresses NF-kappaB activation. *J Med Virol* **79**:1431-9.18. **Folkesson, H. G., M. A. Matthay, C. A. Hebert, and V. C. Broaddus.** 1995. Acid aspiration-induced lung injury in rabbits is mediated by interleukin-8-dependent mechanisms. *J Clin Invest* **96**:107-16.
19. **Fouchier, R. A., T. Kuiken, M. Schutten, G. van Amerongen, G. J. van Doornum, B. G. van den Hoogen, M. Peiris, W. Lim, K. Stohr, and A. D. Osterhaus.** 2003. Aetiology: Koch's postulates fulfilled for SARS virus. *Nature* **423**:240.
20. **Franceschi, C., M. Bonafe, S. Valensin, F. Olivieri, M. De Luca, E. Ottaviani, and G. De Benedictis.** 2000. Inflamm-aging. An evolutionary perspective on immunosenescence. *Ann N Y Acad Sci* **908**:244-54.
21. **Frieman, M., M. Heise, and R. Baric.** 2008. SARS coronavirus and innate immunity. *Virus Res* **133**:101-12.

22. Ganster, R. W., Z. Guo, L. Shao, and D. A. Geller. 2005. Differential effects of TNF-alpha and IFN-gamma on gene transcription mediated by NF-kappaB-Stat1 interactions. *J Interferon Cytokine Res* 25:707-19.
23. Gasse, P., C. Mary, I. Guenon, N. Noulin, S. Charron, S. Schnyder-Candrian, B. Schnyder, S. Akira, V. F. Quesniaux, V. Lagente, B. Ryffel, and I. Couillin. 2007. IL-1R1/MyD88 signaling and the inflammasome are essential in pulmonary inflammation and fibrosis in mice. *J Clin Invest* 117:3786-99.
24. Goeman, J. J., S. A. van de Geer, F. de Kort, and H. C. van Houwelingen. 2004. A global test for groups of genes: testing association with a clinical outcome. *Bioinformatics* 20:93-9.
25. Guo, B., E. Y. Chang, and G. Cheng. 2008. The type I IFN induction pathway constrains Th17-mediated autoimmune inflammation in mice. *J Clin Invest* 118:1680-90.
26. Haagmans, B. L., T. Kuiken, B. E. Martina, R. A. Fouchier, G. F. Rimmelzwaan, G. van Amerongen, D. van Riel, T. de Jong, S. Itamura, K. H. Chan, M. Tashiro, and A. D. Osterhaus. 2004. Pegylated interferon-alpha protects type 1 pneumocytes against SARS coronavirus infection in macaques. *Nat Med* 10:290-3.
27. Haagmans, B. L., and A. D. Osterhaus. 2006. Nonhuman primate models for SARS. *PLoS Med* 3:e194.
28. Hon, K. L., C. W. Leung, W. T. Cheng, P. K. Chan, W. C. Chu, Y. W. Kwan, A. M. Li, N. C. Fong, P. C. Ng, M. C. Chiu, C. K. Li, J. S. Tam, and T. F. Fok. 2003. Clinical presentations and outcome of severe acute respiratory syndrome in children. *Lancet* 361:1701-3.
29. Huang, K. J., I. J. Su, M. Theron, Y. C. Wu, S. K. Lai, C. C. Liu, and H. Y. Lei. 2005. An interferon-gamma-related cytokine storm in SARS patients. *J Med Virol* 75:185-94.
30. Huber, W., A. von Heydebreck, H. Sultmann, A. Poustka, and M. Vingron. 2002. Variance stabilization applied to microarray data calibration and to the quantification of differential expression. *Bioinformatics* 18 Suppl 1:S96-104.
31. Imai, Y., K. Kuba, G. G. Neely, R. Yaghubian-Malhami, T. Perkmann, G. van Loo, M. Ermolaeva, R. Veldhuizen, Y. H. Leung, H. Wang, H. Liu, Y. Sun, M. Pasparakis, M. Kopf, C. Mech, S. Bavari, J. S. Peiris, A. S. Slutsky, S. Akira, M. Hultqvist, R. Holmdahl, J. Nicholls, C. Jiang, C. J. Binder, and J. M. Penninger. 2008. Identification of oxidative stress and Toll-like receptor 4 signaling as a key pathway of acute lung injury. *Cell* 133:235-49.
32. Jiang, Y., J. Xu, C. Zhou, Z. Wu, S. Zhong, J. Liu, W. Luo, T. Chen, Q. Qin, and P. Deng. 2005. Characterization of cytokine/chemokine profiles of severe acute respiratory syndrome. *Am J Respir Crit Care Med* 171:850-7.
33. Kong, K. F., K. Delroux, X. Wang, F. Qian, A. Arjona, S. E. Malawista, E. Fikrig, and R. R. Montgomery. 2008. Dysregulation of TLR3 impairs the innate immune response to West Nile virus in the elderly. *J Virol* 82:7613-23.
34. Kopecky-Bromberg, S. A., L. Martinez-Sobrido, M. Frieman, R. A. Baric, and P. Palese. 2007. Severe acute respiratory syndrome coronavirus open reading frame (ORF) 3b, ORF 6, and nucleocapsid proteins function as interferon antagonists. *J Virol* 81:548-57.
35. Kramer, O. H., D. Baus, S. K. Knauer, S. Stein, E. Jager, R. H. Stauber, M. Grez, E. Pfitzner, and T. Heinzel. 2006. Acetylation of Stat1 modulates NF-kappaB activity. *Genes Dev* 20:473-85.
36. Kuiken, T., R. A. Fouchier, M. Schutten, G. F. Rimmelzwaan, G. van Amerongen, D. van Riel, J. D. Laman, T. de Jong, G. van Doornum, W. Lim, A. E. Ling, P. K. Chan, J. S. Tam, M. C. Zambon, R. Gopal, C. Drosten, S. van der Werf, N. Escriou, J. C. Manuguerra, K. Stohr, J. S. Peiris, and A. D. Osterhaus. 2003. Newly discovered coronavirus as the primary cause of severe acute respiratory syndrome. *Lancet* 362:263-70.
37. Law, H. K., C. Y. Cheung, H. Y. Ng, S. F. Sia, Y. O. Chan, W. Luk, J. M. Nicholls, J. S. Peiris, and Y. L. Lau. 2005. Chemokine upregulation in SARS-coronavirus-infected, monocyte-derived human dendritic cells. *Blood* 106:2366-74.
38. Leung, C. W., and W. K. Chiu. 2004. Clinical picture, diagnosis, treatment and outcome of severe acute respiratory syndrome (SARS) in children. *Paediatr Respir Rev* 5:275-88.
39. Licastro, F., G. Candore, D. Lio, E. Porcellini, G. Colonna-Romano, C. Franceschi, and C. Caruso. 2005. Innate immunity and inflammation in ageing: a key for understanding age-related diseases. *Immun Ageing* 2:8.
40. Livak, K. J., and T. D. Schmittgen. 2001. Analysis of relative gene expression data using real-time quantitative PCR and the 2(-Delta Delta C(T)) Method. *Methods* 25:402-8.
41. Loutfy, M. R., L. M. Blatt, K. A. Siminovitch, S. Ward, B. Wolff, H. Lho, D. H. Pham, H. Deif, E. A. LaMere, M. Chang, K. C. Kain, G. A. Farcas, P. Ferguson, M. Latchford, G. Levy, J. W. Dennis, E. K. Lai, and E. N. Fish. 2003. Interferon alfacon-1 plus corticosteroids in severe acute respiratory syndrome: a preliminary study. *Jama* 290:3222-8.
42. Meyer, K. C. 2005. Aging. *Proc Am Thorac Soc* 2:433-9.

43. Meyer, K. C. 2001. The role of immunity in susceptibility to respiratory infection in the aging lung. *Respir Physiol* **128**:23-31.
44. Modelska, K., J. F. Pittet, H. G. Folkesson, V. Courtney Broaddus, and M. A. Matthay. 1999. Acid-induced lung injury. Protective effect of anti-interleukin-8 pretreatment on alveolar epithelial barrier function in rabbits. *Am J Respir Crit Care Med* **160**:1450-6.
45. Nagata, N., N. Iwata, H. Hasegawa, S. Fukushi, A. Harashima, Y. Sato, M. Saijo, F. Taguchi, S. Morikawa, and T. Sata. 2008. Mouse-passaged severe acute respiratory syndrome-associated coronavirus leads to lethal pulmonary edema and diffuse alveolar damage in adult but not young mice. *Am J Pathol* **172**:1625-37.
46. Nagata, N., N. Iwata, H. Hasegawa, S. Fukushi, M. Yokoyama, A. Harashima, Y. Sato, M. Saijo, S. Morikawa, and T. Sata. 2007. Participation of both host and virus factors in induction of severe acute respiratory syndrome (SARS) in F344 rats infected with SARS coronavirus. *J Virol* **81**:1848-57.
47. Nozell, S., T. Laver, K. Patel, and E. N. Benveniste. 2006. Mechanism of IFN-beta-mediated inhibition of IL-8 gene expression in astrogloma cells. *J Immunol* **177**:822-30.
48. O'Neill, L. A. 2008. When signaling pathways collide: positive and negative regulation of toll-like receptor signal transduction. *Immunity* **29**:12-20.
49. Pauli, E. K., M. Schmolke, T. Wolff, D. Viemann, J. Roth, J. G. Bode, and S. Ludwig. 2008. Influenza A virus inhibits type I IFN signaling via NF-kappaB-dependent induction of SOCS-3 expression. *PLoS Pathog* **4**:e1000196.
50. Peiris, J. S., C. M. Chu, V. C. Cheng, K. S. Chan, I. F. Hung, L. L. Poon, K. I. Law, B. S. Tang, T. Y. Hon, C. S. Chan, K. H. Chan, J. S. Ng, B. J. Zheng, W. L. Ng, R. W. Lai, Y. Guan, and K. Y. Yuen. 2003. Clinical progression and viral load in a community outbreak of coronavirus-associated SARS pneumonia: a prospective study. *Lancet* **361**:1767-72.
51. Peiris, J. S., Y. Guan, and K. Y. Yuen. 2004. Severe acute respiratory syndrome. *Nat Med* **10**:S88-97.
52. Plackett, T. P., E. D. Boehmer, D. E. Faunce, and E. J. Kovacs. 2004. Aging and innate immune cells. *J Leukoc Biol* **76**:291-9.
53. Prinz, M., H. Schmidt, A. Mildner, K. P. Knobeloch, U. K. Hanisch, J. Raasch, D. Merkler, C. Detje, I. Gutcher, J. Mages, R. Lang, R. Martin, R. Gold, B. Becher, W. Bruck, and U. Kalinke. 2008. Distinct and nonredundant *in vivo* functions of IFNAR on myeloid cells limit autoimmunity in the central nervous system. *Immunity* **28**:675-86.
54. Rink, L., I. Cakman, and H. Kirchner. 1998. Altered cytokine production in the elderly. *Mech Ageing Dev* **102**:199-209.
55. Rockx, B., T. Baas, G. A. Zornetzer, B. Haagmans, T. Sheahan, M. Frieman, M. D. Dyer, T. H. Teal, S. Proll, J. van den Brand, R. Baric, and M. G. Katze. 2009. Early upregulation of acute respiratory distress syndrome-associated cytokines promotes lethal disease in an aged-mouse model of severe acute respiratory syndrome coronavirus infection. *J Virol* **83**:7062-74.
56. Rothlin, C. V., S. Ghosh, E. I. Zuniga, M. B. Oldstone, and G. Lemke. 2007. TAM receptors are pleiotropic inhibitors of the innate immune response. *Cell* **131**:1124-36.
57. Rutkute, K., R. H. Asmis, and M. N. Nikolova-Karakashian. 2007. Regulation of neutral sphingomyelinase-2 by GSH: a new insight to the role of oxidative stress in aging-associated inflammation. *J Lipid Res* **48**:2443-52.
58. Smyth, G. K. 2004. Linear models and empirical bayes methods for assessing differential expression in microarray experiments. *Stat Appl Genet Mol Biol* **3**:Article3.
59. Tang, N. L., P. K. Chan, C. K. Wong, K. F. To, A. K. Wu, Y. M. Sung, D. S. Hui, J. J. Sung, and C. W. Lam. 2005. Early enhanced expression of interferon-inducible protein-10 (CXCL-10) and other chemokines predicts adverse outcome in severe acute respiratory syndrome. *Clin Chem* **51**:2333-40.
60. Tukey, J. W. 1977. Some thoughts on clinical trials, especially problems of multiplicity. *Science* **198**:679-84.
61. van Holten, J., K. Reedquist, P. Sattonet-Roche, T. J. Smeets, C. Plater-Zyberk, M. J. Vervoordeldonk, and P. P. Tak. 2004. Treatment with recombinant interferon-beta reduces inflammation and slows cartilage destruction in the collagen-induced arthritis model of rheumatoid arthritis. *Arthritis Res Ther* **6**:R239-49.
62. Ware, L. B. 2005. Prognostic determinants of acute respiratory distress syndrome in adults: impact on clinical trial design. *Crit Care Med* **33**:S217-22.
63. Ware, L. B., and M. A. Matthay. 2000. The acute respiratory distress syndrome. *N Engl J Med* **342**:1334-89.
64. Wei, L., M. R. Sandbulte, P. G. Thomas, R. J. Webby, R. Homayouni, and L. M. Pfeffer. 2006. NFkappaB negatively regulates interferon-induced gene expression and anti-influenza activity. *J Biol Chem* **281**:11678-84.
65. Wong, C. K., C. W. Lam, A. K. Wu, W. K. Ip, N. L. Lee, I. H. Chan, L. C. Lit, D. S. Hui, M. H. Chan, S. S. Chung, and J. J. Sung. 2004. Plasma inflammatory cytokines and chemokines in severe acute respiratory syndrome. *Clin Exp Immunol* **136**:95-103.



66. Wong, G. W., A. M. Li, P. C. Ng, and T. F. Fok. 2003. Severe acute respiratory syndrome in children. *Pediatr Pulmonol* **36**:261-6.
67. Yoon, P., K. T. Keylock, M. E. Hartman, G. G. Freund, and J. A. Woods. 2004. Macrophage hypo-responsiveness to interferon-gamma in aged mice is associated with impaired signaling through Jak-STAT. *Mech Ageing Dev* **125**:137-43.



CHAPTER 7

# Repressed transcriptional host response in SARS-CoV infected ferrets

Based on:

Anna de Lang, Judith M.A. van den Brand, Maarten A. Bijl, Fatiha Zaaraoui-Boutahar, Lisette Provacia, Albert D.M.E. Osterhaus, Arno C. Andeweg, and Bart L. Haagmans

In preparation



## ABSTRACT

SARS-CoV causes a severe infection of the lower respiratory tract in several animal species. Analysis of the host response to experimental SARS-CoV infection in ferrets revealed that several proinflammatory genes, including, IL-1 $\beta$ , IL-6 and IL-8, were not induced despite high levels of SARS-CoV replication and mild to moderate pathological changes in the lower respiratory tract. Compared to SARS-CoV infection in macaques and mice, a repressed transcriptional host response associated with a viral tropism restricted to type II pneumocytes was observed in ferrets. Differentially regulated host pathways in SARS-CoV infected ferrets may relate to the inability of recombinant interferon  $\alpha$  and ACE2 to demonstrate efficacy in this animal species. Thus, comparative transcriptional host response analysis in different animal species may be instrumental in order to successfully design and test intervention strategies that target the host.

## INTRODUCTION

In humans SARS-CoV causes a severe infection of the lower respiratory tract that is hypothesized to be caused by a disproportional host immune response, illustrated by elevated levels of proinflammatory cytokines and chemokines such as IL-1 $\beta$ , IL-6, IL-8, IL-12, CCL2 and CXCL10 (5, 11, 21, 27, 42, 47, 57, 66, 69). The severity of SARS pathology in a SARS-CoV infected host is most likely dependent on a fine balance between the activation of antiviral and pathogenic pathways through the induction of interferons (IFNs) and proinflammatory cytokines, respectively. Eventually, uncontrolled induction of proinflammatory cytokines can lead to acute respiratory distress syndrome (ARDS), characterized by inflammation, pulmonary oedema combined with infiltration of polymorphonuclear leukocytes and macrophages (63). To unravel the pathogenesis of SARS, a range of animal models have been established (14-15, 17, 32, 34-35, 40, 48, 65). In ferrets, commonly used as an animal model for experimental infection with human respiratory viruses, SARS-CoV replicates efficiently, causing macroscopic and microscopic abnormalities in the lungs (40, 56, 62). Several studies have used ferrets to test the efficacy of neutralizing antibodies and vaccines to protect against SARS-CoV challenge (8, 10, 28, 52, 56, 64). In a previous study we have shown that therapeutic treatment of aged SARS-CoV infected macaques with IFN- $\alpha$  significantly decreased SARS induced gross pathology, not by reducing viral titers, but through an anti-inflammatory effect (53). Similarly, mice infected with SARS-CoV show less pathological changes when treated with recombinant IFN- $\alpha$  therapeutically (31). Prophylactic administration of IFN- $\alpha$  in mice and macaques on the other hand, significantly inhibits viral replication in the lungs (2, 18). To further extend these observations we now studied ferrets treated with pegylated recombinant human IFN- $\alpha$  before or after SARS-CoV infection.

Angiotensin converting enzyme-2 (ACE2) is the cellular receptor for SARS-CoV, but this enzyme also is one of the key players in the renin-angiotensin system (RAS) (13, 33, 58). Although mainly known for its role in maintaining blood pressure homeostasis, the key RAS molecule angiotensin II (ANG II) is involved in the development of pulmonary hypertension by affecting pulmonary vasculature, leading to vasoconstriction and proliferation, and by initiating inflammatory processes by signaling through the AT<sub>1</sub> receptor (6, 36, 41, 51). In addition, the RAS has been directly linked to ARDS pathogenesis; polymorphisms in the ACE gene, a RAS enzyme that counterbalances ACE2 function, as well as ACE activity and ACE levels have been associated with ARDS susceptibility and disease outcome (23, 39, 44). In contrast to ACE, ACE2, whose enzymatic activity decreases ANG II levels, has been shown to have a protective role in lung damage. Depletion of the ACE2 gene in mice exposed to different acute lung injury (ALI) inducing treatments leads to increased disease severity while treatment of these mice with AT<sub>1</sub> receptor inhibitors decreased disease severity again, illustrating the important role of ACE2-mediated ANG II degradation in the protection against pulmonary damage (24). In this study we treated SARS-CoV infected ferrets with recombinant ACE2 and subsequently determined viral replication, pathological changes in the lungs and host gene expression.

## MATERIALS AND METHODS

### Experimental set-up of ferret studies

Groups of 6 female ferrets (4-5 months of age, Schimmel, the Netherlands) were treated with pegylated recombinant IFN- $\alpha$ 2b (prIFN-a , Schering), intraperitoneally (IP) in a volume of 0.5 ml at days indicated. prIFN-a blood levels were determined using an ELISA (Bender MedSystems Diagnostics, Vienna, Austria) using PEG-Intron as a standard. For the ACE2 experiment (6 ferrets/group), 1 group of ferrets was IP injected with 4-10 mg/kg rhuACE2 1 day before SARS-CoV infection, a 2<sup>nd</sup> and 3<sup>rd</sup> group were IP injected with 800 ug/kg rhuACE2 or mut-rhuACE respectively at day -1 and day 0 before SARS-CoV infection and day 1 and day 2 after infection. One control group was IP injected with a PBS (0.1%BSA/PBS) buffer instead of rhuACE2 and subsequently SARS-CoV infected. Ferrets were intratracheally (IT) inoculated with  $1 \times 10^5$  TCID<sub>50</sub> SARS-CoV strain HKU39849. Animals were checked daily for clinical signs of disease and euthanized at day 4 after infection. Another group of ferrets was also inoculated with  $1 \times 10^5$  TCID<sub>50</sub> SARS-CoV strain HKU39849, after which 5 ferrets were euthanized at day 1 after infection and 5 at day 4 after infection. A negative control group of 5 ferrets was PBS infected and euthanized at day 4 after inoculation. After euthanization lung tissue was collected and stored in RNAlater (Ambion) for RNA isolation, 10% formalin for histopathology and cell culture medium for SARS-CoV titration. All experiments were executed under biosafety level 3 and approval for animal experiments was obtained from the Institutional Animal Welfare Committee and performed according to Dutch guidelines for animal experimentation.

### IFN bioassay

Primary ferret splenocytes and ferret kidney cells were seeded in 96-well plates (Greiner Bio-one) and incubated with recombinant IFN- $\alpha$  (PEG-Intron, Schering) for 16 hours. Additionally, in parallel cells were incubated with IFN- $\alpha$  as a positive control for antiviral IFN activity, or left untreated as a negative control. After 16 hours cells were either infected with vesicular stomatitis virus ( $1 \times 10^4$  TCID<sub>50</sub>/ml) or left uninfected. Cells were checked for CPE daily and two days after infection VSV induced CPE was complete after which VSV infection was stopped by fixing cells for 15 minutes with 10% formalin. Subsequently cells were stained with 0.05% Crystal Violet solution (VWR) for 30 minutes and washed. Splenocytes were counted and kidney cells were treated with ethanol and absorbance values were measured, with increased CPE leading to lower absorbance levels.

### Recombinant ACE2 proteins

RhuACE2 and mut-rhuACE2 were a kind gift from JM Penninger and generation of these proteins have been described earlier (24). SARS-CoV neutralizing activity of these proteins was evaluated by a neutralization test in which different concentrations of rhuACE2 and mut-rhuACE2 were incubated with  $1 \times 10^4$  TCID<sub>50</sub>/ml SARS-CoV for 1 hour. Subsequently this mixture was added to Vero E6 cell cultures for 1 hour, then cells were washed and fresh medium was added. The SARS-CoV infection was stopped after 8 hours after which SARS-CoV infected cells were stained with a SARS-CoV specific antibody and counted as described before (12).

Catalytic activity of the rhuACE2 and mut-rhuACE2 proteins was measured by using the fluorogenic peptide Substrate VI (Mca-Tyr-Val-Ala-Asp-Ala-Pro-Lys(Dnp)-OH, R&D systems). ACE2 proteins at different concentrations were incubated with the fluorescent substrate after which fluorescence was monitored with the Tecan infinite F200 (Tecan).

### **SARS-CoV titration**

Ferret lung tissue samples were homogenized in 1 ml virus transport medium, using ceramic spheres and an automated homogenizer (MP biomedical). After centrifugation, the homogenates were frozen at  $-70^{\circ}\text{C}$  until they were inoculated on Vero E6 cell cultures in 10-fold serial dilutions and cells were monitored for CPE. The identity of the isolated virus was confirmed as SARS-CoV by performing RT-PCR using the supernatant.

### **SARS-CoV and host gene RT-PCR**

Ferret lung tissue samples were homogenized in 1 ml Trizol Reagent (Invitrogen), using ceramic spheres and an automated homogenizer (MP biomedical). Subsequently, RNA was extracted using the RNeasy mini kit (Qiagen). Quantitative real-time RT-PCR was performed to detect SARS-CoV mRNA levels and to detect host gene expression changes. First cDNA synthesis was performed using Superscript III RT (Invitrogen) and oligo(dT), according to the manufacturer's instructions. Subsequently, each RT-PCR reaction was run in triplicate using Taqman 2x PCR Universal Master Mix (Applied Biosystems) with primers and probe specific for the SARS-CoV nucleoprotein gene (30), or for ferret cellular genes. Sequences for the ferret host gene primers and probes are given in table 1. Differences in gene expression are represented as the fold change in gene expression relative to a calibrator and normalized to a reference, using the  $2^{-\Delta\Delta Ct}$  method (37). GAPDH (glyceraldehydes-3-phosphate dehydrogenase) was used as endogenous control to normalize quantification of the target gene. Samples from PBS-inoculated ferrets were used as a calibrator. As a positive control for the induction of IL-1 $\beta$ , IL-6, IL-8 and CXCL10, ferret PBMCs were incubated with LPS, or medium as a negative control, for 24 hours after which RNA was isolated and used for cDNA synthesis and RT-PCR.



**Table 7.1. Primers and probes used for quantitative RT-PCR**

<i>Gene</i>	<i>Primer sequence</i>
<b><i>GAPDH</i></b>	Fw: 5'-AACATCATCCCTGCTTCCACTGGT-3'
	Rv: 5'-TGTTGAAGTCGCAGGAGACAACCT-3'
	Probe: FAM-TGACCTGCCGCTGGAGAAAGCTGCC-TAMRA
<b><i>CXCL10</i></b>	Fw: 5'-ACCAACCGCTGTACACAA-3'
	Rv: 5'-AGGACCTGGTACGTTCACTAAAA-3'
	Probe: FAM-TCATCCTTCTGTCCGGGCACTAT-TAMRA
<b><i>IL6</i></b>	Fw: 5'-GGTTCATCCTTGGCAAATCTCT-3'
	Rv: 5'-CCTGATTGAATTGAGACTGGAAGC-3'
	Probe: FAM-AGCAAGGAGGCACTGGCAGAGAACAAC-TAMRA
<b><i>IL8</i></b>	Fw: 5'-CCAGGAAGAAACCAGACCAA-3'
	Rv: 5'-TGCACTGGCATCGGAGTT-3'
	Probe: FAM-TGCTTTTGCAGTTCTGTGTGAAGC-TAMRA
<b><i>IFNA2</i></b>	Fw: 5'-ACTACCTCAGCTCTTTGGGATGTG-3'
	Rv: 5'-GGGGGAAGCCAAAGTCGTT-3'
	Probe: FAM-TTGTCGCAGGAGCATCAGGGCCC-TAMRA
<b><i>IFNB</i></b>	Fw: 5'-GAAGGAACATCTGGAGGAAATC-3'
	Rv: 5'-GATTCTGCTTGCACTATTGTCC-3'
	Probe: FAM-TGGCTTTCAGGTACCGCACGAT-TAMRA
<b><i>ACE2</i></b>	Fw: 5'-TTACCGACGAGAATATCCAAAAGA-3'
	Rv: 5'-CACGGATGACCCACTCTGCT-3'
	Probe: FAM-CCCAGCATGCCAAAACCTACCCACTA-TAMRA

### **RNA labeling, microarray hybridization, scanning and data preprocessing**

RNA (100 ng) extracted from ferret lung was labeled using MessageAmp™ Premier RNA Amplification kit (Applied Biosystems) and hybridized onto Affymetrix GeneChip Canine Genome 2.0 arrays, according to the manufacturer's recommendations. Image analysis was performed using Gene Chip Operating Software (Affymetrix). Microarray Suite version 5.0 software (Affymetrix) was used to generate .dat and .cel files for each experiment. All data were normalized using a variance stabilization algorithm (VSN) (22). Transformed probe values were summarized into one value per probe set by the median polish method (61). Primary data is available through <http://www.virgo.nl> in accordance with MIAME standards.

## Microarray data analysis

Probe set (gene) wise comparisons between the different groups (SARS-CoV infected ferrets euthanized either at day 1 or at day 4 after infection compared to PBS infected animals) were performed by LIMMA (version 2.12.0) (54). Correction for multiple testing was achieved by requiring a false discovery rate (FDR) of 0.05, calculated with the Benjamini-Hochberg procedure (3). To understand the gene functions and the biological processes represented in the data and obtain differentially expressed molecular and cellular functions, Ingenuity Pathways Knowledge Base (<http://www.ingenuity.com/>) was used. The heatmap that compares host gene expression in SARS-CoV infected ferret to gene expression in SARS-CoV infected macaques and mice was generated using existing data from these animals (53) (de Lang et al, submitted). The gene-set used for the heatmap was created by combining the 50 most differentially expressed genes in young adult SARS-CoV infected macaques. Subsequently, this list was filtered in order to only include genes that were annotated both on the macaque chip and on the mouse and ferret chips, resulting in a list of 29 genes. With this final set of genes heatmaps were created using expression data from each species, always using the same comparison, namely SARS-CoV infected animals versus PBS inoculated animals at day 4 after infection. In our data analysis, genes were considered differentially expressed when the FDR is smaller than 0.05 and the abs fold change is at least 2.

## Immunohistochemistry

Serial 3  $\mu\text{m}$  lung sections were stained according to standard protocols (18, 30), with the modification that we used mouse-anti-SARS-nucleocapsid IgG1 (Imgenex 5029) 1:400 with citrate buffer 10 mM, pH 6.0 (Sigma) as antigen retrieval. The slides were heated at 100°C for 15 min and after washing, sections were incubated with horseradishperoxidase labeled goat-anti-mouse IgG1 (Southern Biotech) 1/100 in PBS/0.1% BSA for 1 hour at RT. As controls, isotype control antibodies (clone 11711; R&D) were used.

## RESULTS

### Treatment of SARS-CoV infected ferrets with recombinant IFN- $\alpha$ and ACE2

We treated SARS-CoV infected ferrets prophylactically and therapeutically with pegylated recombinant human IFN- $\alpha$ , shown to reduce SARS-mediated immunopathology in aged macaques (18). Although we confirmed the biological activity of pegylated recombinant IFN- $\alpha$  *in vitro* using ferret splenocytes (figure 7.1A) and ferret kidney cells (not shown) challenged with VSV and although we demonstrated high levels of the recombinant protein circulating in ferrets after injection (figure 7.1B), treatment of SARS-CoV infected ferrets with IFN- $\alpha$  did neither lead to significant differences in viral replication in the lung and throat (figure 7.1C-D) nor to differences in gross and histopathology scores (data not shown).

To test whether ACE2 can be used as a therapeutic for SARS we used a recombinant human ACE2 (rhuACE2) protein to prevent SARS-CoV mediated pathology in ferrets. Treatment with rhuACE2 could have an effect on SARS-CoV infection and pathogenesis at different levels, either by neutralizing viral particles

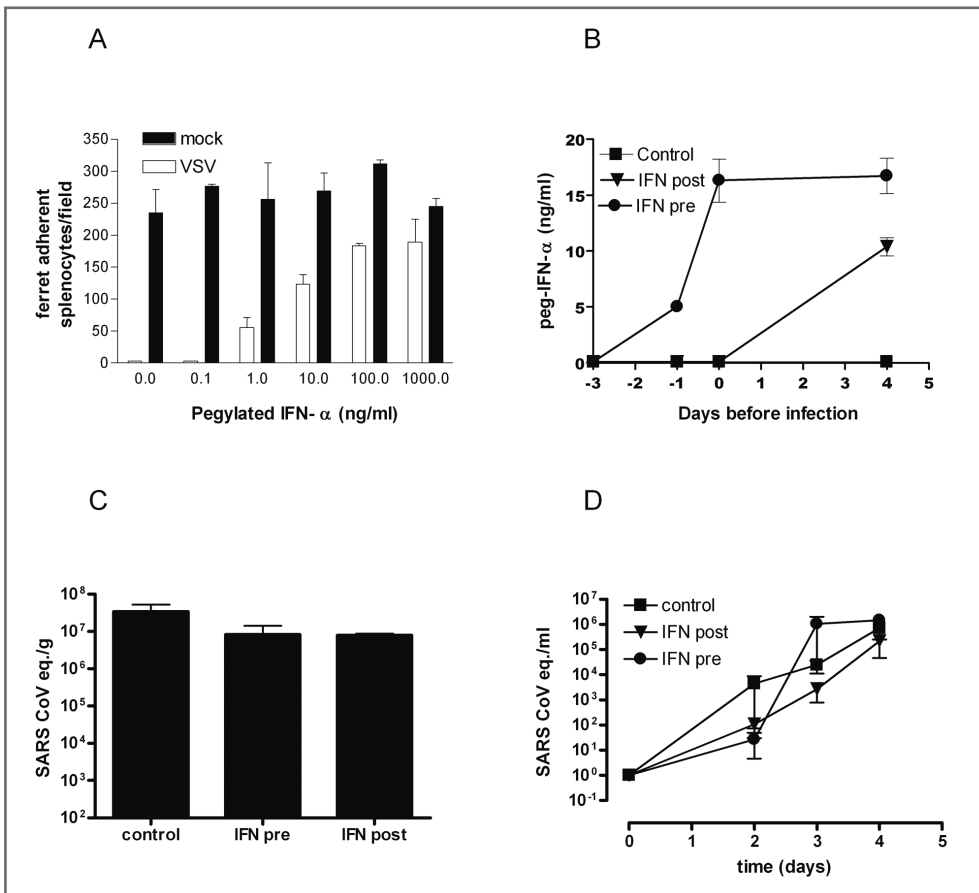


**Figure 7.1. IFN- $\alpha$  treatment of SARS-CoV infected ferrets.** Pegylated recombinant human IFN- $\alpha$  is biologically active and protects ferret splenocytes from VSV induced CPE in a dose dependent manner (A). Levels of circulating recombinant IFN- $\alpha$  in ferrets when injected with IFN- $\alpha$  before (round symbols) or directly after (triangular symbols) SARS-CoV infection in comparison to the PBS control group (square symbols) (B). SARS-CoV titers in lungs of SARS-CoV infected ferrets at day 4 after infection in different treatment groups (C). SARS-CoV titers in throat swabs of SARS-CoV infected ferrets at different time points after infection in the pre-treatment group (round symbols), the post-treatment group (triangular symbols) and the control groups (square symbols).

as a SARS-CoV receptor and thus decreasing the number of infected cells or through its enzymatic activity, degrading ANG II levels and thus preventing lung damage. Therefore, two different treatment strategies were employed; either a high dose single shot of rhuACE2 before SARS-CoV infection to examine the neutralizing effect of ACE2 treatment on viral levels (pre-treatment), and secondly, a lower dose ACE2 treatment for several days after SARS-CoV infection to investigate the effect of the ACE2 enzyme on SARS mediated lung damage (therapeutic treatment). A catalytically inactive mutant recombinant human ACE2 (mut-rhuACE2) protein was taken along as a control for any pathological changes seen after rhuACE2 treatment.

First, the enzymatic activity of the rhuACE2 and the mut-rhuACE2 proteins was evaluated using the fluorogenic ACE2 substrate Mca-Y-V-A-D-A-P-K(Dnp)-OH. As expected, rhuACE2 protein was able to cleave the proline/lysine bonds in the fluorogenic substrate in a dose dependent manner, while the mut-rhuACE2 and the negative control did not, demonstrating that the rhuACE2 protein, but not the mut-rhuACE2 protein, is enzymatically active (figure 7.2A). Subsequently, SARS-CoV neutralizing activity of the rhuACE2 and mut-rhuACE2 proteins was examined in a neutralization assay. Both ACE2 proteins were able to neutralize SARS-CoV in a similar manner, showing that the ACE2 proteins are able to bind SARS-CoV particles thus preventing infection of cells (figure 7.2B). It should be noted that the neutralizing capacity is limited when compared to polyclonal (not shown) and monoclonal antibodies that neutralize SARS-CoV (59).

After establishing the enzymatic and neutralizing activity of the rhuACE2 protein, ferrets were pre-treated with rhu-ACE2 and infected with SARS-CoV. As shown in figure 7.2C, pre-treatment with a high dose single shot of rhuACE2 did not affect SARS-CoV levels in ferret lungs, as determined by titration and RT-PCR. Additionally, no significant differences in viral levels were observed when SARS-CoV infected ferrets were therapeutically treated with a lower dose of either rhuACE2 or mut-rhuACE2 (figure 7.2D). When we analyzed macroscopical and microscopical pathological changes in the rhu-ACE2 treated ferrets compared to those in untreated ferrets, again no significant differences were observed. Gross pathology scores were around 30% in all treatment groups (not shown). Microscopically, mild pathological changes were seen in both the rhuACE2 treated groups as in the control groups, characterized by multifocal mild to moderate alveolar damage with limited numbers of infiltrating inflammatory cells (not shown). Noteworthy, expression of endogenous ACE2 was decreased about 10 times in SARS-CoV infected ferrets, a phenomenon that has been described in several SARS mouse models as well (49). In conclusion, neither pre-treatment nor therapeutic post-treatment with rhuACE2 of SARS-CoV infected ferrets affected SARS-CoV levels or SARS induced pathology in ferret lungs.

### Induction of host gene expression in SARS-CoV infected ferrets

Given the inability of recombinant IFN and ACE2 to exert significant effects on SARS-CoV infection in ferrets, we considered that apart from a potentially limited biological activity of these molecules in ferrets, differences in the host response to this virus in ferrets opposed to macaques and mice could hamper the potency of these drugs. In order to examine the ferret host response to SARS-CoV infection in more detail, ferret-specific RT-PCR assays were performed on the lungs of SARS-CoV ( $n = 6$ ) and mock infected ferrets ( $n = 5$ ) to analyze expression of several host genes that have been reported to be activated in humans and animal species infected with SARS-CoV. As shown in figure 7.3, induction of proinflammatory cytokines IL-1 $\beta$ , IL-6 and IL-8 could not be detected in SARS-CoV infected ferrets at day 4 after infection, whereas CXCL10 was upregulated approximately 10 fold. The fact that transcription of these proinflammatory host genes was hardly induced in SARS-CoV infected ferrets lead us to examine the host response in more detail by performing a microarray analysis on the lungs of SARS-CoV infected ferrets. RNA isolated from the ferret lungs was hybridized to canine microarray chips (similar as described by other groups, (4, 50)) and expression data were directly compared to mock infected ferrets in order to identify genes that were differentially expressed between the two groups. Applying an absolute fold change cut-off of 2 and a FDR < 0.05, a total of 584 genes were found to be differentially expressed in SARS-CoV infected ferrets

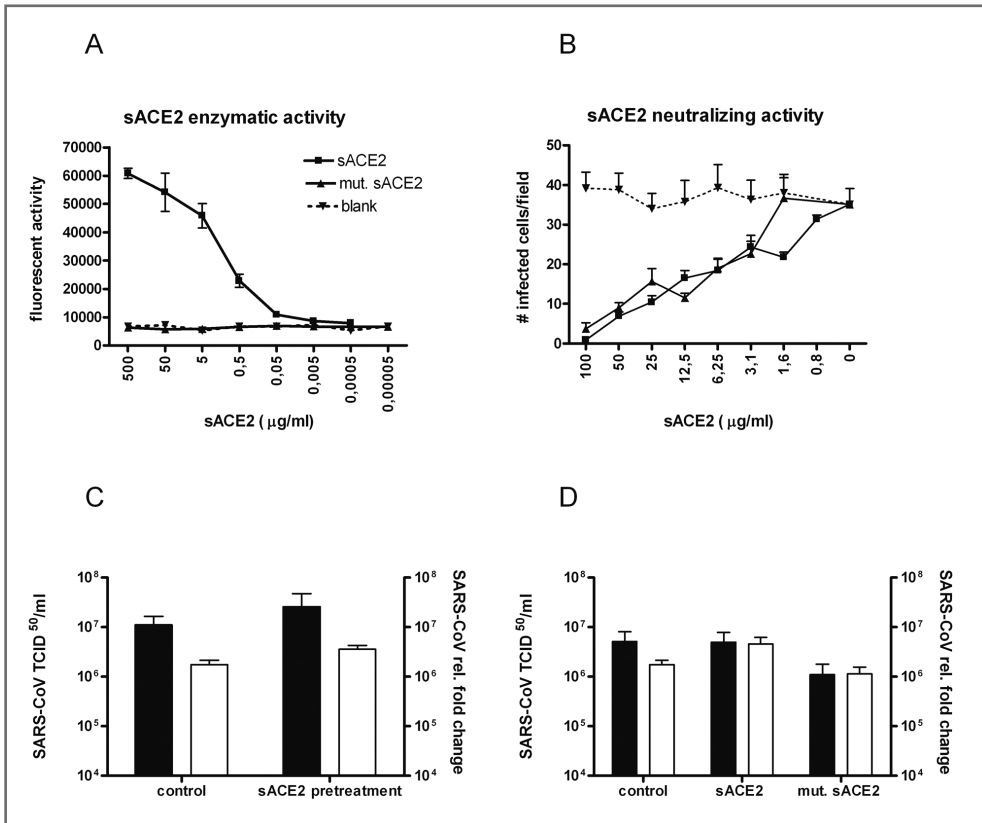


**Figure 7.2. Neutralizing and catalytic activity of rhuACE2 in SARS-CoV infected ferrets.** The rhuACE2 protein but not the mut-rhuACE2 protein has catalytic capacities (A). ACE2 specific enzymatic activity was determined using a fluorogenic ACE2 substrate. The X-axis represents 10 fold dilutions of the ACE2 protein while the Y-axis presents the amount of fluorescence. SARS-CoV neutralizing activity of the rhuACE2 and mut-rhuACE2 proteins was determined with a neutralization assay (B). The Y-axis represents the average number of SARS-CoV infected cells in a random microscopic field after incubation of SARS-CoV with a certain concentration of ACE2, depicted on the X-axis. SARS-CoV levels in ferret lungs. Viral levels were determined in lungs of SARS-CoV infected ferrets that were either pre-treated with a high dose of rhuACE2 (A) or treated before and after infection with a lower dose of either rhuACE2 or mut-rhuACE2 (B). SARS-CoV levels were determined using titration (dark bars), represented on the left Y-axis, and RT-PCR (open bars), represented on the right Y-axis. SARS-CoV titration values are represented by the TCID<sub>50</sub>/ml and RT-PCR values are represented by the relative SARS-CoV fold change in infected animals as compared to PBS infected animals. GAPDH was used as an endogenous control.

at day 4 after infection. Interestingly, more than 95% of these genes (560) were downregulated compared to mock infected animals and only a very small number of genes (24) were upregulated (figure 7.4A). The small group of significantly upregulated genes included genes that have been found to be activated in SARS-CoV infection in other species as well, including CCL2, CXCL10, ISG15 and IFI6. Induction of IFN induced genes like CXCL10, ISG15 and IFI6 is indicative of an active antiviral response in the SARS-CoV

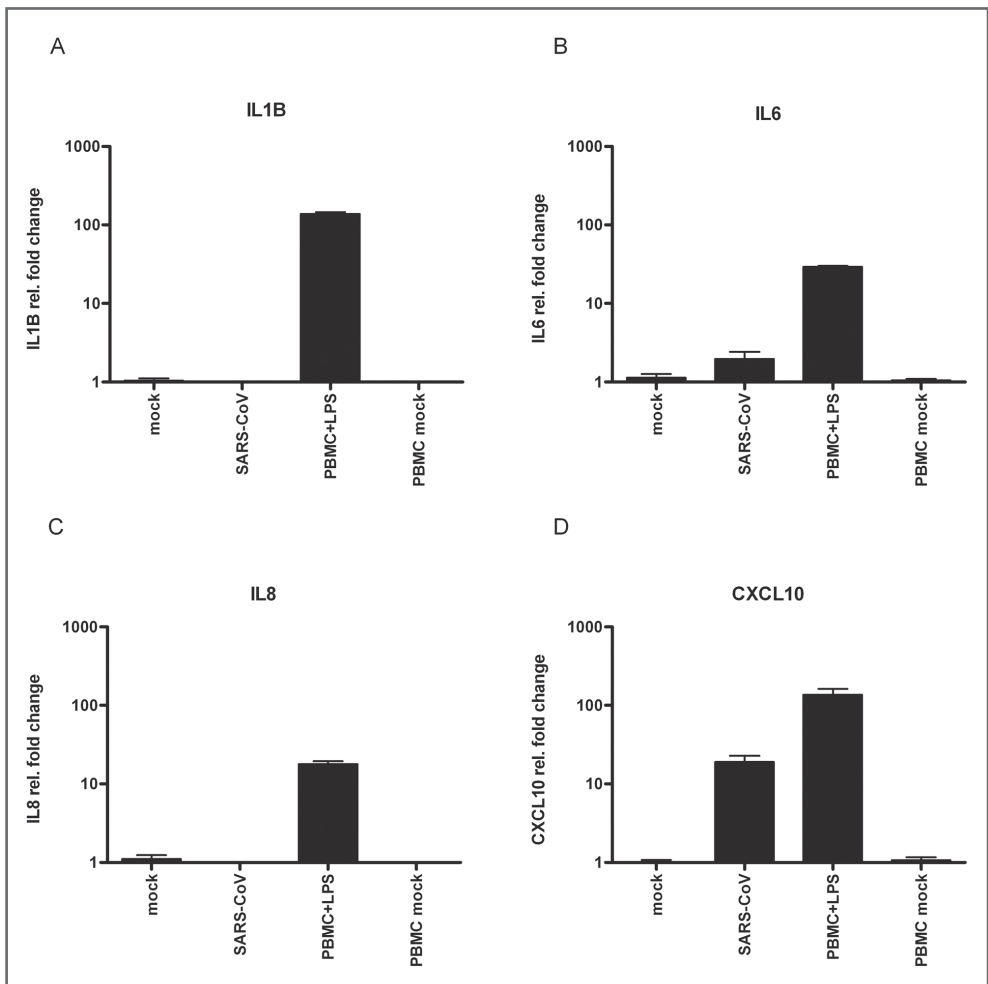


**Figure 7.3. Induction of host cytokines and chemokines in the lungs of SARS-CoV infected ferrets.** Fold increases in gene transcription in SARS-CoV infected animals at day 4 after infection as compared to PBS infected animals were determined using RT-PCR. Data are shown as the mean + the standard of the mean (SEM) for 5 ferrets.

infected ferrets. The total number of differentially expressed genes at day 4 after infection in SARS-CoV infected ferrets was higher when comparing these results to gene expression data from SARS-CoV infected BALB/c mice and cynomolgus macaques. However, both in SARS-CoV infected BALB/c mice as well as in macaques the majority of activated genes are upregulated after infection.

Using Ingenuity, a functional analysis approach that looks for biological relations between genes, we further examined the biological functions of the genes that are differentially expressed in SARS-CoV infected ferrets revealing the top 4 most significantly regulated canonical pathways in SARS-CoV

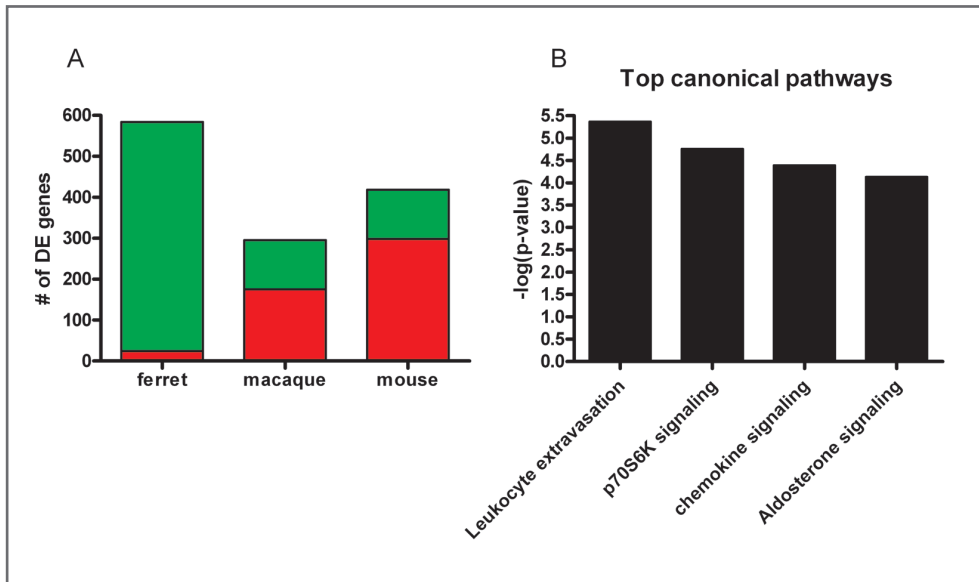


**Figure 7.4. Characteristics of host gene expression in SARS-CoV infected ferrets.** The number of differentially expressed genes (Abs. fc. > 2, p-value < 0.05) in SARS-CoV infected ferrets, macaques and mice at day 4 after infection (A). Up-regulated genes are shown in red while downregulated genes are shown in green. Differentially expressed genes in SARS-CoV infected ferrets were used to create a schematic representation of the 4 most significantly regulated canonical pathways in the lungs of SARS-CoV infected ferrets at day 4 after infection, using Ingenuity Pathways Knowledge Base (B).

infected ferrets at day 4 compared to PBS infected animals (figure 7.4B). Genes differentially expressed in these pathways were mainly downregulated in SARS-CoV infected ferrets compared to mock infected ferrets, such as a number of genes involved in leukocyte extravasation signaling, the process by which leukocytes migrate from blood to tissue during inflammation. In line with this observation, several genes involved in chemokine signaling are downregulated as well. Interestingly, aldosterone signaling in epithelial cells, important for maintaining blood pressure and electrolyte homeostasis and a process associated with the RAS, was downregulated in the lungs of SARS-CoV infected ferrets. Aldosterone secretion from the adrenal cortex increases the blood pressure and can be stimulated by ANG II. Another significantly downregulated pathway in SARS-CoV infected ferrets, linked to the RAS and ANG II, is the p70S6K signaling pathway, involved in cell cycle progression and cell survival. ANG II is one of the proteins that can induce uncontrolled activation of the p70S6K signaling pathway, leading to e. g. excessive and abnormal cell growth. In addition to the pathway analysis we examined expression levels of genes that are directly involved in the RAS, as this might provide more information about the RAS activation state and thus about the potential efficacy of ACE2 treatment. Within the selected gene-set, containing genes like ACE2, ACE, the AT1 and AT2 receptors as well as many downstream genes involved in RAS signaling pathways, practically none of these genes were differentially expressed in ferrets. Remarkably, only expression levels of the ACE gene were significantly downregulated in ferrets. Applying the same set of genes to gene

expression data from SARS-CoV infected macaques and mice revealed that in aged macaques the largest number of genes within the set was activated compared to the other SARS models, coinciding with more severe pathology in these animals. However, expression levels of the genes involved in the RAS were very low (data not shown). The fact that several pathways that can potentially lead to pathology, including the excessive induction of proinflammatory cytokines and pathways involved with the RAS are not upregulated but downregulated in SARS-CoV infected ferrets could explain why treatments that affect those pathogenic pathways are not effective.

While the host response to SARS-CoV infection in mice, macaques and especially aged macaques is characterized by the induction of a wide range of proinflammatory cytokines and genes involved in cellular movement and cell-to-cell signaling, these genes are not activated in SARS-CoV infected ferrets. In order to further compare the different host responses in SARS-CoV infected ferrets, mice and macaques, a set of the most highly regulated genes (either up- or down) in SARS-CoV infected young adult macaques at day 4 after infection was created to examine expression of these genes in SARS-CoV infected ferrets and mice. This set includes genes involved in the antiviral response like ISG15, STAT1, OASL and the MX genes and genes with a proinflammatory function like CCL2, CCL3, CXCL10 and IL-6, but also many genes involved in cellular processes like cellular movement, cell cycle progression and cell differentiation. Results of this comparison are visualized in figure 7.5, a graphic representation of gene expression within this gene set in the lungs of the different SARS-CoV infected animals, demonstrating that many genes that are differentially expressed after SARS-CoV infection in macaques are also significantly regulated in SARS-CoV infected mice. In contrast, in SARS-CoV infected ferrets most of these genes were not activated, suggesting that several pathogenic pathways and many proinflammatory genes that are not only activated in SARS-CoV infected mice and macaques, but also in humans with SARS are not significantly induced in SARS-CoV infected ferrets when analyzing RNA from whole ferret lung tissue.

Since only few genes were activated in SARS-CoV infected ferrets at day 4 after infection, ferrets ( $n = 5$ ) were infected with SARS-CoV and euthanized at day 1 after inoculation to examine early host responses to SARS-CoV infection in these animals (data not shown). The percentage of upregulated genes at day 1 after infection was higher than on day 4, namely almost 50%. This set of upregulated genes contained many genes involved in IRF activation and IFN signaling, such as DHX58, ISG15, STAT1, IRF1, OAS1 and various IFIT genes, indicative of an active antiviral response early during infection, but also genes involved in ubiquitination, like USP18 and HERC5. Only few genes with proinflammatory characteristics were upregulated, such as CCL2 and CXCL10. We also analyzed expression of several antiviral and proinflammatory host genes by RT-PCR and found that both IFN- $\alpha$  and IFN- $\beta$  gene transcription was induced more than 100 times and more than 10 times respectively on day 1 after infection (figure 7.6A-B). The IFN inducible chemokine CXCL10 was also induced about 100 times compared to mock infected animals, but expression of the proinflammatory cytokines IL-1 $\beta$ , IL-6 and IL-8 was hardly upregulated (not shown). These results were further illustrated by the fact that, just as in SARS-CoV infected mice and macaques, phosphorylated STAT1, a marker for active IFN signaling, could be readily detected in ferret lungs using immunohistochemistry (not shown).



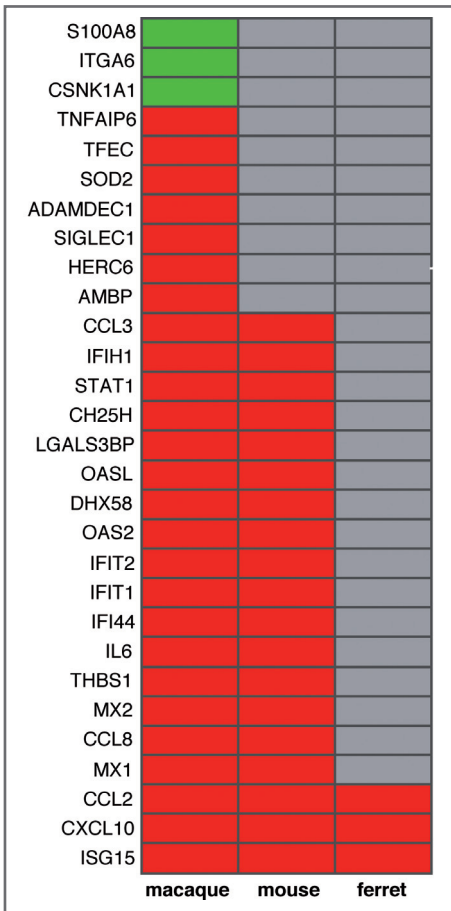


Figure 7.5. Cross-species comparison of SARS-CoV specific host response. A heatmap was generated comparing expression of a gene-set, highly significantly expressed in young adult SARS-CoV infected macaques, in SARS-CoV infected ferrets, mice and macaques. Significantly ( $Abs\ fc > 2$ ,  $p\text{-value} < 0.05$ ) upregulated genes are represented in red, significantly downregulated genes are represented in green. Genes that did not make the  $p$ -value or fold change cutoff are depicted by the light grey bars.

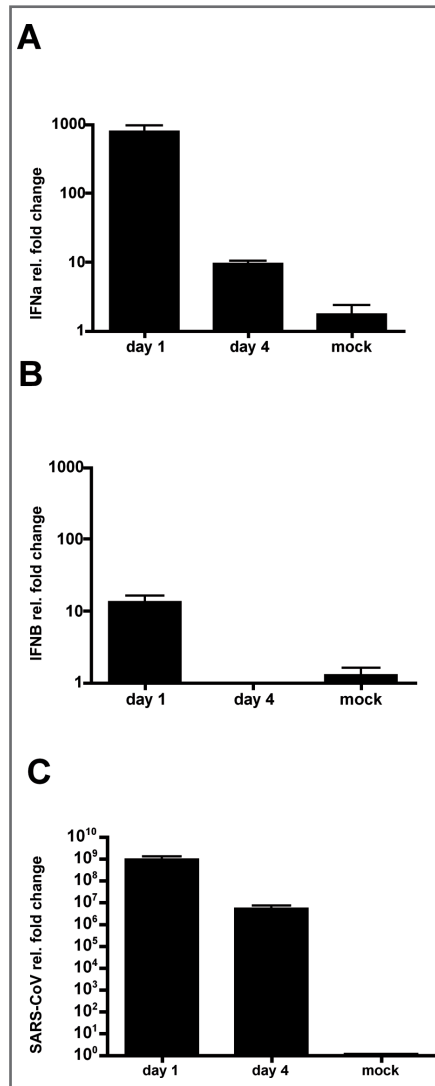
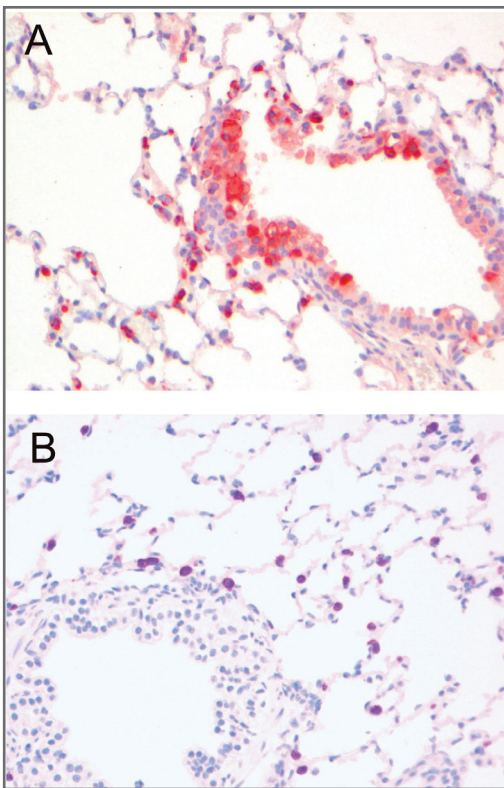


Figure 7.6. Detection of IFNs and SARS-CoV in ferret lungs. Induction of IFN- $\alpha$  (A) and IFN- $\beta$  (B) in the lungs of SARS-CoV infected ferrets. Fold increases in IFN gene transcription in SARS-CoV infected animals at day 1 and day 4 after infection as compared to PBS infected animals were determined using RT-PCR. Data are shown as the mean + the standard of the mean (SEM) for 5 ferrets. SARS-CoV levels were determined in lungs of SARS-CoV infected ferrets at day 1 and at day 4 after infection, compared to PBS infected animals, using RT-PCR (C).

### SARS-CoV replication in ferrets

One explanation for the observed differences in the host response to SARS-CoV infection in ferrets and other SARS models could be the kinetics of viral replication in the lungs. At day 1 after infection SARS-CoV mRNA levels were at least one log higher than what has been previously detected in either SARS-CoV infected mice or macaques at day 1 after inoculation (figure 7.6C). To further analyze the viral replication in ferrets, lungs from SARS-CoV infected ferrets were stained for SARS-CoV nucleocapsid protein. As shown in figure 7.7, in SARS-CoV infected ferrets SARS viral protein could be detected in large numbers of cells morphologically resembling type II pneumocytes at day 1 after infection. Interestingly, no bronchiolar epithelial cells were found to be positive for SARS-CoV antigen, whereas in SARS-CoV infected mice both bronchiolar epithelial cells and type II pneumocytes were SARS-CoV infected equally (figure 7.7).



**Figure 7.7.** Immunohistochemical detection of SARS-CoV infected cells in the lower respiratory tract of mice and ferrets at day 1 after infection. In mice both pneumocytes and bronchiolar epithelial cells are SARS-CoV positive (A). In ferrets mainly cells morphologically resembling type II pneumocytes are SARS-CoV positive (B).

## DISCUSSION

Several animal species, including macaques, African green monkeys, ferrets, hamsters and mice have been used to study SARS-CoV pathogenesis and test intervention strategies. Ferrets are readily infected with SARS-CoV; the virus replicates efficiently to high titers in the lung and infected animals may present clinical symptoms. Macroscopically and microscopically SARS-CoV-mediated pathology in ferrets is characterized by multifocal pulmonary lesions and multifocal mild to moderate diffuse alveolar damage respectively (40, 62). In addition, ferrets have an unusual long trachea, allowing simple compartmentalization of the upper and lower respiratory tracts, making it easier to study virus mediated effects in different areas of the respiratory system.

Analysis of the host response to SARS-CoV infection in ferret lungs revealed that proinflammatory cytokines such as IL-1 $\beta$ , IL-6, and IL-8 - known to be activated after SARS-CoV infection in humans, macaques and mice - are not differentially upregulated in the lungs of SARS-CoV infected ferrets. On the other hand, antiviral type I IFNs and CXCL10 were upregulated in SARS-CoV infected ferrets, just as in SARS-CoV infected humans, macaques and mice. In addition, microarray analysis of gene expression in the lungs of SARS-CoV infected ferrets revealed that, while in macaques and mice the majority of genes differentially expressed after SARS-CoV infection is upregulated, contrarily in SARS-CoV infected ferrets most genes were downregulated at day 4 after infection. Among the few genes upregulated in SARS-CoV infected ferrets there are several genes involved in antiviral pathways, most likely activated by IFNs produced early after infection. Strong activation of antiviral responses early after SARS-CoV infection in ferrets has been described previously and is similar to what is seen for SARS-CoV infection in macaques and mice, however otherwise the host response to SARS-CoV infection in ferrets shows little overlap with what is known from other species (9). It is not yet known what causes the massive downregulation of host genes that we observed in the lungs of SARS-CoV infected ferrets. Noteworthy, Baas et al. found a comparable gene expression pattern in young SARS-CoV infected mice where transcription of the majority of genes was downregulated after infection (1). A similar phenomenon has been observed in case of murine coronavirus mouse hepatitis virus (MHV) (46). MHV induces a host translational shutoff that coincides with the degradation of host mRNAs caused by the induction of a stress response after MHV infection, with the formation of stress granules and processing bodies. SARS-CoV also may cause host mRNA degradation through the expression of the NSP1 protein (43).

It is remarkable that, while SARS-CoV replicates to high titers both in ferrets, macaques and mice, the characteristics of the host response to infection are considerably different. We hypothesize that the differences seen in the host response to SARS-CoV could be explained partly by differences in cell tropism. While in macaques (type I and II) and mice (type II) pneumocytes and bronchiolar epithelial cells are infected by SARS-CoV equally, in ferrets only type II pneumocytes are infected. There are several possible explanations for the difference in SARS-CoV cell tropism between ferrets and other species. Ferret type I pneumocytes do not seem to express ACE2, explaining why these cells do not get infected with SARS-CoV (62). On the other hand, ACE2 is abundantly present on ferret bronchiolar epithelial cells. Theoretically it is possible that SARS-CoV does not use ACE2, but a different, unknown, receptor in ferrets

that is not expressed on ferret bronchiolar epithelial cells. However, unsuitability of ferret ACE2 as a SARS-CoV receptor is unlikely, since it has been shown that cells can be made permissive for SARS-CoV when transfected with ferret ACE2 (68). In addition, while the homology between ferret, human, macaque and mice ACE2 is about 82 % for all species, ferret ACE2 has been reported to be more efficient as a SARS-CoV receptor than mouse ACE2, corroborating the high virus levels we detect in lungs of SARS-CoV infected ferrets (68). Since the ACE2 receptor is expressed on ferret bronchiolar epithelial cells, more likely than the use of a completely different receptor than ACE2, is the use of a second, still unknown, co-receptor to infect this cell type (62). For example, C-type lectins like DC-SIGN and CD209L have been shown to enhance SARS-CoV entry *in vitro* and it is possible that a similar molecule necessary for SARS-CoV infection is not available on ferret bronchiolar epithelial cells (26, 67). Alternatively, specific proteases such as Cathepsin L and TMPRSS2 that are necessary for SARS-CoV infection may not be present in ferret bronchiolar epithelial cells, preventing infection of these cells (16, 20).

Not only the cell type infected by SARS-CoV and the following host response is different in ferrets compared to macaques and mice, interestingly SARS-CoV titers in ferret lungs at day 1 after infection are at least 1 log higher than in macaques and mice. The fact that so many cells in the ferret lung are SARS-CoV infected might also explain why, although pathogenic proinflammatory pathways are not induced, pathology is still observed in SARS-CoV infected ferrets. In contrast to the host response and immune-mediated pathology in SARS-CoV infected macaques and mice, which mainly seems to be driven by uninfected cells like pDCs and infected bronchiolar epithelial cells, the pathology in SARS-CoV infected ferrets might be caused by the huge number of SARS-CoV infected type II pneumocytes in the lungs. In addition, we hypothesize that the massive downregulation of host genes seen in SARS-CoV infected ferrets is a representation of the reaction to SARS-CoV in the infected type II pneumocytes.

During the outbreak of SARS-CoV in 2003 several treatments have been used to prevent or reduce SARS-mediated pathology including antiviral, immunomodulatory drugs and antibiotics, but no consensus of an optimal regimen has been accomplished (7, 19, 38, 55). In this study we tested the efficacy of a soluble ACE2 protein as a treatment for SARS. In the lung, ACE2 is mainly expressed on type I and II pneumocytes, bronchiolar epithelial cells as well as on endothelial cells and its expression changes dynamically depending on physiological conditions (25, 45, 70). In addition, ACE2 expression can also be regulated by several cytokines and by the SARS-CoV Spike protein, illustrated by the fact that ACE2 expression is downregulated in SARS-CoV infected ferrets, as described here, and in SARS-CoV infected mice (12, 29, 49). ACE2 is not only the cellular receptor for SARS-CoV, it has also been shown that the enzymatic activity of ACE2 has a protective role against lung damage; intraperitoneally injected ACE2 prevents acid induced acute lung injury in mice, most likely by decreasing ANG II levels in the lung limiting pathogenic effects through the AT<sub>1</sub> receptor (24). We hypothesized that treatment of SARS-CoV infected ferrets with ACE2, either before infection to neutralize viral particles before they are able to infect their target cell, or post infection to prevent alveolar damage through the catalytic activity of ACE2, might inhibit SARS-CoV mediated pathology. However, ferrets treated either before or after SARS-CoV infection with rhuACE2 did not have less pathology than control animals. In addition, no differences were found in viral replication. Although similar treatment protocols with rhuACE2 have been shown to be effective in mice and pig AI models, no effect could be observed in SARS-CoV infected ferrets (24, 60). In addition, treatment with

pegylated IFN- $\alpha$ , effective in reducing SARS-mediated immunopathology in aged macaques, did not affect SARS-induced pathology in ferrets either. The fact that no differences in pathology could be observed after treatment with either recombinant ACE2 or pegylated IFN- $\alpha$  in SARS-CoV infected ferrets, might be caused by the fact that pathogenic pathways that are targeted by ACE2 and IFN- $\alpha$  treatment are not activated but rather downregulated in ferrets after SARS-CoV infection. Therefore, the fact that both treatment with rhuACE2 and treatment with IFN- $\alpha$  did not have any effect on SARS-CoV induced pathology raised questions about the characteristics of the ferret host response to SARS-CoV compared to other SARS animal models such as non human primates and mice, but also compared to humans.

This study emphasizes that, when comparing SARS-mediated pathology between animal models different degrees of pathology and diverse characteristics of the host response to SARS-CoV infection can be distinguished in the various species. While in mice, macaques, but also African green monkeys, SARS-CoV induces an IFN response and a broad immune response, through pathways involved in inflammation, cell-to-cell signaling, cellular movement, in ferrets most of these pathways - except for the IFN response - are downregulated after SARS-CoV infection. The fact that different species infected with SARS-CoV with comparable levels of viral replication and seemingly comparable degrees of pathology in the lung can have a very different host response to the virus at the gene expression level, could affect efficacy of pathway specific treatments. Using genomics to characterize pathogenesis of SARS is a useful tool to examine species specific differences in pathogenesis.

## REFERENCES

1. Baas, T., A. Roberts, T. H. Teal, L. Vogel, J. Chen, T. M. Tumpey, M. G. Katze, and K. Subbarao. 2008. Genomic analysis reveals age-dependent innate immune responses to severe acute respiratory syndrome coronavirus. *J Virol* **82**:9465-9476.
2. Barnard, D. L., C. W. Day, K. Bailey, M. Heiner, R. Montgomery, L. Lauridsen, P. K. Chan, and R. W. Sidwell. 2006. Evaluation of immunomodulators, interferons and known *in vitro* SARS-CoV inhibitors for inhibition of SARS-CoV replication in BALB/c mice. *Antivir Chem Chemother* **17**:275-284.
3. Benjamini, Y., and Y. Hochberg. 1995. Controlling the False Discovery Rate - a Practical and Powerful Approach to Multiple Testing. *J Roy Stat Soc B Met* **57**:289-300.
4. Cameron, C. M., M. J. Cameron, J. F. Bermejo-Martin, L. Ran, L. Xu, P. V. Turner, R. Ran, A. Danesh, Y. Fang, P. K. Chan, N. Mytle, T. J. Sullivan, T. L. Collins, M. G. Johnson, J. C. Medina, T. Rowe, and D. J. Kelvin. 2008. Gene expression analysis of host innate immune responses during Lethal H5N1 infection in ferrets. *J Virol* **82**:11308-11317.
5. Cameron, M. J., L. Ran, L. Xu, A. Danesh, J. F. Bermejo-Martin, C. M. Cameron, M. P. Muller, W. L. Gold, S. E. Richardson, S. M. Poutanen, B. M. Willey, M. E. DeVries, Y. Fang, C. Seneviratne, S. E. Bosinger, D. Persad, P. Wilkinson, L. D. Greller, R. Somogyi, A. Humar, S. Keshavjee, M. Louie, M. B. Loeb, J. Brunton, A. J. McGeer, S. R. N. Canadian, and D. J. Kelvin. 2007. Interferon-mediated immunopathological events are associated with atypical innate and adaptive immune responses in patients with severe acute respiratory syndrome. *J Virol* **81**:8692-8706.
6. Cheng, Z. J., H. Vapaatalo, and E. Mervaala. 2005. Angiotensin II and vascular inflammation. *Med Sci Monit* **11**:RA194-205.
7. Chu, C. M., V. C. Cheng, I. F. Hung, M. M. Wong, K. H. Chan, K. S. Chan, R. Y. Kao, L. L. Poon, C. L. Wong, Y. Guan, J. S. Peiris, and K. Y. Yuen. 2004. Role of lopinavir/ritonavir in the treatment of SARS: initial virological and clinical findings. *Thorax* **59**:252-256.
8. Czub, M., H. Weingartl, S. Czub, R. He, and J. Cao. 2005. Evaluation of modified vaccinia virus Ankara based recombinant SARS vaccine in ferrets. *Vaccine* **23**:2273-2279.
9. Danesh, A., C. M. Cameron, A. J. Leon, L. Ran, L. Xu, Y. Fang, A. A. Kelvin, T. Rowe, H. Chen, Y. Guan, C. B. Jonsson, M. J. Cameron, and D. J. Kelvin. 2011. Early gene expression events in ferrets in response to SARS coronavirus infection versus direct interferon- $\alpha$ 2b stimulation. *Virology* **409**:102-112.
10. Darnell, M. E., E. P. Plant, H. Watanabe, R. Byrum, M. St Claire, J. M. Ward, and D. R. Taylor. 2007. Severe acute respiratory syndrome coronavirus infection in vaccinated ferrets. *J Infect Dis* **196**:1329-1338.
11. de Lang, A., T. Baas, T. Teal, L. M. Leijten, B. Rain, A. D. Osterhaus, B. L. Haagmans, and M. G. Katze. 2007. Functional genomics highlights differential induction of antiviral pathways in the lungs of SARS-CoV-infected macaques. *PLoS Pathog* **3**:e112.
12. de Lang, A., A. D. Osterhaus, and B. L. Haagmans. 2006. Interferon-gamma and interleukin-4 downregulate expression of the SARS coronavirus receptor ACE2 in Vero E6 cells. *Virology* **353**:474-481.
13. Donoghue, M., F. Hsieh, E. Baronas, K. Godbout, M. Gosselin, N. Stagliano, M. Donovan, B. Woolf, K. Robison, R. Jeyaseelan, R. E. Breitbart, and S. Acton. 2000. A novel angiotensin-converting enzyme-related carboxypeptidase (ACE2) converts angiotensin I to angiotensin 1-9. *Circ Res* **87**:E1-9.
14. Fouchier, R. A., T. Kuiken, M. Schutten, G. van Amerongen, G. J. van Doornum, B. G. van den Hoogen, M. Peiris, W. Lim, K. Stohr, and A. D. Osterhaus. 2003. Aetiology: Koch's postulates fulfilled for SARS virus. *Nature* **423**:240.
15. Glass, W. G., K. Subbarao, B. Murphy, and P. M. Murphy. 2004. Mechanisms of Host Defense following Severe Acute Respiratory Syndrome-Coronavirus (SARS-CoV) Pulmonary Infection of Mice. *J Immunol* **173**:4030-4039.
16. Glowacka, I., S. Bertram, M. A. Muller, P. Allen, E. Soilleux, S. Pfefferte, I. Steffen, T. S. Tsegaye, Y. He, K. Gnirss, D. Niemeyer, H. Schneider, C. Drosten, and S. Pohlmann. 2011. Evidence that TMPRSS2 activates the severe acute respiratory syndrome coronavirus spike protein for membrane fusion and reduces viral control by the humoral immune response. *J Virol* **85**:4122-4134.
17. Guan, Y., B. J. Zheng, Y. Q. He, X. L. Liu, Z. X. Zhuang, C. L. Cheung, S. W. Luo, P. H. Li, L. J. Zhang, Y. J. Guan, K. M. Butt, K. L. Wong, K. W. Chan, W. Lim, K. F. Shortridge, K. Y. Yuen, J. S. Peiris, and L. L. Poon. 2003. Isolation and characterization of viruses related to the SARS coronavirus from animals in southern China. *Science* **302**:276-278.
18. Haagmans, B. L., T. Kuiken, B. E. Martina, R. A. Fouchier, G. F. Rimmelzwaan, G. van Amerongen, D. van Riel, T. de Jong, S. Itamura, K. H. Chan, M. Tashiro, and A. D. Osterhaus. 2004. Pegylated interferon-alpha protects type 1 pneumocytes

against SARS coronavirus infection in macaques. *Nat Med* 10:290-293.

19. Ho, J. C., A. Y. Wu, B. Lam, G. C. Ooi, P. L. Khong, P. L. Ho, M. Chan-Yeung, N. S. Zhong, C. Ko, W. K. Lam, and K. W. Tsang. 2004. Pentaglobin in steroid-resistant severe acute respiratory syndrome. *Int J Tuberc Lung Dis* 8:1173-1179.
20. Huang, I. C., B. J. Bosch, F. Li, W. Li, K. H. Lee, S. Ghiran, N. Vasilieva, T. S. Dermody, S. C. Harrison, P. R. Dormitzer, M. Farzan, P. J. Rottier, and H. Choe. 2006. SARS coronavirus, but not human coronavirus NL63, utilizes cathepsin L to infect ACE2-expressing cells. *J Biol Chem* 281:3198-3203.
21. Huang, K. J., I. J. Su, M. Theron, Y. C. Wu, S. K. Lai, C. C. Liu, and H. Y. Lei. 2005. An interferon-gamma-related cytokine storm in SARS patients. *J Med Virol* 75:185-194.
22. Huber, W., A. von Heydebreck, H. Sultmann, A. Poustka, and M. Vingron. 2002. Variance stabilization applied to microarray data calibration and to the quantification of differential expression. *Bioinformatics* 18 Suppl 1:S96-104.
23. Idell, S., F. Kueppers, M. Lippmann, H. Rosen, M. Niederman, and A. Fein. 1987. Angiotensin converting enzyme in bronchoalveolar lavage in ARDS. *Chest* 91:52-56.
24. Imai, Y., K. Kuba, S. Rao, Y. Huan, F. Guo, B. Guan, P. Yang, R. Sarao, T. Wada, H. Leong-Poi, M. A. Crackower, A. Fukamizu, C. C. Hui, L. Hein, S. Uhlig, A. S. Slutsky, C. Jiang, and J. M. Penninger. 2005. Angiotensin-converting enzyme 2 protects from severe acute lung failure. *Nature* 436:112-116.
25. Ishiyama, Y., P. E. Gallagher, D. B. Averill, E. A. Tallant, K. B. Brosnihan, and C. M. Ferrario. 2004. Upregulation of angiotensin-converting enzyme 2 after myocardial infarction by blockade of angiotensin II receptors. *Hypertension* 43:970-976.
26. Jeffers, S. A., S. M. Tusell, L. Gillim-Ross, E. M. Hemmila, J. E. Achenbach, G. J. Babcock, W. D. Thomas, Jr., L. B. Thackray, M. D. Young, R. J. Mason, D. M. Ambrosino, D. E. Wentworth, J. C. Demartini, and K. V. Holmes. 2004. CD209L (L-SIGN) is a receptor for severe acute respiratory syndrome coronavirus. *Proc Natl Acad Sci U S A* 101:15748-15753.
27. Jiang, Y., J. Xu, C. Zhou, Z. Wu, S. Zhong, J. Liu, W. Luo, T. Chen, Q. Qin, and P. Deng. 2005. Characterization of cytokine/chemokine profiles of severe acute respiratory syndrome. *Am J Respir Crit Care Med* 171:850-857.
28. Kobinger, G. P., J. M. Figueredo, T. Rowe, Y. Zhi, G. Gao, J. C. Sanmiguuel, P. Bell, N. A. Wivel, L. A. Zitzow, D. B. Flieder, R. J. Hogan, and J. M. Wilson. 2007. Adenovirus-based vaccine prevents pneumonia in ferrets challenged with the SARS coronavirus and stimulates robust immune responses in macaques. *Vaccine* 25:5220-5231.
29. Kuba, K., Y. Imai, S. Rao, H. Gao, F. Guo, B. Guan, Y. Huan, P. Yang, Y. Zhang, W. Deng, L. Bao, B. Zhang, G. Liu, Z. Wang, M. Chappell, Y. Liu, D. Zheng, A. Leibbrandt, T. Wada, A. S. Slutsky, D. Liu, C. Qin, C. Jiang, and J. M. Penninger. 2005. A crucial role of angiotensin converting enzyme 2 (ACE2) in SARS coronavirus-induced lung injury. *Nat Med* 11:875-879.
30. Kuiken, T., R. A. Fouchier, M. Schutten, G. F. Rimmelzwaan, G. van Amerongen, D. van Riel, J. D. Laman, T. de Jong, G. van Doornum, W. Lim, A. E. Ling, P. K. Chan, J. S. Tam, M. C. Zambon, R. Gopal, C. Drosten, S. van der Werf, N. Escriou, J. C. Manuguerra, K. Stohr, J. S. Peiris, and A. D. Osterhaus. 2003. Newly discovered coronavirus as the primary cause of severe acute respiratory syndrome. *Lancet* 362:263-270.
31. Kumaki, Y., J. Ennis, R. Rahbar, J. D. Turner, M. K. Wandersee, A. J. Smith, K. W. Bailey, Z. G. Vest, J. R. Madsen, J. K. Li, and D. L. Barnard. 2011. Single-dose intranasal administration with mDEF201 (adenovirus vectored mouse interferon-alpha) confers protection from mortality in a lethal SARS-CoV BALB/c mouse model. *Antiviral Res* 89:75-82.
32. Lau, S. K., P. C. Woo, K. S. Li, Y. Huang, H. W. Tsoi, B. H. Wong, S. S. Wong, S. Y. Leung, K. H. Chan, and K. Y. Yuen. 2005. Severe acute respiratory syndrome coronavirus-like virus in Chinese horseshoe bats. *Proc Natl Acad Sci U S A*.
33. Li, W., M. J. Moore, N. Vasilieva, J. Sui, S. K. Wong, M. A. Berne, M. Somasundaran, J. L. Sullivan, K. Luzuriaga, T. C. Greenough, H. Choe, and M. Farzan. 2003. Angiotensin-converting enzyme 2 is a functional receptor for the SARS coronavirus. *Nature* 426:450-454.
34. Li, W., Z. Shi, M. Yu, W. Ren, C. Smith, J. H. Epstein, H. Wang, G. Crameri, Z. Hu, H. Zhang, J. Zhang, J. McEachern, H. Field, P. Daszak, B. T. Eaton, S. Zhang, and L. F. Wang. 2005. Bats are natural reservoirs of SARS-like coronaviruses. *Science* 310:676-679.
35. Liang, L., C. He, M. Lei, S. Li, Y. Hao, H. Zhu, and Q. Duan. 2005. Pathology of guinea pigs experimentally infected with a novel reovirus and coronavirus isolated from SARS patients. *DNA Cell Biol* 24:485-490.
36. Lipworth, B. J., and K. D. Dagg. 1994. Vasoconstrictor effects of angiotensin II on the pulmonary vascular bed. *Chest* 105:1360-1364.
37. Livak, K. J., and T. D. Schmittgen. 2001. Analysis of relative gene expression data using real-time quantitative PCR and the 2(-Delta Delta C(T)) Method. *Methods* 25:402-408.

38. Loutfy, M. R., L. M. Blatt, K. A. Siminovitch, S. Ward, B. Wolff, H. Lho, D. H. Pham, H. Deif, E. A. LaMere, M. Chang, K. C. Kain, G. A. Farcas, P. Ferguson, M. Latchford, G. Levy, J. W. Dennis, E. K. Lai, and E. N. Fish. 2003. Interferon alfacon-1 plus corticosteroids in severe acute respiratory syndrome: a preliminary study. *Jama* **290**:3222-3228.
39. Marshall, R. P., S. Webb, G. J. Bellingam, H. E. Montgomery, B. Chaudhari, R. J. McNulty, S. E. Humphries, M. R. Hill, and G. J. Laurent. 2002. Angiotensin converting enzyme insertion/deletion polymorphism is associated with susceptibility and outcome in acute respiratory distress syndrome. *Am J Respir Crit Care Med* **166**:646-650.
40. Martina, B. E., B. L. Haagmans, T. Kuiken, R. A. Fouchier, G. F. Rimmelzwaan, G. Van Amerongen, J. S. Peiris, W. Lim, and A. D. Osterhaus. 2003. Virology: SARS virus infection of cats and ferrets. *Nature* **425**:915.
41. Morrell, N. W., P. D. Upton, S. Kotecha, A. Huntley, M. H. Yacoub, J. M. Polak, and J. Wharton. 1999. Angiotensin II activates MAPK and stimulates growth of human pulmonary artery smooth muscle via AT<sub>1</sub> receptors. *Am J Physiol* **277**:L440-448.
42. Nagata, N., N. Iwata, H. Hasegawa, S. Fukushi, M. Yokoyama, A. Harashima, Y. Sato, M. Saijo, S. Morikawa, and T. Sata. 2007. Participation of both host and virus factors in induction of severe acute respiratory syndrome (SARS) in F344 rats infected with SARS coronavirus. *J Virol* **81**:1848-1857.
43. Narayanan, K., C. Huang, K. Lokugamage, W. Kamitani, T. Ikegami, C. T. Tseng, and S. Makino. 2008. Severe acute respiratory syndrome coronavirus nsp1 suppresses host gene expression, including that of type I interferon, in infected cells. *J Virol* **82**:4471-4479.
44. Orfanos, S. E., A. Armaganidis, C. Glynos, E. Psevdi, P. Kaltsas, P. Sarafidou, J. D. Catravas, U. G. Dafni, D. Langleben, and C. Roussos. 2000. Pulmonary capillary endothelium-bound angiotensin-converting enzyme activity in acute lung injury. *Circulation* **102**:2011-2018.
45. Oudit, G. Y., M. A. Crackower, P. H. Backx, and J. M. Penninger. 2003. The role of ACE2 in cardiovascular physiology. *Trends Cardiovasc Med* **13**:93-101.
46. Raaben, M., M. J. Groot Koerkamp, P. J. Rottier, and C. A. de Haan. 2007. Mouse hepatitis coronavirus replication induces host translational shutoff and mRNA decay, with concomitant formation of stress granules and processing bodies. *Cell Microbiol* **9**:2218-2229.
47. Reghunathan, R., M. Jayapal, L. Y. Hsu, H. H. Chng, D. Tai, B. P. Leung, and A. J. Melendez. 2005. Expression profile of immune response genes in patients with Severe Acute Respiratory Syndrome. *BMC Immunol* **6**:2.
48. Roberts, A., L. Vogel, J. Guarner, N. Hayes, B. Murphy, S. Zaki, and K. Subbarao. 2005. Severe acute respiratory syndrome coronavirus infection of golden Syrian hamsters. *J Virol* **79**:503-511.
49. Rockx, B., T. Sheahan, E. Donaldson, J. Harkema, A. Sims, M. Heise, R. Pickles, M. Cameron, D. Kelvin, and R. Baric. 2007. Synthetic reconstruction of zoonotic and early human severe acute respiratory syndrome coronavirus isolates that produce fatal disease in aged mice. *J Virol* **81**:7410-7423.
50. Rowe, T., A. J. Leon, C. J. Crevar, D. M. Carter, L. Xu, L. Ran, Y. Fang, C. M. Cameron, M. J. Cameron, D. Banner, D. C. Ng, R. Ran, H. K. Weirback, C. A. Wiley, D. J. Kelvin, and T. M. Ross. 2010. Modeling host responses in ferrets during A/California/07/2009 influenza infection. *Virology* **401**:257-265.
51. Schiffrin, E. L., and R. M. Touyz. 2003. Inflammation and vascular hypertrophy induced by angiotensin II: role of NADPH oxidase-derived reactive oxygen species independently of blood pressure elevation? *Arterioscler Thromb Vasc Biol* **23**:707-709.
52. See, R. H., M. Petric, D. J. Lawrence, C. P. Mok, T. Rowe, L. A. Zitzow, K. P. Karunakaran, T. G. Voss, R. C. Brunham, J. Gauldie, B. B. Finlay, and R. L. Roper. 2008. Severe acute respiratory syndrome vaccine efficacy in ferrets: whole killed virus and adenovirus-vectored vaccines. *J Gen Virol* **89**:2136-2146.
53. Smits, S. L., A. de Lang, J. M. van den Brand, L. M. Leijten, I. W. F. van, M. J. Eijkemans, G. van Amerongen, T. Kuiken, A. C. Andeweg, A. D. Osterhaus, and B. L. Haagmans. 2010. Exacerbated innate host response to SARS-CoV in aged non-human primates. *PLoS Pathog* **6**:e1000756.
54. Smyth, G. K. 2004. Linear models and empirical bayes methods for assessing differential expression in microarray experiments. *Stat Appl Genet Mol Biol* **3**:Article3.
55. So, L. K., A. C. Lau, L. Y. Yam, T. M. Cheung, E. Poon, R. W. Yung, and K. Y. Yuen. 2003. Development of a standard treatment protocol for severe acute respiratory syndrome. *Lancet* **361**:1615-1617.
56. ter Meulen, J., A. B. Bakker, E. N. van den Brink, G. J. Weverling, B. E. Martina, B. L. Haagmans, T. Kuiken, J. de Kruijf, W. Preiser, W. Spaan, H. R. Gelderblom, J. Goudsmit, and A. D. Osterhaus. 2004. Human monoclonal antibody as prophylaxis for SARS coronavirus infection in ferrets. *Lancet* **363**:2139-2141.



57. Theron, M., K. J. Huang, Y. W. Chen, C. C. Liu, and H. Y. Lei. 2005. A probable role for IFN-gamma in the development of a lung immunopathology in SARS. *Cytokine* **32**:30-38.
58. Tipnis, S. R., N. M. Hooper, R. Hyde, E. Karran, G. Christie, and A. J. Turner. 2000. A human homolog of angiotensin-converting enzyme. Cloning and functional expression as a captopril-insensitive carboxypeptidase. *J Biol Chem* **275**:33238-33243.
59. Traggiai, E., S. Becker, K. Subbarao, L. Kolesnikova, Y. Uematsu, M. R. Gismondo, B. R. Murphy, R. Rappuoli, and A. Lanzavecchia. 2004. An efficient method to make human monoclonal antibodies from memory B cells: potent neutralization of SARS coronavirus. *Nat Med* **10**:871-875.
60. Trembl, B., N. Neu, A. Kleinsasser, C. Gritsch, T. Finsterwalder, R. Geiger, M. Schuster, E. Janzek, H. Loibner, J. Penninger, and A. Loeckinger. 2010. Recombinant angiotensin-converting enzyme 2 improves pulmonary blood flow and oxygenation in lipopolysaccharide-induced lung injury in piglets. *Crit Care Med* **38**:596-601.
61. Tukey, J. W. 1977. Some thoughts on clinical trials, especially problems of multiplicity. *Science* **198**:679-684.
62. van den Brand, J. M., B. L. Haagmans, L. Leijten, D. van Riel, B. E. Martina, A. D. Osterhaus, and T. Kuiken. 2008. Pathology of experimental SARS coronavirus infection in cats and ferrets. *Vet Pathol* **45**:551-562.
63. Ware, L. B., and M. A. Matthay. 2000. The acute respiratory distress syndrome. *N Engl J Med* **342**:1334-1349.
64. Weingartl, H., M. Czub, S. Czub, J. Neufeld, P. Marszal, J. Gren, G. Smith, S. Jones, R. Proulx, Y. Deschambault, E. Grudeski, A. Andonov, R. He, Y. Li, J. Copps, A. Grolla, D. Dick, J. Berry, S. Ganske, L. Manning, and J. Cao. 2004. Immunization with modified vaccinia virus Ankara-based recombinant vaccine against severe acute respiratory syndrome is associated with enhanced hepatitis in ferrets. *J Virol* **78**:12672-12676.
65. Weingartl, H. M., J. Copps, M. A. Drebot, P. Marszal, G. Smith, J. Gren, M. Andova, J. Pasick, P. Kitching, and M. Czub. 2004. Susceptibility of pigs and chickens to SARS coronavirus. *Emerg Infect Dis* **10**:179-184.
66. Wong, C. K., C. W. Lam, A. K. Wu, W. K. Ip, N. L. Lee, I. H. Chan, L. C. Lit, D. S. Hui, M. H. Chan, S. S. Chung, and J. J. Sung. 2004. Plasma inflammatory cytokines and chemokines in severe acute respiratory syndrome. *Clin Exp Immunol* **136**:95-103.
67. Yang, Z. Y., Y. Huang, L. Ganesh, K. Leung, W. P. Kong, O. Schwartz, K. Subbarao, and G. J. Nabel. 2004. pH-dependent entry of severe acute respiratory syndrome coronavirus is mediated by the spike glycoprotein and enhanced by dendritic cell transfer through DC-SIGN. *J Virol* **78**:5642-5650.
68. Zamoto, A., F. Taguchi, S. Fukushi, S. Morikawa, and Y. K. Yamada. 2006. Identification of ferret ACE2 and its receptor function for SARS-coronavirus. *Adv Exp Med Biol* **581**:519-522.
69. Zhang, Y., J. Li, Y. Zhan, L. Wu, X. Yu, W. Zhang, L. Ye, S. Xu, R. Sun, Y. Wang, and J. Lou. 2004. Analysis of serum cytokines in patients with severe acute respiratory syndrome. *Infect Immun* **72**:4410-4415.
70. Zisman, L. S., R. S. Keller, B. Weaver, Q. Lin, R. Speth, M. R. Bristow, and C. C. Canver. 2003. Increased angiotensin-(1-7)-forming activity in failing human heart ventricles: evidence for upregulation of the angiotensin-converting enzyme Homologue ACE2. *Circulation* **108**:1707-1712.



CHAPTER 8

# Summarizing discussion



While it is hypothesized that SARS in humans is caused by a disproportional immune response illustrated by inappropriate induction of inflammatory cytokines, the exact nature of the host response to SARS-CoV infection causing severe pathology that includes diffuse alveolar damage (DAD) and acute respiratory distress syndrome (ARDS) has not been fully revealed. It is complicated to investigate the early events leading up to SARS mediated pathology in humans, since only a limited number of (PBMC) samples is available from SARS patients during the epidemic in 2003/2004 and no new natural SARS-CoV infections in humans have been reported since then. In addition, the samples that are available were taken relatively late during infection, often after different intervention strategies were applied, causing serious difficulties in the analysis of SARS pathogenesis.

Although several studies have investigated the behavior of SARS-CoV in cell lines and primary cell cultures, it is difficult to integrate these results in a model of SARS pathogenesis. In order to further understand early events after SARS-CoV infection contributing to SARS mediated pathology, we studied SARS-CoV pathogenesis in different animal models. A range of techniques to establish parameters such as viral loads, virus tropism and the severity of pathology were employed to analyze SARS-CoV infection in macaques, mice and ferrets. Additionally, functional genomics was used to explore the host response at gene expression level in these animal models. Combining these observations allowed us to further elucidate the pathogenesis of SARS.

### **SARS-CoV activates antiviral and proinflammatory pathways in macaques**

In *chapters 2, 3* and *6* different aspects of SARS pathogenesis in macaques are evaluated, analyzing viral loads, cell types infected and host responses at the gene expression level after SARS-CoV infection. SARS-CoV replicates efficiently to high titers in the lungs of infected macaques, with virus levels peaking around day 2 after infection after which these levels decrease (31, 42). The kinetics of SARS-CoV replication in macaques are significantly different from those described for human SARS-CoV infections where it is estimated that viral levels peak much later, around day 10 after onset of clinical symptoms, after which viral loads in the lung decrease as the level of SARS-CoV specific antibodies increases (55, 69). Differences in viral replication kinetics between macaques and humans might be partly caused by the intratracheal route of infection employed in macaque infection studies. This infection method results in high levels of SARS-CoV in the lungs very early during infection, while in natural infection in humans it takes more time for inhaled viral particles to reach the lungs. In humans it has been proven difficult to determine exactly which cells are infected by SARS-CoV. This is mainly due to the fact that only a limited number of samples are available and suitable for immunohistochemistry and in situ hybridization, since most samples were obtained late during infection or after death of the patient. SARS-CoV positive cells have only been detected in the lungs of patients that died relatively early, within 14 days after the onset of disease, and had high viral loads, as detected by RT-PCR (64). In cases where SARS-CoV positive cells could be detected, these cells were mainly identified as alveolar epithelial cells, primarily type I pneumocytes but also type II pneumocytes (64, 85). In addition, smaller numbers of SARS-CoV positive cells were identified as alveolar macrophages and occasionally SARS-CoV infected bronchiolar epithelial cells were detected, but based on the number of samples available and the number of cells that stained positive it is not clear whether SARS-CoV replicates in these latter two cell types (20-21, 93). In macaques

the main cell type infected by SARS-CoV are the type I and type II pneumocytes, but also bronchiolar epithelial cells are infected.

Although SARS-CoV replicates to high titers in macaque lungs, young adult SARS-CoV infected macaques remain free from clinical symptoms and only very limited pulmonary pathology is developed. Microscopically SARS-CoV infection in young macaques is characterized by mild DAD with multifocal lesions and modest numbers of infiltrating immune cells. Additionally, multifocal mild chronic lymphoplasmacytic tracheo-bronchoadenitis was observed. On the other hand, SARS-CoV infection in aged macaques did result in clinical symptoms, although relatively mild. Body temperatures were increased in all animals infected and in some of the macaques decreased activity and mildly labored breathing was observed. When comparing pulmonary pathology after SARS-CoV infection the difference between young and aged macaques was even more obvious. Although viral loads in the lungs are similar in young and aged macaques, pulmonary pathology in aged macaques is far more severe, with large (multi) focal pulmonary consolidation visible macroscopically while microscopically acute lung injury (ALI) associated lesions and DAD similar to what has been described for human SARS patients were observed. The difference in pathology between young and aged macaques corresponds with natural human SARS-CoV infection where disease symptoms are far more severe in elderly compared to younger patients (28, 45, 57).

Analysis of the macaque host response to SARS-CoV infection at the gene expression level revealed the induction of a broad host immune response with activation of both antiviral and proinflammatory pathways. This was illustrated by induced expression of a range of cytokines and chemokines, many of which also have been reported to be upregulated in human SARS patients. The antiviral response in SARS-CoV infected young adult macaques was characterized by elevated transcription of several IFN genes. IFNs are released by host cells in response to the presence of virus and are key players in the antiviral response to invading pathogens. In most cell types SARS-CoV is able to block or delay the production of type I IFNs (33-34, 52). For instance, studies using expression plasmids containing one of the SARS-CoV proteins, have demonstrated that the SARS-CoV proteins open reading frame (ORF)3b, ORF6 and the N proteins are able to inhibit interferon production by affecting the IRF-3 activation pathway.(52) However, gene expression of type I, type II and type III IFN genes was highly induced in SARS-CoV infected young macaques, as determined by microarray analysis and RT-PCR. Presence of IFN- $\beta$  in macaques was also shown at the protein level. In addition, a number of genes involved in the JAK/STAT signaling pathway or produced as a result of IFN signaling are upregulated in SARS-CoV infected macaques, including several of the IFIT, MX and OAS genes as well as STAT1, among others. Elevated expression of these IFN stimulated genes (ISGs) in macaques suggests that the IFNs produced after SARS-CoV infection are biologically active. Induction of antiviral pathways was further illustrated by immunohistochemical staining of phosphorylated STAT1 in the nuclei of cells in the macaque lung, showing abundant activation of this transcription factor. However, STAT1 was not activated in SARS-CoV infected pneumocytes, most likely due to inhibition of IFN signaling by the SARS-CoV protein ORF6, which has been shown to be able to block translocation of STAT1 to the nucleus (35). Thus, type I IFNs are produced in the lungs of SARS-CoV-infected young adult macaques and are able to activate the JAK/STAT pathway. However, translocation of STAT1 does not occur in SARS-CoV infected pneumocytes suggesting IFNs produced after SARS-CoV infection mainly activate antiviral responses in uninfected cells.

Besides antiviral pathways also proinflammatory pathways are readily induced in SARS-CoV infected macaques. A wide range of inflammatory chemokines and cytokines, such as IL-1 $\beta$ , IL-6, IL-8, CCL2, CXCL9 and CXCL10, are significantly induced after SARS-CoV infection in macaques. Additionally, monocyte chemotactic protein genes like CCL7, CCL8, but also CCL11, a chemotactic protein for eosinophils were upregulated in macaque lungs after SARS-CoV infection. Many of these cytokines and chemokines are also upregulated in human SARS patients. Taken together, SARS-CoV infection in young macaques elicits a strong host immune response, as would be expected during viral infection.

In addition to analyzing host responses in the macaque lung, the main site of viral replication, host responses were also analyzed in PBMCs of young SARS-CoV infected macaques. Since PBMC samples are relatively easy to obtain during infection in a clinical setting, in contrast to lung samples, it is of interest to examine if expression profiles in PBMCs reflect expression profiles in the lungs after SARS-CoV infection. If this is the case, analyzing host gene expression profiles in PBMCs could be a useful tool to help to predict disease outcome and to adjust the type of treatment to individual needs. Determining gene expression profiles in PBMCs for diagnostic and prognostic purposes has already proven to be a useful tool in other diseases including several types of cancer, systemic lupus erythematosus and smallpox infection (3, 8-9, 80, 95). In humans no clear evidence is available that shows that SARS-CoV efficiently infects PBMCs and also in SARS-CoV infected macaques we could not detect viral replication (56, 63). The fact that SARS-CoV does not replicate in macaque PBMCs indicates that host response detected in these cells are driven by host responses in the lung and not by viral particles directly, a condition that must be met in order to use PBMCs as sensing tool for host responses in the lung. Although SARS-CoV was not detected in PBMCs, a strong host response to infection was mounted in these cells, especially at day 1 after infection, after which the number of differentially expressed genes decreased again. Host responses in PBMCs after SARS-CoV infection were dominated by activation of antiviral and proinflammatory pathways, just as in the lungs. A wide range of PRRs, molecules involved in sensing of invading pathogens, were differentially expressed, illustrated by induced expression of several Toll like receptors (TLRs), Nod like receptors (NLRs) and RNA helicases. Downstream of these sensing proteins, numerous antiviral genes such as IFN signaling genes and ISGs were upregulated, but also expression of some of the inflammatory cytokines and chemokines like IL-1 $\beta$ , CXCL3 and CXCL11 was induced. However at day 4 after infection, several of the typically induced cytokines and chemokines induced in the lung like IL-6, CCL4, CCL11 and CXCL9 were not detected in PBMCs. Additionally, in contrast to the lungs, induction of IFNs itself and the proinflammatory chemokine CCL2 are not induced in PBMCs. This is in line with the absence of viral replication in these cells, since both molecules are typically induced in the presence of viral particles in SARS-CoV infection (18). In this thesis we propose that cytokines and chemokines produced in the lung after SARS-CoV infection in macaques are responsible for the gene expression profiles detected in PBMCs. Analysis of host responses in PBMCs derived from hosts were more severe disease is induced after SARS-CoV infection, such as aged macaques, will show if this technique is able to discriminate PBMC expression profiles linked to varying severity of disease in the lungs.

As described in **chapter 6**, in aged macaques the host response to SARS-CoV infection was even more pronounced than in young macaques, despite similar levels of viral replication. Analysis of gene expression in the lungs of SARS-CoV infected macaques revealed that in aged macaques more genes

associated with inflammation were significantly upregulated compared to young macaques, especially genes that center around the transcription factor NF- $\kappa$ B. Age-related differences in proinflammatory immune responses to viral infection have been described earlier and might be (partly) due to disturbances in the redox balance, caused by accumulated oxidative damage over time and a weakened antioxidative defense system in aged individuals (6, 12, 23, 32, 81). This disturbed redox balance results in activation of redox-sensitive transcription factors like NF- $\kappa$ B and subsequently lead to induction of proinflammatory cytokines as observed in aged macaques. Immunohistological staining revealed that, similarly to activation of the STAT1 transcription factor in non-SARS-CoV infected cells in young macaques, also activation of NF- $\kappa$ B seems to be restricted to cells that are not SARS-CoV infected. This suggests that the uninfected cells are mainly responsible for upregulated expression of NF- $\kappa$ B target genes in the lungs of aged macaques and thus the strong immune response to SARS-CoV infection in macaques seems to be primarily driven by uninfected cells instead of SARS-CoV infected cells.

The induction of antiviral pathways and the production of type I IFNs after SARS-CoV infection were far less pronounced in aged macaques compared to young macaques. Decreased levels of type I IFNs after infection in elderly individuals is a phenomenon that has been described in humans (16, 75, 86). Therapeutic treatment with pegylated IFN- $\alpha$  reduced SARS associated pathology in SARS-CoV infected aged macaques, but the beneficial effect of IFN treatment is most likely not derived from its antiviral capacities, considering SARS-CoV levels were not affected by this treatment. This could be explained by the fact that SARS-CoV replication peaks very early after infection in macaques, just after IFN treatment is started. Furthermore, the fact that IFN signaling via the JAK/STAT pathway is inhibited by SARS-CoV proteins in infected cells probably decreases the antiviral effect of therapeutic treatment with IFN in the macaque model. Analysis of gene expression data showed that instead of decreasing virus levels, the beneficial effect of IFN treatment is rather due to its capacity to reduce the excessive induction of proinflammatory pathways in the macaque lung, resulting in decreased pathology. Anti-inflammatory capacities of type I IFNs have been described previously and are further confirmed in this thesis by the fact IL-1 $\beta$  induced production of IL-1 $\beta$  and IL-8 in PBMC could be reduced by IFN- $\alpha$  *in vitro* (2, 10, 41, 70, 97).

### **pDCs are activated by live and inactivated SARS-CoV in mice**

In order to analyze SARS pathogenesis in mice and to compare murine host responses to SARS-CoV infection to host responses in macaques, young mice were infected intratracheally with SARS-CoV instead of intranasally, which is the more commonly used route of infection for murine infection models (**chapter 4**). SARS-CoV replicates to high titers in the lungs of both BALB/c and C57BL/6 mice, similarly to SARS-CoV infection in macaques. In contrast to previously published intranasal wildtype SARS-CoV infections where mainly bronchiolar epithelial cells are infected, in our studies both type II pneumocytes and bronchiolar epithelial cells were the main target cells for SARS-CoV infection at day 1 after infection (38, 76). At day 4 after infection, only few SARS-CoV positive cells were visible in the lungs. Interestingly, Rockx et al. showed that SARS-CoV strains with different spike variants have different tropism in mouse lungs, varying from only infecting bronchiolar epithelial cells to mainly infecting type II pneumocytes or combinations of both, and these subtle differences in tropism also affected SARS pathogenesis and outcome (76).



Despite high levels of viral replication in the lungs BALB/c mice intratracheally infected with SARS-CoV did not show signs of clinical illness. Microscopically however, at day 4 after infection the lungs of SARS-CoV infected BALB/c mice all exhibited alveolar damage to some extent, with the severity ranging from mild to moderate focal lesions, infiltration of inflammatory cells, damage of bronchioles and sometimes fibrin depositions. However, signs of more severe ALI as observed in human SARS patients, such as type II pneumocyte hyperplasia, flooding with edema and hyaline membranes, were not observed in SARS-CoV infected mice. In contrast to young SARS-CoV infected BALB/c mice that did not show any clinical signs of disease, 4 out of 6 aged BALB/c mice did not survive intratracheal SARS-CoV infection. This is the first study that describes mortality caused by a wildtype SARS-CoV strain in immunocompetent mice. Although more studies are required to determine the exact cascade of pathological events causing death in these mice, these results are in line with the increased pathology described for other SARS-CoV aged mouse models as well as our aged macaque model.

When examining the host response to SARS-CoV infection at the gene expression level in young mice, gene expression profiles in BALB/c mice were dominated by activation of antiviral and proinflammatory pathways, similarly to expression profiles in SARS-CoV infected macaques. Several genes involved in sensing of invading pathogens through PRRs were significantly upregulated in SARS-CoV infected BALB/c mice, such as RIG-I, MDA-5 and PKR, as well as genes that engage in the activation of interferon regulatory factors (IRFs) by PRRs. Activation of IRFs by cytosolic PRRs can lead to induction of various antiviral genes, depending on the type of IRF activated. RT-PCR analysis revealed significant induction of the type I, II and III IFNs in BALB/c mice after SARS-CoV infection. The presence of IFNs was further illustrated by the fact that many genes involved in the JAK/STAT signaling pathway were significantly induced as well as a wide range of IFN stimulated genes (ISGs). The proinflammatory host responses in SARS-CoV infected BALB/c mice were dominated by elevated gene transcription levels of genes as IL-6, SAA1, CXCL1, CXCL1, CXCL9, CXCL10 and CXCL11, all induced in SARS-CoV infected macaques as well. Noteworthy, the Th2 chemokine CCL11 (eotaxin), an eosinophil attractant that is induced in SARS-CoV infected macaques, is not induced in mice. The broad host immune response elicited after intratracheal SARS-CoV infection in BALB/c mice seems to be more prominent than what has been described thus far for intranasal infections with wildtype SARS-CoV in young BALB/c mice, coinciding with the more pronounced pathology in these mice (7, 76).

Remarkably, C57BL/6 mice are more resistant to SARS-CoV infection than BALB/c mice, since almost no pathology was observed in lungs of infected animals after intratracheal SARS-CoV infection. In addition to differences observed in pathology between the two mouse strains, the host response to SARS-CoV infection in C57BL/6 mice was less pronounced than in BALB/c mice, with only relatively few genes differentially expressed after infection (60 gene transcripts at day 1 after infection, 18 gene transcripts at day 4 after infection). Just as in BALB/c mice, this set was dominated by a range of upregulated ISGs, although not as many ISGs were differentially expressed as in BALB/c mice and expression levels were lower. In line with this, in contrast to BALB/c mice, in which both type I, II and II IFNs were detected, in C57BL/6 mice only elevated transcript levels of IFN- $\lambda$  could be detected by RT-PCR. In addition to antiviral genes, a limited number of chemokine genes like the SARS-CoV induced CCL2 and the IFN induced CXCL10 as well as a number of heat shock protein genes were significantly upregulated in C57BL/6 mice.

Strikingly, proinflammatory cytokines and chemokines like IL-6, CXCL1 and CXCL11, highly expressed in SARS-CoV infected BALB/c mice, as well as in SARS-CoV infected macaques, were not significantly induced in C57BL/6 mice. When gene expression data from SARS-CoV infected C57BL/6 mice at day 1 after infection were directly compared to gene expression data from BALB/c mice, this set mainly contained genes that remained unchanged in C57BL/6 mice, but were up- or downregulated in BALB/c mice. Interestingly, ACE2 was one of the genes downregulated in BALB/c mice, but not in the C57BL/6 mice. Besides being the SARS-CoV cellular receptor, ACE2 has been shown to protect from lung damage (48). One could speculate that the fact that ACE2 expression is not decreased after SARS-CoV infection in C57BL/6 mice could play a role in the observed lack of pulmonary pathology after infection. Similar strain related differences in disease pathogenesis and host responses to viral infection have been described previously in mice in general as well as between BALB/c mice and C57BL/6 mice specifically (13, 68, 88, 90, 98). Although the reason for these differences is not known yet, several genetic factors may be of influence. It has been proposed that high levels of secretory phospholipase 2, an enzyme for which C57BL/6 mice are genetically deficient, may amplify the induction of proinflammatory cytokines in BALB/c mice (40, 94). Additionally, differential expression and differential activation of PRRs in BALB/c and C57BL/6 mice might influence the characteristics of the subsequent host response to infection (4, 58, 77).

Both in mice as well as in macaques several types of IFN are produced after SARS-CoV infection. *In vitro*, human pDCs are the only cells known to produce type I IFNs when exposed to SARS-CoV (17). As is demonstrated in **chapter 4**, transcription of IFN- $\alpha$ , IFN- $\beta$  and IFN- $\lambda$  is highly induced in pDCs obtained from BALB/c mice, upon exposure to SARS-CoV *in vitro*. Strikingly, not only live SARS-CoV induced expression of IFNs, also stimulation with inactivated virus resulted in elevated levels of IFN gene transcription, showing that the presence of SARS-CoV particles alone is sufficient to activate pDCs and infection of and replication in these cells is not required for activation. As is shown for other CoVs, SARS-CoV infected pDCs are most likely activated through TLR7 by endocytosed viral particles rather than by active viral replication (17). Activation of pDCs by inactivated virus particles, leading to production of IFN- $\alpha$ , has been described for several other viruses as well (27, 59, 92).

Despite relatively high levels of IFN gene transcription in mouse pDCs compared with the specific pDC stimulator ODN-2216, only low, but biologically active, levels of IFN- $\alpha$  protein were detected in the supernatants of pDCs incubated with either live or inactivated SARS-CoV. No IFN- $\beta$  and IFN- $\lambda$  protein could be detected. These data suggest that the production of IFN proteins might be blocked at the translational level. Inhibited or delayed protein production has been described previously for SARS-CoV infections as well as for other CoV infections (51, 78, 100). It remains to be determined which mechanism is responsible for the inhibited IFN protein production in murine pDCs after incubation with (inactivated) SARS-CoV. Noteworthy, when human pDCs were incubated with SARS-CoV, IFNs are produced at high levels both at the mRNA and the protein level (unpublished results). The mechanism behind this discrepancy between activation of murine and human pDCs by SARS-CoV could be due to species differences, for example in PRR responses, and should be investigated further.

Depletion of pDCs in SARS-CoV infected BALB/c mice demonstrated that, although only low levels of IFN protein seem to be produced by murine pDCs *in vitro*, depletion of pDCs significantly reduced activation of antiviral pathways in these mice, compared to control antibody (Ab) treated mice, suggest-

ing pDCs indeed do produce biologically active IFNs upon SARS-CoV infection *in vivo*. Besides decreased activation of genes involved in IFN signaling and the ISGs, also transcription of IFNs was lower in pDC depleted mice, especially at day 1 after infection, when expression of the type I IFNs and IFN- $\lambda$  was reduced compared to Ab treated control mice. Depletion of pDCs in BALB/c mice did not lead to a complete inhibition of IFN gene transcription, which might be due to remaining pDCs and/or other IFN production by other cell types such as alveolar macrophages that also have been reported to produce large amounts of IFNs upon infection with RNA viruses (54). Nevertheless, in pDC depleted mice decreased IFN levels early during infection resulted in SARS-CoV levels that were about 1 log higher than detected in control Ab treated mice at day 4 after infection. This was further illustrated by a higher number of SARS-CoV positive cells in the lung of pDC depleted mice at day 4 after infection, as determined by immunohistological staining. An additional factor leading up to the increased viral levels in the lungs of pDC depleted mice might be the lack of IFN- $\gamma$  expression in these mice. In **chapter 5** we show that IFN- $\gamma$  has antiviral properties in SARS-CoV infection since this cytokine reduces expression of ACE2, the cellular receptor of SARS-CoV. While ACE2 expression might be reduced in control Ab treated mice as a result of the induced transcription of IFN- $\gamma$ , hereby possibly reducing the number of SARS-CoV infected cells, ACE2 expression in pDC depleted mice might be relatively high in the absence of IFN- $\gamma$ . Microarray results support this hypothesis; in control Ab treated mice ACE2 was significantly downregulated both at day 1 and at day 4 after infection, while in pDC depleted mice ACE2 gene transcription was only reduced at day 1 after infection, although differences were modest.

Interestingly, from our pDC depletion studies in SARS-CoV infected mice, we can conclude that activation of pDCs by SARS-CoV is not only important for the induction of an antiviral host response, also proinflammatory host responses are induced through activation of pDCs. Several inflammatory cytokine genes as well as pathogenic proinflammatory pathways were not or less induced in mice in which pDCs were depleted before SARS-CoV infection. Induction of the proinflammatory chemokine CXCL10 was also demonstrated in murine pDCs *in vitro* after incubation with SARS-CoV. Similarly to production of IFNs in these cells, exposure of murine pDCs to both live and inactivated SARS-CoV induced transcription of the CXCL10 gene. The fact that inactivated SARS-CoV is sufficient to induce a proinflammatory response in pDCs raises the question if solely the presence of inactivated SARS-CoV particles would be sufficient to induce a pathogenic immune response in the host. More research would be needed to address this question.

Although depletion of pDC resulted in higher levels of SARS-CoV in the lungs at day 4 after infection compared to control mice, SARS-CoV induced pathology in these young BALB/c mice was not significantly different between both groups. In fact, microscopically the lungs of pDC depleted mice seemed less affected and less infiltrating immune cells were observed than in the lungs of Ab treated control mice. This difference is most likely caused by the diminished activation of proinflammatory pathways in pDC depleted mice compared to the control group as well reduced activation of pathways involved in cross-talk between innate and adaptive immune responses and pathways involved in the lysis by cytotoxic T-cells. In pDC depleted mice less T cell may be drawn to the site of infection, compared to control mice, illustrated by decreased levels of IFN- $\gamma$ . It has been shown that T cells are important to overcome SARS-CoV infection and although in our study infecting young wildtype BALB/c mice with a non-adapted wildtype SARS-CoV T-cells may not be required to overcome infection (19, 101).

In contrast to SARS-CoV infection in young pDC depleted BALB/c mice, aged mice intratracheally infected with SARS-CoV after pDC depletion all died within 4 days after infection. Ab treated control mice survived significantly longer after SARS-CoV infection than pDC depleted mice. This indicates that proper activation of pDCs plays an important role in SARS pathogenesis in mice. Also other studies highlight the importance of the innate immune response in murine SARS-CoV infections (36, 38, 44). Our results in pDC depleted mice show resemblance with studies in young adult C57BL/6 mice that are deficient for the adaptor protein MyD88 and infected with a mouse-adapted SARS-CoV strain. These mice succumb to SARS-CoV infection and show a reduced proinflammatory response in the early phase of infection, indicating that MyD88 plays an important role in generating the proinflammatory responses to infection (84). pDCs might be one of the cell types responsible for these responses, since in these cells detection of positive stranded RNA by TLR7 leads to MyD88-mediated activation of antiviral and proinflammatory pathways

### **SARS-CoV infection leads to downregulated host gene expression in ferrets**

Ferrets are commonly used to study respiratory infections and increasingly more research tools are becoming available in order to study different aspects of disease in these animals. SARS-CoV readily infects ferrets, replicating in the lung with similar kinetics as in macaques and mice. In fact, SARS-CoV replication in ferrets was even more efficient than in mice and macaques. Not only were SARS-CoV mRNA levels in the lung 1-2 logs higher in ferrets, also the number of cells in the lung staining positive for SARS-CoV was higher in ferrets compared to mice and macaques, both on day 1 and day 4 after infection. In contrast to macaques and mice, in ferrets only type II pneumocytes, but not type I pneumocytes or bronchiolar epithelial cells, were SARS-CoV infected. In ferrets, type I pneumocytes do not express ACE2 on the cell surface, explaining the absence of viral antigen in this cell type (96). However, ACE2 is abundantly expressed on bronchiolar epithelial cells. Perhaps an unknown co-receptor, in addition to ACE2, is required to infect bronchiolar epithelial cells in ferrets. C-type lectins like DC-SIGN and CD209L are known to enhance SARS-CoV entry into target cells and a similar molecule required for SARS-CoV infection might not be available on ferret bronchiolar epithelial cells (49, 99). Alternatively, ferret bronchiolar epithelial cells could lack expression of specific proteases such as Cathepsin L and TMPRSS2 that are necessary for SARS-CoV infection, thus preventing infection of these cells (39, 46). Generally, SARS-CoV infected ferrets do not suffer from severe clinical symptoms. However, there is quite some variation in the disease severity induced by SARS-CoV infection in ferrets, ranging from asymptomatic disease to lethargy and even death in rare cases (22, 26, 96). Observed variations may be caused by different infection methods used, ferret strain differences and host factors such as age or underlying morbidities. In our study, as described in **chapter 7**, no severe clinical symptoms were observed in SARS-CoV infected ferrets. Macroscopically, SARS-CoV mediated pathology in ferrets was characterized by multifocal pulmonary consolidation, as described previously (96). Microscopically, multifocal mild to moderate diffuse alveolar damage was observed, with limited numbers of infiltrating inflammatory cells.

Just as in SARS-CoV infected macaques and mice, gene expression analysis was performed in order to get a broader view of the host responses to SARS-CoV infection in ferrets. Since no commercial microarray chip is available for ferrets, a canine microarray chip was used. Although ferret genes show a high

degree of homology with canine genes and canine chips have previously been used to study host responses in ferrets, the current lack of a commercial ferret specific microarray chip is a potential drawback of performing microarray studies in ferrets (15, 25, 29, 79). In order to reduce this problem, expression of several ferret genes was additionally analyzed using a ferret-specific RT-PCR in order to confirm microarray results. More than 500 genes were differentially expressed in SARS-CoV infected ferrets at day 4 after infection, as opposed to 295 genes in young macaques and 418 genes in young BALB/c mice at that time point after infection. Strikingly, in contrast to infection in macaques and mice where more genes were upregulated than downregulated after SARS-CoV infection, the majority of genes differentially expressed in ferrets were downregulated after infection. The small set of upregulated genes contained several genes commonly upregulated after SARS-CoV infection, like ISG15 and CXCL10, typically induced by IFNs, as well as CCL2 which can be induced by SARS-CoV directly (18). The presence of IFNs was confirmed by RT-PCR, revealing significant induction of type I IFNs in ferret lungs. Interestingly, the large set of downregulated genes in ferrets represented decreased activation of pathways involved in processes as extravasation signaling, chemokine signaling, integrin signaling, CCR3 signaling and aldosterone signaling, all indicative of limited inflammatory activity in these animals.

SARS-CoV infected young and aged macaques, as well as SARS-CoV infected BALB/c mice, all elicit a broad host immune response to SARS-CoV infection marked by activation of antiviral and proinflammatory pathways, although the intensity of this response varies between the different animal models. In contrast, in SARS-CoV infected ferrets almost no induction of inflammatory cytokines was detected upon infection. Both at day 1 and at day 4 after infection, the interferon inducible chemokine CXCL10 was induced, but induction of other proinflammatory cytokines commonly upregulated after SARS-CoV infection, like IL-1 $\beta$ , IL-6 and IL-8 was not detected. The characteristics of the host response to SARS-CoV infection in ferrets, induction of antiviral pathways, but not of proinflammatory pathways and massive downregulation of host genes, differ from the typical host response observed in SARS-CoV infected macaques and mice. These differences can not be linked to lower levels of SARS-CoV in the lung as viral loads in ferrets lungs seem to be even higher than those in macaques and mice. However, the different host response to SARS-CoV infection in ferrets did coincide with the observed variation in cell tropism between the animal models. While in ferrets the only cell type infected were the type II pneumocytes, in macaques both type I pneumocytes and bronchiolar epithelial cells were additionally SARS-CoV infected and in mice bronchiolar epithelial cells were SARS-CoV infected in addition to type II pneumocytes.

In this thesis we do not further examine the mechanism by which host gene transcription is downregulated in SARS-CoV infected ferrets, but one could hypothesize that the SARS-CoV NSP1 protein is (partly) responsible. This SARS-CoV protein has been reported to suppress host gene transcription *in vitro* after SARS-CoV infection (51, 62). It would be interesting to examine if infection of ferrets with SARS-CoV deficient for *nsp1* generates similar host gene downregulation as the wildtype virus. Also other CoVs like MHV are known to induce a host shut-off, marked by large-scale mRNA degradation (71). The fact that in SARS-CoV infected ferrets so many genes are downregulated, combined with high levels of virus, suggests that in this SARS model host responses detected with microarray analysis and RT-PCR might be a reflection of responses in the SARS-CoV infected cells, in contrast to the macaque and mouse SARS models, where host responses seem to be dominantly driven by gene expression in non-infected cells. In

addition, we hypothesize that pathology observed in SARS-CoV infected ferrets is mainly due to damage caused directly by the high number of infected cells. Contrarily, pathology in SARS-CoV infected macaques and mice seems to be mostly immune-mediated caused associated with elevated levels of inflammatory cytokines and chemokines. Species-related differences in host responses to SARS-CoV infection are further illustrated by differences in the efficacy of IFN treatment after SARS-CoV infection in macaques and ferrets. In contrast to the anti-inflammatory effect of IFN treatment in aged macaques, resulting in less severe pathology, when SARS-CoV infected ferrets were treated with IFN, no favorable effect on pathology was observed. The fact that proinflammatory host responses were not induced in SARS-CoV infected ferrets might explain this discrepancy, as the pathways on which IFN acts are not induced in these animals. Besides excessive induction of proinflammatory pathways also other pathogenic pathways might be involved in SARS pathogenesis. One of the more obvious ones would be the role of the renin angiotensin system (RAS), considering the role of ACE2 in SARS-CoV infection. Not only is ACE2 the cellular receptor for SARS-CoV, ACE2 is one of the key regulating enzymes in the RAS (11, 24). ACE2 has been shown to protect lungs from damage in mouse ALI models and activation of endogenous ACE2 prevents development of pulmonary hypertension in mice (30, 48). On the other hand, SARS-CoV has been shown to downregulate expression of ACE2 (53). Moreover, in **chapter 5** of this thesis we show that  $\text{INF-}\gamma$ , which is produced in the lungs during SARS-CoV infection, downregulates expression of ACE2 as well. ACE2 is not the only RAS component that plays a role in pulmonary pathology. While ACE2 has a protective role against lung damage, its counter-regulatory homologue ACE is involved in pathogenic processes in the lungs associated with ARDS. Involvement of components of the RAS in the development of ARDS might be linked to genetic factors. Already in the 1980s large variations in ACE plasma levels between individuals were described, which were later shown to be partly linked to an insertion/deletion polymorphism in the ACE gene (14, 74). More recently it was shown that this insertion/deletion polymorphism in ACE is associated with the ARDS susceptibility and disease outcome (50, 60). Several studies have shown that the RAS is activated in ARDS patients, illustrated by the fact that increased levels of activated ACE in the lungs are associated with more severe disease (47, 67).

The fact that the RAS is activated in ARDS and considering SARS-CoV interacts with ACE2 raised the question if members of the RAS could serve as therapeutics or therapeutical targets in SARS-CoV infection. We prophylactically and therapeutically treated SARS-CoV infected ferrets with a recombinant ACE2 protein in order to address this question. However, we did not observe a change in viral levels or pathology after SARS-CoV infection in ferrets that were treated with recombinant ACE2. The gene expression profile in SARS-CoV infected ferrets might explain why no treatment effect of recombinant ACE2 was observed, since most genes in ferrets were downregulated after SARS-CoV infection, including pathogenic proinflammatory pathways that would be affected by ACE2 treatment. In addition to the analysis of proinflammatory pathways, we examined if expression levels of genes directly involved in the RAS were significantly up- or downregulated in SARS-CoV infected ferrets, as this might provide more information about the RAS activation state and thus about the potential efficacy of ACE2 treatment. Within the set of genes that were selected, that contained genes like ACE2, ACE, the AT1 and AT2 receptors as well as many downstream genes involved in RAS signaling pathways, practically none of these genes were differentially expressed in ferrets. Remarkably, within this set ACE was the only gene significantly down-

regulated in ferrets. Analysis of the same set in SARS-CoV infected macaques and mice revealed that in aged macaques the largest number of genes within the set was activated compared to the other SARS models, although expression levels were very low. Downregulation of ACE2 expression was most obvious in SARS-CoV infected mice. Since gene expression levels of RAS genes were very low and many RAS components are activated at the peptide level as opposed to the gene expression level more research is needed to determine the RAS activation status in the different models.

Treatment with ACE2 might be more beneficial in a model where more pathogenic genes are upregulated after SARS-CoV infection like aged macaques or aged BALB/c mice. Also other drugs influencing the RAS, such as ACE and AT<sub>1</sub> receptor blockers that are currently used to treat hypertension, might be effective in preventing SARS-CoV induced pathology. Since many of these drugs are commonly used it would be interesting to examine, through a retrospective study in SARS patients, if usage of these drugs was correlated with less severe pathology during SARS-CoV infection as such a relation has been suggested for the prior outpatient use of an ACE inhibitor in subgroups of patients with pneumonia (72).

### **SARS pathogenesis revisited**

In this thesis we show that, although SARS-CoV replicates efficiently to high titers in the lungs of macaques, ferrets and mice, characteristics of the host response to SARS-CoV infection are different in each animal model. The differential activation of host responses in these different animal models resulted in multiple SARS phenotypes, dependent on host factors such as age, species and strain differences. In macaques and mice strong host responses are driven by uninfected cells, while in ferrets SARS-CoV infected cells may dominate the observed pathogenesis. The fact that SARS-CoV leads to a range of host dependent phenotypes has implications for development of SARS treatments and the use of SARS animal models.

Several aspects of SARS-CoV infection in the animal models described in this thesis indicate that SARS pathogenesis in macaques and mice is immune-mediated. In macaques and mice, SARS-CoV infection leads to a strong activation of proinflammatory and antiviral pathways as a consequence of a rapid increase of viral replication. Remarkably, viral replication is controlled quite rapidly thereafter. In macaques, activation of antiviral pathways is characterized by induced transcription of IFNs, ISGs as well as phosphorylation and nuclear translocation of STAT1 in alveolar cells. However, in SARS-CoV infected cells activation of STAT1 is inhibited, preventing JAK/STAT signaling in infected cells. In line with this, the transcription factor NF- $\kappa$ B, a key player in inflammation, was also primarily activated in uninfected cells. This suggests that the antiviral and proinflammatory host responses that dominate gene expression profiles in SARS-CoV infected macaques and mice are mainly driven by uninfected cells.

Reduced activation of antiviral and proinflammatory pathways in pDC depleted mice indicates that activation of pDCs by SARS-CoV is, at least partly responsible for the induction of antiviral genes and proinflammatory genes during SARS-CoV infection. Remarkably, inactivated SARS-CoV stimulated production of antiviral and proinflammatory cytokines in murine pDCs, in line with the immunopathological characteristic of SARS. The induction of antiviral and anti-inflammatory IFNs by pDCs during SARS-CoV infection may be needed to balance the proinflammatory responses that are elicited simultaneously. Thus, activation of pDCs and subsequent IFN production possibly prevents severe pathology, as might be the case

in young adult macaques and young mice. In aged individuals, the number of circulating pDCs as well as the amount of IFN produced by pDCs upon stimulation is decreased, which could explain the reduced IFN response in aged macaques and the effectiveness of IFN treatment in these animals (1, 87, 89, 91).

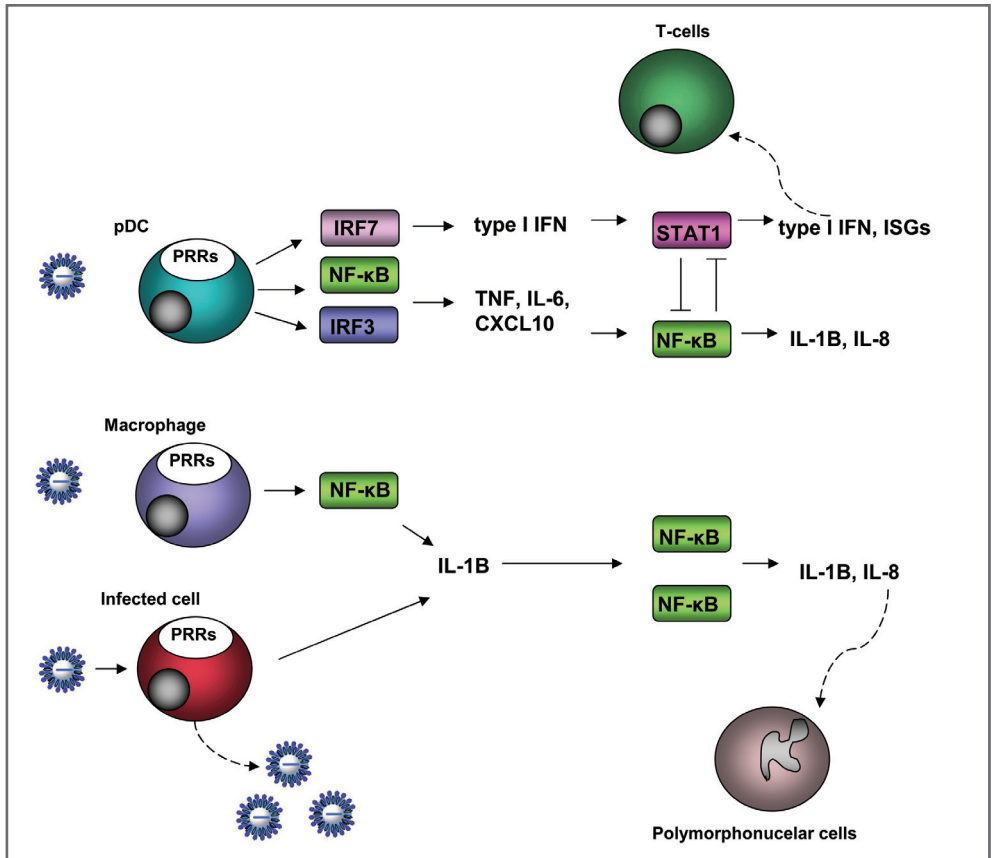


**Figure 8.1. Differential activation of antiviral and proinflammatory pathways by SARS-CoV.** Detection of SARS-CoV by PRRs can lead to activation of multiple pathways in the host cell, dependent on the type of PRR and the types of transcription factors involved. In pDCs, uninfected by SARS-CoV, activation of PRRs induces IRF6 mediated production of IFN- $\alpha$ , which subsequently activates JAK/STAT signaling in surrounding cells. In addition, T cells are recruited. On the other hand, activation of transcription factors like NF- $\kappa$ B and IRF3 in pDCs can lead to production of proinflammatory cytokines as TNF and IL-6. These cytokines activate NF- $\kappa$ B in neighboring cells as well, resulting in production of IL-1 $\beta$  and IL-8 and recruitment of polymorphonuclear cells, such as neutrophils. Also other uninfected cells, depicted here as macrophages, as well as subpopulations of SARS-CoV infected cells produce proinflammatory mediators upon activation of host PRRs, resulting in NF- $\kappa$ B activation neighboring cells. Differential activation of these pathways as well as cross-regulation between these pathways can lead to unbalanced induction of antiviral and proinflammatory host responses, thereby affecting pathology.



In contrast to SARS-CoV infected macaques and mice, only few genes were upregulated after SARS-CoV infection in ferrets while the majority of genes were downregulated. We hypothesize that the reduced transcription of host genes observed in SARS-CoV infected ferrets is a reflection of reduced gene transcription in SARS-CoV infected cells. Although cytokines and chemokines are not strongly induced upon SARS-CoV infection in ferrets and transcription of most genes is downregulated, mild to moderate pathology did develop in ferret lungs. Considering that a large number of cells are SARS-CoV positive in ferret lungs 4 days after infection, more than in macaques and mice at that time point, SARS-CoV mediated pathology in ferrets is possibly caused directly by damage from SARS-CoV infected cells. Given the fact that few proinflammatory pathways are activated in SARS-CoV infected ferrets and pathology remains relatively mild in ferrets, despite very efficient SARS-CoV replication in the lungs and upper respiratory tract, the pathogenesis of SARS-CoV in ferrets may resemble that of civet cats, an intermediate host that spread SARS-CoV. On the other hand disease characteristics in (aged) macaques, more closely resemble the end-stage host in which infection can lead to severe immune-mediated disease.

Differences in host responses and subsequent pathology in SARS-CoV infected macaques, mice and ferrets might be explained by distinct viral tropism. The absence of SARS-CoV replication in bronchiolar epithelial cells in ferrets suggests a proinflammatory role of these cells in macaques and mice. Host and cell type dependent variations in expression, regulation and activation of pathogen recognition receptors (PRRs) on target cells might influence host responses in SARS-CoV infected animals. Expression and activation of toll like receptors (TLRs), a family of PRRs, varies extensively between different cell types within an individual, between individuals of the same species and between different species (5, 37, 43, 58, 61, 66). Aging also influences TLR expression levels and host responses generated after TLR stimulation (83, 89). This is thought to be a major cause of the increased morbidity and mortality from infectious disease in the elderly (82). For instance, in pDCs derived from aged individuals increased oxidative stress was detected after TLR9 stimulation compared to pDCs derived from young individuals (89). Future studies may need to focus on variations in TLR expression levels and differential TLR responses upon stimulation with SARS-CoV particles and differences observed in SARS-CoV mediated host responses in different SARS animal models.

We have integrated our findings in a model that depicts the differential activation of antiviral and proinflammatory pathways by SARS-CoV in different host cells. Depending on expression and regulation of PRRs in the host cell different signaling cascades in the cell are activated upon detection of SARS-CoV leading to antiviral and proinflammatory responses in the host. The extent to which these pathways are activated as well as the balance between induction of antiviral and proinflammatory pathways is dependent on host factors and affects SARS pathogenesis (figure 8.1). The analysis of SARS-CoV infection and subsequent host responses in various SARS animal models lead us to conclude that SARS pathogenesis cannot be explained by one route of host factor regulation, but that several SARS phenotypes exist. Host factors such as species and strain differences, age and disease state influence activation of antiviral and proinflammatory pathways, especially in the non-infected cells. In human patients SARS pathogenesis is not identical in all infected individuals; SARS-CoV infection in children is mostly asymptomatic while mortality rates in older individuals are as high as 50% (28). Probably, several intermediate forms of SARS-CoV pathogenesis exist in humans as well, but remain unseen. Also in severe cases of SARS in hospitalized

patients it was concluded that observed pathology was not uniform in all patients (65). Similarly, recent investigations have revealed that multiple disease phenotypes of “one” disease may exist for other chronic inflammatory diseases like asthma, allergies and autoimmune disorders (73). Also these diseases are caused by a complex interaction between genes differentially regulated in each host resulting in a distinct disease phenotype in each individual. Genomics provides a useful tool to examine the differential activation of host responses, especially when combined with other read-outs. It should be kept in mind that induced expression of gene transcription not necessarily corresponds to induced levels of protein and subsequent phenotype. The fact that SARS pathogenesis is determined by individual host factors and not uniform, implies that intervention strategies in humans, but also animal models, should be adjusted accordingly. In this thesis we report that therapeutical treatment with pegylated recombinant IFN- $\alpha$  reduced SARS-CoV mediated disease in aged macaques without affecting viral levels, while IFN treatment did not reduce pathology in SARS-CoV infected ferrets. Differential activation of host responses upon infection can also influence effectiveness and side-effects of vaccinations. We found extensive infiltration of eosinophils in the lungs of SARS-CoV vaccinated and challenged macaques, possibly caused by the SARS-CoV induced production of the eosinophil attractant eotaxin in macaque lungs. However, in ferrets that were vaccinated and challenged in a similar way, no eosinophil infiltration was observed. Thus, differential host responses to infections can affect efficacy of treatment and vaccinations, which can also be of importance to other viral infections that cause immunopathology. Furthermore, rather than searching for one single effective pharmacological target, personalized treatment might be required to effectively treat SARS. Further identification of the range of phenotypes after SARS-CoV infection in humans and animal models and identifying putative molecular signaling cascades involved is of importance. Additional techniques to quickly determine the SARS phenotype in clinical settings would be useful to determine the most appropriate treatment.

## REFERENCES

1. **Abb, J., H. Abb, and F. Deinhardt.** 1984. Age-related decline of human interferon alpha and interferon gamma production. *Blut* **48**:285-289.
2. **Abreu, S. L.** 1982. Suppression of experimental allergic encephalomyelitis by interferon. *Immunol Commun* **11**:1-7.
3. **Alizadeh, A. A., M. B. Eisen, R. E. Davis, C. Ma, I. S. Lossos, A. Rosenwald, J. C. Boldrick, H. Sabet, T. Tran, X. Yu, J. I. Powell, L. Yang, G. E. Marti, T. Moore, J. Hudson, Jr., L. Lu, D. B. Lewis, R. Tibshirani, G. Sherlock, W. C. Chan, T. C. Greiner, D. D. Weisenburger, J. O. Armitage, R. Warnke, R. Levy, W. Wilson, M. R. Grever, J. C. Byrd, D. Botstein, P. O. Brown, and L. M. Staudt.** 2000. Distinct types of diffuse large B-cell lymphoma identified by gene expression profiling. *Nature* **403**:503-511.
4. **Anderson, A. E., M. L. Worku, W. Khamri, K. B. Bamford, M. M. Walker, and M. R. Thursz.** 2007. TLR9 polymorphisms determine murine lymphocyte responses to Helicobacter: results from a genome-wide scan. *Eur J Immunol* **37**:1548-1561.
5. **Ashton, K. A., A. Proietto, G. Otton, I. Symonds, M. McEvoy, J. Attia, and R. J. Scott.** 2010. Toll-like receptor (TLR) and nucleosome-binding oligomerization domain (NOD) gene polymorphisms and endometrial cancer risk. *BMC Cancer* **10**:382.
6. **Aw, D., A. B. Silva, and D. B. Palmer.** 2007. Immunosenescence: emerging challenges for an ageing population. *Immunology* **120**:435-446.
7. **Baas, T., A. Roberts, T. H. Teal, L. Vogel, J. Chen, T. M. Tumpey, M. G. Katze, and K. Subbarao.** 2008. Genomic analysis reveals age-dependent innate immune responses to severe acute respiratory syndrome coronavirus. *J Virol* **82**:9465-9476.
8. **Baechler, E. C., F. M. Batliwalla, G. Karypis, P. M. Gaffney, W. A. Ortmann, K. J. Espe, K. B. Shark, W. J. Grande, K. M. Hughes, V. Kapur, P. K. Gregersen, and T. W. Behrens.** 2003. Interferon-inducible gene expression signature in peripheral blood cells of patients with severe lupus. *Proc Natl Acad Sci U S A* **100**:2610-2615.
9. **Bennett, L., A. K. Palucka, E. Arce, V. Cantrell, J. Borvak, J. Banchereau, and V. Pascual.** 2003. Interferon and granulopoiesis signatures in systemic lupus erythematosus blood. *J Exp Med* **197**:711-723.
10. **Billiau, A.** 2006. Anti-inflammatory properties of Type I interferons. *Antiviral Res* **71**:108-116.
11. **Boehm, M., and E. G. Nabel.** 2002. Angiotensin-converting enzyme 2--a new cardiac regulator. *N Engl J Med* **347**:1795-1797.
12. **Bruunsgaard, H., M. Pedersen, and B. K. Pedersen.** 2001. Aging and proinflammatory cytokines. *Curr Opin Hematol* **8**:131-136.
13. **Buer, J., and R. Balling.** 2003. Mice, microbes and models of infection. *Nat Rev Genet* **4**:195-205.
14. **Cambian, F., F. Alhenc-Gelas, B. Herbeth, J. L. Andre, R. Rakotovo, M. F. Gonzales, J. Allegrini, and C. Bloch.** 1988. Familial resemblance of plasma angiotensin-converting enzyme level: the Nancy Study. *Am J Hum Genet* **43**:774-780.
15. **Cameron, C. M., M. J. Cameron, J. F. Bermejo-Martin, L. Ran, L. Xu, P. V. Turner, R. Ran, A. Danesh, Y. Fang, P. K. Chan, N. Mytle, T. J. Sullivan, T. L. Collins, M. G. Johnson, J. C. Medina, T. Rowe, and D. J. Kelvin.** 2008. Gene expression analysis of host innate immune responses during Lethal H5N1 infection in ferrets. *J Virol* **82**:11308-11317.
16. **Canaday, D. H., N. A. Amponsah, L. Jones, D. J. Tisch, T. R. Hornick, and L. Ramachandra.** 2010. Influenza-induced production of interferon-alpha is defective in geriatric individuals. *J Clin Immunol* **30**:373-383.
17. **Cervantes-Barragan, L., R. Züst, F. Weber, M. Spiegel, K. S. Lang, S. Akira, V. Thiel, and B. Ludewig.** 2007. Control of coronavirus infection through plasmacytoid dendritic-cell-derived type I interferon. *Blood* **109**:1131-1137.
18. **Chen, I. Y., S. C. Chang, H. Y. Wu, T. C. Yu, W. C. Wei, S. Lin, C. L. Chien, and M. F. Chang.** 2010. Upregulation of the chemokine (C-C motif) ligand 2 via a severe acute respiratory syndrome coronavirus spike-ACE2 signaling pathway. *J Virol* **84**:7703-7712.
19. **Chen, J., Y. F. Lau, E. W. Lamirande, C. D. Paddock, J. H. Bartlett, S. R. Zaki, and K. Subbarao.** 2010. Cellular immune responses to severe acute respiratory syndrome coronavirus (SARS-CoV) infection in senescent BALB/c mice: CD4+ T cells are important in control of SARS-CoV infection. *J Virol* **84**:1289-1301.
20. **Chen, P. C., and C. H. Hsiao.** 2004. Re: To KF, Tong JH, Chan PK, et al. Tissue and cellular tropism of the coronavirus associated with severe acute respiratory syndrome: an in-situ hybridization study of fatal cases. *J Pathol* 2004; **202**: 157-163. *J Pathol* **203**:729-730; author reply 730-721.
21. **Chow, K. C., C. H. Hsiao, T. Y. Lin, C. L. Chen, and S. H. Chiou.** 2004. Detection of severe acute respiratory syndrome-associated coronavirus in pneumocytes of the lung. *Am J Clin Pathol* **121**:574-580.
22. **Chu, Y. K., G. D. Ali, F. Jia, Q. Li, D. Kelvin, R. C. Couch, K. S. Harrod, J. A. Hutt, C. Cameron, S. R. Weiss, and C. B. Jonsson.** 2008. The SARS-CoV ferret model in an infection-challenge study. *Virology* **374**:151-163.

23. Chung, H. Y., B. Sung, K. J. Jung, Y. Zou, and B. P. Yu. 2006. The molecular inflammatory process in aging. *Antioxid Redox Signal* 8:572-581.
24. Crackower, M. A., R. Sarao, G. Y. Oudit, C. Yagil, I. Kozieradzki, S. E. Scanga, A. J. Oliveira-dos-Santos, J. da Costa, L. Zhang, Y. Pei, J. Scholey, C. M. Ferrario, A. S. Manoukian, M. C. Chappell, P. H. Backx, Y. Yagil, and J. M. Penninger. 2002. Angiotensin-converting enzyme 2 is an essential regulator of heart function. *Nature* 417:822-828.
25. Danesh, A., C. M. Cameron, A. J. Leon, L. Ran, L. Xu, Y. Fang, A. A. Kelvin, T. Rowe, H. Chen, Y. Guan, C. B. Jonsson, M. J. Cameron, and D. J. Kelvin. 2011. Early gene expression events in ferrets in response to SARS coronavirus infection versus direct interferon- $\alpha$ 2b stimulation. *Virology* 409:102-112.
26. Darnell, M. E., E. P. Plant, H. Watanabe, R. Byrum, M. St Claire, J. M. Ward, and D. R. Taylor. 2007. Severe acute respiratory syndrome coronavirus infection in vaccinated ferrets. *J Infect Dis* 196:1329-1338.
27. Deal, E. M., M. C. Jaimes, S. E. Crawford, M. K. Estes, and H. B. Greenberg. 2010. Rotavirus structural proteins and dsRNA are required for the human primary plasmacytoid dendritic cell IFN $\alpha$  response. *PLoS Pathog* 6:e1000931.
28. Donnelly, C. A., A. C. Ghani, G. M. Leung, A. J. Hedley, C. Fraser, S. Riley, L. J. Abu-Raddad, L. M. Ho, T. Q. Thach, P. Chau, K. P. Chan, T. H. Lam, L. Y. Tse, T. Tsang, S. H. Liu, J. H. Kong, E. M. Lau, N. M. Ferguson, and R. M. Anderson. 2003. Epidemiological determinants of spread of causal agent of severe acute respiratory syndrome in Hong Kong. *Lancet* 361:1761-1766.
29. Fang, Y., T. Rowe, A. J. Leon, D. Banner, A. Danesh, L. Xu, L. Ran, S. E. Bosinger, Y. Guan, H. Chen, C. C. Cameron, M. J. Cameron, and D. J. Kelvin. 2010. Molecular characterization of *in vivo* adjuvant activity in ferrets vaccinated against influenza virus. *J Virol* 84:8369-8388.
30. Ferreira, A. J., V. Shenoy, Y. Yamazato, S. Sriramula, J. Francis, L. Yuan, R. K. Castellano, D. A. Ostrov, S. P. Oh, M. J. Katovich, and M. K. Raizada. 2009. Evidence for angiotensin-converting enzyme 2 as a therapeutic target for the prevention of pulmonary hypertension. *Am J Respir Crit Care Med* 179:1048-1054.
31. Fouchier, R. A., T. Kuiken, M. Schutten, G. van Amerongen, G. J. van Doornum, B. G. van den Hoogen, M. Peiris, W. Lim, K. Stohr, and A. D. Osterhaus. 2003. Aetiology: Koch's postulates fulfilled for SARS virus. *Nature* 423:240.
32. Franceschi, C., M. Bonafe, S. Valensin, F. Olivieri, M. De Luca, E. Ottaviani, and G. De Benedictis. 2000. Inflamm-aging. An evolutionary perspective on immunosenescence. *Ann N Y Acad Sci* 908:244-254.
33. Frieman, M., M. Heise, and R. Baric. 2008. SARS coronavirus and innate immunity. *Virus Res* 133:101-112.
34. Frieman, M., K. Ratia, R. E. Johnston, A. D. Mesecar, and R. S. Baric. 2009. Severe acute respiratory syndrome coronavirus papain-like protease ubiquitin-like domain and catalytic domain regulate antagonism of IRF3 and NF-kappaB signaling. *J Virol* 83:6689-6705.
35. Frieman, M., B. Yount, M. Heise, S. A. Kopecky-Bromberg, P. Palese, and R. S. Baric. 2007. Severe acute respiratory syndrome coronavirus ORF6 antagonizes STAT1 function by sequestering nuclear import factors on the rough endoplasmic reticulum/Golgi membrane. *J Virol* 81:9812-9824.
36. Frieman, M. B., J. Chen, T. E. Morrison, A. Whitmore, W. Funkhouser, J. M. Ward, E. W. Lamirande, A. Roberts, M. Heise, K. Subbarao, and R. S. Baric. 2010. SARS-CoV pathogenesis is regulated by a STAT1 dependent but a type I, II and III interferon receptor independent mechanism. *PLoS Pathog* 6:e1000849.
37. Genc, M. R., S. Vardhana, M. L. Delaney, A. Onderdonk, R. Tuomala, E. Norwitz, and S. S. Witkin. 2004. Relationship between a toll-like receptor-4 gene polymorphism, bacterial vaginosis-related flora and vaginal cytokine responses in pregnant women. *Eur J Obstet Gynecol Reprod Biol* 116:152-156.
38. Glass, W. G., K. Subbarao, B. Murphy, and P. M. Murphy. 2004. Mechanisms of Host Defense following Severe Acute Respiratory Syndrome-Coronavirus (SARS-CoV) Pulmonary Infection of Mice. *J Immunol* 173:4030-4039.
39. Glowacka, I., S. Bertram, M. A. Muller, P. Allen, E. Soilleux, S. Pfeifferle, I. Steffen, T. S. Tsegay, Y. He, K. Gnirss, D. Niemeyer, H. Schneider, C. Drosten, and S. Pohlmann. 2011. Evidence that TMPRSS2 activates the severe acute respiratory syndrome coronavirus spike protein for membrane fusion and reduces viral control by the humoral immune response. *J Virol* 85:4122-4134.
40. Granata, F., A. Petraroli, E. Boilard, S. Bezzine, J. Bollinger, L. Del Vecchio, M. H. Gelb, G. Lambeau, G. Marone, and M. Triggiani. 2005. Activation of cytokine production by secreted phospholipase A2 in human lung macrophages expressing the M-type receptor. *J Immunol* 174:464-474.
41. Guo, B., E. Y. Chang, and G. Cheng. 2008. The type I IFN induction pathway constrains Th17-mediated autoimmune inflammation in mice. *J Clin Invest* 118:1680-1690.

42. Haagmans, B. L., T. Kuiken, B. E. Martina, R. A. Fouchier, G. F. Rimmelzwaan, G. van Amerongen, D. van Riel, T. de Jong, S. Itamura, K. H. Chan, M. Tashiro, and A. D. Osterhaus. 2004. Pegylated interferon-alpha protects type 1 pneumocytes against SARS coronavirus infection in macaques. *Nat Med* 10:290-293.
43. Heinz, S., V. Haehnel, M. Karaghiosoff, L. Schwarzfischer, M. Muller, S. W. Krause, and M. Rehli. 2003. Species-specific regulation of Toll-like receptor 3 genes in men and mice. *J Biol Chem* 278:21502-21509.
44. Hogan, R. J., G. Gao, T. Rowe, P. Bell, D. Flieder, J. Paragas, G. P. Kobinger, N. A. Wivel, R. G. Crystal, J. Boyer, H. Feldmann, T. G. Voss, and J. M. Wilson. 2004. Resolution of primary severe acute respiratory syndrome-associated coronavirus infection requires stat1. *J Virol* 78:11416-11421.
45. Hon, K. L., C. W. Leung, W. T. Cheng, P. K. Chan, W. C. Chu, Y. W. Kwan, A. M. Li, N. C. Fong, P. C. Ng, M. C. Chiu, C. K. Li, J. S. Tam, and T. F. Fok. 2003. Clinical presentations and outcome of severe acute respiratory syndrome in children. *Lancet* 361:1701-1703.
46. Huang, I. C., B. J. Bosch, F. Li, W. Li, K. H. Lee, S. Ghiran, N. Vasilieva, T. S. Dermody, S. C. Harrison, P. R. Dormitzer, M. Farzan, P. J. Rottier, and H. Choe. 2006. SARS coronavirus, but not human coronavirus NL63, utilizes cathepsin L to infect ACE2-expressing cells. *J Biol Chem* 281:3198-3203.
47. Idell, S., F. Kueppers, M. Lippmann, H. Rosen, M. Niederman, and A. Fein. 1987. Angiotensin converting enzyme in bronchoalveolar lavage in ARDS. *Chest* 91:52-56.
48. Imai, Y., K. Kuba, S. Rao, Y. Huan, F. Guo, B. Guan, P. Yang, R. Sarao, T. Wada, H. Leong-Poi, M. A. Crackower, A. Fukamizu, C. C. Hui, L. Hein, S. Uhlig, A. S. Slutsky, C. Jiang, and J. M. Penninger. 2005. Angiotensin-converting enzyme 2 protects from severe acute lung failure. *Nature* 436:112-116.
49. Jeffers, S. A., S. M. Tusell, L. Gillim-Ross, E. M. Hemmila, J. E. Achenbach, G. J. Babcock, W. D. Thomas, Jr., L. B. Thackray, M. D. Young, R. J. Mason, D. M. Ambrosino, D. E. Wentworth, J. C. Demartini, and K. V. Holmes. 2004. CD209L (L-SIGN) is a receptor for severe acute respiratory syndrome coronavirus. *Proc Natl Acad Sci U S A* 101:15748-15753.
50. Jerng, J. S., C. J. Yu, H. C. Wang, K. Y. Chen, S. L. Cheng, and P. C. Yang. 2006. Polymorphism of the angiotensin-converting enzyme gene affects the outcome of acute respiratory distress syndrome. *Crit Care Med* 34:1001-1006.
51. Kamitani, W., K. Narayanan, C. Huang, K. Lokugamage, T. Ikegami, N. Ito, H. Kubo, and S. Makino. 2006. Severe acute respiratory syndrome coronavirus nsp1 protein suppresses host gene expression by promoting host mRNA degradation. *Proc Natl Acad Sci U S A* 103:12885-12890.
52. Kopecky-Bromberg, S. A., L. Martinez-Sobrido, M. Frieman, R. A. Baric, and P. Palese. 2007. Severe acute respiratory syndrome coronavirus open reading frame (ORF) 3b, ORF 6, and nucleocapsid proteins function as interferon antagonists. *J Virol* 81:548-557.
53. Kuba, K., Y. Imai, S. Rao, H. Gao, F. Guo, B. Guan, Y. Huan, P. Yang, Y. Zhang, W. Deng, L. Bao, B. Zhang, G. Liu, Z. Wang, M. Chappell, Y. Liu, D. Zheng, A. Leibbrandt, T. Wada, A. S. Slutsky, D. Liu, C. Qin, C. Jiang, and J. M. Penninger. 2005. A crucial role of angiotensin converting enzyme 2 (ACE2) in SARS coronavirus-induced lung injury. *Nat Med* 11:875-879.
54. Kumagai, Y., O. Takeuchi, H. Kato, H. Kumar, K. Matsui, E. Morii, K. Aozasa, T. Kawai, and S. Akira. 2007. Alveolar macrophages are the primary interferon-alpha producer in pulmonary infection with RNA viruses. *Immunity* 27:240-252.
55. Li, G., X. Chen, and A. Xu. 2003. Profile of specific antibodies to the SARS-associated coronavirus. *N Engl J Med* 349:508-509.
56. Li, L., J. Wo, J. Shao, H. Zhu, N. Wu, M. Li, H. Yao, M. Hu, and R. H. Dennin. 2003. SARS-coronavirus replicates in mononuclear cells of peripheral blood (PBMCs) from SARS patients. *J Clin Virol* 28:239-244.
57. Liang, W., Z. Zhu, J. Guo, Z. Liu, W. Zhou, D. P. Chin, and A. Schuchat. 2004. Severe acute respiratory syndrome, Beijing, 2003. *Emerg Infect Dis* 10:25-31.
58. Liu, T., T. Matsuguchi, N. Tsuboi, T. Yajima, and Y. Yoshikai. 2002. Differences in expression of toll-like receptors and their reactivities in dendritic cells in BALB/c and C57BL/6 mice. *Infect Immun* 70:6638-6645.
59. Manuse, M. J., C. M. Briggs, and G. D. Parks. 2010. Replication-independent activation of human plasmacytoid dendritic cells by the paramyxovirus SV5 Requires TLR7 and autophagy pathways. *Virology* 405:383-389.
60. Marshall, R. P., S. Webb, G. J. Belligan, H. E. Montgomery, B. Chaudhari, R. J. McAnulty, S. E. Humphries, M. R. Hill, and G. J. Laurent. 2002. Angiotensin converting enzyme insertion/deletion polymorphism is associated with susceptibility and outcome in acute respiratory distress syndrome. *Am J Respir Crit Care Med* 166:646-650.
61. Muzio, M., D. Bosisio, N. Polentarutti, G. D'Amico, A. Stoppacciaro, R. Mancinelli, C. van't Veer, G. Penton-Rol, L. P. Ruco, P. Allavena, and A. Mantovani. 2000. Differential expression and regulation of toll-like receptors (TLR) in human leukocytes: selective expression of TLR3 in dendritic cells. *J Immunol* 164:5998-6004.

62. Narayanan, K., C. Huang, K. Lokugamage, W. Kamitani, T. Ikegami, C. T. Tseng, and S. Makino. 2008. Severe acute respiratory syndrome coronavirus nsp1 suppresses host gene expression, including that of type I interferon, in infected cells. *J Virol* **82**:4471-4479.
63. Ng, E. K., D. S. Hui, K. C. Chan, E. C. Hung, R. W. Chiu, N. Lee, A. Wu, S. S. Chim, Y. K. Tong, J. J. Sung, J. S. Tam, and Y. M. Lo. 2003. Quantitative analysis and prognostic implication of SARS coronavirus RNA in the plasma and serum of patients with severe acute respiratory syndrome. *Clin Chem* **49**:1976-1980.
64. Nicholls, J. M., J. Butany, L. L. Poon, K. H. Chan, S. L. Beh, S. Poutanen, J. S. Peiris, and M. Wong. 2006. Time Course and Cellular Localization of SARS-CoV Nucleoprotein and RNA in Lungs from Fatal Cases of SARS. *PLoS Med* **3**:e27.
65. Nicholls, J. M., L. L. Poon, K. C. Lee, W. F. Ng, S. T. Lai, C. Y. Leung, C. M. Chu, P. K. Hui, K. L. Mak, W. Lim, K. W. Yan, K. H. Chan, N. C. Tsang, Y. Guan, K. Y. Yuen, and J. S. Peiris. 2003. Lung pathology of fatal severe acute respiratory syndrome. *Lancet* **361**:1773-1778.
66. O'Mahony, D. S., U. Pham, R. Iyer, T. R. Hawn, and W. C. Liles. 2008. Differential constitutive and cytokine-modulated expression of human Toll-like receptors in primary neutrophils, monocytes, and macrophages. *Int J Med Sci* **5**:1-8.
67. Orfanos, S. E., A. Armaganidis, C. Glynos, E. Psevdi, P. Kaltsas, P. Sarafidou, J. D. Catravas, U. G. Dafni, D. Langleben, and C. Roussos. 2000. Pulmonary capillary endothelium-bound angiotensin-converting enzyme activity in acute lung injury. *Circulation* **102**:2011-2018.
68. Packiam, M., S. J. Veit, D. J. Anderson, R. R. Ingalls, and A. E. Jerse. 2010. Mouse strain-dependent differences in susceptibility to *Neisseria gonorrhoeae* infection and induction of innate immune responses. *Infect Immun* **78**:433-440.
69. Peiris, J. S., C. M. Chu, V. C. Cheng, K. S. Chan, I. F. Hung, L. L. Poon, K. I. Law, B. S. Tang, T. Y. Hon, C. S. Chan, K. H. Chan, J. S. Ng, B. J. Zheng, W. L. Ng, R. W. Lai, Y. Guan, and K. Y. Yuen. 2003. Clinical progression and viral load in a community outbreak of coronavirus-associated SARS pneumonia: a prospective study. *Lancet* **361**:1767-1772.
70. Prinz, M., H. Schmidt, A. Mildner, K. P. Knobloch, U. K. Hanisch, J. Raasch, D. Merkler, C. Detje, I. Gutcher, J. Mages, R. Lang, R. Martin, R. Gold, B. Becher, W. Bruck, and U. Kalinke. 2008. Distinct and nonredundant *in vivo* functions of IFNAR on myeloid cells limit autoimmunity in the central nervous system. *Immunity* **28**:675-686.
71. Raaben, M., M. J. Groot Koerkamp, P. J. Rottier, and C. A. de Haan. 2007. Mouse hepatitis coronavirus replication induces host translational shutoff and mRNA decay, with concomitant formation of stress granules and processing bodies. *Cell Microbiol* **9**:2218-2229.
72. Rafailidis, P. I., D. K. Matthaiou, I. Varbobitis, and M. E. Falagas. 2008. Use of ACE inhibitors and risk of community-acquired pneumonia: a review. *Eur J Clin Pharmacol* **64**:565-573.
73. Renz, H., E. von Mutius, P. Brandtzaeg, W. O. Cookson, I. B. Autenrieth, and D. Haller. 2011. Gene-environment interactions in chronic inflammatory disease. *Nat Immunol* **12**:273-277.
74. Rigat, B., C. Hubert, F. Alhenc-Gelas, F. Cambien, P. Corvol, and F. Soubrier. 1990. An insertion/deletion polymorphism in the angiotensin I-converting enzyme gene accounting for half the variance of serum enzyme levels. *J Clin Invest* **86**:1343-1346.
75. Rink, L., I. Cakman, and H. Kirchner. 1998. Altered cytokine production in the elderly. *Mech Ageing Dev* **102**:199-209.
76. Rockx, B., T. Baas, G. A. Zornetzer, B. Haagmans, T. Sheahan, M. Frieman, M. D. Dyer, T. H. Teal, S. Proll, J. van den Brand, R. Baric, and M. G. Katze. 2009. Early upregulation of acute respiratory distress syndrome-associated cytokines promotes lethal disease in an aged-mouse model of severe acute respiratory syndrome coronavirus infection. *J Virol* **83**:7062-7074.
77. Rodriguez-Martinez, S., M. E. Cancino-Diaz, L. Jimenez-Zamudio, E. Garcia-Latorre, and J. C. Cancino-Diaz. 2005. TLRs and NODs mRNA expression pattern in healthy mouse eye. *Br J Ophthalmol* **89**:904-910.
78. Roth-Cross, J. K., L. Martinez-Sobrido, E. P. Scott, A. Garcia-Sastre, and S. R. Weiss. 2007. Inhibition of the alpha/beta interferon response by mouse hepatitis virus at multiple levels. *J Virol* **81**:7189-7199.
79. Rowe, T., A. J. Leon, C. J. Crevar, D. M. Carter, L. Xu, L. Ran, Y. Fang, C. M. Cameron, M. J. Cameron, D. Banner, D. C. Ng, R. Ran, H. K. Weirback, C. A. Wiley, D. J. Kelvin, and T. M. Ross. 2010. Modeling host responses in ferrets during A/California/07/2009 influenza infection. *Virology* **401**:257-265.
80. Rubins, K. H., L. E. Hensley, P. B. Jahrling, A. R. Whitney, T. W. Geisbert, J. W. Huggins, A. Owen, J. W. Leduc, P. O. Brown, and D. A. Relman. 2004. The host response to smallpox: analysis of the gene expression program in peripheral blood cells in a nonhuman primate model. *Proc Natl Acad Sci U S A* **101**:15190-15195.
81. Rutkute, K., R. H. Asmis, and M. N. Nikolova-Karakashian. 2007. Regulation of neutral sphingomyelinase-2 by GSH: a new insight to the role of oxidative stress in aging-associated inflammation. *J Lipid Res* **48**:2443-2452.

82. Shaw, A. C., S. Joshi, H. Greenwood, A. Panda, and J. M. Lord. 2010. Aging of the innate immune system. *Curr Opin Immunol* 22:507-513.
83. Shaw, A. C., A. Panda, S. R. Joshi, F. Qian, H. G. Allore, and R. R. Montgomery. 2011. Dysregulation of human Toll-like receptor function in aging. *Ageing Res Rev* 10:346-353.
84. Sheahan, T., T. E. Morrison, W. Funkhouser, S. Uematsu, S. Akira, R. S. Baric, and M. T. Heise. 2008. MyD88 is required for protection from lethal infection with a mouse-adapted SARS-CoV. *PLoS Pathog* 4:e1000240.
85. Shieh, W. J., C. H. Hsiao, C. D. Paddock, J. Guarner, C. S. Goldsmith, K. Tatti, M. Packard, L. Mueller, M. Z. Wu, P. Rollin, I. J. Su, and S. R. Zaki. 2005. Immunohistochemical, in situ hybridization, and ultrastructural localization of SARS-associated coronavirus in lung of a fatal case of severe acute respiratory syndrome in Taiwan. *Hum Pathol* 36:303-309.
86. Shiozawa, S., Y. Tanaka, I. Morimoto, A. Miyauchi, T. Yamatani, and T. Fujita. 1989. Radioimmunoassay of circulating alpha-interferon with reference to aging and osteoporosis. *Gerontology* 35:305-310.
87. Shodell, M., and F. P. Siegal. 2002. Circulating, interferon-producing plasmacytoid dendritic cells decline during human ageing. *Scand J Immunol* 56:518-521.
88. Srivastava, B., P. Blazejewska, M. Hessmann, D. Bruder, R. Geffers, S. Mauel, A. D. Gruber, and K. Schughart. 2009. Host genetic background strongly influences the response to influenza A virus infections. *PLoS One* 4:e4857.
89. Stout-Delgado, H. W., X. Yang, W. E. Walker, B. M. Tesar, and D. R. Goldstein. 2008. Aging impairs IFN regulatory factor 7 upregulation in plasmacytoid dendritic cells during TLR9 activation. *J Immunol* 181:6747-6756.
90. Sumaria, N., S. L. van Dommelen, C. E. Andoniou, M. J. Smyth, A. A. Scalzo, and M. A. Degli-Esposti. 2009. The roles of interferon-gamma and perforin in antiviral immunity in mice that differ in genetically determined NK-cell-mediated antiviral activity. *Immunol Cell Biol* 87:559-566.
91. Teig, N., D. Moses, S. Gieseler, and U. Schauer. 2002. Age-related changes in human blood dendritic cell subpopulations. *Scand J Immunol* 55:453-457.
92. Teleshova, N., J. Kenney, J. Jones, J. Marshall, G. Van Nest, J. Dufour, R. Bohm, J. D. Lifson, A. Gettie, and M. Pope. 2004. CpG-C immunostimulatory oligodeoxyribonucleotide activation of plasmacytoid dendritic cells in rhesus macaques to augment the activation of IFN-gamma-secreting simian immunodeficiency virus-specific T cells. *J Immunol* 173:1647-1657.
93. To, K. F., J. H. Tong, P. K. Chan, F. W. Au, S. S. Chim, K. C. Chan, J. L. Cheung, E. Y. Liu, G. M. Tse, A. W. Lo, Y. M. Lo, and H. K. Ng. 2004. Tissue and cellular tropism of the coronavirus associated with severe acute respiratory syndrome: an in-situ hybridization study of fatal cases. *J Pathol* 202:157-163.
94. Triggiani, M., F. Granata, A. Oriente, M. Gentile, A. Petraroli, B. Balestrieri, and G. Marone. 2002. Secretory phospholipases A2 induce cytokine release from blood and synovial fluid monocytes. *Eur J Immunol* 32:67-76.
95. van de Vijver, M. J., Y. D. He, L. J. van't Veer, H. Dai, A. A. Hart, D. W. Voskuil, G. J. Schreiber, J. L. Peterse, C. Roberts, M. J. Marton, M. Parrish, D. Atsma, A. Witteveen, A. Glas, L. Delahaye, T. van der Velde, H. Bartelink, S. Rodenhuis, E. T. Rutgers, S. H. Friend, and R. Bernards. 2002. A gene-expression signature as a predictor of survival in breast cancer. *N Engl J Med* 347:1999-2009.
96. van den Brand, J. M., B. L. Haagmans, L. Leijten, D. van Riel, B. E. Martina, A. D. Osterhaus, and T. Kuiken. 2008. Pathology of experimental SARS coronavirus infection in cats and ferrets. *Vet Pathol* 45:551-562.
97. van Holten, J., K. Reedquist, P. Sattone-Roche, T. J. Smeets, C. Plater-Zyberk, M. J. Vervoordeldonk, and P. P. Tak. 2004. Treatment with recombinant interferon-beta reduces inflammation and slows cartilage destruction in the collagen-induced arthritis model of rheumatoid arthritis. *Arthritis Res Ther* 6:R239-249.
98. Weinberg, J. B., M. L. Lutzke, R. Alfinito, and R. Rochford. 2004. Mouse strain differences in the chemokine response to acute lung infection with a murine gammaherpesvirus. *Viral Immunol* 17:69-77.
99. Yang, Z. Y., Y. Huang, L. Ganesh, K. Leung, W. P. Kong, O. Schwartz, K. Subbarao, and G. J. Nabel. 2004. pH-dependent entry of severe acute respiratory syndrome coronavirus is mediated by the spike glycoprotein and enhanced by dendritic cell transfer through DC-SIGN. *J Virol* 78:5642-5650.
100. Yoshikawa, T., T. E. Hill, N. Yoshikawa, V. L. Popov, C. L. Galindo, H. R. Garner, C. J. Peters, and C. T. Tseng. 2010. Dynamic innate immune responses of human bronchial epithelial cells to severe acute respiratory syndrome-associated coronavirus infection. *PLoS One* 5:e8729.
101. Zhao, J., N. Van Rooijen, and S. Perlman. 2009. Evasion by stealth: inefficient immune activation underlies poor T cell response and severe disease in SARS-CoV-infected mice. *PLoS Pathog* 5:e1000636.





# Nederlandse samenvatting

De uitbraak van de ziekte SARS aan eind 2002/begin 2003 had wereldwijd een enorme impact. In razend tempo verspreidde de ziekte zich vanuit China naar andere landen in Azië, Europa en Noord-Amerika. Uiteindelijk werden ruim 8000 mensen ziek, waarvan ongeveer 10% is overleden. Al heel snel na de uitbraak van SARS werd een coronavirus (CoV) geïdentificeerd als de veroorzaker van deze ziekte. CoVs infecteren naast de mens een groot aantal verschillende zoogdieren en vogels en transmissie van CoVs vindt voornamelijk plaats via respiratoire aerosolen of via de fecale-orale route. De meeste CoVs veroorzaken in de mens slechts relatief milde klachten zoals verkoudheid. Echter, infectie met SARS-CoV kan leiden tot zeer ernstige ziekte die gekenmerkt wordt door de ontwikkeling van een progressieve longontsteking die gepaard gaat met schade aan de longen. Dit kan resulteren in het ontstaan van het Acuut Respiratoir Distress Syndroom (ARDS). Bij ARDS faalt de longfunctie door de aanwezigheid van vocht in de longen waardoor de ademhaling wordt belemmerd. ARDS is moeilijk te behandelen met medicijnen en de mortaliteit geassocieerd met ARDS is dan ook erg hoog. Karakteristiek voor de ontwikkeling van ARDS is een overvloedige productie van verschillende proinflammatoire cytokinen en chemokinen die gepaard gaat met massale migratie van cellen van het immuunsysteem, waaronder neutrofielen en macrofagen, vanuit het bloed naar de longen. De aanwezigheid van veel van deze cytokinen en chemokinen is ook aangetoond in SARS patiënten met ARDS en wordt vaak geassocieerd met een ernstig ziekteverloop.

De immunrespons van het lichaam tegen binnendringende virussen bestaat uit een aspecifieke (aangeboren) respons en een specifieke (adaptieve) respons. De aspecifieke respons wordt gekenmerkt door de zeer snelle productie van een scala aan cytokinen en chemokinen, waaronder interferonen. Deze interferonen, maar ook andere cytokinen en chemokinen worden geproduceerd nadat Toll-like receptoren van de gastheer cel in contact komen met een virusdeeltje. Verschillende factoren, zoals het betrokken celtype, het subtype Toll-like receptor maar ook het soort pathogeen, bepalen welke cytokinen en chemokinen uiteindelijk geproduceerd worden door de gastheer cel. In het menselijk lichaam komen verschillende soorten interferonen voor, elk met hun eigen specifieke taken. Deze interferonen spelen een belangrijke rol het controleren en opruimen van infecties doordat zij op meerdere manieren kunnen interfereren met de virale replicatie in de gastheer cel. Veel virussen zijn in staat de antivirale mechanismen van de gastheer te ontlopen doordat zij bijvoorbeeld de productie en werking van interferonen blokkeren of verminderen. Zo zijn er ook verschillende SARS-CoV eiwitten bekend die de productie van interferon en de signaaltransductie van interferon via de JAK/STAT route inhiberen. Een van de weinige celtypen waarvan bekend is dat zij wel in staat is om interferonen te produceren na contact met SARS-CoV zijn de humane plasmacytoïde dendritische cellen (pDCs). Dit komt doordat zij een unieke methode gebruiken om interferon te produceren waar de SARS-CoV eiwitten geen invloed op hebben.

Algemeen wordt aangenomen dat de ziekte SARS wordt veroorzaakt door een disproportionele immunrespons van de gastheer. Aangezien een adequate respons van het immuunsysteem natuurlijk noodzakelijk is om de SARS-CoV infectie te klaren, is het nog niet duidelijk welke omstandigheden ervoor zorgen dat een normale immunrespons doorslaat naar een ongepaste immunrespons, en of dit uiteindelijk leidt tot het ziektebeeld horend bij SARS. SARS-CoV infectie is bestudeerd in een groot aantal

celtypen *in vitro*, maar er is nog niet zoveel bekend over SARS pathogenese *in vivo*, welke celtypen daarbij betrokken zijn en welke gastheer factoren hier invloed op hebben. In tegenstelling tot SARS-CoV infectie in de mens, is SARS in dieren zelden dodelijk en infectie met SARS-CoV resulteert over het algemeen in zeer beperkte klinische verschijnselen. Echter, het feit dat SARS-CoV wel goed in staat is om cellen in de longen van verschillende diersoorten te infecteren en zich daar te vermenigvuldigen, biedt kansen om de verscheiden aspecten van de gastheer respons op SARS-CoV infectie in verschillende diersoorten in kaart te brengen. In dit proefschrift wordt de SARS pathogenese bestudeerd in makaken, muizen en fretten door gebruik te maken van een combinatie van technieken die verscheidene parameters van infectie bepalen, zoals de hoeveelheid virus in de longen, de celtypen die geïnfecteerd worden, de mate van schade aan de longen. Additioneel is de gastheer respons na infectie bestudeerd met behulp van “genomics”, een techniek die de mate van expressie, en dus activiteit, van gastheer genen in kaart brengt.

In **hoofdstuk 2** wordt het verloop van SARS-CoV infectie in jong volwassen makaken beschreven. Deze makaken worden niet ziek na infectie met SARS-CoV, alhoewel het virus tot hoge titers replicateert in de longen van deze dieren. Wanneer stukjes van de longen van de SARS-CoV geïnfecteerde makaken worden bestudeerd met de microscoop blijkt dat SARS-CoV infectie wel degelijk leidt tot (milde) schade in de longen met karakteristieken vergelijkbaar met de schade die SARS-CoV in humane long veroorzaakt. Echter de schade in de longen van jong volwassen makaken herstelt vanzelf en is niet in de gehele long aanwezig. Analyse van genexpressie in deze longen laat zien dat er een sterke aspecifieke (aangeboren) gastheer respons op gang komt na SARS-CoV infectie, gekenmerkt door verhoogde expressie van verscheidene typen interferon, zowel als de verhoogde expressie van interferon gestimuleerde genen. Dit laat zien dat de interferonen *in vivo* wel degelijk geproduceerd worden na infectie met SARS-CoV, mogelijk door de makaak pDCs, ondanks de vele mechanismen van het virus om interferon productie tegen te houden. Naast toegenomen expressie van antivirale interferonen, is ook de expressie van een scala van proinflammatoire cytokinen en chemokinen zoals interleukine (IL)-6, IL-8 en CXCL10 verhoogd in SARS-CoV geïnfecteerde makaken. Opvallend is dat de gastheer respons op gen expressie niveau voornamelijk gestuurd lijkt te worden door cellen die niet SARS-CoV geïnfecteerd zijn; interferon signaal transductie via STAT1, resulterend in verhoogde expressie van interferon gestimuleerde genen, was alleen zichtbaar in de niet-geïnfecteerde cellen.

In **hoofdstuk 3** worden de gastheer responsen in de longen van SARS-CoV geïnfecteerde makaken vergeleken met de gastheer respons in het bloed van dezelfde makaken met behulp van genomics. Ook al werd er, in tegenstelling tot de longen, geen viraal RNA gevonden in het bloed, waren er verschillende antivirale en proinflammatoire processen geactiveerd in bloedcellen. De meeste genen die verhoogd tot expressie kwamen in het bloed zijn betrokken bij het herkennen van binnendringende pathogenen en daarop volgende processen als interferon signaal transductie. Echter, er werd geen toename gevonden in de expressie van de interferon genen zelf, dus de geobserveerde activatie van interferon signaal transductie wordt waarschijnlijk veroorzaakt door interferonen die in de longen worden geproduceerd en vervolgens in het bloed terecht komen. Hoewel er relatief weinig overlap is tussen de genen geactiveerd in het bloed en de genen geactiveerd in de longen na SARS-CoV infectie, laat de analyse van de gastheer respons in het bloed na SARS-CoV infectie zien dat bloedcellen wel als bio-indicatoren zouden kunnen fungeren en een afspiegeling vormen van de vroege responsen in de long.

Celtypen verantwoordelijk voor de productie van interferonen na SARS-CoV infectie en de rol van interferonen tijdens SARS pathogenese worden verder beschreven in **hoofdstuk 4**. Infectie van BALB/c muizen met SARS-CoV leidt, net als in de makaak, tot verhoogde gen expressie van verschillen typen interferon, interferon gestimuleerde genen en een groot aantal proinflammatoire cytokinen en chemokinen. Expressie van veel van deze genen wordt ook geïnduceerd door zowel levend SARS-CoV als geïnactiveerd SARS-CoV in muizen pDCs *in vitro*, zonder dat deze cellen geïnfecteerd worden door het virus. Hoewel slechts beperkte hoeveelheden cytokine en chemokine eiwit worden uitgescheiden door deze pDCs, leidt depletie van pDCs in jonge BALB/c muizen niet alleen tot een daling van zowel de expressie van een groot aantal proinflammatoire cytokinen en chemokinen maar ook tot een afgenomen expressie van interferonen en andere antivirale genen, gepaard met hogere virus titers in de long. Dit laat zien dat pDCs een belangrijke rol spelen in de totstandkoming van zowel de proinflammatoire als de antivirale gastheer respons. In tegenstelling tot jonge BALB/c muizen overleven oude BALB/c muizen infectie met SARS-CoV niet wanneer de pDCs gedepleteerd zijn. Dit suggereert dat een juiste activatie van pDCs met ene goede balans in de inductie van zowel antivirale als proinflammatoire genen belangrijk is om infectie met SARS-CoV te overwinnen. Conditie waarin pDCs niet goed functioneren of in mindere mate aanwezig zijn zouden de pathogenese van SARS ten nadele kunnen beïnvloeden.

Een van de mogelijke antivirale processen die wordt geïnduceerd door cytokinen zoals interferon- $\gamma$  wordt verder beschreven in **hoofdstuk 5**. Hier laten we zien dat, *in vitro*, interferon- $\gamma$  cellen minder toegankelijk maakt voor infectie met SARS-CoV door de expressie van de SARS-CoV receptor ACE2 op het oppervlak van de gastheer cel te verlagen. Niet alleen de expressie van het ACE2 eiwit gaat omlaag na behandeling met interferon- $\gamma$ , ook de transcriptie van ACE2 op mRNA niveau is lager na behandeling met dit type interferon. Het verlagen van de expressie van de SARS-CoV receptor door cytokinen, resulterend in een verminderde infectiviteit van SARS-CoV in deze cellen, is een van de manieren waarop cytokinen een antivirale werking kunnen hebben.

In de **hoofdstukken 6 en 7** ligt de focus op de proinflammatoire processen die worden geïnduceerd na infectie met SARS-CoV. In **hoofdstuk 6** laten we zien dat SARS-CoV infectie in oude makaken leidt tot ernstigere ziekteverschijnselen dan SARS-CoV infectie in jong volwassen makaken, net als in de humane situatie. Infectie met SARS-CoV veroorzaakt in oude makaken meer klinische verschijnselen dan in jonge makaken en een aanzienlijk groter deel van de longen is aangetast in deze dieren. De laesies die ontstaan in de longen van oude makaken na infectie lijken veel op de laesies die zijn waargenomen in humane SARS patiënten. Aangezien de hoeveelheid virus in de longen van jonge en oude makaken gelijk is, kunnen deze verschillen niet verklaard door een verschil in virale replicatie. Een analyse van de genexpressie in de longen van oude makaken laat zien dat een breed scala van proinflammatoire genen verhoogd tot expressie komt na infectie met SARS-CoV, veel meer dan in jonge makaken. Echter, expressie van interferonen is in de oude makaken niet verhoogd, in tegenstelling tot de verhoogde interferon expressie in jonge makaken na infectie met SARS-CoV. Wanneer interferon wordt toegediend aan oude makaken direct na infectie, ontstaat geen longschade en is de expressie van proinflammatoire genen sterk gereduceerd, zonder dat de hoeveelheid virus in de longen verandert. Dit laat zien dat interferon in SARS een anti-inflammatoire werking heeft en een geschikte behandeling zou kunnen zijn voor virus geïnduceerde longschade.

Er zijn verschillende pathogene processen die kunnen bijdragen aan de ernst van SARS. Niet alleen overvloedige productie van proinflammatoire cytokinen en chemokinen na SARS-CoV infectie kan de pathogenese van SARS beïnvloeden, ook de receptor die SARS-CoV gebruikt om gastheer cellen te binden en te infecteren, ACE2, zou een rol kunnen spelen in de SARS pathogenese. ACE2 is naast de receptor voor SARS-CoV namelijk vooral bekend als een enzym dat deel uit maakt van het renine angiotensine systeem (RAS). Dit systeem van peptiden en hormonen coördineert een aantal belangrijke processen in het lichaam, waaronder de regulatie van bloeddruk. De acties van het enzym ACE2 beschermen tegen negatieve verschijnselen als hoge bloeddruk en vasoconstrictie die gestuurd worden door de acties van de ACE2 homoloog, ACE. Er is bovendien in verschillende modellen aangetoond dat de acties van ACE2 beschermen tegen longschade. Opmerkelijk is dat SARS-CoV de expressie van ACE2 op het oppervlak van de gastheercel verlaagt, wat zou kunnen bijdragen aan de schade in de longen veroorzaakt door infectie met SARS-CoV. In **hoofdstuk 7** worden twee mogelijke behandelingen voor SARS geëvalueerd in fretten. Ten eerste worden SARS-CoV geïnfecteerde fretten behandeld met interferon, wat effectief is gebleken in oude makaken. Ten tweede, worden SARS-CoV geïnfecteerde fretten behandeld met een recombinant ACE2 eiwit, waarvan in muizen is beschreven dat het beschermt tegen longschade. Opvallend genoeg waren geen van beide behandelingen effectief in SARS-CoV geïnfecteerde fretten. Een analyse van de genexpressie in fretten na SARS-CoV infectie laat zien dat veel van de proinflammatoire cytokinen en chemokinen die in makaken en muizen geactiveerd zijn, niet zijn geactiveerd in geïnfecteerde fretten, ondanks het feit dat veel virus aanwezig is in de longen en er ook (milde) longschade ontstaat na infectie met SARS-CoV. Sterker nog, de expressie van de meeste genen in de longen van SARS-CoV geïnfecteerde fretten was verlaagd vergeleken met expressie van dezelfde genen in niet-geïnfecteerde dieren, in tegenstelling tot genexpressie in SARS-CoV geïnfecteerde makaken en muizen, die sterk verhoogd is. Het feit dat juist de processen waarop interferon en ACE2 een effect zouden moeten hebben niet geactiveerd zijn in SARS-CoV geïnfecteerde fretten, zou kunnen verklaren waarom deze behandelingen niet effectief zijn in het verminderen van SARS-CoV veroorzaakte longschade. Mogelijk wordt de longschade in fretten veroorzaakt door de grote hoeveelheid virus in deze dieren of door nog ongedefinieerde processen. Deze studie benadrukt het belang van vergelijkende analyses van gastheer genexpressie na infectie met SARS-CoV, of andere virussen, in verschillende diersoorten, aangezien de uitkomst van deze analyse belangrijk kan zijn voor het kiezen voor het ontwikkelen van een succesvolle interventiestrategie.

In dit proefschrift laten we zien dat infectie met SARS-CoV uiteenlopende gastheer responsen induceert in de verschillende diermodellen, die sterk afhankelijk zijn van gastheer factoren, terwijl de mate van virale replicatie in de longen van makaken, muizen en fretten vergelijkbaar is. De gastheer respons en het daarop volgende ziektebeeld is afhankelijk van het soort gastheer, maar kan ook beïnvloed worden door de stam (bij muizen), de leeftijd van de gastheer en de locatie in het lichaam waarin de gastheer respons wordt bestudeerd. Ook is het aannemelijk dat de gezondheid, het gebruik van medicatie en bijvoorbeeld een vaccinatie effect hebben op de pathogenese van SARS. Deze verschillende gastheer responsen leiden tot diverse SARS ziektebeelden, die vragen om een individuele behandeling. Terwijl in makaken en muizen de sterke SARS-CoV geïnduceerde gastheer respons op genexpressie niveau gedomineerd lijkt te worden door niet-geïnfecteerde cellen en de pathogenese immuun-gemedieerd is, suggereren onze data dat de sterk verlaagde expressie van gastheer genen zoals gezien in SARS-CoV

geïnfekteerde fretten voornamelijk gestuurd wordt door de geïnfekteerde cellen. Het feit dat infectie met SARS-CoV leidt to een scala van gastheer afhankelijke fenotypen heeft implicaties voor de keuze van diermodellen bij het doen interventie studies, niet alleen bij het bestuderen van SARS-CoV maar mogelijk ook bij onderzoek naar andere virussen die immuun-gemedieerde ziektes veroorzaken.



# Dankwoord

Zo lang naar toegeleefd en nu is het eindelijk zo ver, mijn proefschrift is klaar! Maar promoveren lukt je niet alleen. Alle mensen die geholpen hebben bij het tot stand komen van mijn proefschrift wil ik hierbij bedanken. In het bijzonder richt ik mijn dankwoord tot de volgende personen:

Allereerst wil ik natuurlijk mijn promotor en copromoter bedanken voor hun bijdrage. Ab, het “lab van Ab” is een gave plek om te werken, interessant onderzoek, altijd midden in de actualiteit, kortom; never a dull moment! Bedankt voor de kans om hier deel van uit te mogen maken. Bart, ik ben blij dat het, wat later dan verwacht, nu dan toch echt af is. Bedankt voor je tomeloze inzet en enthousiasme, juist op momenten dat ik zelf niet meer zo enthousiast was. Je gedrevenheid en creatieve ideeën als onderzoeker zijn inspirerend en je redigeer kwaliteiten voor deze “koningin van de bijzin” onmisbaar! Heel veel dank voor alle tijd en energie die jullie in mijn project hebben gestoken. Zonder jullie was het niet zo’n mooi resultaat geworden!

Graag wil ik benadrukken dat dit proefschrift tot stand is gekomen met behulp van vele mensen. Mijn collega’s op de afdeling virologie dank ik voor de samenwerking, hulp, kritische discussie, adviezen, materialen en natuurlijk vooral gezelligheid. Dat laatste geldt zeker ook voor al mijn kamergenoten de afgelopen jaren op de virologie. Annemiek, Suwanna, Byron, Jessica, Hans, Rui, Monique, Werner, Sander, Pascal, Bernadette, Jonneke, Sacha, Martin Marina, Marine & Kim, zonder de welkome lachbuien (wall of shame!), zoete en hartige versnaperingen en de broodnodige peptalks zouden onze -toch al kleine- werk-kamers nog véél kleiner zijn geweest.

In het bijzonder wil ik een aantal mensen bedanken die mij hebben geholpen met de experimenten die zijn beschreven in dit proefschrift: Lonneke, Lisette, Peter en Judith voor hun hulp met de immunohistochemie en pathologie; Arno, Maarten en Fatiha voor hun onmisbare bijdrage aan de genomics; Robert en Geert voor hun hulp bij de dierexperimenten; Rob, Richard en Byron voor het doen van SARS-CoV infecties op het ML-III lab; en natuurlijk Corine en Femke voor hun hulp bij het isoleren en sorten van de muizen DCs en de depletie experimenten. Daarnaast wil ik Léonie graag bedanken voor het opmaken van dit proefschrift.

One of the best experiences of the past years was to conduct part of my PhD research in Seattle at the University of Washington. I would like to thank prof. dr. Michael Katze for this opportunity. Also I would like to thank all the people at the Katze lab for their help with performing the experiments and subsequent analysis, but also for their hospitality and for the fun times we had. It was great!

Natuurlijk wil ik ook mijn paranimfen bedanken, Saskia en Talita. Heel erg fijn dat jullie mij op de promotiedag terzijde willen staan. Saskia, niet alleen ben je een van mijn weinige echte “SARS” collega’s

en hebben we de laatste jaren regelmatig samengewerkt, overlegd etc., ook ben je gewoon een super gezellige collega! Nieuwe data bespreken, frustraties uiten of gewoon even bijkletsen tijdens onze dagelijkse lunch, vaak voorzien van nuchtere inzichten van jouw kant, doet me altijd goed. Laten we die traditie nog even vasthouden! Lieve Talita, we zijn elkaar tegen gekomen op het Jv0, compleet verschillende opleidingen gevolgd en nu allebei (bijna) klaar met de promotie! Wie had dat nou kunnen denken ruim 20(!) jaar geleden... Super fijn dat we al die jaren zulke goede vriendinnen zijn gebleven en hopelijk hebben we allebei straks weer wat meer tijd om af te spreken. Vinden Naäma en Malte vast ook leuk!

Ik wil ook graag alle lieve vrienden en familie bedanken voor het meeleven gedurende het hele project. Carla, Marjolein, Inge, Maaïke, Jose, Kirsten, Rutger en Anna, Helmer en Inge, heel erg bedankt voor alle gezellige etentjes en koffiedates, maar vooral ook voor het luisterende oor! Sven en Mo, Maaïke en Ronald, het was een heftige zomer, heel fijn dat jullie konden bijspringen wanneer ik geen tijd had. Volgend jaar met z'n allen BBQen in Degerbyn? Lieve papa en mama, bedankt voor jullie vertrouwen en onvoorwaardelijke steun, ik waardeer het enorm!

Tenslotte wil ik Joris bedanken voor alles! Voor je geduld, je betrokkenheid, intelligentie, knappe uiterlijk, bijzonder sympathieke houding en voor het typen van de laatste zin van mijn dankwoord ;-)







# Curriculum Vitae

Anna de Lang was born on December 16<sup>th</sup>, 1978 in Leusden, the Netherlands. In 1997 she finished high school at the Stedelijk Gymnasium Johan van Oldenbarnevelt in Amersfoort and started to study Biotechnology at Wageningen University. After finishing the first year, she switched to Biology at the same university and specialized in molecular and cellular biology in the Bachelor phase. During the Master phase, she specialized further into virology and immunology. She did an extended research project at the department of Virology, Wageningen University, studying the VP15 protein of White Spot Syndrome Virus. Afterwards, she performed a study on Human Papilloma Virus at the department of Immunology, Genetics and Pathology at the University of Uppsala, Sweden. Finally, she did an internship at the department of Immunology at the Dutch Cancer Institute studying the use of the Sindbis virus replicon as a DNA vaccine for melanoma. In 2004 she started as a PhD student at the department of Virology in the Erasmus Medical Center in Rotterdam under supervision of prof.dr. Ab Osterhaus and dr. Bart Haagmans. This project, focusing on the pathogenesis of SARS, has resulted in the present thesis.



# Publications

**A. de Lang**, C.H. GeurtsvanKessel, G. van Amerongen, M.A. Bijl, F. Zaaaraoui-Boutahar, L. Boon, A.D.M.E. Osterhaus, A.C. Andeweg and B.L. Haagmans. Plasmacytoid dendritic cells drive early antiviral and proinflammatory host responses in severe acute respiratory syndrome coronavirus infected mice.

*Submitted for publication*

S.L. Smits, J.M. van den Brand, **A. de Lang**, L.M. Leijten, W.F. van IJcken, G. van Amerongen, A.D.M.E. Osterhaus, A.C. Andeweg and B.L. Haagmans.

Distinct severe acute respiratory syndrome coronavirus-induced acute lung injury pathways in two different nonhuman primate species.

*Journal of Virology*, 2011: 85(9):4234-4245

S.L. Smits, **A. de Lang**, J.M. van den Brand, L.M. Leijten, W.F. van IJcken, M.J. Eijkemans, G. van Amerongen, T. Kuiken, A.C. Andeweg, A.D.M.E. Osterhaus and B.L. Haagmans.

Exacerbated innate host response to SARS-CoV in aged non-human primates.

*PLoS Pathogens*, 2010: 5;6(2):e1000756

**A. de Lang**, T. Baas, S.L. Smits, M.G. Katze, A.D.M.E. Osterhaus and B.L. Haagmans.

Unraveling the complexities of the interferon response during SARS-CoV infection.

*Future Virology*, 2009: 1;4(1):71-78

**A. de Lang**, T. Baas, T. Teal, L.M. Leijten, B. Rain, A.D.M.E. Osterhaus, B.L. Haagmans and M.G. Katze.

Functional genomics highlights differential induction of antiviral pathways in the lungs of SARS-CoV-infected macaques.

*PLoS Pathogens*, 2007; 10;3(8):e112

**A. de Lang**, A.D.M.E. Osterhaus and B.L. Haagmans.

Interferon- $\gamma$  and interleukin-4 downregulate expression of the SARS-CoV receptor ACE2 in Vero E6 cells.

*Virology*, 2006: 30;353(2):474-481

**A. de Lang** and E. Wilander.

Sensitivity of HPV tests on stained vs. unstained cervical smears.

*Acta Cytologica*, 2005: 49(6):595-599

**A. de Lang**, I. Wikström and E. Wilander.

Significance of HPV tests on women with cervical smears showing ASCUS.

*Acta Obstetrica et Gynecologica Scandinavica*, 2005: 84(10):1001-1005.

J. Witteveldt, A.M. Vermeesch, M. Langenhof, **A. de Lang**, J.M. Vlak and M.C. van Hulten.

Nucleocapsid protein VP15 is the basic DNA binding protein of white spot syndrome virus of shrimp.

*Archives of Virology*, 2005: 150(6):1121-1133



# PhD portfolio

<b>Name PhD student:</b>	Anna de Lang
<b>Erasmus MC department:</b>	Virology
<b>Research school:</b>	Post-graduate Molecular Medicine
<b>PhD period:</b>	2004-2011
<b>Promotor:</b>	Prof. dr. A.D.M.E. Osterhaus
<b>Copromotor:</b>	Dr. B.L. Haagmans

## In-depth courses

2009	Practical Course on Analysis and Informatics of Microarray Data, provided by EMBO, Cambridge, England
2007	Molecular Immunology, provided by the postgraduate school Molecular Medicine, Erasmus MC, Rotterdam, The Netherlands
2007	Analysis of microarray gene expression data, provided by the Medical Genetics Center, Erasmus MC/Leiden University, Rotterdam, The Netherlands
2006	Classical Methods for Data-analysis CCo2, provided by the Netherlands Institute for Health Sciences, Rotterdam, The Netherlands
2005	Course on medical ethics and philosophy, provided by the department of Medical Philosophy and Ethics, Erasmus MC, Rotterdam, The Netherlands
2005	English Biomedical Writing and Communication, provided by the Postgraduate School Molecular Medicine, Erasmus MC, Rotterdam, The Netherlands
2005-present	Internal and external presentations at the Department of Virology twice a week

## Presentations

2011	Role of plasmacytoid dendritic cells in the host response to SARS-CoV infection. (XII <sup>th</sup> International Nidovirus Symposium, Acme, United States) (oral presentation) Interferon response in murine plasmacytoid dendritic cells after SARS-CoV infection (Molecular Medicine day, Rotterdam, The Netherlands) (poster)
2009	Differential host responses to SARS-CoV infection. (EMBO course, Cambridge, England) (poster) Interferon response in murine plasmacytoid dendritic cells after SARS-CoV infection (Joint meeting of the ICS/ISICR, Lissabon, Portugal) (poster)

- 2007 Type I interferon induction and STAT1 phosphorylation in lungs of SARS-CoV infected macaques. (Dutch Annual Virology Symposium, Amsterdam, The Netherlands) (oral presentation)
- 2006 Differential gene expression in macaques infected with SARS-CoV. (SARS-CoV grant meeting, Seattle, United States) (oral presentation)
- Interleukin-4 downregulates ACE2 expression and inhibits SARS-CoV replication in Vero E6 cells. (Molecular Medicine day, Rotterdam, The Netherlands) (oral presentation)
- 2005 Interferon- $\gamma$  and Interleukin-4 down regulate SARS-CoV Receptor Expression. (X<sup>th</sup> International Nidovirus Symposium, Colorado Springs, United States) (poster)
- Regulation of the SARS-CoV receptor ACE2. (Department of Microbiology, University of Washington, Seattle, United States) (oral presentation)

## Attended

- 2011 Molecular Medicine day, Rotterdam, The Netherlands
- 2010 Dutch Annual Virology Symposium, Amsterdam, The Netherlands
- 2009 Dutch Annual Virology Symposium, Amsterdam, The Netherlands.  
Molecular Medicine day, Rotterdam, The Netherlands
- 2008 XIth International Nidovirus symposium, Oxford, England.  
Dutch Annual Virology Symposium, Amsterdam, The Netherlands  
Molecular Medicine day, Rotterdam, The Netherlands
- 2007 Vaccine Symposium, Utrecht, The Netherlands  
Dutch Annual Virology Symposium, Amsterdam, The Netherlands.  
Molecular Medicine day, Rotterdam, The Netherlands  
SARS-CoV grant meeting, Chapel Hill, United States
- 2006 SARS-CoV grant meeting, Seattle, United States  
Molecular Medicine day, Rotterdam, The Netherlands
- 2005 X<sup>th</sup> International Nidovirus Symposium, Colorado Springs, United States
- 2005 Dutch Annual Virology Symposium, Amsterdam, The Netherlands

## Other

- 2008/2009 Supervision of MSc student
- 2006 2-month research project “functional genomics” at the department of microbiology, University of Washington, Seattle, United States
- 2005 3-month research project “functional genomics” at the department of microbiology, University of Washington, Seattle, United States